Factors controlling the properties of the Cds – Cu (_2)s photovoltaic cell

B. G. Caswell

FACTORS CONTROLLING THE PROPERTIES OF THE $CdS - Cu_2S$ PHOTOVOLTAIC CELL

by

B. G. CASWELL, B.Sc.

Presented in candidature for the degree of
Doctor of Philosophy
in the
University of Durham

August 1976

ACKNOWLEDGEMENTS

It is a pleasure to express my thanks to friends and colleagues who have helped me during the course of this research project. I would especially like to thank Dr. J. Woods, my supervisor, for his encouragement and guidance. Thanks are also due to Dr. G.J. Russell for instructing me in the use of the electron microscope and for the many valuable discussions concerning the results.

I would also like to thank Professor D.A. Wright for allowing me to use the departmental research facilities and I am grateful to the workshop staff headed by Mr. F. Spence for their technical help and advice. For the growth of the CdS single crystals, I am indebted to Messrs. J.R. Cutter and N.F. Thompson.

Special thanks are due to the Solid State Physics Section of I.R.D. Co. Ltd. (Newcastle upon Tyne) for permitting me to use the research facilities there. I am also grateful for the valuable discussions with members of the group, especially Mr. R.J. Mytton, Dr. L. Clark and Dr. R.W. Gale.

I am indebted to the Science Research Council for the award of a C.A.S.E. Research Studentship in conjunction with I.R.D. Co. Ltd.

Finally I would like to express my gratitude to my parents for their many sacrifices and constant encouragement over the years and to my wife, Christiana, for her understanding and support.

ABSTRACT

Large area sprayed or silk screen printed CdS/Cu_2S solar cells are potentially cheap and efficient devices for the direct conversion of sunlight into electrical energy. They do not require the expenditure of large amounts of energy during fabrication as do silicon cells. There are, however, various degradation processes associated with the operation of the cells and the major mechanism is thought to be associated with a gradual oxidation of the copper sulphide. It is clear therefore that the degradation of single crystal and evaporated thin film cells must be better understood before the more difficult problems associated with the fabrication and operation of sprayed or printed layer cells can be solved.

This thesis describes an investigation into the photovoltaic properties of CdS/Cu_2S heterojunctions. The cells were prepared by forming layers of Cu_2S on single crystals and thin films of CdS. Undoped crystals with both high and low resistivity have been used as have low resistivity samples containing grown-in copper, indium and chlorine impurities. A study of the spectral dependence of the open circuit voltage and of the current-voltage characteristics, after baking in air at 200°C, shows that the maximum spectral sensitivity of the cells in the range 0.6 to 0.7 μm is associated with a photoconductive region in the cadmium sulphide caused by a diffusion of copper into the cadmium sulphide. The effects of forming the cuprous sulphide layers on basal planes of opposite polarity have also been investigated. It was shown that the conversion of cadmium sulphide to cuprous sulphide proceeds 1.5 times faster on sulphur than on cadmium planes and the photovoltages of unbaked cells with the cuprous

sulphide formed on sulphur faces are some 20% larger than the photovoltages from cells in which the cuprous sulphide is formed on cadmium faces. It was further shown that the plating temperature must be carefully controlled at 90°C to ensure production of stoichiometric Cu_2S.

CONTENTS

CHAPTER 1

INTRODUCTION

Since the late 1960's, there has been great interest in cadmium sulphide/copper sulphide heterojunction photovoltaic cells. Such devices show promise for space and terrestrial use. Silicon cells are at present used as satellite power sources but they degrade severely when exposed to cosmic and other radiation. On earth, silicon solar cells are used as power sources in remote places such as marker buoys but much electrical energy is consumed during their production. Cadmium sulphide solar cells are known to be more radiation resistant than silicon solar cells and large area devices can be fabricated in thin film form. The production of such cells is inherently less energy consuming than the silicon technology. However, the power output of cadmium sulphide/copper sulphide solar cells degrades during exposure to illumination or on thermal cycling. To combat these effects, better attempts must be made to understand the operation of the device so that more stable and efficient devices can be fabricated.

The work in this thesis has been carried out under the Science Research Council's C.A.S.E. award Scheme in collaboration with the International Research and Development Company of Newcastle upon Tyne. This company has been involved in the research and development of thin film solar cells since the middle of the last decade.

It is possible to fabricate thin film and single crystal cells. The basic structure of both types of device consists of some sort of substrate which serves as an ohmic contact to the CdS. A copper sulphide 'barrier' layer is formed on the CdS and finally an ohmic contact usually in the form of a grid is formed on the copper sulphide. Such devices may be encapsulated to retard the various degradation processes.

Earlier work carried out at I.R.D. and Durham has been concerned mainly with the properties of the CdS layer. Although the ultimate aim was to produce evaporated layers of CdS for eventual device fabrication, work was carried out on single crystal material to give basic information about the material. Evaporated layers of good quality and optimum resistivity have been produced in these earlier studies.

More recently in the field of solar cell research, attention has been increasingly focused on changes which occur on the copper sulphide side of the boundary. The Cu-S phase diagram is complex and several workers have explained the degradation effects in terms of the gradual oxidation of the copper sulphide to a copper deficient phase.

The studies reported in this thesis are all concerned with the factors controlling the properties of CdS/Cu_2S photovoltaic cells. Solar cells in both single crystal and thin film form were fabricated during this study. Chapter 2 is a general review of photo-effects in group II - group VI compounds. The photovoltaic effect in the cadmium sulphide/copper sulphide heterojunction is discussed in Chapter 3. Since the aim is to produce large area devices, Chapters 4 and 5 are concerned with general methods of production of thin films and the particular arrangements used at Durham and I.R.D. The formation of copper sulphide topotaxially on cadmium sulphide is described in Chapter 6 together with a method for the direct identification of the phase of copper sulphide produced by standard procedures in this laboratory. A study was also made of the influence of the heat treatment in air of cells fabricated on single crystal CdS of different resistivities and dopants. This is described in Chapter 7. Photoconductive effects associated with device characteristics are shown to be related to the diffusion of copper from the copper sulphide into the cadmium sulphide.

Investigations of the effects of heat treatment are continued in Chapter 8 when the effects of surface oxidation are discussed. Attempts were made to produce stoichiometric cuprous sulphide by applying potentials to the Cu_2S surface during its formation. The importance of controlling the formation temperature is also reported and cell spectral response characteristics are correlated with the phase of copper sulphide present as identified directly by techniques discussed in earlier chapters.

CHAPTER 2

PHOTOEFFECTS AND II-VI COMPOUNDS

2.1 Photoelectric Effects

The three main photoelectric effects were discovered in the nineteenth century and have descriptive names in contrast to many contemporary physical effects which were named after their discoverer or a leading investigator. The photovoltaic effect (P.V.E.) forms the basis of the work to be described in this thesis, although the other two main effects of photoconduction and photoemission have been investigated to a much greater extent by other workers and are exploited in many applications.

The first of the photoelectric effects to be discovered was the P.V.E. (Becquerel 1839). It required a wet cell comprising two non-identical electrodes immersed in an electrolyte. When one electrode was illuminated with photons of certain energies, a potential difference developed between the two electrodes and on connecting a load, a current was observed to flow.

The Becquerel type P.V.E. is one of the most difficult photoeffects to explain fully and not many theories were put forward until the work on Cu/Cu_2O photocouples had been performed. Early models proposed by Frenkel (1933,1935), Landau and Lifshitz (1936), Davydov (1938) and Mott (1939) concluded correctly that the photo-emf arose as a consequence of the production of a non-equilibrium concentration of minority carriers. A more recent exposition of the Becquerel P.V.E. was given by Williams (1960). Both cadmium sulphide (CdS) and gallium arsenide (GaAs) were investigated as electrode materials, but this wet cell arrangement does not appear to have any applications or particular

advantage. When Chapin et al (1954) discovered the photovoltaic effect in p-n homojunctions in silicon, much of the then recently developed semiconductor device theory was used to explain the processes involved. However, attempts by Reynolds et al (1954) to apply this theory to the Cu/CdS or Cu_2S/CdS heterojunction cell, which had also been reported by them at about the same time, were not so successful, and even now no model for this device is universally accepted.

The second photoelectric phenomenon discovered was the photoconductive effect (P.C.E.). It was first observed in selenium by Smith (1873). The resistivity of a bulk sample decreased when it was illuminated with light of the appropriate photon energy. Identical electrodes were used and no photo-emf was generated. Consequently a power source was needed to operate the device. Most of the compounds formed from the elements of groups II and VI of the periodic table have large photoconductive effects. Cadmium sulphide in particular has high dark resistivity and good sensitivity and CdS photoconductive cells are used in the exposure meters of many cameras. In many practical devices, a compromise has to be reached between the speed of response and sensitivity (Rose 1963, Bube 1955,1960).

The third major photoelectric process is the photoemissive effect which Hertz (1887) first observed during his series of experiments on electric induction. It was found that a spark in a secondary circuit passed more easily across a gap when the gap was illuminated with the light from the primary spark (which was a source of ultra-violet light). Hallwachs (1888) corroborated these results and concluded that negative charge was emitted from the cathode under excitation from high energy photons.

Elster and Geitel (1895) discovered that the electron emission was much larger from the electrochemically positive metals such as sodium or cesium. This eventually led to the development of present day photocathodes such as Cs_3Sb and Cs-O-Ag which are used in the first stage of modern photomultipliers for example.

For completeness, other relatively minor photoelectric phenomena should be mentioned although at present they do not form the basis of any practical devices nor have they been investigated in this present work. They are however used in the determination of material parameters such as carrier mobility for example. These are:

(a) The Dember effect in which a voltage is produced in a sample in a direction parallel to that of illumination by incident photons. The voltage is produced as a result of the different recombination rates of electrons and holes which do not possess the same mobilities and therefore diffuse at different rates.

(b) The photopiezoelectric effect which arises from a small local change in energy gap of a semiconductor when the bulk material between two opposite contacts is compressed and the sample is illuminated. This phenomenon gives rise to a small photovoltage.

(c) The photoelectromagnetic effect which is analogous to the Hall effect. When a magnetic field is applied to a sample which is being illuminated in a direction perpendicular to the field, a potential difference appears across the crystal in the third orthogonal direction. The electrons and holes which are created by the absorption of photons are separated by the magnetic field and a potential difference is developed across the sample.

All of these effects are discussed in Tauc's book (1962) but the detailed theory may require modification in the light of more recent developments.

A photovoltaic effect can be produced in several different situations:-

(1) A bulk effect may occur if a sample is illuminated non-uniformly or if it has a non-uniform impurity distribution contained within it.

This effect was reported by Wallmark (1957) who observed a transverse photovoltaic effect in certain materials when they were illuminated non-uniformly. A potential difference parallel to a junction just below the surface was produced when the junction was illuminated perpendicularly to the surface. The magnitude and sign of the voltage produced was very sensitive to the location of the focused spot of incident light. The effect could be exploited in a position indicator.

(2) Barrier effects arise whenever an electrostatic barrier is present in a sample. These effects cause charge separation of the optically created electron-hole pairs. As a result of which, an electrostatic potential difference occurs across the barrier. The barrier may arise in several different ways. It may be due to a diffusion potential between an n-type and a p-type region, or to an interface region between semiconductors with different band gaps or simply to a blocking contact between a metal and a semiconductor. The CdS solar cell which is so called for historical reasons, but which is really a heterojunction between p-type copper sulphide and n-type cadmium sulphide falls into the first category. Further complications arise from the probable existence of a copper compensated cadmium sulphide interface region which is present in at least some CdS solar cells.

(3) A photovoltage many times larger than the energy gap may arise in single crystals of certain group II - group VI compounds. The potential gradient may be several hundred volts per centimetre of length (Goldstein and Pensak 1959, Brandhorst et al 1968) and depends on sample perfection or the method of production of the thin films. One explanation of the effect suggests that the cubic/hexagonal stacking faults which are present in some group II - group VI compounds (especially zinc sulphide) are in effect potential barriers (Ellis et al 1958). It is further suggested that the different band gaps of the cubic and hexagonal materials cause a series of discontinuities in potential energy which is additive, hence a total barrier of several hundred electron volts is formed (Cutter and Woods 1975). However the high impedance of samples which show this effect has prevented any useful application up to the present time.

2.2 Solar Cells

Semiconducting photovoltaic devices were initially used only to detect or measure radiation in such applications as photographic exposure meters, light actuated switches and light detectors with lower noise and faster response than photoconductive devices. However, during the past two decades, technological improvements have led to photovoltaic cells in which the electrons and holes can be collected much more efficiently, and useful conversion of solar energy into electrical power has been achieved.

On a cloudless sunny day at latitude 55°N at sea-level, about 800 W m^{-2} of solar energy falls on the earth's surface. At present, most of our power is generated from the burning of fossil fuels such as coal and oil. These were produced indirectly by the sun in the first place by photosynthesis. This is an inherently inefficient and time consuming

process and it would clearly be better to convert the sun's energy directly into electricity. Solar cells were recognised to have great potential as energy converters as silicon technology developed and other materials with low conversion losses were found. A 20% "limiting conversion efficiency" was calculated for silicon p-n junctions and even higher values for materials such as aluminium antimonide, gallium arsenide and indium phosphide (Cummerow 1954, Pfann and Roosbroek 1954, Rittner 1954, Prince 1955, Rappaport 1959 and Wolf 1960). Much recent work has been directed towards realising these efficiencies and the greatest advances have been made as a result of the U.S.A. space projects. Beyond the earth's atmosphere, the available solar energy is ~ 1.4 kW m^{-2}. A commonly occurring term used to describe the relative power falling on a solar cell is that of relative air mass. The optical air mass is a function of height above sea level, i.e. atmospheric pressure and the length of path in the atmosphere through which the sunrays must pass and hence the global position of the cell is important. A power of 1.4 kW m^{-2} is received at the equator at midday outside the earth's atmosphere and these are air mass zero conditions (A.M.O). The A.M.1 condition occurs on a cloudless day at sea level at the equator and corresponds to a received power density of 1 kW m^{-2}. Equivalent A.M.O or A.M.1 conditions assume that the power source has the same spectral response as that of the sun. Since such a large amount of solar power is available in space, even assuming a low power conversion efficiency of say 10%, communication satellites can be powered from a solar cell array of acceptable dimensions (several tens of square metres in area).

When solar cell materials and array designs are chosen, the following criteria must be considered.

(i) The cost of materials should be low.

(ii) The processes used in making the materials and the devices should not consume excessive amounts of energy.

(iii) The method of fabrication should lend itself to mass production.

In addition the solar cell should be designed to fulfil the following conditions:-

(a) It should have a high radiation resistance especially for space use.

(b) It should have a large area to reduce cell interconnection problems.

(c) The cells should be flexible.

(d) They should have a high power to weight ratio.

(e) There should be low reflection losses at the surface.

(f) The cell must have a high efficiency for production of electron-hole pairs from absorbed photons.

(g) The carrier mobilities should be high to reduce recombination losses.

(h) A cell should have a high fill factor (ratio of maximum power rectangle to product of open circuit voltage and short circuit current).

(i) The internal series resistance should be low (this has been partly solved by better grid design).

The first devices to be fabricated were based on single crystals. Although silicon solar cells were the most efficient for a long time, gallium arsenide cells and cadmium sulphide/indium phosphide have been reported more recently as having higher efficiencies (Wagner and Shay 1975).

All of these cells however are fabricated from thin slices of material cut from single crystals which have to be grown at high temperatures. Not only is this process wasteful of materials, it is also wasteful of energy. Moreover the areas of the cells are limited to a few square centimetres by the crystal growth processes and the thin wafers are exceedingly fragile.

Present day efficiencies of silicon cells are quoted as $\sim$15% but 12 to 13% is more typical. Most of the present applications of silicon cells are in space environments and the cells degrade to an efficiency of about 6% in a few months because they are subjected to particle and cosmic radiation in space. It has been suggested (Brucker et al 1966) that this damage can be minimised by using a silicone coating or by heavily doping the silicon with lithium. This latter modification is thought to promote a self repairing mechanism.

Up to the present time, the power level requirement of the single crystal silicon cells used in unmanned space missions has been less than 1 kW. Future missions will probably require power levels of several kilowatts and it will not be possible to meet this using body mounted devices. A space deployable array will be required and much research sponsored by N.A.S.A. has been done on a flexible thin film cell for use in such an array. Thin film cells (Moss 1961) offer the advantages of potential cheapness, light weight, mechanical flexibility and a large total output power level from an array of practical size. A comparison between the parameters of silicon single crystal solar cells and cadmium sulphide thin film cells is given in Table 2.1 which is taken from Mytton, 1973.

Although some of the production problems can be overcome using more advanced technology, the basic properties of the materials which

Parameter	CdS Roll up Array	Si Roll up Array 150 μm cells
Efficiency when first fabricated	7%	11%
Efficiency after 5 years in synchronous orbit	5.9%	9.6%
Power to weight ratio $W\ Kg^{-1}$	82.1	71.2
Cost per watt In 1973	£30	£120

Table 2.1: Comparison between CdS and Si solar cells (mainly for space applications).

make up the heterojunctions are the real limiting factors of the cadmium sulphide/copper sulphide cell. A curve of efficiency as a function of energy gap has been deduced theoretically (Loferski 1956, Wolf 1960) and this suggests that a maximum performance should be attained with an energy gap of 1.6 eV when A.M.O. illumination is employed. On this basis silicon (energy gap $\sim$1.1 eV) is worse than gallium arsenide (1.34 eV) or aluminium arsenide (1.52 eV). Indium phosphide (1.27 eV) ought to be slightly better than silicon and this has recently been demonstrated to be true (Wagner and Shay 1975). From energy gap considerations, it was originally assumed that CdS solar cells would be very poor, but the band gap of cadmium sulphide of 2.4 eV should, from this point of view, be replaced by an effective band gap of 1.2 eV which is attributable to the copper sulphide layer.

Consideration of all of these factors suggests that the flexible thin film CdS/Cu_2S cells may present a strong challenge to the overall supremacy of silicon. In theory and in practice, heterojunctions fabricated from cadmium telluride (CdTe) (Vodakov et al 1960, Cusano 1963), aluminium arsenide (AlSb) (Rittner 1954), and indium phosphide (InP) (Wagner and Shay 1975) are better than either cadmium sulphide or silicon. However in practice, difficulties in growing single crystals rule out most of these materials. In contrast CdS/Cu_2S solar cells can easily be prepared in thin film form and efforts to produce a sprayed solar cell are continuing in this laboratory.

2.3 II-VI Compounds

We shall define II-VI compounds as the compounds formed between elements from groups IIb and VIb of the periodic table.

Crystals of all of the II-VI compounds have been grown from the melt and by vapour phase growth. The growth of a II-VI compound from the vapour phase was first reported by Lorenz (1891). The technique was used much later in a modified form by Frerichs (1947). In this latter dynamic method, separate sources of the elements were required with a carrier gas supplied externally. The basic requirement for growth is simply that of the provision of a vapour containing the group II and group VI elements. This can be achieved either by the dissociation of a permanent compound (e.g. CdS) or by the vapourisation of the separate elements. The gas molecules diffuse or flow to a region where super-saturation occurs and growth follows.

A static method of crystal growth was developed later by Reynolds and Czyzak (1950) and Greene et al (1958) in which transport occurs by diffusion within the gas phase. In this method, the starting materials are required to be in powder form. Further modifications to the technique were carried out by Piper and Polich (1961) and since then, this method has been used with good results to grow crystals of several II-VI compounds.

Growth from the melt has many advantages in the preparation of large single crystals. Only certain II-VI compounds which have a relatively low melting point such as cadmium telluride, cadmium selenide and zinc telluride can be melted without a high pressure being applied (Lorenz 1962).

The II-VI compounds crystallize in two main forms, namely the cubic zinc blende (sphalerite) structure and the hexagonal wurtzite structures. Although cadmium sulphide and cadmium selenide are dimorphic, they normally crystallize in the hexagonal form whereas cadmium telluride crystallizes with the cubic sphalerite structure. Polytypes may also exist but they are essentially derived from the sphalerite or wurtzite

structures. Some II-VI compounds (e.g. CdS) exist in the more stable wurtzite form at room temperature. However by means of external constraints it is possible to produce the less stable sphalerite form. Co-ordination is tetrahedral in both cases. The more covalently bonded II-VI compounds form the sphalerite structure, but as ionicity increases, there is a tendency to form the wurtzite structure.

Both the wurtzite and sphalerite crystal structures of II-VI and III-V compounds are characterized by a tetrahedral Sp^3 bond configuration of the component elements. The elements are arranged in double layers perpendicular to the <111> directions of the zincblende structures or the [0001] direction of the wurtzite structure (Fig. 2.1). As a result of the greater bond density between the close packed layers and the lack of inversion symmetry, both of these structures possess a crystallographic polarity. The $\{111\}$ faces of the zincblende structure and the (0001) face of the wurtzite structure terminate with cations, i.e. ions from groups II or III, while the $\{\bar{1}\bar{1}\bar{1}\}$ faces of the zincblende structure and the $(000\bar{1})$ face of the wurtzite structure are composed of anions, i.e. ions from groups VI or V. The polar nature leads to different etch rates for different faces of these crystals.

Crystals of II-VI compounds grown in practice are usually non-ideal and contain many defects which often control their semiconducting properties. Typically, point defects such as vacancies or impurity atoms are present as well as line or plane defects such as dislocations or stacking faults. The cooling of the crystal growth capsule and the subsequent slicing of boules produces strain which is relaxed mainly by the formation of dislocations. More complex defects can arise from combinations of these elementary ones. Some II-VI compounds such as zinc sulphide are prone to the intergrowth of both crystal forms, there are then gross defect structures associated with this polytypism.

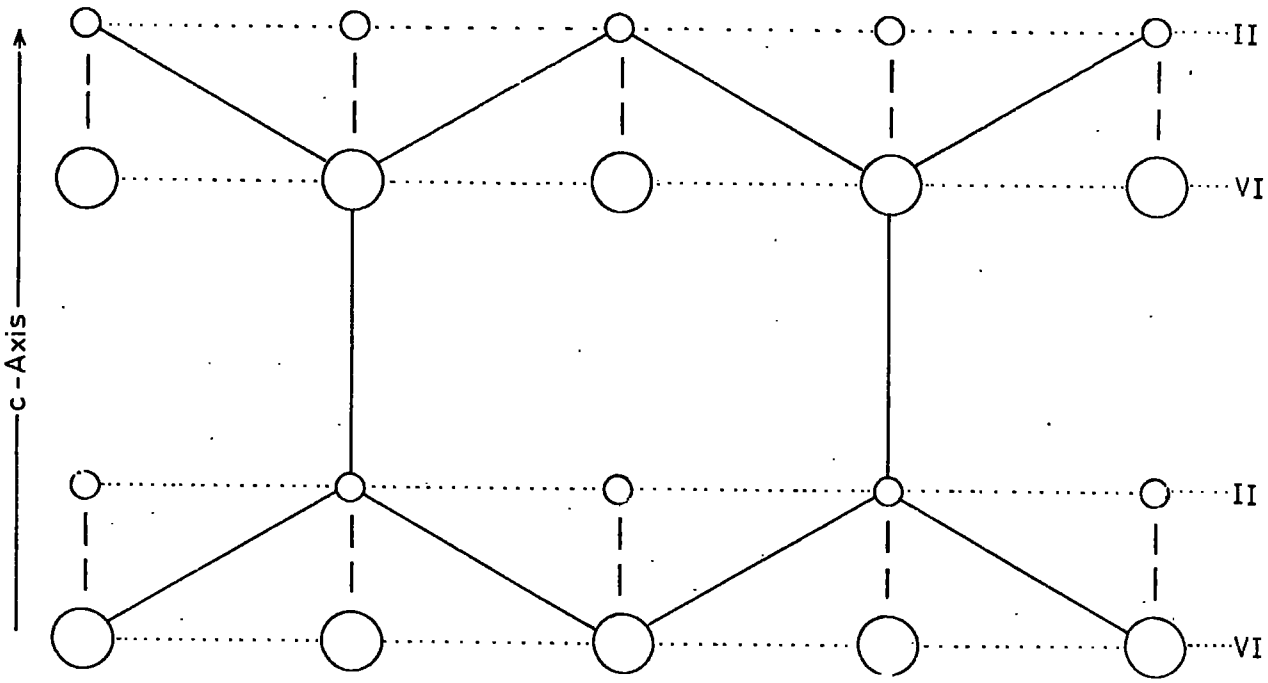

FIG. 2.1 ALTERNATE LAYERS OF GROUP II AND VI ATOMS PERPENDICULAR TO THE [0001] DIRECTION OF A WURTZITE II-VI COMPOUND.

As is well known, the group IV elemental semiconductors all crystallize with the diamond structure in which each atom is in tetrahedral co-ordination with four like atoms. The interatomic bonding is predominantly covalent. In the II-VI compounds, the bonding cannot adequately be described as of any one extreme, but is intermediate between ionic and covalent. Regardless of whether the bonding is predominantly more ionic or covalent, the spins of the bonding electrons are paired and the net electron spin is zero. A perfect defect free crystal is therefore diamagnetic. In fact the interesting electrical, magnetic and optical effects of the II-VI compounds arise from the number and nature of defects incorporated during growth.

Most of the II-VI compounds can be made photoconductive. This photoelectronic process is controlled by charge carriers. Both free electrons and holes are generated by the exciting radiation and it is the increase in free carrier concentration which is responsible for the photoconductivity. It is possible to reduce the resistivity by many orders of magnitude when the crystals are illuminated. Furthermore the large range of values of bandgaps from zinc sulphide ($\sim$3.7 eV) to cadmium telluride ($\sim$1.45 eV) allows for a wide range in the wavelength of maximum response from the ultraviolet to the infrared with direct band gap transitions.

The photoconductivity process in II-VI compounds can be characterized in the following manner.

(a) Electrons provide the main contribution to the photocurrent. Although free electrons and holes are created by the absorption of photons, the holes are rapidly captured at sites when recombination with free electrons occurs at a later time.

(2) The centres which give rise to the high photosensitivity are compensated acceptors. They have a capture cross section for holes which is 10^4 to 10^6 times larger than their subsequent cross section for free electrons. These centres are usually associated with defect impurity complexes or intrinsic crystal defects.

(3) The location of the energy levels of the sensitizing centres in the forbidden gap determines many of the characteristic properties of particular II-VI photoconductors such as the dependence of photocurrent on intensity, optical quenching and speed of response.

2.4 Properties of Cadmium Sulphide

Cadmium sulphide is a IIb-VIb semi-insulating compound which crystallizes normally in the hexagonal wurtzite form and has a direct band gap of about 2.4 eV. Under certain growth conditions, a metastable cubic sphalerite structure may predominate. Thin films with a cubic structure can be grown on cubic crystal substrates such as sodium chloride if the unit cell is similar to that of cadmium sulphide (Wilcox and Holt 1969).

Since the energy gap is direct, the optical absorption coefficient changes as the square of the incident photo energy and has a very large magnitude for photon energies just greater than the energy gap.

Cadmium sulphide begins to sublime at about 700°C and melts at about 1750°C, but only under many atmospheres pressure. It is possible to grow cadmium sulphide from the melt using a high pressure autoclave (Fischer 1963, Medcalf and Fahrig 1958), but it is much easier to grow crystals from the vapour phase. In fact such was the method employed in this laboratory.

It is only possible to prepare n-type samples of cadium sulphide. Pure crystals of cadmium sulphide or cadmium sulphide containing acceptor like impurities are essentially insulators in the dark with resistivities of approximately 10^{12} Ωcm. Any attempt to incorporate acceptor impurities such as copper results in self compensation by vacancies of metal (A) and non-metal (B) vacancies, i.e. Schottky defects. During cooling to room temperature, some of the high temperature vacancy concentration is frozen in. If an undoped crystal is fired under conditions which promote the formation of one type of vacancy over the other, a non-stoichiometry is produced which leads to self-doped conductivity as it were. Cadmium sulphide for instance may be made n-type by heating in cadmium vapour. However firing in the vapour of the non-metal constituent does not produce p-type conductivity. The ratio of cation radius (r_c) to anion radius (r_a) describes the experimentally observed limitations. If $r_c/r_a > 1$, then n-type conductivity occurs and if $r_c/r_a < 1$, p-type conductivity arises. For crystals in which $r_c/r_a \approx 1$, amphoteric conduction occurs as in the case of cadmium telluride. A more detailed account of self compensation in wide energy gap semiconductors may be found in Fischer 1966.

At one time it was thought that p-type cadmium sulphide had been formed using bismuth and phosphorous ion implantation techniques (Anderson and Mitchell 1968, Chernow et al 1968), but the radiation damage produced is now thought to explain the p-type behaviour observed (Tell and Gibson 1969). Because of the impossibility of producing p-type cadmium sulphide, copper sulphide in the chalcocite phase (Cu_2S) has been used to form the p-type side of the heterojunction in the CdS solar cell. The chalcocite can be grown topotaxially on the n-type cadmium sulphide using a chemical exchange reaction which will be described later.

The high resistivity of pure crystals of cadmium sulphide makes measurements of transport properties quite difficult. Not only does the resistivity decrease as a function of light intensity, but the Hall mobility may be dependent on it also. In the dark and at room temperature, the Hall mobility of electrons is approximately 300 $cm^2 V^{-1} sec^{-1}$ in good single crystals, whereas the hole mobility is only about 20 $cm^2 V^{-1} sec^{-1}$. In single crystals, the mobility is limited by ionised impurity scattering at low temperatures and polar optical mode scattering at higher temperatures. In thin films there may be additional geometrical effects limiting mobilities and the inter-granular boundaries will also be important.

Cadmium sulphide has been extensively studied over the last two decades and has been found to exhibit many interesting phenomena. Some of the more important properties are listed below:

(1) High photoconductivity.

(2) A large piezoelectric effect (since there is no centre of inversion symmetry).

(3) Acoustoelectric amplification.

(4) Luminescence (thermo-, photo-, tribo-, cathodo- and electroluminescence).

(5) Laser emission.

(6) Electrical conductivity storage (Wright et al 1968).

For more information and reference to original papers, Aven and Prener (1967) or Ray (1969) should be consulted.

2.5 Properties of Copper Sulphide

Chalcocite (Cu_2S) which is used as the p-type layer in the CdS solar cell is one of the many stable phases of copper sulphide.

A general review of the electrical and optical properties of the copper sulphides has been given by Abdullaev et al (1968) and Vlasenko and Kononets (1971). The performance of the CdS/Cu_2S photovoltaic cell is very dependent on the stoichiometry of the copper sulphide formed during the fabrication of the device and it is relatively easy to produce a copper deficient phase. As a consequence, the copper sulphide is often referred to as Cu_xS with $1.8 \leq x \leq 2$.

A layer of chalcocite can be formed topotaxially on cadmium sulphide by dipping the cell, either in thin film or single crystal form, into a hot solution of Cu^+ ions. The following chemical substitution reaction then takes place:

$$CdS + 2Cu^+ \longrightarrow Cu_2S + Cd^{++}$$

On heating in air, chalcocite is partially converted to djurleite, $Cu_{1.96}S$. Further heating in air produces some digenite, $Cu_{1.8}S$. More detailed discussion on the phase diagram of the Cu—S system and phase transformations will be given later.

By means of this chemical plating process, it is possible to convert a single crystal of cadmium sulphide into a single but cracked crystal of chalcocite (Singer and Faeth 1967, Cook 1970). This process will be discussed in greater detail later.

Chalcocite has an indirect band gap of 1.2 eV and a second threshold for direct transitions at about 1.8 eV (Marshall and Mitra 1965). The optical absorption coefficient changes slowly with increasing photon energy up to 1.8 eV and then increases more rapidly. As a result, high energy photons with energies greater than 1.8 eV are absorbed close to the surface of the chalcocite when the cell is used in the conventional front wall mode. This leads to low conversion efficiencies for shorter

wavelength illumination since the electrons and holes are then created nearer to surface states which promotes rapid recombination. Some of the photons with energies between 1.2 eV and 2.4 eV will be allowed to pass into the intermediate layers between the cadmium sulphide and copper sulphide, and then modify the electro-optic properties of the device.

Chalcocite is a heavily degenerate p-type semiconductor which has a hole mobility of about 10 $cm^2\ V^{-1}\ sec^{-1}$ (Martinuzzi et al 1970). It shows appreciable ionic conduction at room temperature with a mobility of $\sim 3 \times 10^{-6}\ cm^2\ V^{-1}\ sec^{-1}$ due to the high diffusion rate of Cu^+ ions in chalcocite which increases with increasing temperature (Hirahara 1951). When chalcocite is heated in a vacuum, copper whiskers grow on the surface, but when the heating is done in air, the copper which migrates to the surface is oxidised to copper oxide (Cu_2O). This is an irreversible reaction. At the same time, the bulk undergoes a compositional change as follows:

$$Cu_2S \longrightarrow Cu_{1.96}S \longrightarrow Cu_{1.8}S$$

It is this reaction which is thought to be responsible for the degradation in the efficiency of the CdS solar cell.

The high mobility of the Cu^+ ions in chalcocite is thought to account for the high resistance of CdS solar cells to radiation damage. This is a similar principle to that exploited in silicon cells heavily doped with lithium.

The interface region between the n-type cadmium sulphide and p-type chalcocite is very important. This region of copper compensated cadmium sulphide is about 1 μm thick. By using radioactive tracer techniques, it has been shown (Clarke 1959, Woodbury 1965, Szeto and

Somorjai 1966) that the diffusion rate of copper in cadmium sulphide is anisotropic. From these investigations it was found that copper diffused more rapidly in a direction perpendicular to the 'c' axis than parallel to it. Purohit (1969) showed that the diffusion rate was much slower when the diffusion coefficient of copper in cadmium sulphide was measured using chalcocite as a source of Cu^+ ions. This would suggest that only a very long heat treatment would cause copper ions to penetrate to the substrate and so alter the shunt resistance dramatically.

The effects of successive periods of heat treatment in air and other ambients on both single crystal and thin film cells have been investigated and are described in this thesis.

2.6 Conclusions

At present, the CdS/Cu_2S heterojunction solar cell appears sufficiently promising to compete with other photovoltaic cells and has the following advantages.

(a) It is easy and potentially cheap to fabricate in thin film form (Clark et al 1971) and it may be possible to mass produce a sprayed powder solar cell (Vojdani et al 1973).

(b) The power to weight ratio of thin film devices is very good ($\sim$ 82 W Kgm^{-1}).

(c) The cell has a high resistance to radiation damage which is advantageous for space applications (Brucker et al 1966).

(d) It is flexible and easy to store in thin film form.

(e) The current-voltage characteristics display a large voltage and curve factor.

The main problem associated with the cells is the degradation which they suffer when subjected to long term simulated solar illumination. Not only does the cover plastic darken under ultra-violet irradiation, but there is a loss of power output which is due to a fundamental mechanism known as load effect degradation. This latter effect manifests itself when the cell is exposed to sunlight under open circuit or near open circuit conditions and can be minimised. The greatest problem at present is that the chemistry of the copper sulphides is not totally understood and neither is the way in which the copper/sulphur ratio changes with time and cell treatment.

CHAPTER 3

THE CdS SOLAR CELL

3.1 Brief history of CdS solar cell

The CdS solar cell was discovered by Reynolds et al (1954) who were studying the properties of various rectifying contacts on CdS. When copper contacts were employed and the devices were illuminated by an intense source of visible light, open circuit voltages of 400 mV and short circuit currents of 15 mA/cm^2 were obtained. It was also reported that there was an anomalous response to wavelengths greater than the band gap of CdS. Towards the end of 1954, 1% efficient single crystal cells of 0.5 cm^2 area were being fabricated. At about this time, there followed several years of research into the optoelectronic properties of doped and undoped CdS. A CdS cell in thin film form was first reported by Nadzhakov et al (1954). They used a thin film of CdS evaporated on to a comb-like structure on aluminium or gold which had previously been evaporated on to glass substrates. Relatively low photocurrents were observed. In retrospect it would appear that if they had investigated copper comb patterns, they might have obtained high photocurrents similar to those observed by Reynolds. Copper electrodes were later investigated by Fabricus (1962) and found to produce reasonable results. It is now fairly evident that the copper electrodes used by Reynolds and Fabricus led to the formation of a layer of copper sulphide when the device was heated and hence a copper sulphide/cadmium sulphide heterojunction had been produced.

In 1962, Shirland et al evaporated thin films of CdS on to conducting metal substrates of molybdenum. Flexible, plastic substrates which had been metallised were also under investigation at this time for possible future use in satellite arrays. The techniques of preparing

thin films on flexible metallised substrates, and the production of a layer of copper sulphide on top of them were well established by the mid 1960's. As a consequence of the high sheet resistance of the copper sulphide, the first thin film cells which were prepared had low efficiencies. A compromise had to be reached over this matter; if a small contact to the copper sulphide layer was made, the sheet resistance was high, whereas if a large contact was made, the sheet resistance was acceptable but a large area of the cell was masked from the incoming radiation. The problem was largely solved by bonding a gold plated copper grid to the copper sulphide. In this arrangement, the optical transmission was 80-90% and the sheet resistance was acceptable. Much other work was carried out during this early period on the subjects of array design and the relative merits of front and backwall illumination. Several authors discuss these modifications, see for instance Shirland (1966) and McMahan (1967).

The efficiency of the CdS solar cell has increased gradually over the past 10 years and the values quoted at various conferences are shown in Figure 3.1. In the late 1960's, various improvements were implemented. These were (1) protection from atmospheric humidity and (2) better stability of the cells against thermal cycling. Both of these criteria were satisfied by packaging the cells in between epoxy coated covers (Hietanen and Shirland 1967, Spakowski 1967, Bowman et al 1967). Evidence of the next degradation mechanism then emerged. This was called load effect degradation since its observation depended strongly upon the degree of circuit loading of the cell. This type of degradation was observed first by Spakowski and Forestieri (1968) and Stanley (1968). It occurs when cells are exposed to sunlight under open circuit or near open circuit conditions or when the cell output rises to a value greater

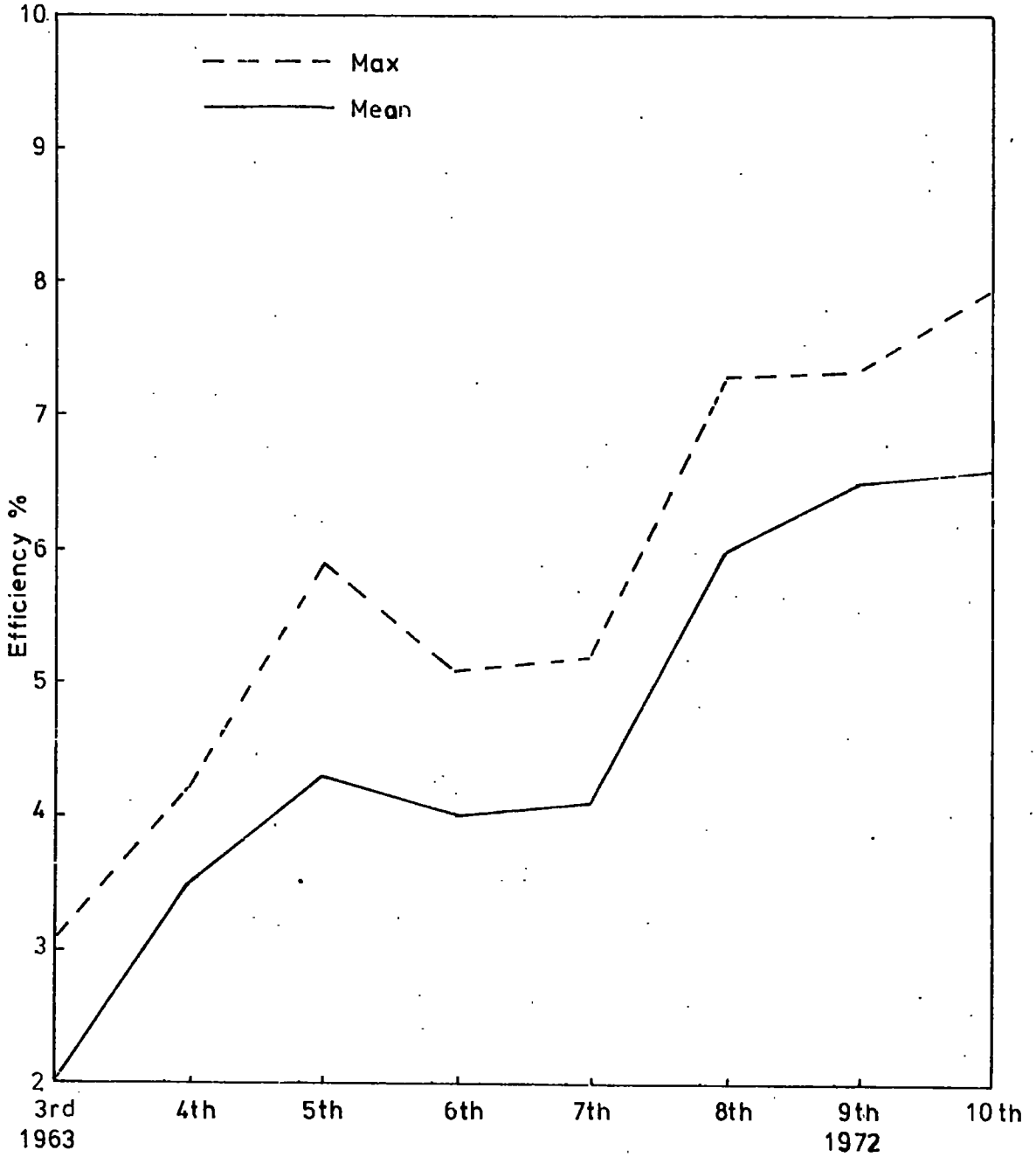

FIG. 3.1 PROGRESS IN CdS CELL EFFICIENCIES REPORTED AT PHOTOVOLTAIC SPECIALISTS CONFERENCES

than some threshold voltage. This was ascribed (Shiozawa et al 1969) to the fact that during formation of the copper sulphide layer, shorts of this material to the substrate are formed down cracks and grain boundaries in the cadmium sulphide film. Under the influence of the photovoltage which appears across these shorts, copper ions migrate through the copper sulphide to the metallized substrate and metallic copper is deposited along the path length until it reaches the top surface. Nodules of copper attached to the shorting whiskers of copper are often formed on the surface. The degradation associated with this electrolytic process was found to be reversible in the dark (Palz 1968). Thermodynamically it can be shown that a potential of 390 mV is required to dissociate Cu_2S into Cu and CuS. The whole sequence can be avoided by running the cell just below this threshold, at say 380 mV which is usually close to the maximum power point (see later). However several degradation mechanisms still remain, especially for sun orientated arrays when the surface temperature can rise to 60°C. It is these which are now being investigated. In recent photovoltaic conferences, improvements in both efficiency and stability of the cells have been reported (Bogus and Mattes 1972, Palz et al 1972, Mytton et al 1972, Palz et al 1974). These researchers, working independently, have identified the major problem as being associated with continuous oxidation of the copper sulphide. The reaction appears to be accelerated under illumination and increases with temperature. Palz et al (1972) reported no degradation at 60°C when cells were tested under high vacuum conditions (which would be experienced in space).

One method of reducing the rate of oxidation is to ensure exact stoichiometry in the copper sulphide layer especially if the cells are going to be used in ambients containing quite small amounts of oxygen.

It should also be emphasized that a stoichiometric copper sulphide phase produces a more efficient cell than a copper deficient one. Much of the work being done on CdS solar cells at the present is devoted to methods of measuring and controlling the stoichiometry of the copper sulphide present.

3.2 Alternative II-VI photovoltaic devices

During the time that progress was being made on CdS/Cu_2S solar cells, the possibility of using other heterojunctions was also being investigated. Reynolds' idea of a P-V effect at a rectifying junction using copper, aluminium or gold on CdS was developed by Bockermuehl (1961) and later by Bujatti and Muller (1965). Devices were fabricated by them in which the photovoltage was a linear function of light intensity. By evaporating CdS on to selenium, Kunioka and Sakai (1965) formed a photovoltaic cell with a spectral response close to that of the eye. Goryunova et al (1970) formed a thin film of Cu_2S on top of single crystals of $CdSnP_2$ and obtained photovoltages up to 200 mV. The following heterojunctions have also been investigated: CdS-SnS (Stoyanov et al 1971), Cu_2Te-CdTe (Cusano 1963), Cu_2S-CdSe (Otake et al 1972), CdS-PbS (Watanabe and Mita 1972) and CdS-InP (Wagner and Shay 1975). An efficiency of 6% was reported by Bonnet and Rabenhorst (1972) for a CdTe-CdS abrupt junction and efforts are being made to produce a graded junction between these two materials. However, the CdS/Cu_2S heterojunction is still thought to offer the best possibility for commercial applications although the recent work on InP-CdS devices, giving efficiencies of about 12%, is interesting.

3.3 Formation of a Photovoltage at a p-n Junction

Although the optimised CdS-Cu_2S solar cell is a p-i-n structure, it is easier in discussing the origin of the photovoltage to explain first how the P-V effect arises in a straightforward p-n homojunction. In the bulk material, of either p or n type, absorbed photons with suitable wavelength impart sufficient energy to raise electrons from the valence to the conduction band. The electrons and holes produced within a diffusion length of the junction, are swept to the n and p-type regions respectively (Figure 3.2) by the built-in electric field. This charge separation of the electrons and holes causes two effects:

(1) The p-type region charges positively and n type region charges negatively.

(2) A photogenerated current I_g flows across the junction. If there are no external connections between the n and p layers, the cell is in forward bias and a forward current I_f just balances out I_g. When the p and n regions are connected through an external load (Figure 3.3), a fraction of the photogenerated current flows through the load and the device acts as a solar energy converter.

3.4 Suggested Mechanisms at the CdS/Cu_2S Junction

Since the CdS solar cell was first reported in 1954, many models have been put forward to explain the experimental observations. In each model, account has to be taken of the particular method of construction used and such models have to explain the strong photovoltaic behaviour at the band edge of CdS and the importance of heat treatment in obtaining optimum cell performance and its effect on spectral response. Some of the many models put forward are mentioned below.

FIG. 3.2 THE PVE IN A p-n HOMOJUNCTION

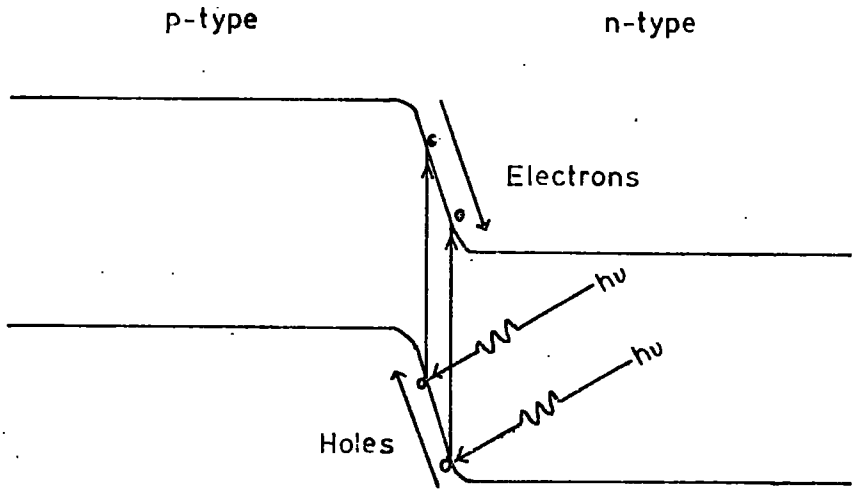

FIG. 3.3 SCHEMATIC DIAGRAM OF A p-n JUNCTION SOLAR CELL

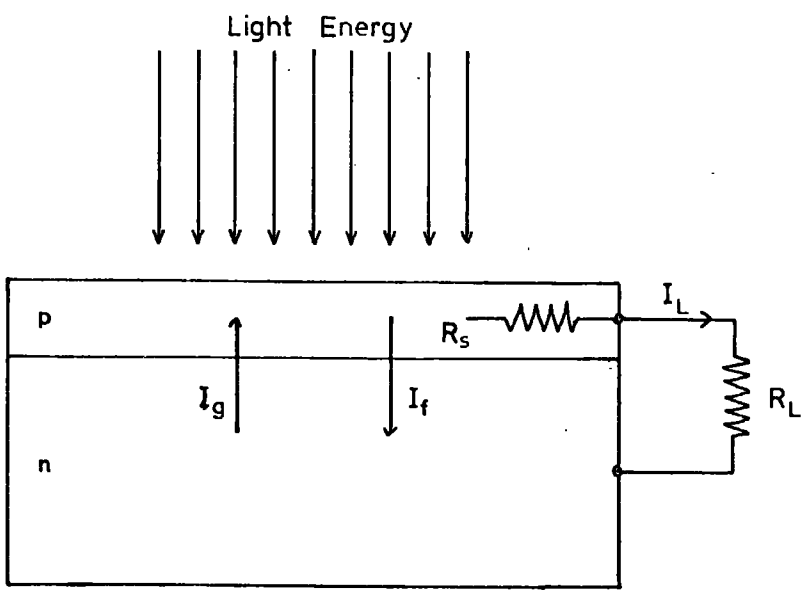

The first devices were formed by evaporating copper on to cadmium sulphide and Woods and Champion (1959) and Grimmeis and Memming (1962) explained the P.V.E. in photovoltaic cells on the basis of a p-n homojunction of cadmium sulphide, i.e. a p-type CdS formed by copper diffusion on an n-type CdS substrate. The existence of an impurity band in the forbidden gap was earlier postulated by Reynolds and Czyzak (1954). Later, Williams and Bube (1960) proposed that electrons are emitted photoelectrically from the copper layer into the cadmium sulphide and Bockenmuehl et al (1961) proposed a double junction model of copper on high resistivity copper doped cadmium sulphide on low resistivity cadmium sulphide.

Chamberlin and Skarman (1966) and Pavelots and Federous (1966) both proposed a straightforward heterojunction between the cadmium and copper sulphides. It was suggested by Balkanski and Chone (1966) that there is a very localised P.V.E. at interface states between p-type Cu_2S and n-type CdS which results in electrons being emitted from these states into the CdS. The authors further proposed that photon absorption by impurities in the CdS influences the long wavelength response of these types of cell.

The impurity P.V.E. at copper centres in CdS was attributed to the creation of additional minority carriers by electronic transitions from the valence band to these impurity levels (Duc Cuong and Blair 1966). Shitaya and Sato (1968) suggested further that the copper contact creates a surface barrier.

The P.V.E. has also been attributed to photoemission from the Cu_2S (Energy gap $\approx$ 1.2 eV) and an impurity P.V.E. (1.8 eV response) by Gill et al (1968). Massicot (1972) suggested that the spectral

sensitivity in the region of 1.8 eV is due to the formation of a thin layer of djurleite ($Cu_{1.96}S$).

In addition, electroluminescence observed in some CdS/Cu_2S heterojunction devices is thought to be caused by hole injection from the copper sulphide into the cadmium sulphide (Keating 1963).

Further models have been suggested by Potter and Schalla 1967 (Lewis model), Hill and Keramidas 1966 (Harshaw model), Shiozawa et al 1966 (Clevite model) and Van Aershodt et al 1968 (E.S.R.O. model). These models all contain certain common features but differ in the details of the way in which the potential energy is supposed to vary with distance from the CdS/Cu_2S interface. However, the Clevite model is currently accepted to be the most satisfactory since it has undergone gradual modification in the light of experimental evidence.

The experimental observations which must be explained by any model are that:

(1) There is a crossover of the current-voltage characteristics measured in the dark and under illumination with an apparent change in the barrier height.

(2) The low energy threshold of the photovoltaic response occurs at 1.2 eV, but a sharp dip in the spectral response of the photocurrent and photovoltage is observed when the device is irradiated by photon energies at 2.4 eV when the copper sulphide layer is thin.

(3) Various enhancement and quenching effects are produced when the cell is irradiated by an additional monochromatic source.

(4) The response time is slow, of the order of seconds or more, for heat-treated devices.

(5) There is a slow shift of points on the current-voltage characteristics curve during constant current or voltage measurements with the possible formation of copper nodules under or near open circuit voltage operation due to an electrodecomposition process.

(6) The squareness of the current-voltage characteristics improves after heating and the junction capacitance decreases as a function of heat treatment.

(7) Impurities such as indium when incorporated into the cadmium sulphide cause a shift in the enhancement spectrum towards longer wavelengths.

(8) The highest recorded open circuit voltage of a cell at 4.2 K under an illumination intensity of several times AmO is about 800 mV.

(9) Cells have a high resistance to radiation damage but degradation is rapid when a cell is heated to a temperature greater than 150°C.

3.5 The Clevite model for solar cell

It is possible, using the so-called Clevite model suggested by Shiozawa et al (1969), to explain most of these experimental observations. The energy band diagram is shown in Figure 3.4 for an optimised cell under both dark and illuminated short circuit conditions. The cell is regarded as a p-i-n heterojunction between degenerate p-type Cu_2S, copper compensated (intrinsic) CdS and n-type CdS. By varying the stoichiometry of the CdS layer, the carrier concentration can also be altered, but values in the range of 10^{16} to 10^{18} cm^{-3} are usually encountered. The model incorporates the following features.

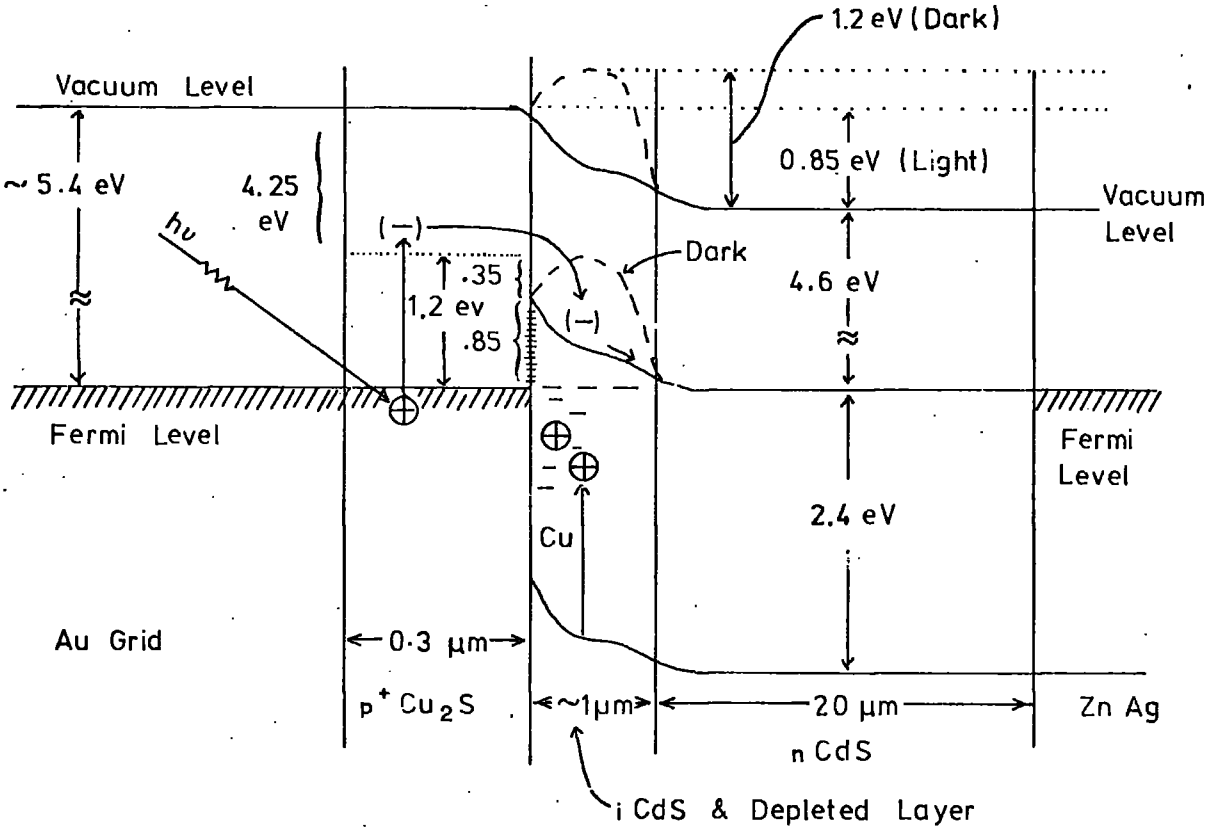

FIG. 3.4 ENERGY BAND DIAGRAM FOR Cu_2S-CdS SOLAR CELL UNDER ILLUMINATED SHORT CIRCUIT CONDITIONS ('CLEVITE MODEL')

(1) The gold grid makes an ohmic contact to the p-type Cu_2S, and the Zn/Ag substrate makes a good ohmic contact to n-CdS.

(2) Most of the photons are absorbed in the thin layer of Cu_2S. Thin films usually have a highly non-planar topology and this aids absorption.

(3) The copper compensated i-layer results from diffusion of copper into the CdS during fabrication and is relatively insulating in the dark whilst being relatively conducting under illuminated conditions. This layer is thus photoconductive and behaves like weakly n-type CdS under illumination.

(4) In the dark, the main junction occurs between the n-CdS and the i-CdS. Under these conditions, an electrostatic barrier height of 1.2 eV is encountered. There is, however, a small reverse junction between the p^+ Cu_2S and i-CdS with a barrier height of 0.35 eV. This disappears under illumination.

(5) Under illumination, the main p-v junction occurs between the Cu_2S and i-CdS, when the barrier height is 0.85 eV.

All of the photons with energies less than 1.2 eV pass straight through the Cu_2S, i-CdS and CdS layers without appreciable absorption. They are reflected, or absorbed in the metallic substrate. Since Cu_2S has an indirect band gap (Vlasenko and Kononets 1971), the absorption coefficient of photons with energies greater than 1.2 eV rises rather slowly with increasing photon energy. Photons with energies between 1.2 and 2.4 eV are absorbed mainly in the Cu_2S but since the copper sulphide layer is quite thin (0.3 μm), a small but significant number

of photons pass into the i-layer. These may be absorbed there and induce a substantial photoconductivity in the i-region.

Most of the electron-hole pairs are generated in the Cu_2S with the most energetic photons being absorbed close to the illuminated surface. Since the electrons are minority carriers in the p^+ Cu_2S, they must diffuse to the Cu_2S-CdS:Cu interface. Diffusion without recombination is aided by the apparently long minority carrier lifetime in Cu_2S (Shiozawa et al 1969). The electrons pass through the interface region and are collected into the n-CdS region where they become majority carriers. Eventually, the carriers are gathered by the ohmic contact. Assuming that the p and n sides are connected to an external load, the electrons flow round the circuit and annihilate the photogenerated holes at the ohmic gold contact.

This model explains quite well the cross-over of current-voltage curves measured in the dark and under illumination for heat treated cells. It also explains why the effective band gap of the 'CdS' cell is 1.2 eV which is quite close to the optimum band gap of $\sim$1.4 eV for solar energy conversion (Loferski 1956). The improved squareness of the current-voltage curves after heating can also be explained by the p-i-n structure. Tunnelling can occur in the abrupt p-n junction but after the heat treatment stages, the i layer would minimize these effects. Moreover, the formation of an i layer indicates high copper mobility which may account for the slow displacement of the current-voltage curves during constant current or voltage measurements. The high radiation resistance may also be associated with the high Cu^+ ion mobility.

A slightly different energy band diagram was suggested by Gill et al (1968). In their scheme the conduction band of CdS was placed 0.1 eV above the bottom of the Cu_2S band instead of 0.3 eV below

it. This gives rise to a narrow energy spike which would permit electrons to tunnel through it. With this model, the effective energy gap would be 1.2 eV which is much larger than the maximum observed O.C.V. at liquid helium temperatures. The feasibility of the argument depends on the width of the spike. Gill et al (1968) proposed that the net donor concentration was about 10^{17} cm^{-3}. This is probably too high for heat treated cells but could be reasonable for unheat-treated cells and the tunnelling effects observed would support this argument.

3.6 Equivalent circuit of CdS cell

In this following section, reference should be made to Figure 3.5. The constant current generator represents the optical generation of electron hole pairs in the copper sulphide layer. Current flow through the effective shunt diode represents that part of the photo-generated current which is lost due to recombination in the copper sulphide layer and at various interface states. An effective resistance R_d can be ascribed to the diode but it should be noted that it is a strongly non-linear function of the voltage appearing across it. R_d is the reciprocal of the differential slope of the true current-voltage curve of the Cu_2S-CdS:Cu junction. This latter curve is the one which would predominate in the dark if all other resistive elements were absent and if the barrier height remained constant. It is broadly the same as the current-voltage curve of the photovoltaic device measured at high light intensities with the origin displaced by the short circuit current. R_i is the resistance of the copper compensated layer and is approximately inversely proportional to the light intensity. R_{ser} is a combined resistance which corresponds to the Cu_2S layer, grid contact resistance, n-type CdS layer and metallic substrate. For most cells,

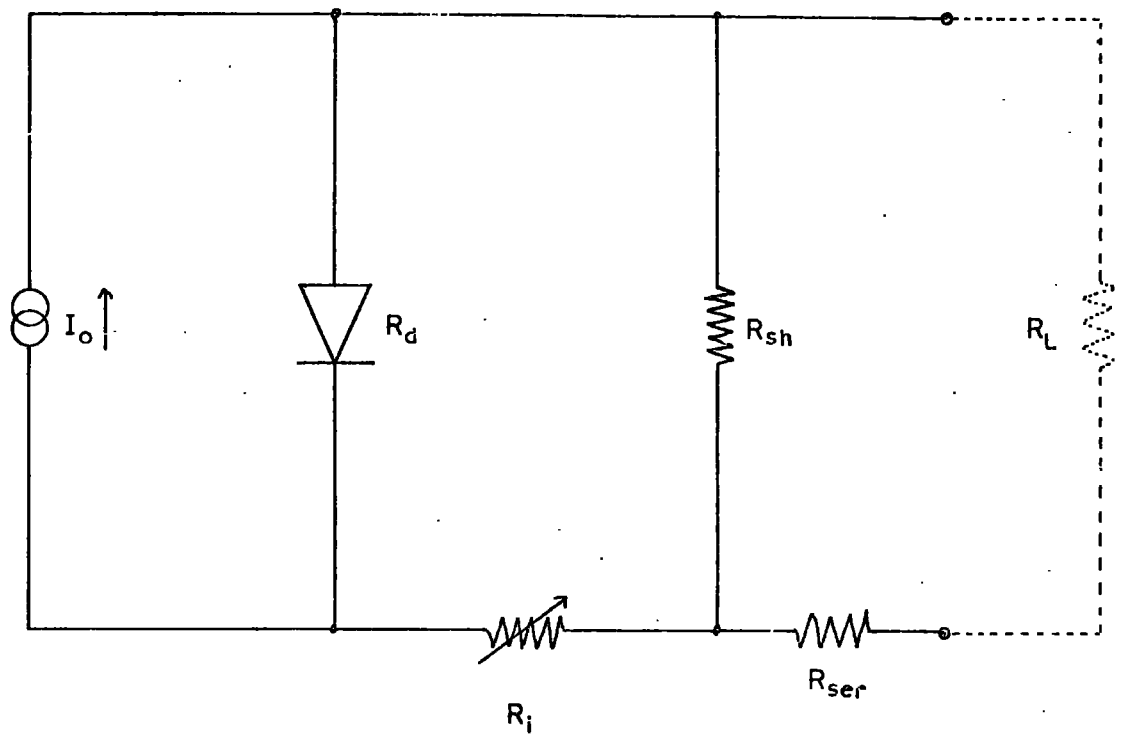

FIG. 3.5 CdS SOLAR CELL EQUIVALENT CIRCUIT

R_{ser} is small and may be neglected under certain conditions. R_{sh} is the lumped shunt resistance of the distributed shorting paths which occur between grid and substrate, copper sulphide layer and substrate and gold grid and substrate. For a particular cell at a specific stage of heat treatment, R_{sh} and R_{ser} are constant and not significantly dependent on wavelength. R_d depends on the voltage across it which in turn depends on the light intensity, hence R_d is indirectly dependent on the light intensity. In this model the junction capacitance has not been allowed for, so that this scheme cannot be used to explain transient effects.

3.7 Cell parameters

In this section, reference should be made to Figure 3.6. This diagram shows the current voltage curves measured with the cell in the dark and under illumination. The four main parameters which can be derived from this type of diagram are: (1) The open circuit voltage (O.C.V.) which is the voltage developed across the cell under no load conditions. This parameter can be measured directly with a very high input impedance voltmeter. It is typically of the order of 400 mV under fairly intense illumination. (2) The short circuit current (S.C.C.). This is the current which flows when the p and n regions are connected externally through a 'load' of zero resistance. This parameter may be measured using a very low impedance ammeter but may have to be measured using a low resistance connected in parallel with the cell so that it is then necessary to measure the voltage across this resistor. An alternative method of measuring short circuit currents using operational amplifier techniques has been developed here and will be discussed later in greater detail. At both the S.C.C. and O.C.V.

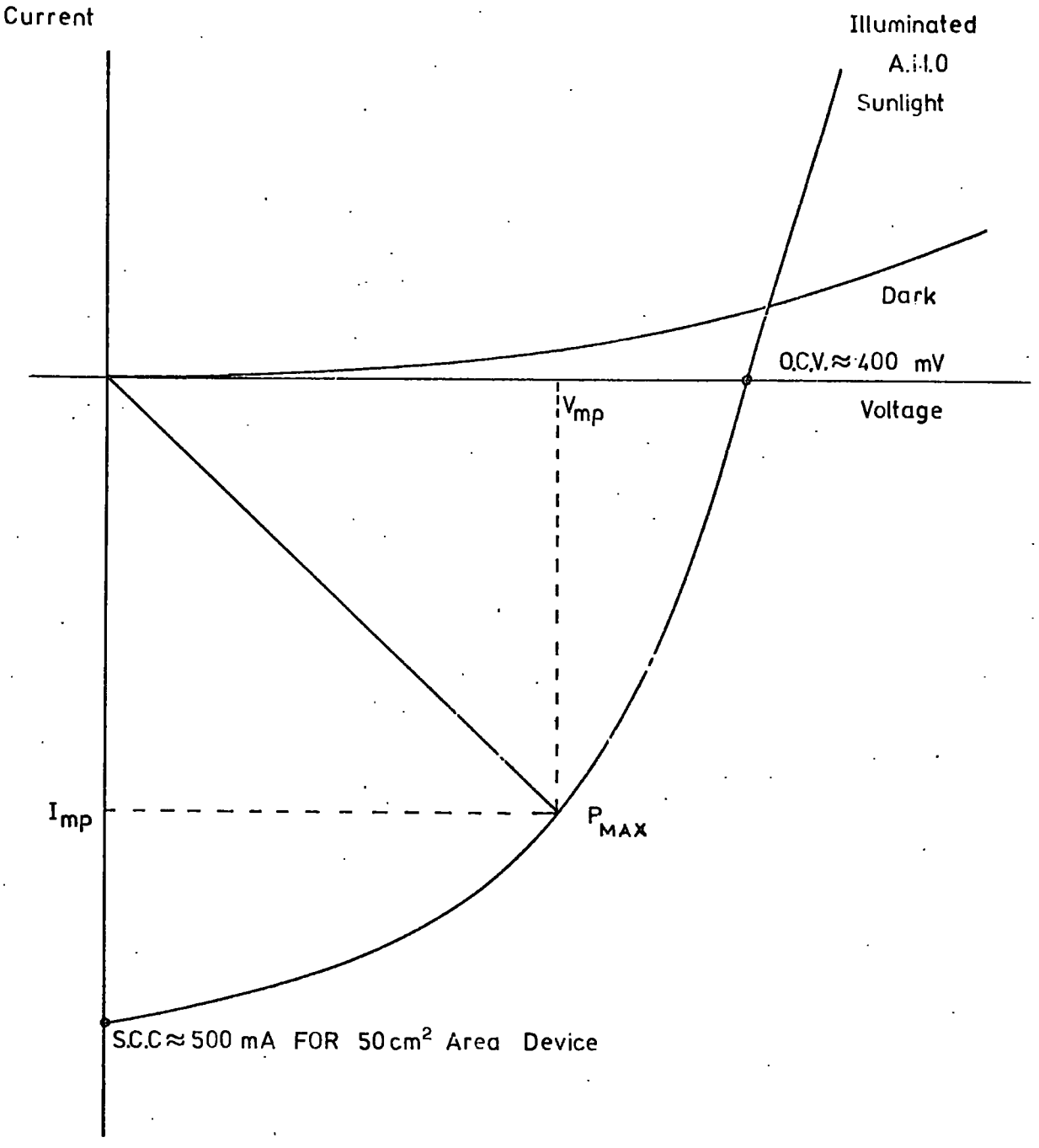

FIG. 3.6 I(V) FOR A LARGE AREA CdS SOLAR CELL

points, the output power obtainable from the cell is zero, but at a point intermediate between O.C.V. and S.C.C., there exists a maximum power point (M.P.P.). This point defines the third parameter. (3) Fill or curve factor (F.F. or C.F.). This is defined as the ratio of the area under the curve at the maximum power point to the product of O.C.V. and S.C.C. It is usually quoted as a percentage and is measured directly from the current-voltage curve. The parameter really defines the degree of squareness of the I(V) characteristics and is at best of the order of 60 to 70%. (4) The efficiency is perhaps the most important parameter. It depends on the series and shunt resistance present in the cell, the fraction of the incident light which passes through any cover and the grid and the percentage of this light which is absorbed with the useful generation of current carriers within a diffusion length of the collecting junction. The efficiency is defined as the ratio of power generated at the m.p.p. to the power of the light incident on the cell.

3.8 Calculation of parameters

Let P_{MAX} be the output power of the device, I_{mp} the current drawn from the device at the maximum power point and V_{mp} the voltage across the device at M.P.P.

Then $$P_{MAX} = I_{mp} \times V_{mp}$$

$$F.F. = \frac{P_{MAX}}{S.C.C. \times O.C.V.}$$

$$\text{Efficiency, } \eta = \frac{P_{MAX}}{P_{in}} \times 100\%$$

where P_{in} is the power of the light incident on the cell.

For the solar spectrum, there are two defined incident power densities. They are:

Air mass zero (A.M.O.) which is equivalent to 140 mW cm^{-2}

Air mass one (A.M.1) which is equivalent to 100 mW cm^{-2}

Using the equivalent circuit in Figure 3.5, it can be deduced for short circuit conditions, i.e. $R_L = 0$, that the short circuit current (I_{SC}) is given by

$$I_{SC} = I_o \left[\frac{R_d R_{sh}}{R_d (R_{ser} + R_{sh}) + R_{ser} R_{sh} + R_i (R_{ser} + R_{sh})} \right]$$

For most devices, $R_{ser} \ll R_{sh}$ so the expression reduces to

$$I_{SC} \approx I_o \left[\frac{R_d}{R_d + R_{ser} + R_i} \right]$$

Furthermore at low light intensities, $(R_{ser} + R_i) \ll R_d$

Hence

$$I_{SC} \approx I_o$$

where I_o is directly proportional to light intensity.

Similarly under open circuit conditions, i.e. $R_L = \infty$ and $I_{SC} = 0$, it can be shown that the open circuit voltage (V_{OC}) is given by:

$$V_{OC} = I_o \left[\frac{R_{sh} R_d}{R_d + R_{sh} + R_i} \right]$$

making a similar approximation for low light levels, i.e. $(R_i + R_{sh}) \ll R_d$, the expression reduces to

$$V_{OC} \approx I_o \cdot R_{sh}$$

Furthermore I_o is directly proportional to light intensity L_o and R_{sh} is a constant so at low light levels:

$$V_{OC} \propto I_{SC}$$

and O.C.V. spectral distributions of cells obtained using low intensity monochromatic radiation from the exit slit of a monochromator should have the same shape as the S.C.C. spectral response curves.

3.9 Optimisation of Parameters

3.9.1 Influence of cadmium sulphide

It is clearly important to reduce the series resistance associated with the i-CdS and n-CdS layers to a minimum and this may be done by reducing the resistivity of the n-type CdS layer to values less than 1000 Ω cm. With thin film cells, the shunt resistance is determined indirectly by the thickness of the CdS layer since the Cu_2S is formed down grain boundaries during plating and will therefore reach the substrate more readily in thinner samples. This criterion explains why the CdS must be at least 15 to 20 μm thick so that the shunt resistance is greater than 100 Ω for a 50 cm^2 cell. Shunt resistances less than 100 Ω lead to reductions in efficiency and fill factor. However in the interests of power to weight ratio for space applications, the layers of CdS must not be too thick in view of the high density of CdS of about 4.8 gm/cc.

The structure of the thin films also plays a significant part. Films with crystallites of diameter 1 to 3 μm are required. They should be of a long needle shape with a high degree of orientation with the crystallographic 'c' axis perpendicular to the substrate. Preferential

etching at the grain boundaries occurs when such films are etched in a K.I. solution. This produces a large surface area but etching must be controlled to keep the shunt resistance high. When the films are dipped in a hot solution of Cu^+ ions, the Cu_2S layer is formed all over the exposed surface including part of the way down the grain boundaries and so a relatively large amount of light is absorbed. This feature is essential for high efficiency devices and explains why the short circuit current and efficiency of single crystal devices is less than for thin film ones.

3.9.2 Cu_2S layer influence

It has been found possible to reduce the series resistance of the Cu_2S contact to about 30 mΩ by using a gold grid which allows 90 - 95% optical transmission (Clark et al 1971). This Cu_2S layer which is approximately 0.3 μm thick is formed in a chemical exchange reaction by immersing the CdS in a bath of copper ions at 90°C after the pH value has been set at 2.5. Although precautions are taken to ensure that the solution contains only cuprous ions, some cupric ions do co-exist in the solution and there is a possibility of forming Cu_xS where $1 < x < 2$. Normally x is very close to 2, but in view of the exceedingly complex phase diagram of the Cu-S system, a very small change in x can result in a large change in the properties of the copper sulphide layer. Rickert and Mathieu (1969) have shown that it is possible to control the stoichiometry by applying a potential to the CdS/Cu_2S as it is being formed.

The actual stoichiometry of the copper sulphide controls several parameters. It is known that the heterojunction between the

chalcocite (Cu_2S) phase and CdS produces the most efficient CdS/Cu_xS devices (Nakayama et al 1971). The open circuit region and short circuit current depend strongly on the stoichiometry of the copper sulphide (Palz et al 1972). The higher the O.C.V. and S.C.C., the higher is the maximum power output provided that the fill factor is not adversely affected. The sheet resistance of Cu_2S is higher than for other phases (Palz 1972, Ellis 1967) and consequently the series resistance is higher than for lower phase Cu_xS cells. This disadvantage is compensated by the increased overall efficiency of Cu_2S/CdS cells and two other factors associated with stability. These are:

(1) The threshold potential at which the Cu_xS dissociates to form copper nodules increases as $x \longrightarrow 2$. The rate of deposition of copper is proportional to the deficiency δ in the formula $Cu_{2-\delta}S$ (Mytton 1972). Hence a more stoichiometric copper sulphide leads to a higher threshold potential and a slower rate of degradation when the cell is operated above this point.

(2) It is known that degradation under illumination is accelerated at 60°C and above due to oxidation of Cu_2S. Palz (1972) and Bogus and Mattes (1972) have shown that the rate of degradation is slower for more nearly stoichiometric layers. It is therefore essential that the physical and chemical properties of the copper sulphides be investigated so that a means of producing a stable, stoichiometric form of Cu_2S is found. The Cu_2S should not be affected by the fabrication process. The target is to produce CdS/Cu_2S solar cells with lifetimes of five years or more and conversion efficiencies of 6-7%. This can only be achieved by a better understanding of the processes involved in the fabrication and production of such devices.

3.10 Conclusion

Over the last two decades, many models have been put forward to explain the operation of the CdS photovoltaic cell. However, the Clevite model, which was discussed earlier in this chapter, appears to explain most of the optoelectronic properties of this type of cell.

The Clevite model emphasizes the properties of the cadmium sulphide side of the heterojunction and attributes the changes in spectral response and efficiency of a cell during optimisation heat treatments to the formation of a photoconductive copper compensated i-layer between the cadmium sulphide and the chalcocite.

More recently, attention has been increasingly focused on changes which may occur on the copper sulphide side of the junction during fabrication and subsequent operation. For example, changes in efficiency and spectral response are now thought to be due to oxidation of the chalcocite or a copper deficient phase.

It can be seen from the equivalent circuit of the photovoltaic cell which was described earlier that the properties of a cell are influenced by the series and shunt resistances as well as by a light dependent resistance which may be present. The work in this thesis partly concerns the effect of varying the resistivity and dopants of the cadmium sulphide base material. However the principal objective was to discover if the changes in spectral response and O.C.V. during heat treatment are due mainly to the formation of the i-layer or the oxidation of the copper sulphide.

CHAPTER 4

CdS THIN FILMS

4.1 Introduction

Most of the recent developments reported at the 9th and 10th Photovoltaic Specialists Conferences have been centred around solar cells fabricated on flexible thin film bases. These types of solar cell produce high current densities and have higher power to weight ratios than devices formed on single crystal material. However, interest has been awakened in cells produced on powdered layers of CdS, but the relevant work is in the early development stage.

Thin films of II-VI compounds have been investigated extensively in recent years because of the demand for smaller and lighter photo-detectors etc. Much work has been carried out on ZnS thin films in the past, but for the applications envisaged at that time a high degree of crystallinity was not required. However, modern developments have led to an increasing interest in the crystalline structure of thin films and many applications require that their physical properties are as close to those of the bulk material as possible. Films of II-VI compounds in general and CdS in particular, have been used as: (1) ultrasonic transducers (Curtis 1969), (2) photoresistors, (3) phosphors, (4) electroluminescent layers (Andrews and Haden 1969), (5) evaporated triodes and diodes (Dresner and Shallcross 1962), (6) heterojunction diodes (Aven and Cook 1961) and (7) insulated gate thin film transistors (Haering 1964).

Some of the techniques of fabricating thin films of II-VI compounds are reviewed in this chapter with special reference to CdS.

4.2 Preparation of Thin Films

The particular method used to produce a thin film can have a strong influence on its optoelectronic properties and devices for different applications may require different methods of production. Relatively crude techniques may be adequate for applications in which a polycrystalline structure is acceptable, but it is necessary to resort to more elaborate methods if a single crystal film or even just a highly orientated film is required. Reviews of various growth methods in common use are given in the books by Anderson (1966) and Chopra (1969). Some of the methods successfully used for the production of CdS thin layers are described below.

(a) Sintered randomly orientated layers of CdS in powder form were prepared by Thomsen and Bube (1955), Kitamura (1960) and Micheletti and Mark (1968). Dopants such as chlorine and copper were sometimes used to increase the photosensitivity of the layers. Chockalingham (1970) produced photoconductive devices with a spectral response extending from 0.63 to 1.12 μm. Nakayama (1969) reported a 6 - 9% efficient CdS solar cell based on a ceramic substrate. This mode of fabrication could be used to produce cheap but heavy devices. Their low power to weight ratio would make them useless for space applications, but suitable for terrestrial applications.

(b) By using a chemical spray technique, Micheletti and Mark (1967) were able to prepare CdS layers 3000 to 5000 Å thick. In order to achieve this, cadmium chloride and thiourea in aqueous solution were sprayed on to a heated ceramic substrate. The cadmium chloride and thiourea were decomposed by further heating and subsequently formed a polycrystalline layer of CdS. The other components escaped in vapour form, but there

was a strong possibility of chlorine contamination of the film. Imaoka (1972) concluded that the orientation and Hall mobility of such layers depended on the actual chemicals used.

Chamberlin and Skarman (1966a,b) also employed a chemical spray technique to form a CdS/Cu_2S photovoltaic junction which produced an O.C.V. of 1.04 V and a S.C.C. of 2 mA/cm^2 when illuminated by 100 mW/cm^2 of visible radiation. Lawrance (1959) studied similar layers for photoconductive applications. In his technique, the cadmium chloride was decomposed in the presence of hydrogen sulphide. Marchenko et al (1970) prepared films in this way and fabricated them into solar cells. However in all of these methods, there are many problems associated with contamination.

(c) Vapour phase epitaxy as used for silicon and III-V compound devices has been used to grow films of II-VI compounds on single crystal substrates. The vapours of the constituent elements are allowed to react and form a film on the heated crystalline substrates. By using this method, Ratcheva et al (1972) produced films of CdS 1 - 2 μm in thickness. Heyraud and Capella (1968) also produced films 15 to 25 μm thick in much the same way on substrates such as the alkali halides or Muscovite (mica). They reported that the photoelectronic properties of such films were comparable to those of the bulk material. Unfortunately although the method produced high quality films, it was not practicable for deposition on large area amorphous substrates.

(d) Present thick film technology based on silk screen printing is mainly concerned with the selective deposition of conductors and insulators. Much work has been done on semiconducting "inks", but very little of it has been reported. Silk screening techniques using CdS ink

for fabricating field effect transistors (Witt et al, 1966) and large area photoconductive cells (Nicoll and Kazan, 1955) have however been reported. Progress in this area is held back since the composition of the semiconducting inks are industrial secrets and the bonding of conductive material to glassy or ceramic substrates is not fully understood. However, Vojdani et al (1973a,1973b) have succeeded in printing a CdS ink on to a ceramic substrate to produce a 20 μm thick CdS layer. A heterojunction between CdS/Cu_2S was formed by dipping the layer in a hot acidified copper chloride solution. A solar cell with an O.C.V. of 460 mV and an S.C.C. of 22 μ_A was produced. This achievement is of great importance since ultimately silk screening techniques offer the advantage of simplified fabrication. Moreover, this process is not expensive in terms of energy.

(e) The firmly established process for producing both thin and thick films of CdS is that of vacuum evaporation. The major consideration in such methods is the choice of supplying energy to the source such that the vapour is able to condense on a substrate to form the film.

Vacuum sputtering methods utilize several different electrode and source arrangements. During sputtering, the target surface, i.e. the cathode, is bombarded by energetic ions which leads to the ejection of surface atoms. These ejected atoms are then condensed in a similar way to thermally evaporated ones. R.f. sputtering has been used to produce CdS layers as well as argon ion sputtering (Comas and Cooper 1966). Honda et al, 1972, have formed stoichiometric layers with excellent photoconductive properties using the latter method. Reactive sputtering of Cd in H_2S (Durand 1972, Lakshmanen and Mitchell 1963)

has been used to form photoconducting layers. This type of process, however, is difficult to control and the high electric fields present can affect the structure of the film.

Thermal evaporation of CdS on CdS and an excess of either Cd or S has been the most popular technique for production of CdS films (Nelson 1955, Wendland 1962 and Bleha 1969). A modified vacuum furnace has also been used (Bujatti 1968) to grow CdS thin films. Well orientated layers of high resistivity CdS have been produced by controlling the temperature gradient at the substrate. Tyagi (1971) sublimed CdS from a single or polycrystalline slice of starting material on to a closely spaced sapphire substrate. The close spacing of source and substrate meant that only a small temperature difference existed between them and hence the evaporation proceeded under equilibrium conditions to give a large grain size stoichiometric film. This particular method has two main advantages. These are:

(1) It is economical since material is only deposited where it is needed.

(2) At a given temperature, it produces a higher deposition rate than other methods.

The main disadvantage is that although this method may be used successfully to produce integrated circuits, it cannot easily be used to deposit films on large area amorphous substrates.

Co-evaporation of CdS and S has been carried out by Pizzorello (1964) and Suzanne and Male (1971) in order to ensure that the resultant film is stoichiometric. Similar co-evaporation of Cd and S has been carried out by de Klerk and Kelly (1965) and King (1969). This type of

process seems a complex way of controlling the film properties since the stoichiometry may be determined by the substrate temperature and the source evaporation rate (Dresner and Shallcross 1962, Sakai and Okimura 1964). It is of note, however, that co-evaporation can yield films with very high resistivities $\approx 10^{10}$ Ω cm.

In order to obtain reproducible results, it is beneficial to reduce the number of variables involved in the evaporation of CdS by supplying energy in one of the following forms, i.e. laser beam, R.F. field, electron beam, thermal radiation or electrical conduction in a resistively heated filament. Most workers in this field, in common with ourselves, use resistively heated or electron beam bombarded sources in vacua approaching 10^{-6} torr.

In theory, an ultra high vacuum of better than 10^{-8} torr is the only environment in which to prepare and investigate thin films in order to ensure a low impurity content. Commercially this is impossible to achieve because of the expense and the long duty cycles of U.H.V. systems. It would be of greater commercial use if reproducible films could be produced in normal high vacuum ($\approx 10^{-6}$ torr) systems. Furthermore it would be better if evaporation techniques could be discarded altogether in favour of sprayed or silk screen printed methods, but these techniques are still at an early stage of investigation at the moment.

4.3 Properties of CdS thin Films

The first researchers in this field did not realise the importance of controlling as many parameters as possible during the growth of a thin film. One of the main problems was that the source material was of dubious and variable quality and post deposition

treatments were necessary to 'activate' the films. The most common impurities were chlorine and various metals (Nelson 1955).

Veith (1950), Aitchson (1951) and Bramley (1955), who investigated the photosensitivity of evaporated CdS layers, demonstrated the importance of controlling the pressure, substrate temperature and impurity content. It is now realised that equally important are parameters such as the evaporation rate, source temperature, film thickness, together with the composition of the residual gas in the vacuum chamber and the surface finish and properties of the substrate. (Shalimova et al 1964, Thomas et al 1970 and Kitada et al 1972). The film structure may however be modified by post evaporation heat treatment to override some of the constraints introduced by these parameters.

When CdS films are deposited in a beam which is perpendicular to a heated substrate, they take the hexagonal wurtzite structure with a fibre axis orientation of microcrystallites. The films are polycrystalline with the individual c axes roughly aligned perpendicular to the substrate surface (Rozgonyi and Foster 1967, Shallcross 1967). However with films deposited with the beam incident obliquely on the substrate, the c axes of the crystallites tend to align themselves parallel to the vapour beam (Foster 1967). The effect may be enhanced by increasing the deposition rate (Fukunishi and Niizeki 1969) and is employed in making CdS ultrasonic transducers. The crystallite size is a function of both film thickness and deposition rate and may be several microns across for a 20 μm thick film (Addiss 1963, Shallcross 1967, Berger et al 1968).

The substrate temperature has a considerable influence on the structure of a film since at low temperature, i.e. below 150°C, the cubic sphalerite modification predominates. Film stoichiometry

is determined by the substrate temperature and it manifests itself in the colour of the film. CdS deposited on to a substrate at room temperature is quite black in colour since it contains so much excess cadmium. As the substrate temperature is increased above 150°C, the film becomes orange in colour and then changes to yellow above 250°C. The structure therefore is predominantly hexagonal wurtzite (Bujatti 1967,1968, Galkin et al 1968). As the substrate temperature is increased beyond 400°C, re-evaporation from the substrate occurs and it becomes difficult to form a deposit (Wendland 1962). Any deposit which does form is yellow in colour.

In order to produce reproducible films, attention has to be paid to the surface finish and cleanliness of the substrate. This is especially important with single crystals where freshly cleaved surfaces often provide the best substrates. Under these conditions it is possible to grow epitaxial cubic or hexagonal CdS layers depending upon the evaporating conditions and substrate temperature (Holloway and Wilkes 1968, Wilcox and Holt 1969). If the vacuum system is relatively uncontaminated, a better vacuum is produced and the epitaxial limits are less constrained. This leads to films with a lower defect content (Holt and Wilcox 1971). Chopra and Khan 1967, produced both cubic and hexagonal CdS films on mica and rock salt substrates by altering the film thickness and the substrate temperatures.

The dark resistivity of polycrystalline CdS films changes with the deposition conditions but there are conflicting reports on the variation of dark resistivity with substrate temperature and evaporation rate. It is however generally accepted that the resistivity increases with increasing substrate temperature, but decreases with increasing

evaporation rate. Variations in the dark resistivity as a function of film thickness has also been reported by Bleha et al (1969), Wilson and Woods (1973) and Buckley and Woods (1973). The photosensitivity changes in the predicted manner; the higher the resistivity, the higher is the photosensitivity (Shalimova et al 1961).

Another important parameter, the electrical Hall mobility μH, is also affected by the deposition conditions which determine the crystal structure. The mobility is lower for polycrystalline films than for single crystal ones, but much lower than for bulk CdS. Typical values of about 10 $cm^2 V^{-1} sec^{-1}$ (Mankarious 1964) have been observed and can be shown to be consistent with the Petritz model (1956) which was first demonstrated for polycrystalline films of PbS, PbSe and PbTe. According to this model the carriers are scattered and trapped by the intercrystalline boundaries and hence μ_H is an exponential function of temperature and barrier height according to the following equation.

$$\mu_H = \mu_o \exp(-\Delta\varepsilon/kT) \qquad \text{(Berger 1961)}$$

However ionized impurity scattering leads to a variation of μ as $T^{3/2}$ and the two mechanisms are difficult to distinguish experimentally (Shallcross 1967). Many workers however favour the Petritz intercrystalline barrier model (Shallcross 1966, Neugebauer 1968) since the existence of intercrystalline barriers is supported by measurements of the drift mobility in CdS films (Waxman et al 1965).

Photoluminescent effects have been observed in normally evaporated CdS films (Bleha and Peacock 1970) and also in thin films evaporated in an enclosed vacuum system (Buckley and Woods 1973).

It has been reported that post deposition heat treatment in

a variety of gas ambients including vacuum, air, H_2S and Ar (Berger et al 1964, Sakai and Okimura 1964 and Esbitt 1965) can increase or decrease the dark resistivity depending on the substrate temperature used during the initial preparation (Wendland 1962). These effects may be explained by (1) substantial recrystallisation, or (2) reaction with oxygen which is known to change the photosensitivity of CdS (Kuwabara 1954).

The recrystallisation phenomenon which is observed when CdS films are heated in contact with a thin metal layer has been investigated by many workers. Addiss (1963) increased the Hall mobility of films from values near 1 to between 20 and 70 $cm^2\ V^{-1}\ sec^2$ (cf the bulk value of 250) by evaporating a thin layer of silver on CdS and then annealing it in an inert atmosphere at 500°C to 600°C. Similar experiments have been carried out more recently by Kahle and Berger (1970). The activation and re-crystallisation of evaporated layers of II-VI compound layers has been reviewed by Vecht (1966).

4.4 Conclusion

Much work on CdS thin films has been published because of their numerous applications. However many of the early results are conflicting because of lack of control over the parameters during evaporation. Absolute cleanliness of the evaporating system and source material is essential. By controlling the evaporation rate and substrate temperature it is possible to produce films with low resistivity ($\sim 10^3\ \Omega$ cm) and of a thickness ($\approx 20\ \mu$m) suitable for the fabrication of thin film photovoltaic devices. The following chapter gives a description of the apparatus used to produce such films for use in fabricating thin film CdS/Cu_2S photovoltaic cells.

CHAPTER 5

PREPARATION OF CdS THIN FILMS

5.1 Vacuum Systems

Figure 5.1 is a schematic diagram of the vacuum system used when films were evaporated from the resistively heated source. This arrangement was used for the deposition of most of the thin films produced at Durham which were later fabricated into solar cells. The pressure in the bell jar was measured with a thermocouple gauge (A.E.I. type V.C.12) for pressures above 10^{-2} torr and a Penning gauge (Edwards Speedivac Type 5A) for pressures in the range 10^{-2} to 10^{-5} torr. The lowest pressure obtainable from this sytem used Silicone 705 pump oil in the 3" diffusion pump and either liquid air or nitrogen in the cold trap was better than 10^{-5} torr. However, most of the evaporations were carried out at pressures of about 2×10^{-5} torr.

A large system using Edwards components and an electron beam evaporator unit was used for a few evaporations, but the high quality films produced were generally too thin for fabrication into solar cells.

A third system manufactured by G.V.C. was used at I.R.D. Ltd. This system had an 18" diameter bell-jar and incorporated an oil diffusion pump and cold trap. The system was controlled by an automatic valve sequence switching unit. Within 30 minutes of the system being started up, a vacuum of about 10^{-7} torr could be obtained. A Sloan deposition control meter (type OMN I 11) was installed to monitor both film thickness and deposition rate. The complete evaporation cycle could be controlled by means of an oscillating crystal detector and relays.

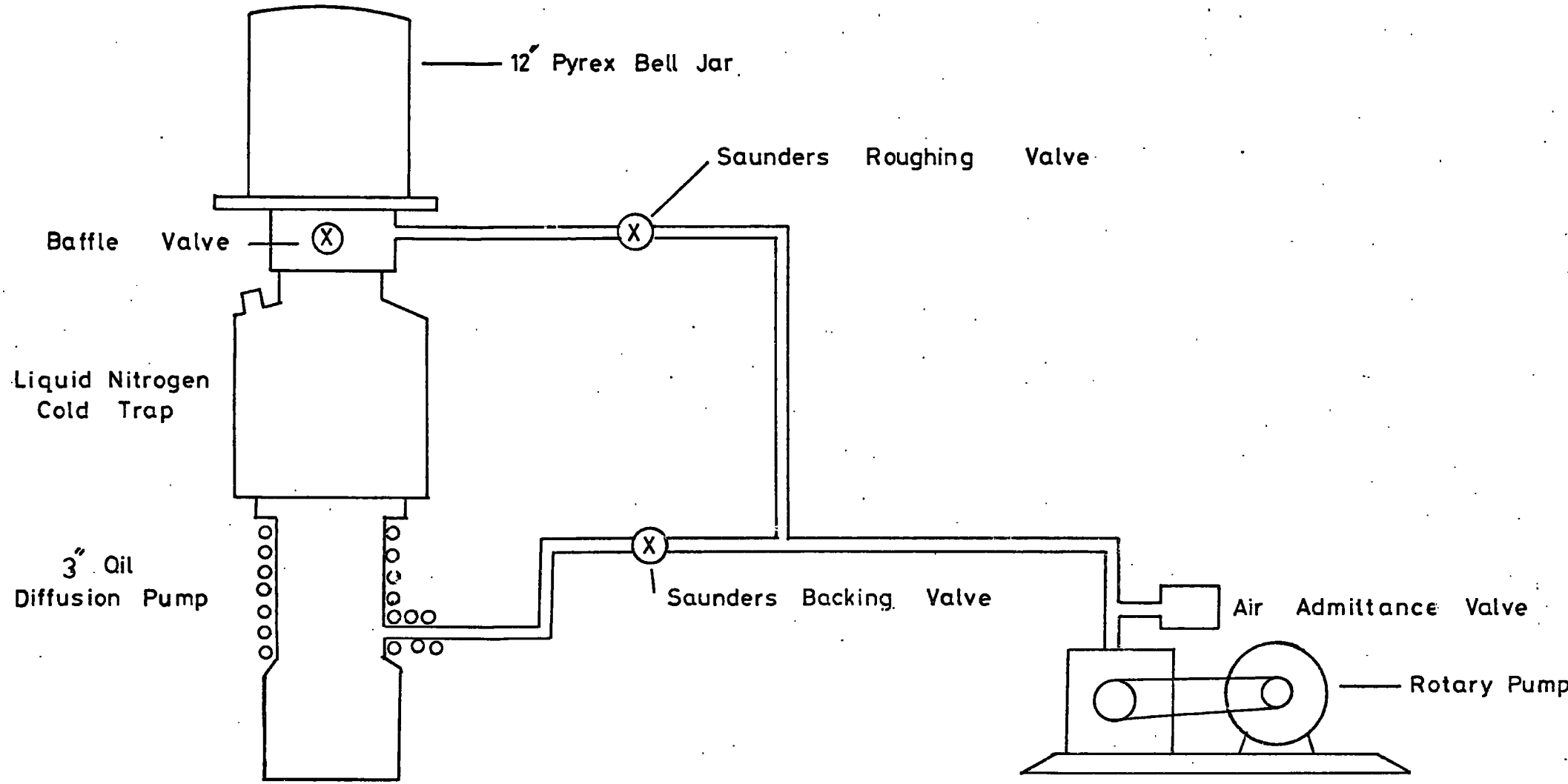

Fig 5.1

Schematic Diagram Of Pumps And Valves Of 12" Evaporator

5.2 Vacuum Chamber Fixtures

Figure 5.2 shows the arrangement of fittings in the bell jar of the 3" pump system used for the resistively heated source. Several shapes of silica crucible were employed but a simple straight sided type is shown in the diagram. The crucibles were wound spirally with molybdenum wire. This filament was prepared in the following way: two strands of 0.5 mm diameter molybdenum wire were twisted together, one end being clamped in a vice and the other in the chuck of a hand-drill. This technique produced a two strand twisted filament which was less prone to deform at high temperatures so that the possibility of shorting between turns was reduced. Tungsten wire was also used but generally proved unsatisfactory. The filament was of sufficiently low resistivity (at the evaporation temperature used) to enable all of the 900 V.A. (30 V, 30 A) available from the transformer to be dissipated if necessary. A high evaporation rate of several thousand Å/minute could be obtained in this system. The substrate and mask were clamped to a stainless steel block containing an insulated tungsten heating element supplied by a 12 V 20 A transformer. The substrate temperature was controlled by an ether 'mini' controller with a NiCr/NiAl thermocouple clamped to the substrate surface.

The volume between the source and the substrate was surrounded by an 8.5 cm I/D pyrex cylinder which was usually heated by radiation from the source. However, a cylindrically wound heater was made to fit round this "hot wall" chimney for use during some of the evaporations. The heater was wound from Kanthal resistance wire and was supplied by a 12 V 20 A transformer unit. The glass chimney was included in the system in an attempt to retain both components of the vapour in the vicinity of the substrate, and to increase the stoichiometry of the resulting

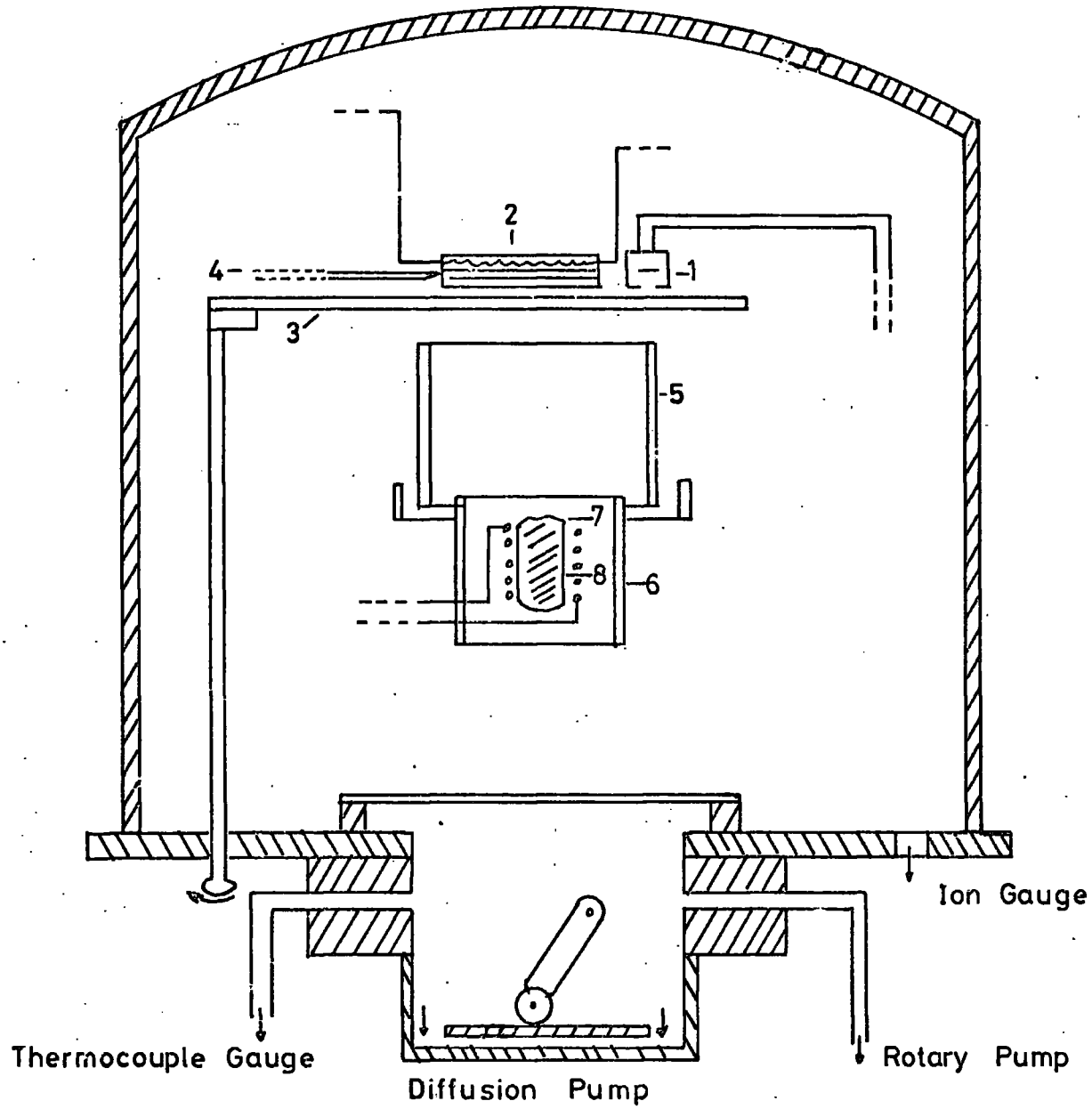

1. Deposit Thickness Monitor
2. Substrate Heater, Subsrate and Copper Mask
3. Shutter
4. Thermocouple
5. Silica Cylinder
6. Mo Radiation Shield
7. Silica Crucible and Molybdenum Heater
8. Charge and Quartz Wool Baffle

Fig. 5.2

Bell Jar Fixtures - Resistively Heated System

films by preventing preferential condensation of one of the components on the cold walls of the bell jar.

A stainless steel shutter operated through a rotary seal was positioned immediately below the substrate so that the source could be outgassed before evaporation on to the substrate began.

Facilities for evaporation from conventional molybdenum boats and baskets were also available inside the bell jar, but they were only used for the preparation of conducting films of gold on chromium on glass.

5.3 The I.R.D. System

The source in the I.R.D. Ltd. evaporation system is shown in Figure 5.3. This was a directly heated tantalum crucible which contained 40 gms of powder when full. Evaporation rates faster than 1 μm/minute were obtained and it was possible for layers of CdS 25 μm thick to be deposited on substrates up to approximately 8 x 8 cm in area. A silica "hot wall" chimney was also used with the source and substrate 36 cm apart and a shutter and radiant heater were incorporated in the chamber.

5.4 Source Material

Commercially produced CdS (B.D.H. Optran grade polycrystalline lump) was purified by sublimation in a manner similar to that described by Stanley (1956). The 60 gm charge was heated to 1150°C in a long silica tube and a stream of 0.2 ℓ min^{-1} of argon was passed over it. Rods and platelets of yellow crystalline CdS were deposited downstream in a cooler part of the tube. Mass spectroscopic analysis of the starting material showed that the major impurities present were Se, Zn,

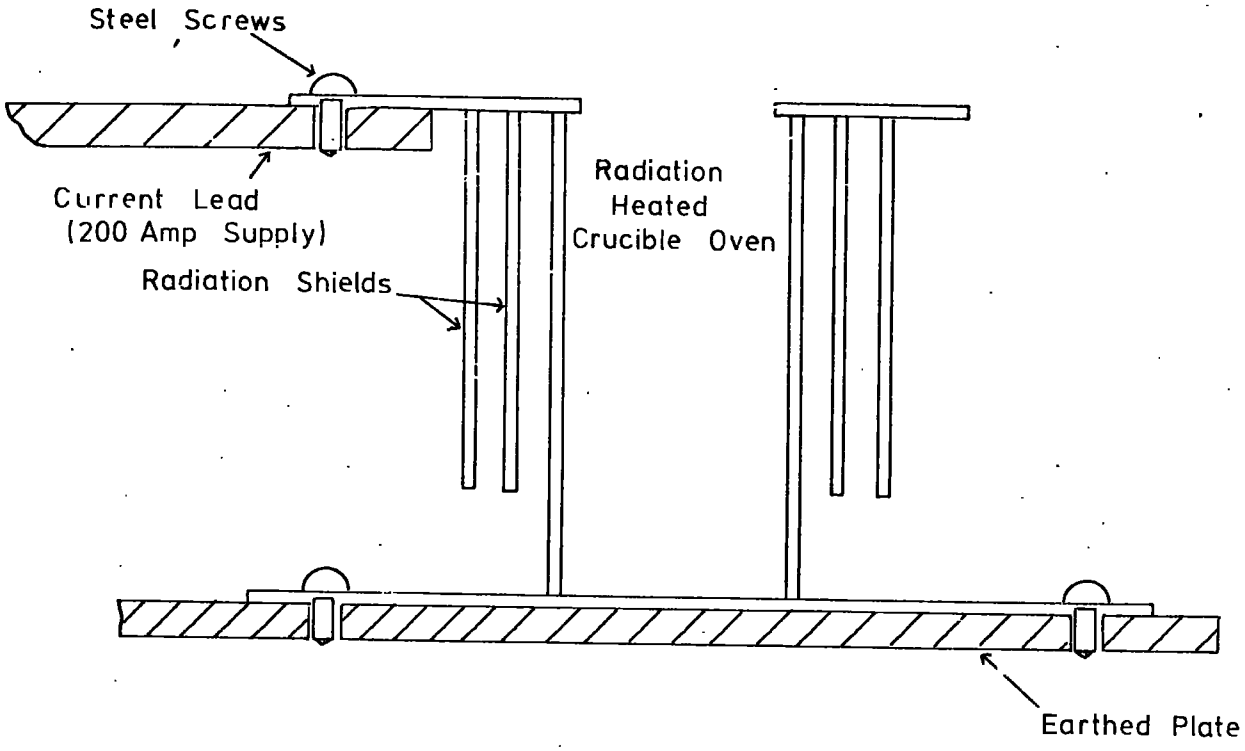

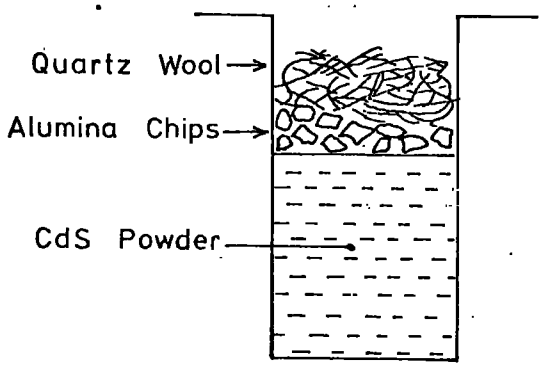

TANTALUM CRUCIBLE

FIG. 5.3
TANTALUM RADIATION-HEATED EVAPORATION SOURCE

Fe, Mn and Si, but only in quantities less than 2 p.p.m. After flow run purification, some of the selenium would be carried to exhaust by the argon and some of the less volatile Zn, Fe and Mn would be left in the charge as the 'heavy' residue. However the Si content would probably increase because of the silica glassware used. The sublimed CdS produced in this so called 'flow run' process was then crushed into fine powder and used as the source material for the evaporations carried out at Durham. The I.R.D. evaporation sources were filled with CdS powder supplied by Leuchstoffurer.

5.5 Substrates

There are many suitable substrates available for the deposition of CdS, all with contrasting properties. They require different cleaning and handling techniques before successful film deposition is possible. Some of the substrates used included molybdenum, soda glass, tin-oxide coated glass. Au/Cr on glass and metallised Kapton (a polyimide plastic).

Only Au/Cr on glass substrates were fabricated by us. Successive layers of Au and Cr were deposited on to the glass substrates after a cleaning process similar to one described below.

5.5.1 Cleaning Procedures

Much work has been carried out to optimise the cleaning processes of glass substrates. Undoubtedly one of the most efficient methods is to immerse the glass in a glow discharge, and much of the work on this subject has been reviewed by Holland (1958). However glow discharge cleaning cannot remove gross contaminants from a surface, so thick contaminant layers are normally removed by chemical methods before glow discharge cleaning. Putner (1959) however came to the conclusion that

under certain conditions, glass surfaces could be cleaned equally well by chemical methods.

Chemical methods of cleaning glass with detergents, hydrocarbon solvents and acids are well described in the literature (see for example Strong 1944). One of the simplest methods is to wash the surface with a detergent (such as teepol or quadralene) and water, and then polish with a lint free cloth steeped in a solvent such as isopropyl alcohol (propan 2-01). Another and more effective process for removing molecular contamination from glass surfaces is by vapour degreasing using an alcohol. This is a method which has become fairly well established in the lens coating industry. Ultrasonic agitation of cleaning fluids has also been used successfully for removing gross contamination such as pitch and jewellers rouge from the surfaces of optical components (Manufacturing Optician 1958). With our substrates the best way of removing gross contamination was by ultrasonic agitation in a detergent type solvent followed by degreasing in propan-2-ol vapour. For the plain glass substrates, a short immersion of the degreased substrate in cold concentrated hydrofluoric acid often proved beneficial. It was unnecessary to perform glow discharge cleaning after this. The metallised Kapton substrates used mainly at I.R.D. were gently swabbed with cotton wool soaked in acetone.

5.5.2 Production of Au/Cr on Glass Substrates

Although it is unlikely that a gold-chromium contact with CdS forms an ohmic contact, this substrate is used in several industrial applications (see for example Pinder and Clark 1974). Chromium adheres very well to glass and gold clings well to chromium. Gold does not adhere very well to glass and rubs off during cleaning processes. The

most important advantage of this multilayer substrate is that CdS films adhere tenanciously to gold. Since problems with adherence are experienced with thick films (>10 μm), the reduced tendency of the thicker films to peel off the Au-Cr substrates was a great advantage.

After degreasing by the method described in Section 5.5.1, large area glass plates 8.7 cm x 6.25 cm x 1 mm thick, were mounted in the evaporating chamber of the 12" bell jar system. The glass sheets used were electron microscope plates made of green soda-lime glass, which had had the photographic emulsion removed. The chromium plated tungsten basket and a molybdenum strip boat were suitably positioned in the vacuum chamber. Gold wire was placed in the molybdenum boat and small pieces of resublimed chromium were placed in the chromium plated tungsten basket. The chromium was first evaporated until it was thick enough to obscure the incandescent basket. Gold was then evaporated on to the Cr film. After cooling to room temperature, the metallised substrates were removed from the chamber. The gold top layer was quite soft and could be partially removed by rubbing, consequently it was cleaned by a simple swabbing with propan-2-ol.

5.6 The CdS Evaporation Cycle

This section describes the sequence of steps in the evaporation of CdS on tc tin-oxide or Au/Cr coated glass using the resistively heated source system.

(1) The glass or SnO_x/glass ($1 < x < 2$) substrates were cleaned by ultrasonic agitation in a 10% w.w. solution of "quadralene Q.I.C." instrument cleaner, then rinsed in distilled water and washed in propan-2-ol and finally suspended in propan-2-ol vapour for several minutes to ensure that no stains persisted on the dry surface.

(2) The substrates were clamped to the substrate heater by the 2½ cm sq mask and were mounted horizontally above the source and 'hot-wall' chimney. Other pieces of SnO_x/glass or Au/Cr/glass were bonded to glass microscope slides and were mounted vertically on the inside of the 'hot-wall' chimney. The source crucible was filled with crushed CdS powder.

(3) The system was evacuated to a pressure of $\approx 10^{-5}$ torr and the substrate was preheated to 200°C for an hour before evaporation commenced.

(4) The filament current was increased gradually to outgas the CdS powder. Too rapid an increase in temperature simply caused the contents of the crucible to spatter out.

(5) The substrate temperature was set to 200°C and the shutter was opened when steady state conditions had been attained.

(6) After the evaporation on to the substrate (usually ½ hr) or when the substrate temperature rose above 220°C or the pressure to 10^{-4} torr, the substrate and source heaters were switched off.

(7) The substrate was allowed to cool down to room temperature and was removed from the vacuum system. It was then usually stored in a vacuum dessicator.

5.7 The Totally Enclosed System

Since the method of enclosing the space between the source and substrate with a'hot-wall' chimney proved successful, a totally enclosed system was used for some evaporations. In this technique (Buckley and Woods 1973), the evaporation chamber is not pumped during the formation

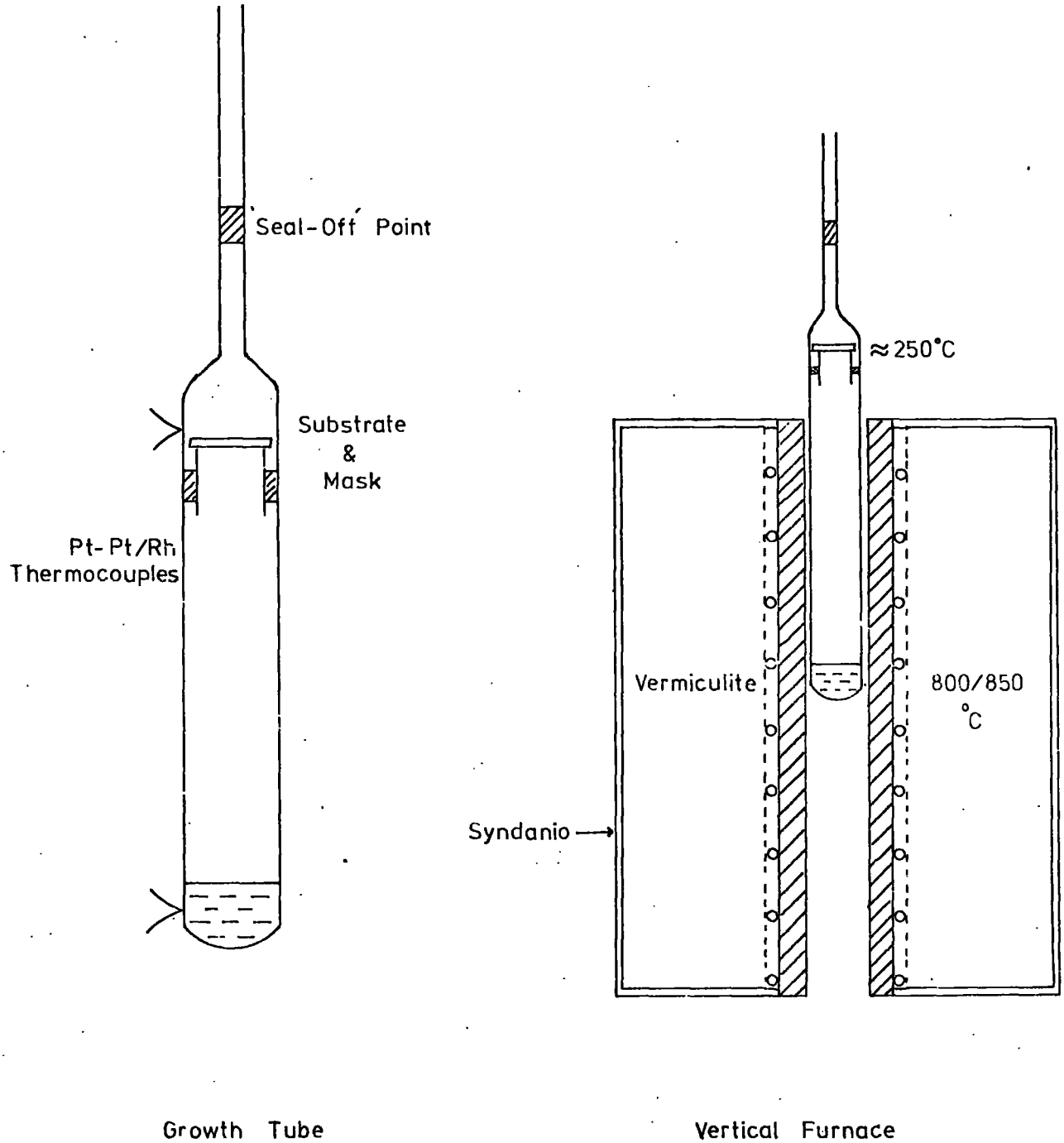

FIG. 5.4

METHOD OF GROWING FILMS IN A TOTALLY ENCLOSED SYSTEM

of the film thus allowing evaporation to be carried out under equilibrium conditions. Furthermore, none of the constituents in the vapour phase are lost preferentially to exhaust.

The 10 gm charge of crushed flow-run, purified CdS powder was placed at the bottom of a vertical 12 mm bore silica glass tube of 25 cm length, Figure 5.4. A 2.5 cm sq. glass substrate coated with tin oxide which had previously been cleaned in the manner described in Section 5.6, was supported on an inner cylinder of silica as near as possible to the top of the large diameter tube, with the tin oxide coating facing downwards. The wide bore silica tube was rounded at the top and joined to a 5 mm bore silica tube through which it was connected to a high vacuum system pumped by a mercury in glass diffusion pump via a liquid nitrogen cold trap. Evacuation of the tube was carried out overnight after it had been mounted horizontally in a furnace with a hot zone at 250^{o}C. This procedure was calculated to outgas the powder and glass components before beginning the evaporation. After pumping on the hot tube, a vacuum of 2×10^{-6} torr was obtained. After cooling, the tube was sealed off from the vacuum system.

Evaporation was carried out by placing the tube in a vertical furnace similar to those used by Clark and Woods (1968) to grow single crystals. It was possible to maintain some degree of control over the substrate and source temperature by adjusting the position of the tube in the vertical furnace. Using this method it was possible to grow thin polycrystalline films up to a few micrometers thick.

The source and substrate temperatures were measured with Pt-PtRh thermocouples in contact with the outside tube adjacent to source and substrates. This was not an ideal situation but it was not possible to measure substrate temperature directly.

5.8 Measurement of Film Thickness

Chopra (1969) has reviewed the various methods used to measure the thickness of films. Since the films prepared by us lay in two ranges of thickness, (a) less than 10 μm and (b) 10 to 20 μm, two different techniques were used. For the thinner films it was necessary to use a 'Watson Interference objective'. However with this method, a metallised layer over the film edge was essential since evaporated CdS layers are much more absorbent to light than is glass. Indium electrical contacts proved ideal for this purpose provided that high evaporation rates and low pressure were used. Unfortunately this is a destructive technique as far as eventual solar cell production from thin CdS films is concerned.

This optical technique of measuring film thickness employed double beam interferometry with monochromatic illumination from a sodium lamp to produce Fizeau interference fringes from the metallised areas. Without the metallisation, contrast of the fringes across the step was very poor. The film thickness was calculated from the fringe displacement across the step which arose from the path difference of the reflected beams since the separation of like intensity fringes is equal to half the wavelength of the illuminating light.

In the case of films greater than 10 μm thick, the large numbers of displacement fringes were difficult to count and a Moore and Wright dial indicator was used in conjunction with an Eclipse type 104 surface gauge positioned on an engineers marking off table to measure the step height directly. This technique was non-destructive so that after measurement these thick films could be fabricated into thin film solar cells. The I.R.D. films with thicknesses greater than 20 μm were measured using a calibrated microscope stage by focusing successively on the film and adjacent substrate or by the use of a Talystep thickness scanning machine.

5.9 Conclusion

A number of samples were prepared using the following methods: (1) electron beam evaporator, (2) resistively heated evaporators and (3) furnace evaporators (enclosed system). The films were grown with low resistivity, $\leqslant 10^3$ Ωcm, and with thicknesses up to 25 μm. However most of these films were thinner than 15 μm and therefore unsuitable for solar cell fabrication. In addition, many of the films produced in the enclosed system were of higher resistivities. One of the main problems in preparing thick films was the great tendency for them to peel off the substrates. However using substrates of gold on chromium on glass seemed to solve this problem.

CHAPTER 6

GROWTH OF Cu_2S ON CdS

6.1 Introduction

In the past, much work has been carried out to study how single crystal cadmium sulphide can be converted into single crystal copper sulphide with one or more phases present. The most detailed investigations were carried out by Cook et al (1970) but other workers have endeavoured to produce the chalcocite phase of copper sulphide on its own (Mulder 1972). In this chapter, the techniques used in the present work to examine the composition and structure of copper sulphide produced on various crystal planes of cadmium sulphide are described, together with the results of the investigations.

6.2 Mechanism of Displacement Reaction

It was mentioned earlier in Chapter 2 that the copper sulphide/cadmium sulphide heterojunction is produced as a result of a chemical displacement reaction between the cuprous and cadmium ions according to the equation

$$2\,Cu^{+} + CdS \longrightarrow Cu_2S + Cd^{2+}$$

Once the initial monolayer of Cu_2S has been formed on the CdS, the rate of formation of further Cu_2S is determined by the diffusion of Cu^{+} ions through the Cu_2S and the out-diffusion of Cd^{2+} ions through the growing layer into solution. This process is similar in many respects to the oxidation of a metal surface for which a parabolic rate of formation has been observed by several workers (Pilling and Bedworth1923, and Hirashima 1955). Singer and Faeth 1967 and Sreedhar et al (1970) reported that the increase in weight of undoped CdS immersed in a solution containing

cuprous ions obeyed a parabolic relationsip with time. Conversely, Shiozawa et al, 1969, concluded that the rate of formation of Cu_2S was linear with time. Buckley and Woods (1974) however showed that a single parabolic law could be used to describe the rate of formation of Cu_2S on copper doped CdS whereas the growth of Cu_2S on indium or gallium doped samples was governed by two parabolic laws.

If the reaction is taken to its limits, a cracked but single crystal of orthorhombic chalcocite (Cu_2S) may be obtained (Cook et al 1970, Singer and Faeth 1967). The transformation of CdS into Cu_2S takes place topotaxially (Te Velde and Dieleman 1973). Since CdS has a molecular weight of 144.46 compared with Cu_2S with a molecular weight of 159.14, conversion must be accompanied by a change in weight of the sample. For complete transformation, the sample must undergo a weight increase of 10.1%. Furthermore, because of lattice constant mismatch, strain will be set up in the sample which is eventually released by cracking. These changes will be discussed later in connection with the results from optical microscopy studies.

6.3 Preparation of the cuprous Ion Bath

The cuprous (Cu^+) ion plating bath used to form the p-type Cu_2S layers on both single crystal and thin film CdS was prepared in the following way.

(a) 75 ml of distilled water was heated in a closed reaction vessel and then oxygen free nitrogen gas was bubbled through the liquid to remove any dissolved oxygen.

(b) 12 ml of concentrated Hydrochloric acid was added to the water and the heating and nitrogen gas flow was continued.

(c) 1 gm of cuprous chloride was added when the temperature was approximately 60°C.

(d) Approximately 7.5 ml of hydrazine hydrate solution was added to the solution to produce a resultant pH of 2 to 3 as measured by indicator papers.

(e) After heating the solution to 90°C, the pH was measured again and corrected to 2.5 using a small amount of hydrochloric acid or hydrazine hydrate. The solution was made up to 100 ml by the addition of a little deoxygenated distilled water. During preparation and while using the bath, a constant flow of oxygen free nitrogen was maintained through the solution. The purpose of this was to keep as much oxygen away from the solution as possible and to keep the solution fully mixed. Plating of Cu_2S on to CdS occurred immediately the CdS crystals or films were dipped into the hot solution.

6.3.1 Oxidation of the Plating Solution

The flow of nitrogen gas through the solution during preparation and use, and the strong reducing agent, hydrazine hydrate, present in the solution had the effect of slowing down the oxidation of colourless cuprous (Cu^+) ions to the blue coloured cupric (Cu^{2+}) ions. Displacement of CdS by cupric ions would produce copper deficient phases of copper sulphide and this was clearly not desirable. Even when the solution was left for a short time with a gas flow maintained through it, a deep blue precipitate formed on the surface of the solution. The compound was a complex between copper, nitrogen and oxygen, similar to the cuprammonium ion. If the solution was reheated and the pH corrected to 2.5 using hydrazine hydrate, the deep blue precipitate could be made to redissolve.

On the other hand, if the solution was left for a long time without a continuous flow of nitrogen gas through it, the solution itself developed a blue/green colour which could not be easily removed. The change in colour was due to the oxidation of Cu^{+} to Cu^{2+}. When a solution was cooled to room temperature with oxygen being kept away as much as possible, thin white needles of cuprous chloride were precipitated from the saturated solution.

A short investigation of the effects of oxidation in the plating bath was carried out where the solution was prepared in a nitrogen filled glove box. CdS/Cu_2S heterojunctions were prepared in this box and the solution was cooled and stored in an atmosphere of nitrogen.

No blue precipitate was formed even after several days and the solution remained colourless. White needle shaped crystals of cuprous chloride were however precipitated. The devices prepared using this method were not any better than those prepared using the conventional method, so it was decided that plating experiments could be carried out without the aid of the glove box. This more controlled environment was of course a very inconvenient constraint in the preparation of devices. To reduce the effects of oxidation, fresh plating solutions were made up on each occasion.

6.4 X-ray Orientation of Crystals

As mentioned in Chapter 2, cadmium sulphide displays polar properties in the [0001] direction. It was decided to orientate all of the boules so that thin slices could be cut perpendicular to the 'c' axis direction. Since the growth axis of the cadmium sulphide boules did not usually lie parallel to the 'c' axis of the single crystal, it was not possible to determine the orientation of the crystal by simple inspection.

However it was feasible to identify the six-fold symmetry axis of the basal plane of the crystal by taking a series of X-ray back reflection photographs and re-aligning the sample by means of information obtained from the photographs using a Greninger Chart. After this alignment process the boule was ready for sectioning.

6.5 Sample Preparation

The orientated boules were cut into 2 mm thick slices using a diamond impregnated cutting wheel. This process left deep cutting marks on the surfaces of the slices which were later removed by grinding the (0001) cadmium and $(000\bar{1})$ sulphur faces using a slurry of 1200 grade carborundum paste on a lapping plate. The slices were then further polished with diamond paste down to a grit size of 1 μm. For the series of experiments concerned with thickness measurements, and electron microscope studies of the copper sulphide layers formed on both (0001) and $(000\bar{1})$ faces, further sectioning was carried out to produce cuboids of size 5 x 5 x 2 mm. The two large area faces were the polar faces of the cadmium sulphide. Both the cutting and polishing processes led to work damage of the crystal surface layers. Some of this damage was removed by lightly etching the samples in cold concentrated hydrochloric acid. The other purpose of the etching was to identify the (0001) and $(000\bar{1})$ faces. Etching in hydrochloric acid produced an optically matt finish on the $(000\bar{1})$ sulphur faces while the cadmium faces became highly reflective. The polished samples were not etched for long enough to reveal many hexagonal etch features on the (0001) face.

6.6 Thickness of the Plated Layer

In order to investigate the relative thicknesses of the copper

sulphide layers formed on both the (0001) and (000$\bar{1}$) faces, the lightly etched samples were placed in the hot Cu^{+} ion bath at a temperature of 90^{o}C for 45 minutes. The converted (0001) and (000$\bar{1}$) faces were examined using an optical microscope and photographs of the faces were taken. It was possible to identify the (0001) and (000$\bar{1}$) planes since the copper sulphide formed on the matt finish sulphur plane was similarly highly light absorbing, in contrast to the highly reflective layer formed on the (0001) cadmium plane. The partially converted samples were embedded in a clear resin with the 'c' axis of the CdS parallel to the surface and the (0001) and (000$\bar{1}$) faces marked. Sectioning of the embedded samples was carried out using grade 600 carborundum paste followed by 1200 grade paste and finally by a series of polishes using diamond paste down to a 1 μm grit size. This process removed approximately half of the sample in all. Photomicrographs of the sections were obtained and are discussed in the next section.

6.6.1 Experimental Results

The lightly etched sulphur plane of the cadmium sulphide was very light absorbing and no etch features could be detected on this face. In contrast the cadmium plane was highly reflective and several hexagonal etch features were present, but the etch pits were not present in great numbers. It was assumed that the etch features would produce local perturbations in the thickness of the copper sulphide layers produced on this face and this was the reason why only a short etch treatment was given. After the plating process, the copper sulphide layers retained the surface finishes of the cadmium and sulphur planes on which they were formed. It was not possible to detect any features on the (000$\bar{1}$) sulphur face layer but in contrast, the copper sulphide surface

on the (0001) face contained numerous cracks lying in three directions at 120^{o} to each other (Figure 6.1). The micrographs in Figures 6.2 and 6.3 show typical copper sulphide layers formed on $(000\bar{1})$ and (0001) planes of the same crystal. In these photographs the copper sulphide layers may be identified as the regions of lighter contrast. Copper sulphide layers on both planes exhibit cracks as dark lines which should not be confused with the micro-scratch marks caused by polishing. The most obvious feature of these two sections is that the copper sulphide layer on the sulphur face is significantly thicker than that formed on the corresponding cadmium face of the same sample. It was noticeable that the copper sulphide was locally thicker in the vicinity of a crack on either face. The highly light reflecting cadmium plane had a relatively flat surface compared to the rough sulphur plane which was highly light absorbing as indicated by the boundary between the very dark resin and the copper sulphide layers. It can be seen by comparing Figures 6.2 and 6.3 that the thickness of copper sulphide formed on a sulphur plane was approximately 1.5 times greater than that formed on the corresponding cadmium plane.

6.7 Electron Microscope Examination of the Copper Sulphide Layers

Several samples of equal size to the ones used for thickness measurements were cut from the same polished slices and were treated in the same plating solution for equal lengths of time. They were then bonded to a reflection electron diffraction mounting stud using 'durofix' adhesive. These samples were mounted off centre on the stud so that it was possible to diffract the electron beam from layers formed on either the sulphur or cadmium faces by a simple translation of the stud within the microscope itself. The technique of reflection electron diffraction is discussed in the next section.

6.8 Reflection Electron Diffraction

Reflection electron diffraction (R.E.D.) was used in preference to methods employing X-rays to investigate the structure of the copper sulphide layer for several reasons. It is known that the depth of penetration of X-ray beams into the surface of a material under investigation is of the order of hundreds of micrometers and the thickness of the copper sulphide layers produced by the methods used was of that order. This would imply that diffraction from the underlying CdS might be produced as well as the desired patterns from the copper sulphide layers. By contrast, the depth of penetration of the electron beam at glancing incidence is only of the order of 100 Å for very flat surfaces. Thus no problems associated with diffraction from the CdS were encountered. A further advantage of the R.E.D. technique was that the diffraction pattern could be studied while the sample orientation was altered.

Each real space plane (h,k,ℓ) produces a reciprocal lattice point which is given the same set of indices as the corresponding plane. The reciprocal lattice point lies on a line perpendicular to the real space planes and passing through the origin. It is situated at a distance from the origin which is inversely proportional to the interplanar spacing, $d_{hk\ell}$. The condition for Bragg reflection of the electron beam may be considered in the following geometrical way. It is assumed that the crystal under investigation is located at the edge of the reflecting sphere (or circle if simplified to 2 dimensions) of radius $1/\lambda$ where λ = wavelength of the electron beam, which is 0.037 Å for 100 KeV electrons. Diffraction only occurs when a reciprocal lattice point arising from the real space planes touches the circle. This condition is illustrated in Figure 6.4. The geometrical representation of the Bragg condition is called the Ewald Construction. Examination of

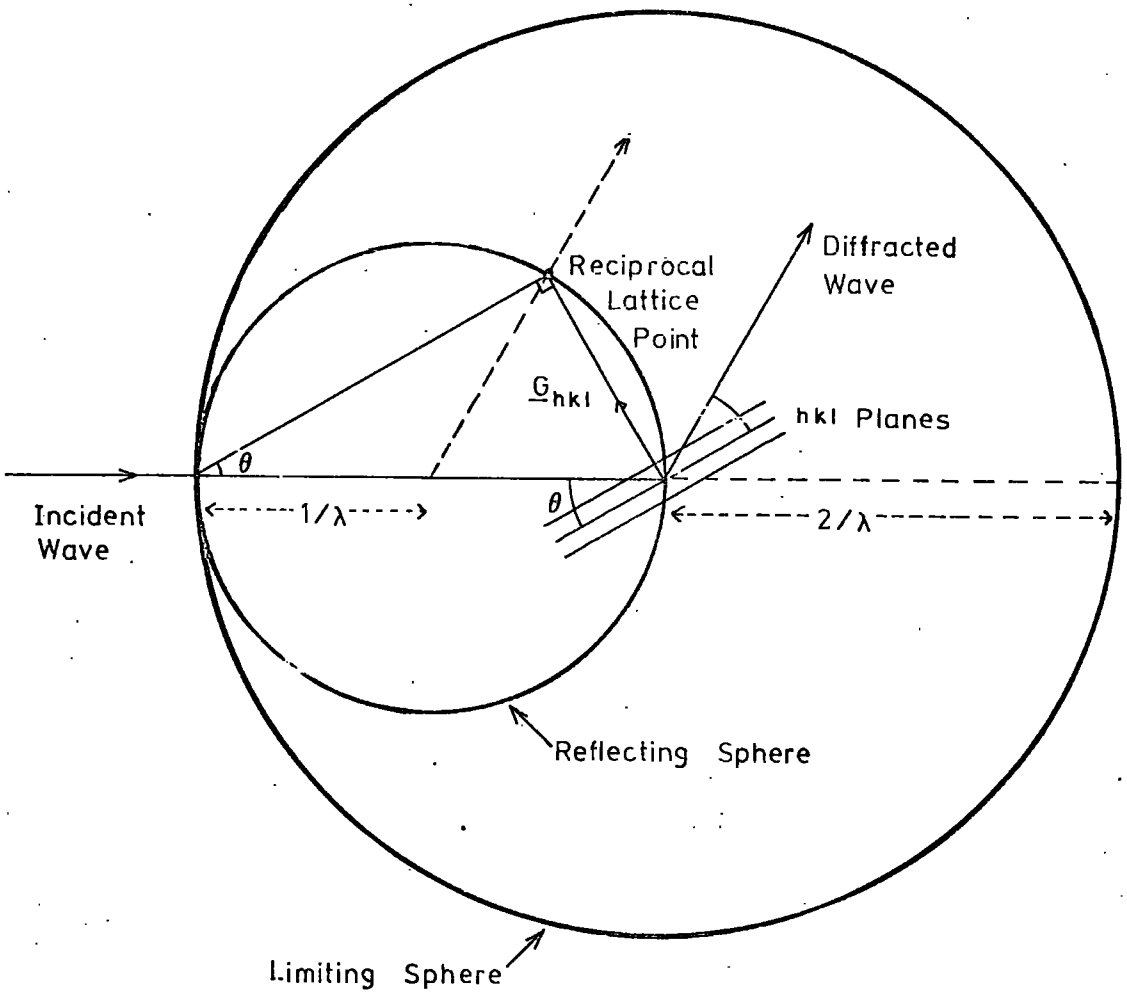

FIG. 6.4 SPHERE OF REFLECTION IN A RECIPROCAL LATTICE

the diffraction pattern obtained from a series of real space planes enables the lattice parameters of samples to be calculated. It should be noted that certain crystal orientations lead to standard, easily recognisable patterns which enable easier calculation of the unit cell dimensions. Before any measurements of the lattice parameters of crystalline materials can be made, the camera constant ($\lambda.L$) for the particular electron microscope used must be evaluated (Barrett and Massalski (1966)). This was carried out using a gold polycrystalline layer and was found to be

$$\lambda.L = 4.12 \pm 0.05 \text{ Å}^{-1} \text{ cm}$$

6.9 Examination of CdS Single Crystals

In order that later comparison between the R.E.D. patterns of cadmium sulphide and copper sulphide could be carried out, a pattern was obtained from the sulphur plane of etched CdS. The sample was rotated and tilted until an easily recognisable symmetrical pattern was obtained (Figure 6.5). This was indexed (Figure 6.6) using the information presented in Hirsch et al (1965).

For the hexagonal crystal system:-

$$\frac{1}{d^2_{hki\ell}} = \frac{4}{3a_o^2}(h^2 + kh + k^2) + \frac{\ell^2}{c_o^2}$$

where a_o and C_o are the lattice parameters of the hexagonal unit cell and $d_{hk\ell}$ is the interplanar spacing. If the (0002) planes are considered, the above equation simplifies to:-

$$\frac{1}{d^2_{0002}} = \frac{4}{c_o^2}$$

or $$c_o = 2d_{0002}$$

FIG. 6.6. INDEXED R.E.D. PATTERN FROM CdS LOOKING DOWN A [120] ZONE AXIS.

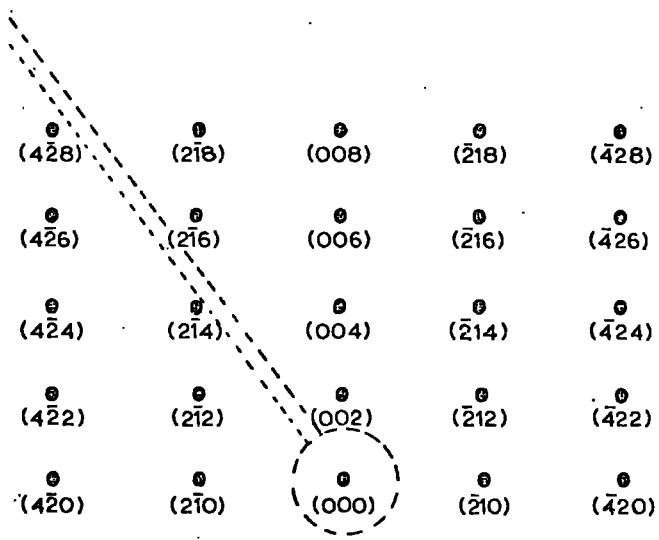

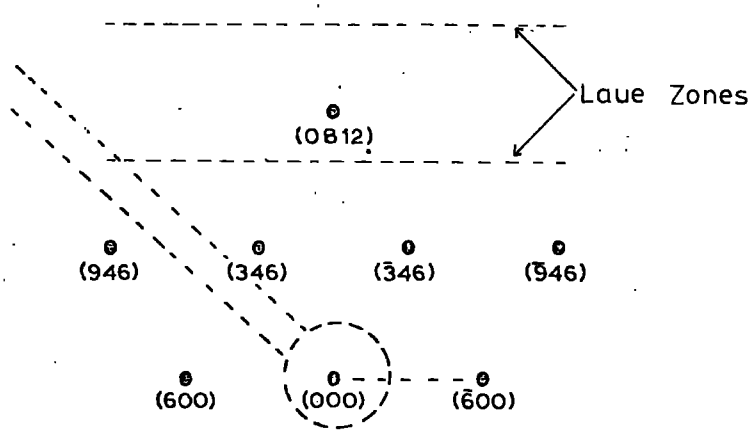

FIG 6.8 PARTIALLY INDEXED R.E.D. PATTERN FROM Cu_2S ON THE S PLANE OF CdS LOOKING DOWN A [0$\bar{3}$2] ZONE AXIS

FIG. 6.10 PARTIALLY INDEXED R.E.D. PATTERN FROM Cu_2S ON THE S PLANE OF CdS LOOKING DOWN A [100] ZONE AXIS

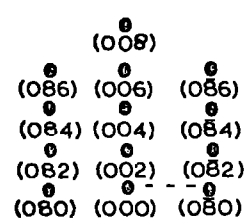

Thus the C_o parameter can be directly calculated from the measured interplanar spacing of the (0002) planes. By measurement of the distance between the origin and (0002) point on an enlargement of Figure 6.5 and a knowledge of the camera constant, it was possible to deduce a value of the C_o parameter as

$$C_o = 6.7 \pm 2\% \text{ Å}$$

It can similarly be shown that for $(2\bar{1}\bar{1}0)$ planes ,

$$a_o = 2d_{2\bar{1}\bar{1}0}$$

This led to a value of a_o of

$$a_o = 4.2 \pm 2\% \text{ Å}$$

These values compared quite well with the lattice parameters of CdS of $a_o = 4.1367$ Å and $C_o = 6.7161$ Å as measured by X-ray diffraction (Cook et al 1970).

The purpose of examining the CdS was to confirm that the gold calibration was correct and to give an indication of the errors incurred using this R.E.D. technique.

6.10 Examination of Copper Sulphide formed on CdS

A number of copper sulphide R.E.D. patterns were obtained from the cadmium and sulphur planes of CdS crystals which had been immersed in a solution of cuprous ions at 90°C for 45 minutes to ensure no diffraction from the underlying CdS, particularly on rough sulphur surfaces. It was only possible to take accurate measurements from copper sulphide layers formed on the sulphur planes of the CdS. R.E.D. patterns

originating from copper sulphide layers formed on the cadmium planes are discussed later. A photograph of the R.E.D. pattern of a particular orientation of the sample is shown in Figure 6.7. Measurements of the distance between the intense 'spots' and the origin from the enlargement of this photograph enabled interplanar spacings characterised by the intense reflections to be calculated. By reference to the A.S.T.M. index for the copper sulphides, it was possible to say that the layer had the chalcocite structure and it was also possible to index some of the diffraction spots. The indexed points are shown in Figure 6.8 By measuring the distances between the diffraction 'spots' and the origin in the [100] direction and using the camera constant it was possible to calculate the a_o parameter of the orthorhombic chalcocite unit cell as $a_o = 12.03 \pm 2\%$ Å. Since the axis perpendicular to the [100] direction was not [010] or [001] but intermediate, it was not possible to calculate the b_o and c_o parameters directly. However two simultaneous equations in b_o and c_o could be written down in terms of the calculated value of a_o using the relationship:-

$$\frac{1}{d_{hk\ell}^2} = \left(\frac{h^2}{a_o^2} + \frac{k^2}{b_o^2} + \frac{\ell^2}{c_o^2} \right) \quad \text{(for orthorhombic crystals)}$$

There was also evidence of the existence of Laue zones (Hirsch et al 1965, pg. 112) which can be seen in Figures 6.7 and 6.8 as the regularly spaced brightened up zones running parallel to the [100] direction. This meant that measurements from the (0 8 12) point to the (0 0 0) point (Figures 6.7 and 6.8) would be inaccurate.

The sample was orientated and tilted so that another type of regular pattern was observed (Figure 6.9). This pattern was indexed (Figure 6.10) in a similar way to that used previously. The intensities

of alternate diffraction spots observed in the [001] direction did not match exactly with those given in the A.S.T.M. index for chalcocite (but the positions did correspond). According to the tables given in the A.S.T.M. index for the various copper sulphides, it would not be expected that (00ℓ) type planes would produce intense diffraction maxima. However it should be noted that the A.S.T.M. intensity data refers specifically to X-ray diffraction and does not always correlate exactly with electron diffraction intensities (see for instance Hirsch et al, pg.91). The diffraction spots not along the 'c' axis e.g. (082) (084) were intense as predicted for chalcocite according to the A.S.T.M. index. Calculation of the b_o and c_o values from the photograph (Figure 6.9) gave values of

$$b_o = 27.74 \pm 2\ \% \text{ Å} \quad \text{and} \quad c_o = 13.59 \pm 2\% \text{ Å}$$

Comparison of the a_o, b_o and c_o parameters for the material topotaxially formed on the CdS surface with the lattice parameter confirmed that the material was orthorhombic copper 1 sulphide (form 3) or chalcocite

$a_o = 11.881$ Å $\quad b_o = 27.323$ Å $\quad c_o = 13.497$ Å (A.S.T.M. index for Cu_2S)

$a_o = 12.03 \pm 2\ \%$ Å $\quad b_o = 27.74 \pm 2\%$ Å $\quad c_o = 13.59 \pm 2\%$ Å (calculated from R E D patterns)

In similar experiments reported by Caswell et al (1975) it was suggested that the material formed was α (low) chalcocite. This form is orthorhombic and very similar to chalcocite but with a slightly smaller b_o parameter of 27.05 Å. In fact α (low) chalcocite is a rare geological form of chalcocite.

Other polished slices of CdS which had been immersed in the hot solution of cuprous ions were mounted on an R.E.D. mounting stud in such a way that R.E.D. patterns could be obtained from both Cd and S plane sides of the CdS by simple translation of the sample inside the electron microscope. Figure 6.11 shows a typical diffraction pattern obtained from a layer formed on an S plane whereas Figure 6.12 shows a typical diffraction pattern from a layer on the corresponding Cd plane of the same crystal. The pattern shown in Figure 6.11 could be obtained over the whole area of the S surface, whereas the pattern shown in Figure 6.12 could only be observed in certain places on the Cd plane. Measurement of the distances in the [010] and [001] directions in Figure 6.11 gave values of b_o and c_o directly:-

$$b_o = 27.69 \pm 2\% \text{ Å} \qquad c_o = 13.48 \pm 2\% \text{ Å}$$

It was impossible to calculate a_o from this orientation of the sample. The R.E.D. pattern shown in Figure 6.12 had a similarly distorted hexagonal array of the intense spots but because of the smeared out appearance of these diffraction maxima, it was not possible to make accurate measurements, but the layer was almost certainly chalcocite. The large number of closely spaced reflections observed with the layer formed on the S plane of CdS were absent from the R.E.D. pattern from the corresponding Cd plane. These close reflections indicate good long range order on the S plane side and it is likely that extensive micro cracking of the layer formed on Cd faces had removed this order and with it the weak reflections. The streaked appearance of the spots from the Cd plane layers was due to the very flat surface of the layer which gives rise to the relaxation of the Laue conditions for the set of

planes parallel to the surface and hence causes streaks perpendicular to the surface (Thomson and Cochrane 1939).

6.11 Examination of Copper Sulphide phase formed at low temperatures

Later in this thesis (Chapter 8), work is reported concerning the O.C.V. spectral responses of devices fabricated at 45°C. Indirect evidence of the formation of a copper deficient phase at this temperature is given and so R.E.D. was carried out to attempt to identify the phase directly. A temperature of 45°C was employed for reasons discussed in Chapter 8.

Polished undoped cadmium sulphide cuboids were dipped in the copper ion plating solution at 45°C for 45 minutes. A typical R.E.D. pattern obtained from the layer of copper sulphide formed on the sulphur (0001) plane of the sample is shown in Figure 6.13. This pattern should be compared with that shown in Figure 6.11 which was obtained from an identical sample prepared at 90°C. It can be seen that there are rows of closely spaced diffraction spots running parallel to the 'c' axis. From measurements made on this pattern is was possible, using the camera constant, to calculate b_o and c_o directly. These were found to be

$$b_o = 13.73 \pm 2\% \text{ Å} \quad \text{and} \quad c_o = 26.84 \pm 2\% \text{ Å} .$$

In the particular orientation from which the pattern was obtained it was not possible to calculate a_o but the b_o and c_o parameters matched those of orthorhombic Djurleite ($Cu_{1.96}S$) i.e.

$$a_o = 15.71 \text{ Å} \qquad b_o = 13.56 \text{ Å} \qquad c_o = 26.84 \text{ Å}$$

obtained from the A.S.T.M. index. Further R.E.D. patterns taken from the layers in different orientation would have been necessary to evaluate

a_o and to confirm the identification of the layer more accurately.

6.12 Examination of CdS thin films

Thin films of cadmium sulphide were evaporated in high vacuum using a resistively heated source as discussed in Chapter 5. A substrate temperature of approximately 300°C was employed. Figure 6.14 shows a typical R.E.D. pattern obtained from a film 10 μm thick (as measured by interferometry techniques). The pattern shows characteristics of a film with a fibre axis and also contains extra reflections which may be attributed to pseudo-double positioning which is described below. Similar patterns have been obtained by Wilson (1971) in an investigation of the degree of preferred orientation of crystallites as a function of film thickness and deposition rate. Such patterns have not been indexed when previously reported.

Examination of the reciprocal lattice pattern of the most densely populated reciprocal lattice planes of face centred cubic and hexagonal crystal structures (Hirsch 1965), shows that for crystallites with a fibre axis in a $\langle 111 \rangle$ type direction for the cubic phase, or for a $[0001]$ direction in the case of hexagonal crystallites, there are two low index directions in the plane perpendicular to the fibre axis for each crystal type. The two lowest index directions for the cubic phase are the $\langle 110 \rangle$ and $\langle 211 \rangle$ directions and the $\langle 12\bar{3}0 \rangle$ and $\langle 10\bar{1}0 \rangle$ for the hexagonal form. These four directions can be identified as zone axes in Figure 6.15. From calculations using the lattice parameters of cadmium sulphide in the cubic and hexagonal phases as given in the A.S.T.M. index, it can be seen that reflections from the $[211]$ (cubic) coincide with those from the $[12\bar{3}0]$ zone within the accuracy of the measuring techniques employed. Perhaps the most interesting features

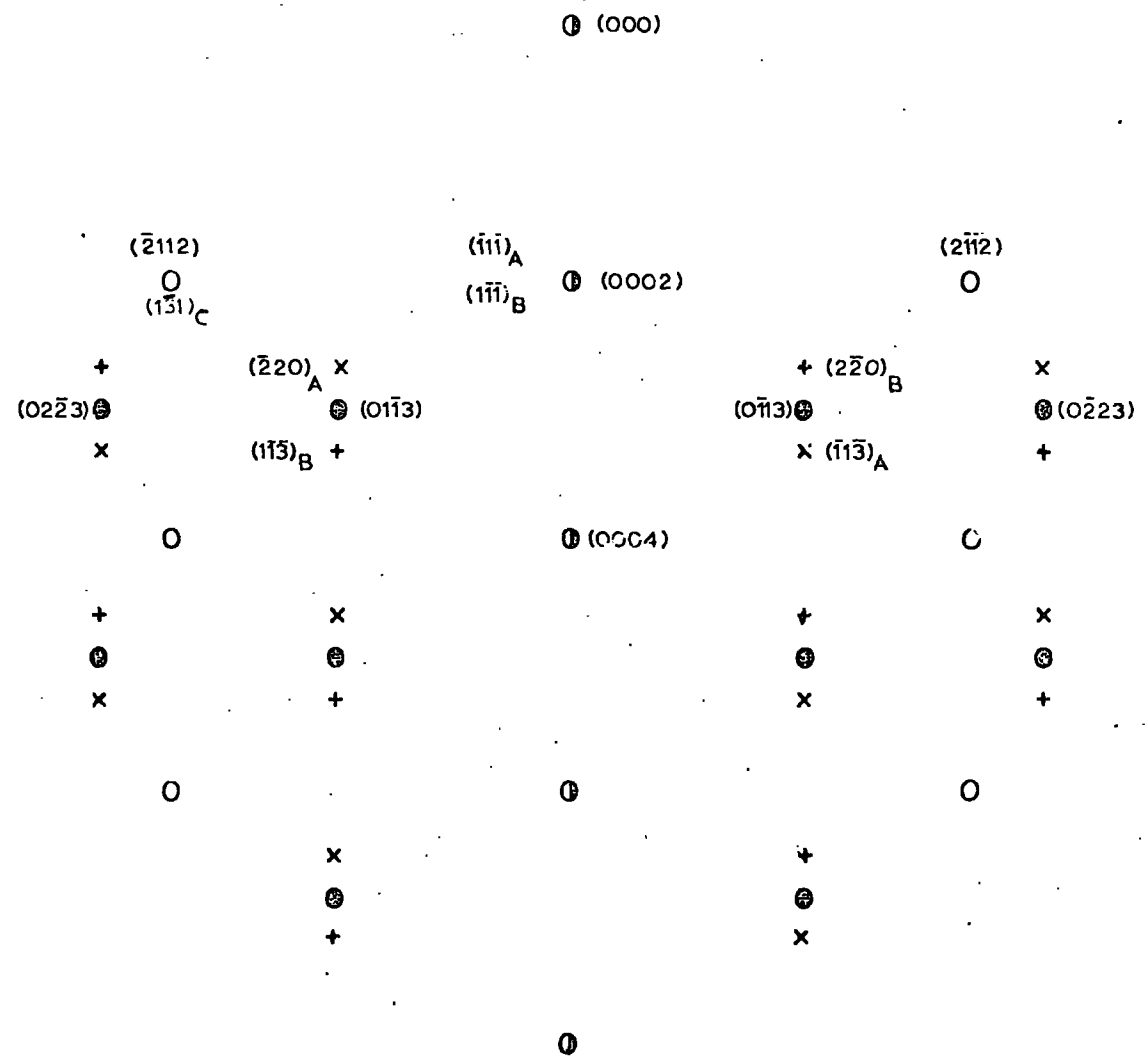

FIG. 6.15 THE INDEXING OF THE R.E.D. PATTERN SHOWN IN FIG. 6.14

$O\{^{(hki\ell)}_{(hk\ell)_C}$ = reflection from the wurtzite phase for $[12\bar{3}0]$ zone axis coincident with sphalerite $[211]$ zone axis

$\ominus$ $(hki\ell)$ = reflection from the wurtzite phase for $[10\bar{1}0]$ zone axis

$\times$ $(hk\ell)_A$ = reflection from the sphalerite phase for $[110]$ zone axis with $[\bar{1}1\bar{1}]$ fibre axis

$+$ $(hk\ell)_B$ = reflection from the sphalerite phase for $[110]$ zone axis with $[1\bar{1}1]$ fibre axis

of the pattern shown in Figure 6.14 are the spots which exhibited 'streak' effects perpendicular to the sample surface. The indexed pattern shows that crystallites with two different $\langle 110 \rangle$ type zone axes are mainly responsible for this. The reflection from the two sets of crystallites are not symmetrical about the fibre axes. One set is a mirror image about the fibre axis of the other. This effect may be considered as being analogous to the 'double' positioning of grains of wurtzite material in a sphalerite structure (Woodcock and Holt 1969).

6.13 R.E.D. Examination of Converted Thin Films

Some of the cadmium sulphide thin films of the type discussed in the previous section were dipped in the solution of cuprous ions at 90°C for 5 to 10 seconds. This is the time used in the preparation of thin film CdS/Cu_2S solar cells. A longer immersion time caused the film to peel off the substrate because of the combination of cracks in it and the action of surface tension of the solution. As can be seen from Figure 6.16, the cadmium sulphide substrate on which the copper sulphide was formed gave rise to extra reflections. The copper sulphide layer was approximately 0.1 μm thick. Weak reflections due to the copper sulphide can be seen as a series of lines in the fibre axis direction.

The results obtained from such partially converted thin films of cadmium sulphide showed that copper sulphide layers under investigation should be at least several microns thick in order to avoid confusing reflections from the under-lying cadmium sulphide. It was for this reason that most experiments on the conversion of cadmium sulphide were carried out on single crystal samples and why long dip times were employed.

6.14 Investigation of Surface Layers using E.S.C.A.

Another technique which was used to provide information about the layers of copper sulphide topotaxially formed on cadmium sulphide was that of E.S.C.A. This is an abbreviation for 'Electron Spectroscopy for Chemical Analysis'. The E.S.C.A. technique relies upon X-rays interacting with deep core electrons. Electrons are emitted and materials may be analysed by counting the number and measuring the velocity of the various photo-electrons emitted. The technique is a very sensitive one but can be used to probe the first few Å of the surface. As a consequence, the effects of surface contamination are very important. Elements and molecules detected in the surface layers of a converted CdS layer by means of this technique were:- carbon, water and cadmium. No significant identification of copper could be shown in what was supposed to be a copper sulphide layer. The conclusion reached was that the technique was too sensitive for our purposes and is much better suited to the identification of complex organic molecules. More information would have been provided if an ultra high vacuum chamber had been available. It was, however, interesting to note that cadmium ions were present in the copper sulphide layer and it was likely that they were in the process of diffusing out through the copper sulphide when the samples were removed from the plating solution. Flow run purified cadmium sulphide crystals were also partially converted and investigated using E.S.C.A. but no meaningful results were obtained since a very flat surface is essential for this technique.

6.15 Orientation Effects of Cadmium Sulphide films

It is a well known phenomenon that when thin films of cadmium sulphide are evaporated on to hot glass substrates, the first crystallites deposited are in random orientation, but as evaporation proceeds, the

crystallites tend to line up with the 'c' axis of hexagonal cadmium sulphide grains approximately normal to the substrate. See for instance Wilson and Woods (1973). A piece of evaporated cadmium sulphide film of thickness greater than ≈ 15 μm was removed from the substrate and was mounted on a R.E.D. mounting stud with the side of the film which had grown first, bonded to the stud. Inside the electron microscope, the stud was orientated such that the electron beam could impinge on the edge of the film. The R.E.D. pattern obtained is shown in Figure 6.17. There are two different halves to this pattern. The side of the film which grew first gives rise to a polycrystalline ring pattern whereas the opposite side shows evidence of fibre axis orientation. It is not possible to identify the axis, probably because of the buckled nature of the film. This experiment showed that for a cadmium sulphide film thicker than a few microns, the crystallites are beginning to orientate themselves with the 'c' axis normal to the substrate.

6.16 Evaporation of Cadmium Sulphide on to single crystal substrates

Cadmium sulphide films were evaporated on to freshly cleaved $\{100\}$ surfaces of rocksalt held at various temperatures between 150° and 325° using the resistively heated source system. The films were floated off the NaCl in water and were examined in transmission in the electron microscope. A T.E.M. diffraction pattern from a CdS film deposited at 300°C is shown in Figure 6.18. The evaporation rate was too high to permit good epitaxy but the film contained a large proportion of the sphalerite phase. Figure 6.18 has been indexed in Figure 6.19 (see Wilcox and Holt 1969, Holt 1969). The pattern is a composite one which arises from a sphalerite structure with a <100> type zone axis and a hexagonal one which is present in two preferred orientations. These are such that

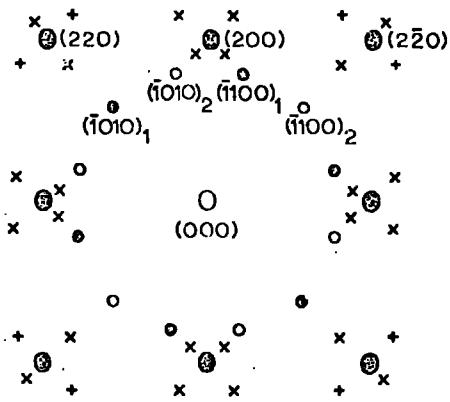

FIGURE 6.19: THE INDEXING OF THE T.E.D. PATTERN SHOWN IN FIG. 6.18.

$\circledcirc_{(hk\ell)}$ = reflection from cubic phase

$\times_{(hki\ell)}$ = reflection from wurtzite grains orientated with basal planes parallel to $\{111\}$ planes of the matrix

$+_{(hki\ell)}$ = double diffraction of wurtzite grains

$\bullet_{(hki\ell)_1}$ = reflection from wurtzite grains in position 1

$\circ_{(hki\ell)_2}$ = reflection from wurtzite grains in position 2

the 'c' axis is parallel to the electron beam for each direction. The $(\bar{1}100)$ planes of one orientation are parallel to the $(2\bar{2}0)$ planes of the cubic lattice and the $(\bar{1}010)$ planes of the other orientation are parallel to the (220) planes of the cubic lattice. These two hexagonal patterns arise from doubly positioned wurtzite grains of CdS as discussed by Wilcox and Holt (1969). In addition there are four satellite spots present around each sphalerite reflection. It is proposed that these are partly due to wurtzite grains orientated with basal planes parallel to the $\{111\}$ type planes of the matrix. The remainder of the spots in satellite positions are thought to be due to double diffraction processes. While it is possible that the satellite reflections could be attributable to twins on the $\{111\}$ planes of the sphalerite matrix, (Holt 1969), the asymmetric disposition of the reflection about the main sphalerite matrix spots would suggest that this is less likely, especially since the films were of poor epitaxy in any case.

The film was re-examined after it had been stored in the laboratory for two months (Figure 6.20). Comparison of the intensities of the reflections from the sphalerite structure with those from the wurtzite structure in both patterns shows that in two months the prominent reflections have changed from those of the sphalerite to those of the wurtzite phase. Wilson (1971) reported a similar effect and attributed this intensity reversal to a relaxation of the crystallites from the cubic phase, in which they were constrained to grow by the rocksalt substrate to the more energetically favourable hexagonal phase.

6.17 Summary of Conclusions

The etch rate of the $(000\bar{1})$ S face of CdS is greater than that of the (0001) Cd face and so during the etching process, the Cd plane is

chemically polished and the S plane is etched. It is possible therefore to identify each face from the great difference in reflectivity of light. When Cu_2S is topotaxially grown on both Cd and S planes of orientated CdS, the surface morphology of the black Cu_2S takes the same form as the underlying Cd or S faces. In the topotaxial growth process, elastic strain is developed, since although the C_o parameters of CdS and Cu_2S match to within 0.4% there are mismatches of about 5% in each of the other parameters. The mismatch causes cracks running at 120^o to each other to be formed on the Cd and S planes. Because of the highly absorbent nature of the Cu_2S layer formed on the S plane, it was only possible to observe the cracks directly on the highly reflecting Cd plane.

By taking sections through partially converted single crystals of CdS, it was demonstrated that the rate of conversion to cuprous sulphide proceeded 1.5 times faster on sulphur faces than on the corresponding cadmium plane. Local perturbations in thickness in the vicinity of cracks were observed on both faces.

The R.E.D. patterns obtained from layers formed on both faces were quite different. With Cu_2S formed on an S plane, there was a single crystal pattern containing a distorted hexagonal array of intense spots with a large number of weaker closely spaced reflections. This type of pattern was obtained over the whole S plane indicating good long-range order. The diffraction pattern was positively identified as that arising from orthorhombic chalcocite (Cu_2S). In contrast, the R.E.D. pattern obtained from the layer formed on the Cd plane contained only the distorted hexagonal array with the individual reflections smeared out due to the very smooth surface. The close spaced weaker spots which depend on Bragg reflection from widely spaced planes in real space were not observed. It is proposed that it is easier to relieve the mismatch strain

on the relatively rough S plane than on the smooth Cd plane. In the latter case, it is suggested that numerous microcracks are formed which destroy the long range order. Furthermore, the pattern arising from the layer formed on a Cd plane could only be obtained from a limited number of regions on that plane.

In each experiment where the single crystal CdS was dipped in the Cu^{+} ion solution at $90^{o}C$, the resulting topotaxial layer was of chalcocite. However when experiments were carried out involving the standard solution at the lower temperature of $45^{o}C$, a different R.E.D. pattern was observed. The layers were identified as djurleite ($Cu_{1.96}S$) which is a copper deficient phase.

It proved impossible to identify the phases of copper sulphide formed on thin films of CdS since the Cu_2S layers were so thin that the reflections from the CdS base material obscured the reflection from the copper sulphide layer. The attempts to identify the layers using the E.S.C.A. technique were unsuccessful because of surface contamination and the greater sensitivity of the technique to carbon atoms.

Thin films of CdS evaporated on to glass showed evidence of a fibre axis and in addition showed extra reflections which were attributed to pseudo double positioning. Low quality epitaxial films of CdS were also evaporated on to $\{100\}$ faces of rocksalt and true double positioning was observed. Films which contained a large proportion of sphalerite grains immediately after deposition relaxed to a lower energy form containing a higher proportion of wurtzite grains when left for several months in the laboratory.

FIG. 6.1 SURFACE OF A POLISHED (0001) PLANE OF CdS PLATED WITH Cu_2S (x270)

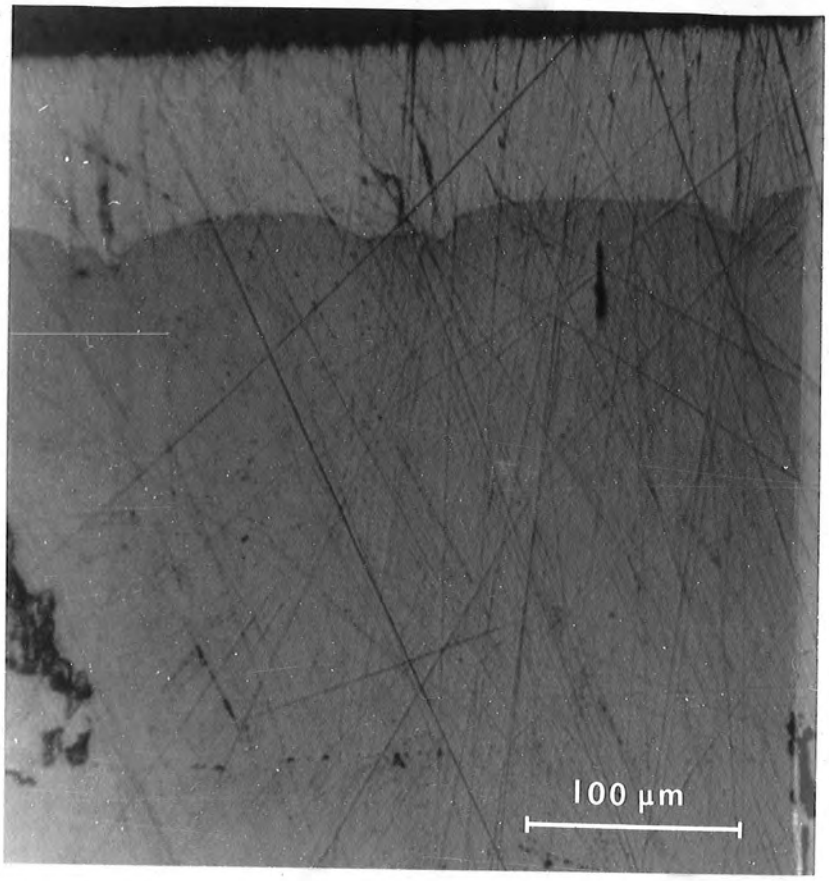

FIG. 6.2 SECTION THROUGH Cu_2S FORMED ON THE S PLANE

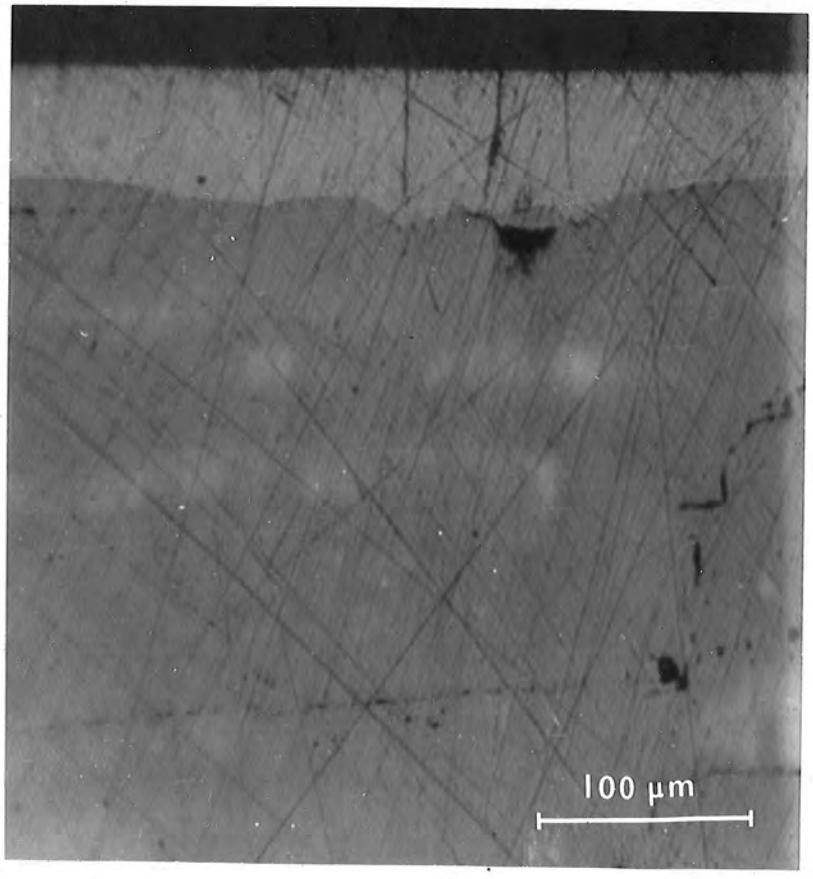

FIG. 6.3 SECTION THROUGH Cu_2S FORMED ON THE Cd PLANE

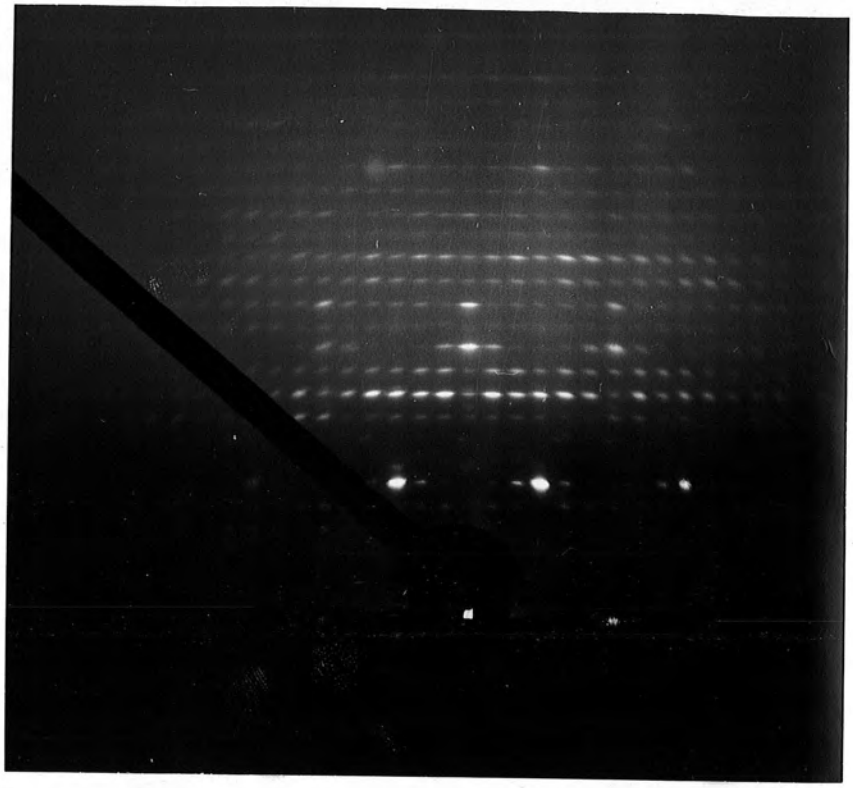

FIG. 6.7 R.E.D. PATTERN FROM THE [0$\bar{3}$2] ZONE AXIS OF Cu_2S

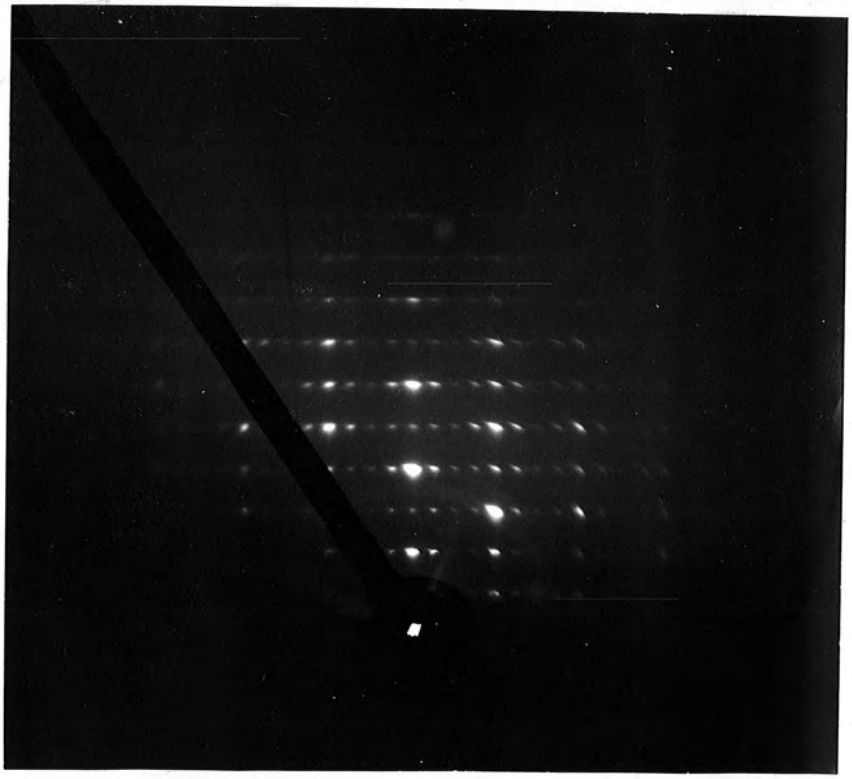

FIG. 6.9 R.E.D. PATTERN FROM THE [100] ZONE AXIS OF Cu_2S

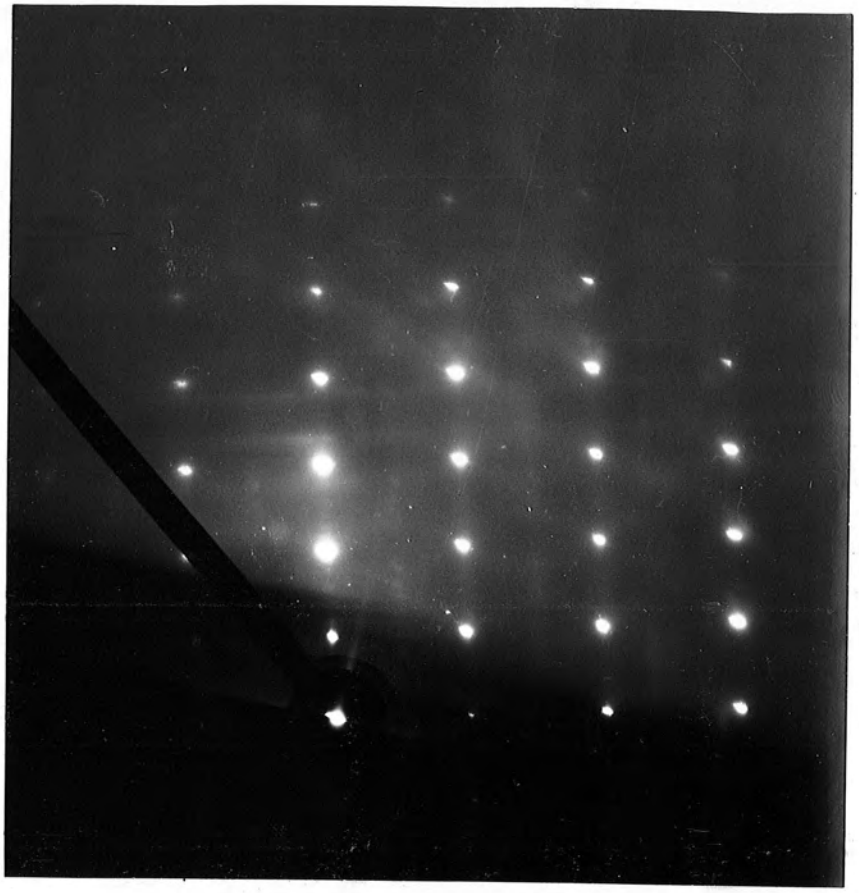

FIG. 6.5 R.E.D. PATTERN FROM THE S PLANE OF CdS

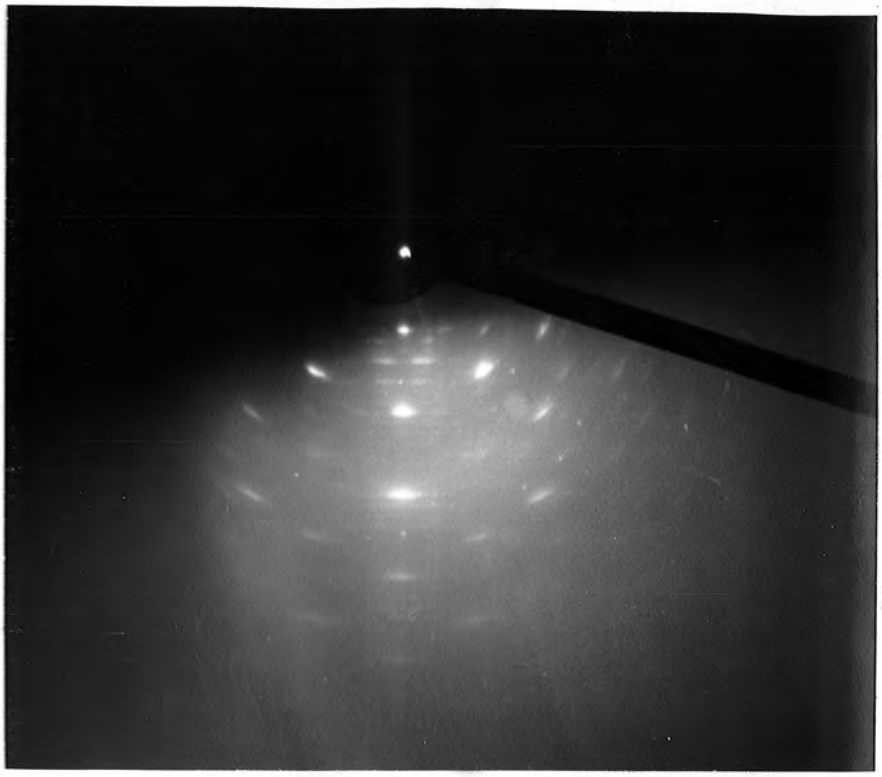

FIG. 6.16 R.E.D. PATTERN FROM A THIN FILM OF CdS WHICH HAS BEEN PARTIALLY CONVERTED TO A PHASE OF COPPER SULPHIDE

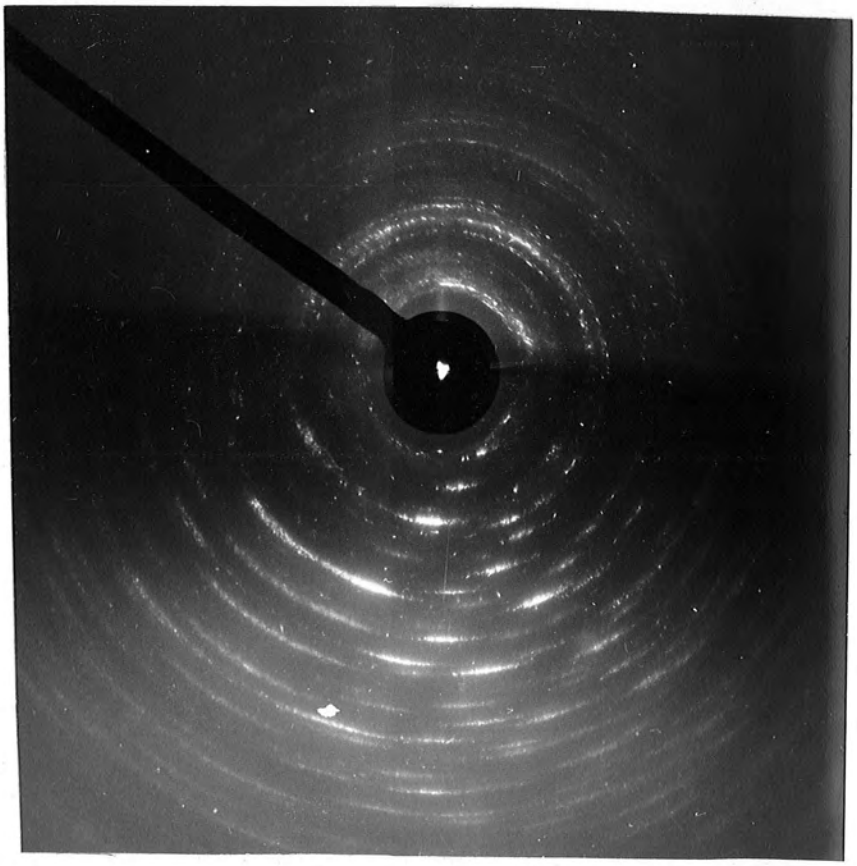

FIG. 6.17 R.E.D. FROM A LAYER OF EVAPORATED CdS SHOWING ORIENTATION EFFECTS

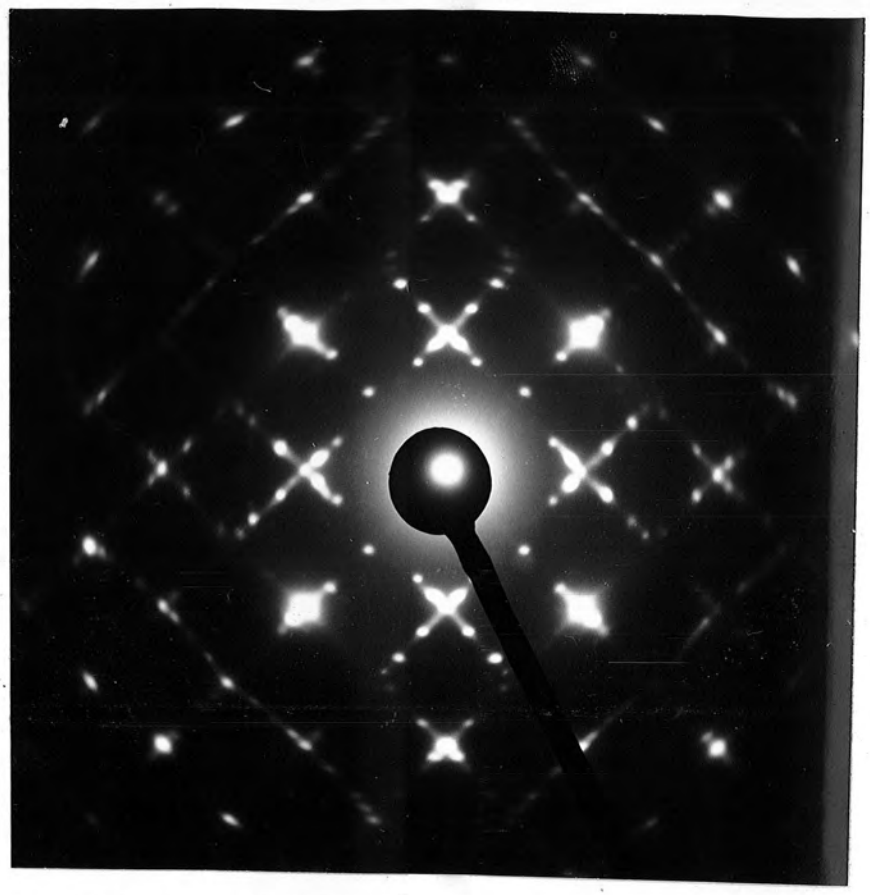

FIG. 6.18 T.E.D. FROM A CdS FILM DEPOSITED ON TO {100} NaCl AT 300°C

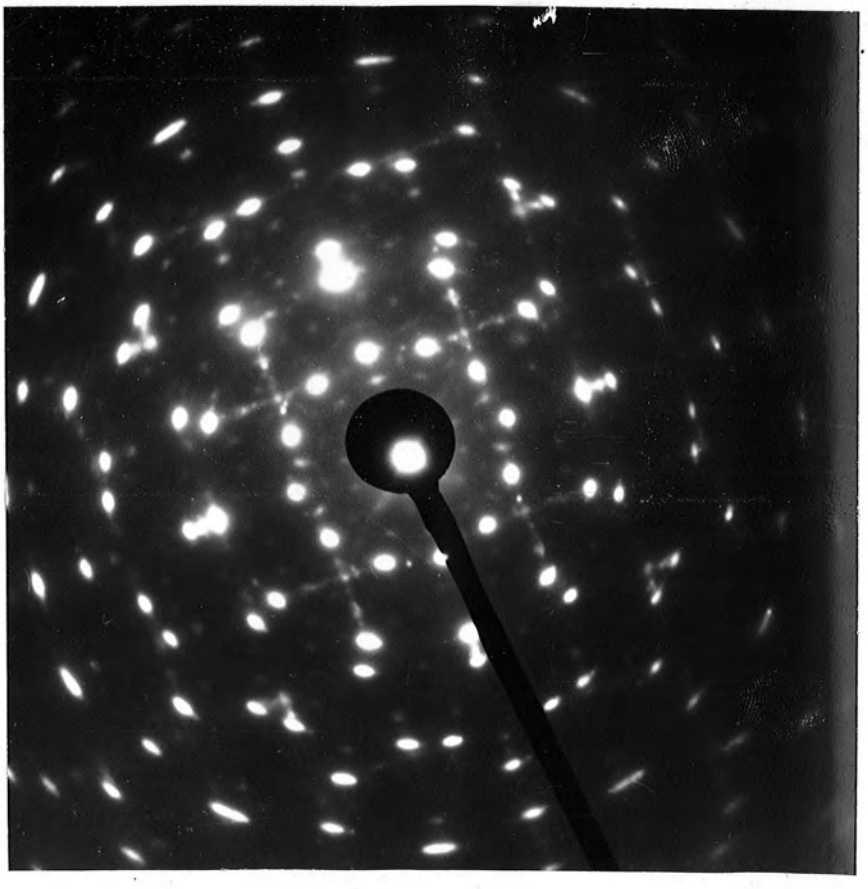

FIG. 6.20 T.E.D. FROM THE SAME FILM AS ABOVE AFTER STORAGE IN THE LABORATORY FOR 2 MONTHS

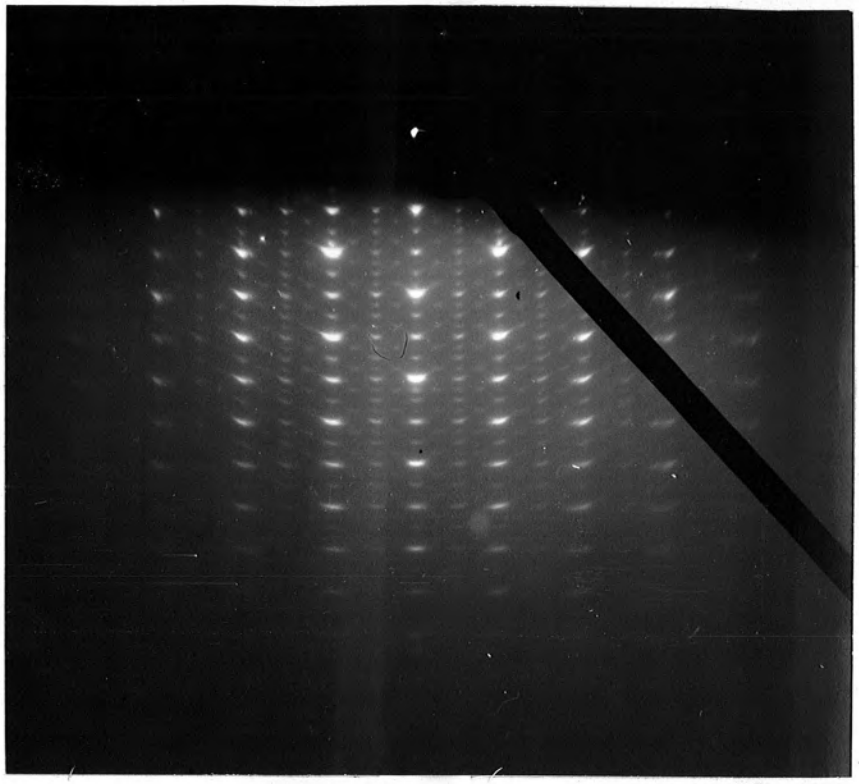

FIG. 6.13 R.E.D PATTERN OF Cu_xS FORMED AT 45°C ON THE S PLANE OF CdS

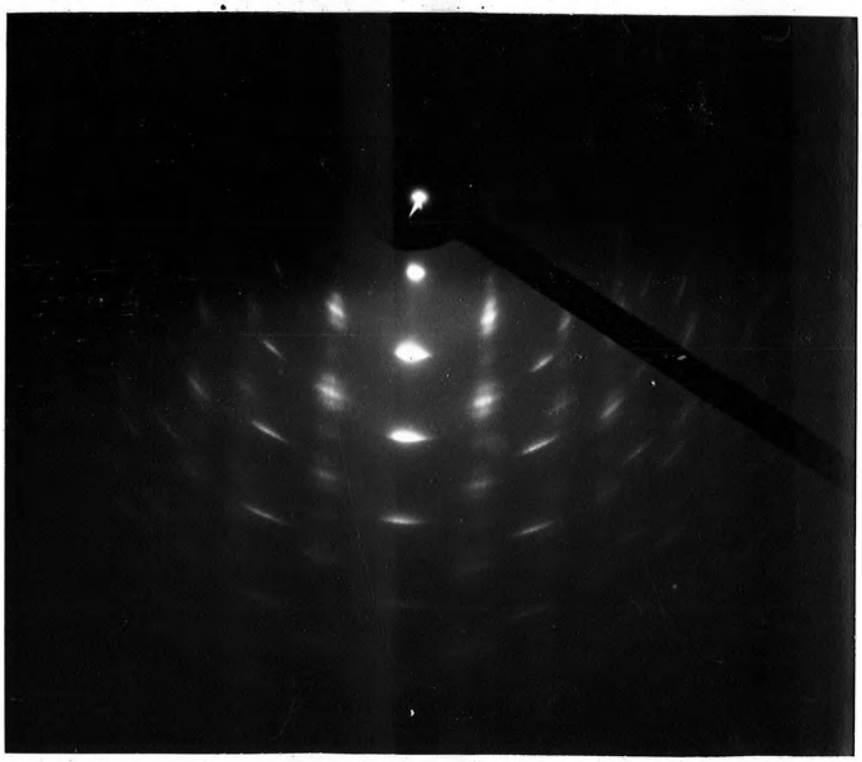

FIG. 6.14 R.E.D PATTERN FROM A 10 μm THICK FILM OF CdS DEPOSITED ON T GLASS

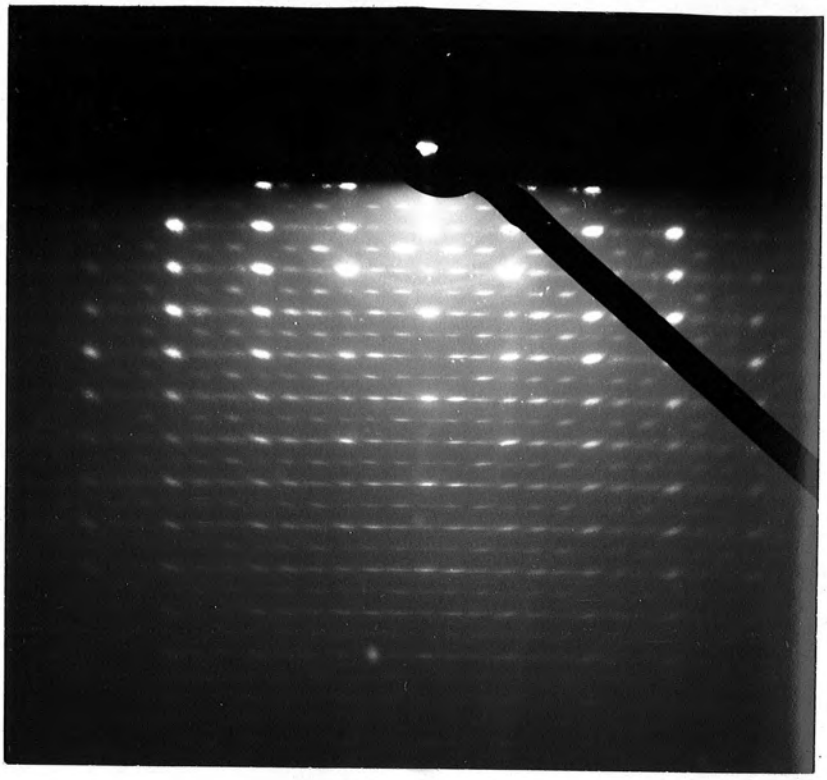

FIG. 6.11 Cu_2S R.E.D. PATTERN FROM THE S PLANE OF CdS

FIG. 6.12 Cu_2S R.E.D. PATTERN FROM THE Cd PLANE OF CdS

CHAPTER 7

PHOTOVOLTAIC AND PHOTOCONDUCTIVE SPECTRAL RESPONSE

7.1 Introduction

If, as it has been proposed, the optimised CdS/Cu_2S solar cell is a p-i-n structure, the dependence of the O.C.V. on incident photon wavelength will be modified by the photoconductive behaviour of the copper compensated region between the p and n type materials. The extent of the contribution of the photoconductive i-region may be reversed by comparison with devices prepared on highly photoconductive base material, where the as-prepared spectral distribution (i.e. prior to baking) should be at least partly determined by the photoconductive response of the bulk material. In view of the fact that Cu_2S grows faster on a CdS single crystal sulphur $(000\bar{1})$ surface than a cadmium plane, it was decided to investigate whether there is a difference in output and spectral response of these two types of device. The effects of different dopants and resistivities of the base material on the spectral distribution, especially as a function of bake time, were investigated.

7.2 Ohmic Contacts

In order to investigate the photoconductive properties of the cadmium sulphide single crystals and to fabricate CdS/Cu_2S solar cells, it was necessary to make good electrical contacts. With bulk CdS samples, good ohmic contact can be made between a metal and the n-type CdS if the work function, ϕ, of the metal is less than that of the n-type semiconductor. Similarly when contact was required to p-type Cu_2S, it

is necessary to use a metal with a larger work function. Both of these cases are examples of 'ohmic' contact where no barrier exists for the flow of electrons in either direction for n-type material or for holes in p-type specimens. If these constraints had not been considered, then rectifying contacts between metal and semiconductor would have existed and the photoconductive properties of the bulk CdS or the photovoltaic behaviour of the CdS/Cu_2S junction would have been modified by the potential barriers produced. Oxide layers between metal and semiconductor would also cause strongly non-ohmic behaviour to be observed. The work functions of most materials and substrates encountered in the investigations are given in Table 7.1. It is well known (Smith 1955) that indium makes an excellent ohmic contact to cadmium sulphide whereas gold does not. Inspection of Table 7.1 and the criteria mentioned earlier show that this is to be expected. However with heavily doped n-type CdS as produced by evaporation in the resistively heated system, both gold and tin oxide coated glass were found to be satisfactory ohmic substrates, whereas indium could not be used because of the high temperatures employed. An intermediate alloy of silver and zinc is also reported to be a good ohmic contact and substrate for evaporated films of CdS, (Shiozawa et al 1969). Unfortunately, thick films of CdS did not adhere to this type of substrate as well as they did to gold or tin oxide coated glass. Indium was used as a contact with all of the single crystal samples.

7.3 Measurement of Spectral Response

7.3.1 General description

All of the spectral response measurements were made over the wavelength range from 0.35 to 1.5 μm, using a Barr and Stroud type

Table 7.1

Work functions of various materials

Material	ϕ eV				
Ag				4.31	Riviere (1957)
Au	4.90	5.38-5.45	Sacher et al (1966)	4.7	Riviere (1957)
Cu	4.4			4.52	Riviere (1957)
In	3.8				
SnO_2	4.7				
$Cu_{2-x}S$	5.4	4.25	Shiozawa et al (1969)		
CdS	5.4 Werring (1973)	4.6	Shiozawa et al (1969)	4.2	Smith (1955)

VL2 monochromator fitted with Spectrosil 'A' prisms. The light source used in all of the experiments was a 250 w tungsten lamp which was powered by a 200 v stabilised d.c. supply. The energy distribution of the source is given in Appendix 1. Relatively large monochromator slit widths of ~1 mm were employed. These were necessary because some of the devices produced very low O.C.V's. when illuminated by light from the exit slit of the monochromator. The large slit widths reduced the resolution of the instrument and since the monochromator was a prism instrument, the dispersion varied with the wavelength of light. For the particular experimental arrangement employed, the bandwidth decreased from 760 Å at 1.15 μm to 140 Å at 0.5 μm.

7.3.2 Setting up Procedure

Before each set of spectral response measurements was obtained the monochromator was calibrated in the following manner. A sodium line source instead of the white light source was positioned at L_1 (Figure 7.1). Mirrors M_1 and M_2 were adjusted until a sharp image of the light source was focused on the entrance slit S_1. A low power microscope was focused on the exit slit S_3 and the wavelength drum D_1 was rotated until the image of the sodium line was observed. Narrow entrance and exit slit widths were employed to obtain maximum resolution. A sensitive light detector which was contained in a metal tube with variable aperture and a shutter assembly was coupled to the exit slit. The detector was an E.M.I. photomultiplier type 9558 with a trialkali S20 photocathode. A Brandenburg power supply unit type 472R was used to provide the 200 v supply to the photomultiplier. The output from the collector electrode of the PM was earthed via a 10 kΩ load resistor and the voltage developed across this was measured using a Philips

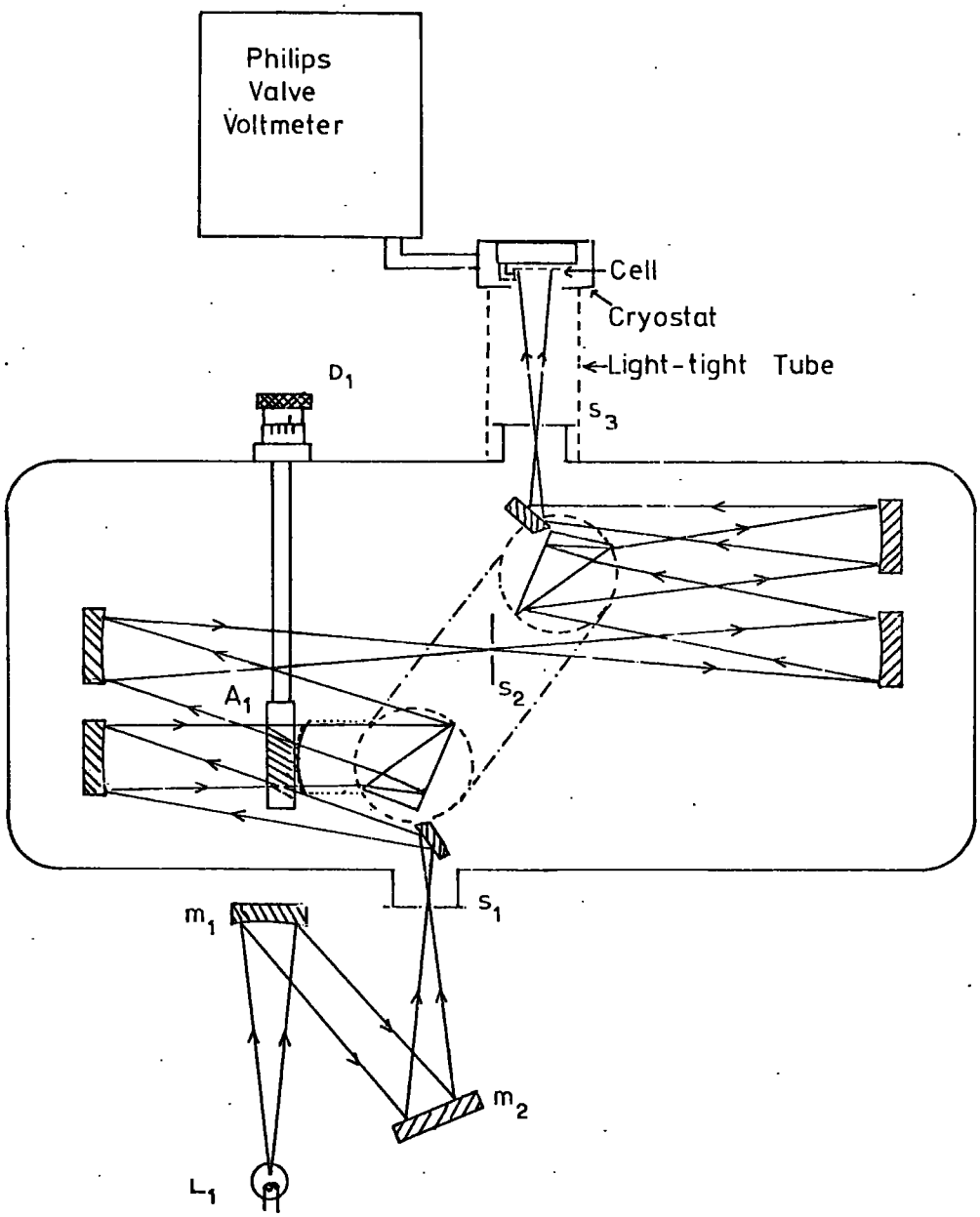

FIG. 7.1 MONOCHROMATOR AND O.C.V MEASUREMENT APPARATUS

valve voltmeter type G.M. 2440. The wavelength drum was adjusted manually for maximum signal across the load. From the manufacturers calibration chart for spectrosil type 'A' prisms, it was found that a drum reading of 22^{o} 35 should correspond to a wavelength of .5896 μm (sodium D_1 line). Slight adjustments were made to the coupling on the spindle (A_1) linking the worm drive and wavelength drum. The monochromator was now calibrated for use. In order that the same amount of light would fall on each sample investigated, adjustments to the mirrors and light source were carried out. This was done in the following manner. A standard silicon solar cell was mounted in a light proof container at the exit slit and the wavelength was adjusted to that of the cells maximum sensitivity. The anode and cathode of the cell were connected via a 1 Ω standard resistor and the voltage developed across this was measured. This was in effect a measurement of the S.C.C. of the cell. The S.C.C. of a silicon cell is a highly dependent function of incident light intensity.

7.4 Bulk Photoconductive Behaviour

7.4.1 Photoconductivity

When certain bulk materials, which are usually insulators or semiconductors, are irradiated with light, their electrical conductivity is found to increase. This phenomenon is termed photoconductivity. The photoconductive gain of a bulk sample may be defined as the number of charge carriers passing between the electrodes per photon absorbed. A gain of less than one means that the electron recombines with a hole before it has reached the anode. The case in which the electron passes through the sample but is not replaced at the negative contact which does not inject another electron to maintain charge neutrality, corresponds to a gain of one. However the best situation for sensitive

photoresponse is when the gain is greater than one. The two main conditions for high gain are (1) the cathode contact must be ohmic and (2) the electron lifetime in the conduction band must be greater than the transit time. The mechanism for high photoconductive gain is as follows. A photon is absorbed and an electron-hole pair is created. Since the electron is more mobile than the hole, at least in II-VI compounds such as CdS, it reaches the anode before the hole has time to reach the cathode. Furthermore, free hole lifetimes are short so that holes are usually trapped very rapidly. Another electron must be injected from the cathode to conserve charge neutrality. It is impossible to produce a fast, sensitive photoconductor since a constant gain . (response time)$^{-1}$ product exists. Long electron lifetime is required for high photosensitivity and this may be achieved by incorporating certain recombination centres into the photoconductor. These defects are called sensitizing centres. The capture cross section, S, of recombination centres for electrons and holes may differ widely. Conventionally there are two types of centre in CdS: Class 1 where $S_e \simeq S_h$ and Class 2 where $S_e \ll S_h$. Where the material contains only class 1 centres short electron lifetime occurs and poor photoresponse is obtained. However if both class 1 and class 2 centres are present, free holes become localised at the latter sites and electrons occupy the class 1 centres. The fast recombination route is effectively blocked and free electrons have long lifetimes. For a much more detailed discussion on photoconductivity, reference should be made to Bube (1960).

7.4.2 Photoconductive Sample Preparations

Most of the single crystal boules from which devices were

fabricated were not photoconductive. This was especially true of low resistivity, cadmium rich, indium or chlorine doped samples. However, high resistivity cadmium sulphide either undoped or containing copper showed substantial bulk photoconductivity.

Specimens from the boules were prepared in the following manner. Several slices 2 mm thick were cut perpendicular to the 'c' axis and after mechanically polishing the cadmium and sulphur faces, the slices were further sectioned into cubes of side 2 mm. After a light etch for 30 s to 120 s in cold concentrated hydrochloric acid, the cubes were washed in distilled water and dried in a stream of nitrogen gas. The purpose of the etch was to remove the oxidised and work damaged surface layers which would otherwise produce non-ohmic contacts. Ohmic contacts to two opposite cube faces were made using indium. This was effected by pressing small slices of 1 mm diameter indium wire on to the appropriate faces and then heating at 200^{o}C for 15 mins in an inert argon atmosphere.

The specimens of high resistivity ($\sim 10^{6}$ Ω cm) undoped CdS and low resistivity ($\sim 5 \times 10^{3} \Omega$cm) copper doped CdS were then placed in a dark enclosure and the forward and reverse current-voltage characteristics were plotted to confirm ohmic behaviour. This was done using a standard power supply and measuring instruments and typical recorder traces for the two types of boule shown in Figure 7.2. It should be noted that pressed/alloyed indium contacts were utilised rather than evaporated indium contacts because the latter occasionally gave rise to non ohmic behaviour, whereas consistent results were obtained using the alloying method.

FIG. 7.2 I-V CHARACTERISTICS (DARK)

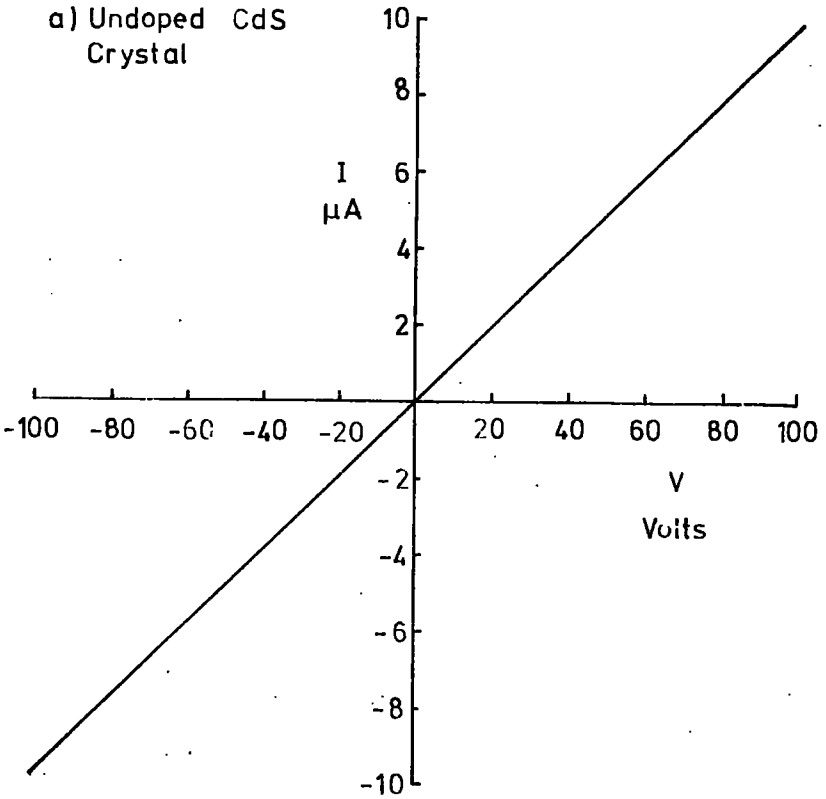

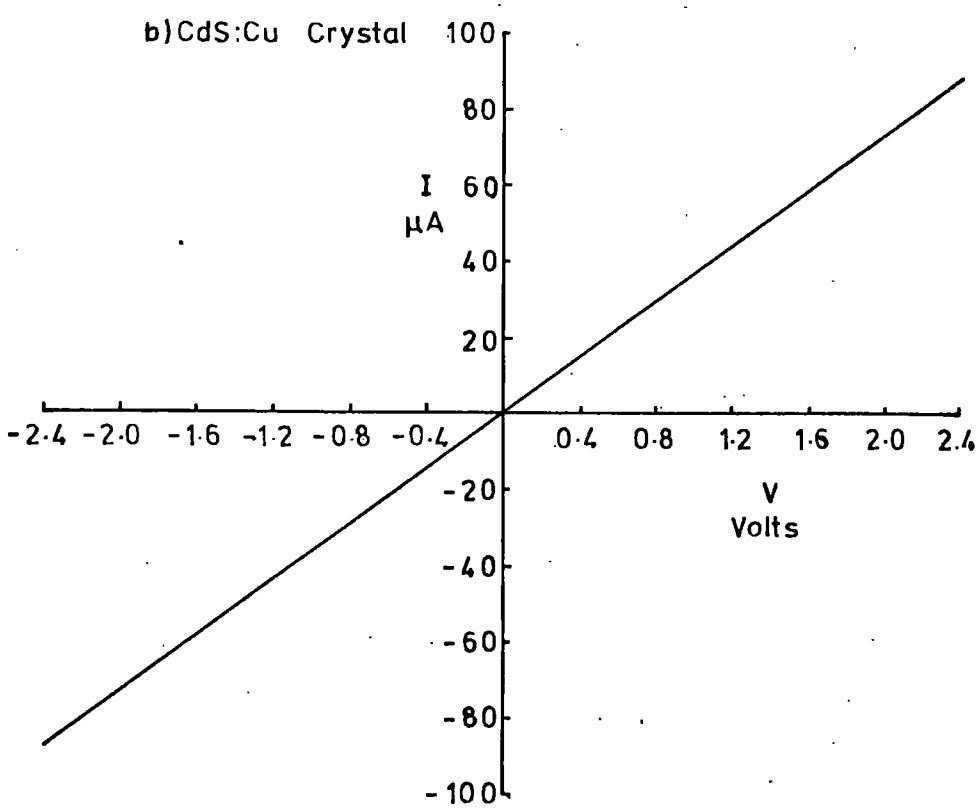

7.4.3 Photoconductive Spectral Distribution

The photoconductive spectral responses of various samples of cadmium sulphide were measured using the Barr and Stroud type VL2 prism monochromator discussed earlier in this chapter. Photoconductive response curves were obtained by applying a constant voltage across the sample and measuring the current flowing through a sensitive microammeter as the wavelength of the radiation falling on the sample container was scanned manually from high to low wavelengths. Some crystals had very long photoconductive response times of up to several minutes and measurements were therefore taken under steady state conditions. None of the samples with resistivity less than 5 Ω cm (i.e. CdS:Cd, CdS:Cl and CdS:In) showed any photoconductive behaviour. On the other hand the undoped CdS and CdS containing copper or chlorine and copper showed sensitive photoconductive behaviour. Consequently, response curves were obtained from undoped CdS and CdS:Cu samples. Typical response curves are shown in Figure 7.3. These curves have not been corrected for the energy distribution of the light source or the varying dispersion of the monochromator. Response curves of both CdS and CdS:Cu have been normalised on the same graph and each curve is a relative response. The relative change in resistivity as a function of wavelength was much greater for the undoped CdS samples than for the copper doped material.

7.4.4 Discussion of Photoconductive Responses

The spectral response of the photocurrent from the undoped CdS was very narrow (bandwidth ~1000 Å) and was centred at approximately 0.53 μm. This would correspond to the bandgap excitation of intrinsic CdS. On the other hand, the response of the copper doped CdS was very

FIG. 7.3 UNCORRECTED PHOTOCONDUCTIVE RESPONSE CURVES OF BULK SAMPLES

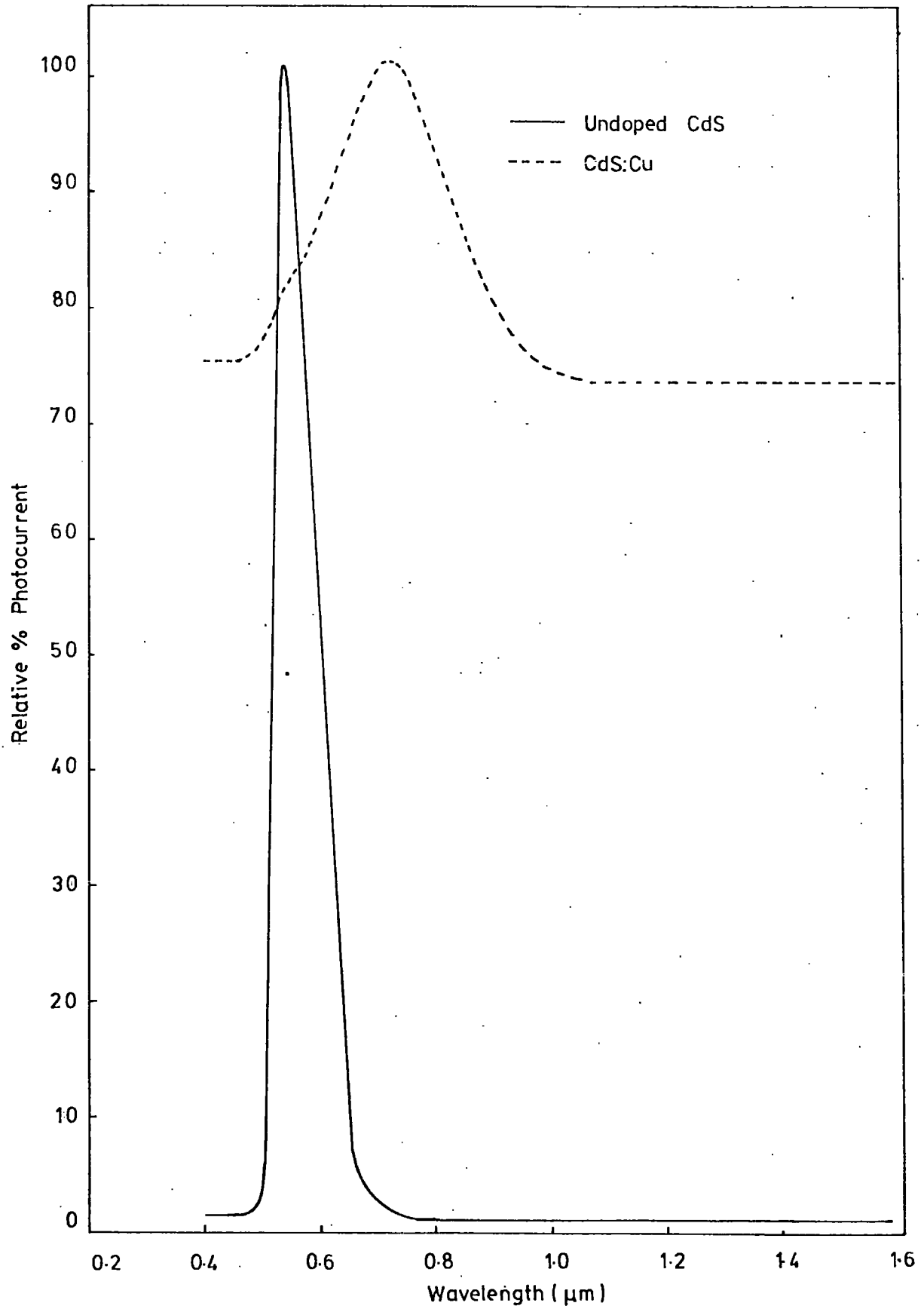

broad. The bandwidth was approximately 3000 Å and was centred at about 0.67 μm. In addition there was an unresolved peak in the vicinity of 0.51 μm. Copper impurities produce deep acceptor levels and in most crystals there are also small amounts of chlorine donor impurities. The copper levels are distributed over a range of energies about 1 eV above the valence band, and the response associated with transitions between these levels and the conduction band is broad. It is worth noting that the response of the copper doped CdS samples was similar to that of a commercially obtainable ORP 12 photoconductive cell which is fairly heavily doped with copper.

7.5 Fabrication of CdS/Cu_2S Solar Cells (Single Crystal)

Orientated single crystal slices of cadmium sulphide were cut from the doped and undoped boules using a diamond impregnated saw and the cadmium and sulphur planes were polished to remove cutting marks as described in Chapter 6. Further sectioning of these polished slices was carried out to produce many 2 mm cubes. Indium contacts were formed on the cadmium or sulphur planes as required and the dice were bonded to a microscope slide, eight at a time, with the cube faces to receive the copper sulphide layers uppermost. After bonding, the four unpolished faces were coated with an acid resistant lacquer and the simple exposed faces of the cubes were etched lightly in hydrochloric acid to remove any oxide layers. The cubes were then plated with copper sulphide under nearly identical conditions by immersing the slide in the standard copper ion plating bath as discussed earlier. A plating temperature of 90°C was employed and all of the devices were dipped for 10 seconds. This dip time was known to produce a copper sulphide layer

~ 0.1 μm thick. After removal from the plating bath, the slides were rinsed in distilled water and then dipped in acetone to remove the bonding agent and lacquer. Each individual cube was mounted on a copper disc by embedding the indium contact in Johnson Matthey silver paste type FSP 51. The devices were stored in a vacuum dessicator away from light until required for evaluation. Storage times of less than three days were usually employed. A very simple approximate evaluation of the O.C.V. of a device was carried out by placing it under a high intensity light source and measuring the O.C.V. by means of a high impedance voltmeter.

Various parameters of the devices were measured including the O.C.V., S.C.C., O.C.V. vs λ and O.C.V. vs light intensity. Several parameters were also investigated as a function of the heat treatment to which the device was subjected.

7.6 Dependence of O.C.V. on junction polarity

To investigate the effects of preparing layers of copper sulphide on cadmium and sulphur planes of the cadmium sulphide cubes, a number of samples of both polarities were irradiated with light from a 1.5 Kw tungsten halogen strip lamp (colour temperature ~3200 K) filtered by 1 cm of water to remove some of the infra-red radiation. This source gave a power density ~100 mw/cm^2 over a small area, but the spectral distribution was not very close to that of the sun. The O.C.V's. of all the cells were measured under the same intensity of illumination. It was not possible to measure S.C.C. accurately because its value was very sensitive to the size and quality of the contact to the copper sulphide layer. A spring loaded phosphor bronze probe was used as a contact to the p-type copper sulphide. The O.C.V. could be measured with much greater

reproducibility. Under illumination with light from the 1.5 Kw lamp, the O.C.V's. of the as-prepared sulphur plane cells were on average some 20% larger than the O.C.V's. of cells formed on cadmium faces.

7.7 Effect of Crystallographic Polarity on Spectral Response

The photovoltaic spectral responses of devices formed on both cadmium and sulphur planes were investigated using the monochromator and tungsten light source. For the reason given in the previous section it was decided to measure O.C.V. as a function of wavelength rather than S.C.C. O.C.V's. were measured using a high impedance (10^8 Ω) voltmeter (Philips type GM 6020) except for devices made on material with a resistivity in excess of 10^6 Ω cm when either a buffer amplifier or a Vibron electrometer model 33B was used. This was only necessary for investigations on devices formed on high resistivity undoped material. After measurements of the spectral response, the devices formed on the cadmium and sulphur planes of undoped material were heated in air at 200°C for varying periods of time up to 20 mins. Spectral distributions were re-assessed after each heat treatment. The variation in spectral response as a function of heat treatment is shown in Figures 7.4 and 7.5 for typical devices formed on cadmium and sulphur planes. The curves have not been corrected for the distribution of energy with wavelength of the source, or the varying dispersion of the prism monochromator.

There was little discernible difference between the spectral distributions of the O.C.V's. of cells prepared on cadmium or sulphur faces; in both devices three major peaks were observed in the vicinity of 0.5, 0.68 and 0.9 μm. Their spectral location was not apparently affected by the polar faces on which the junction had been prepared.

FIG. 7.4 O.C.V. SPECTRAL RESPONSE OF Cd PLANE DEVICE

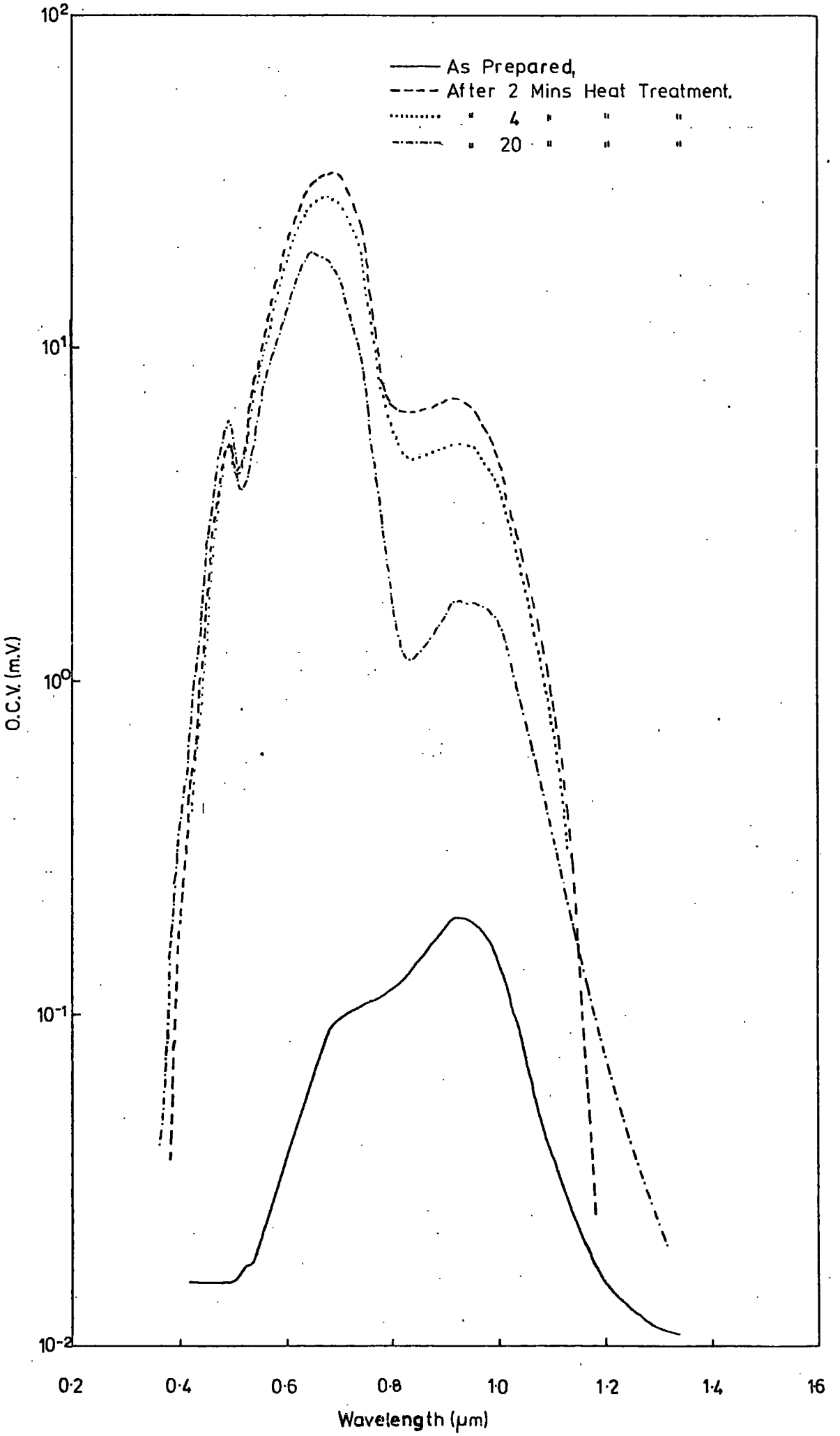

FIG. 7.5 O.C.V. SPECTRAL RESPONSE OF 'S' PLANE DEVICE

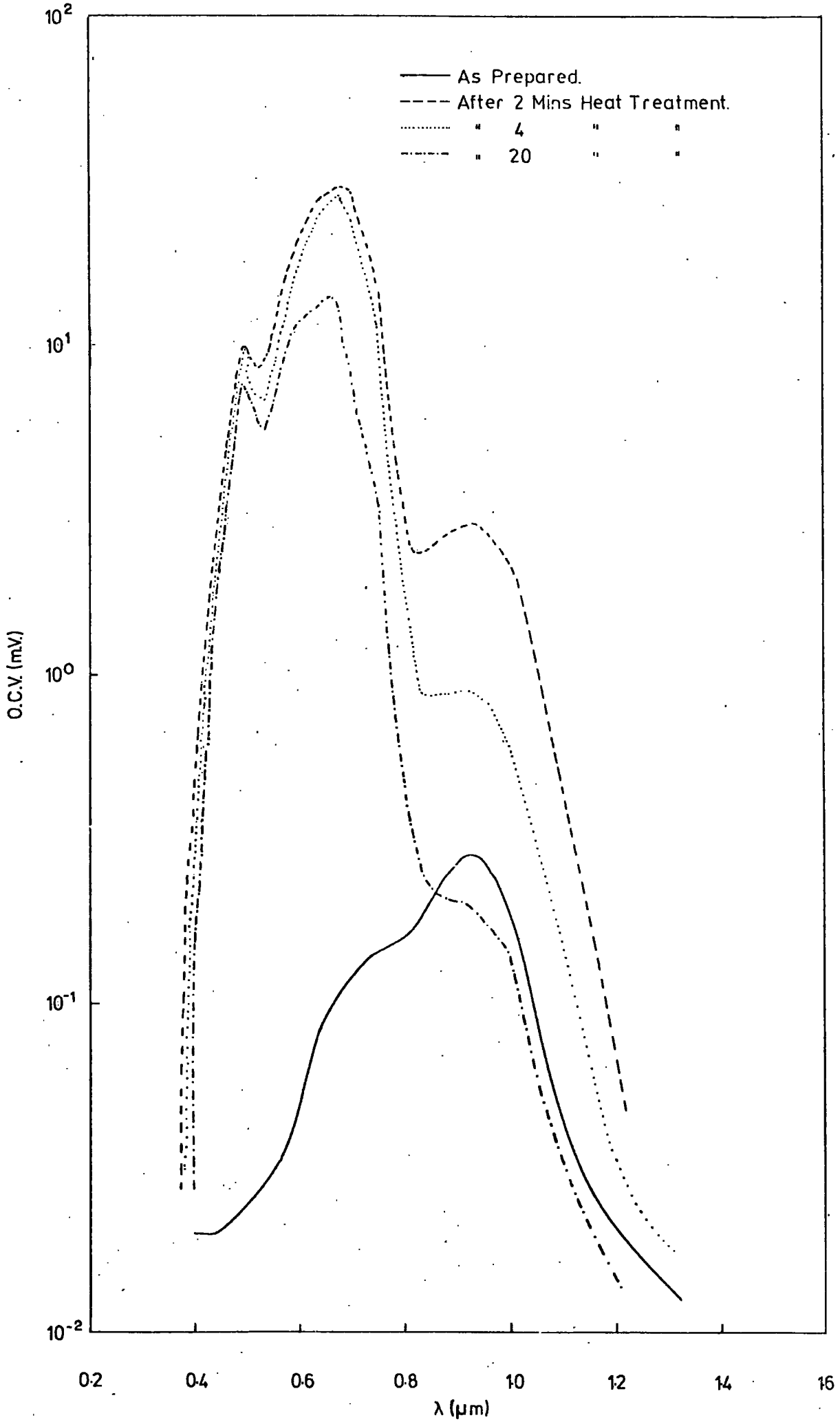

What was apparent was that baking at 200°C for 2 min greatly enhanced the response in the bands at 0.68 and 0.9 μm. However prolonged baking led to a small reduction in the photovoltaic sensitivity at 0.68 μm and a larger reduction at 0.9 μm. The only difference between cadmium and sulphur plane devices subjected to the same 20 min bake in air at 200°C was that there was a larger relative depression of the 0.9 μm band for the sulphur plane device.

Following these experiments, it was decided that all future devices would be prepared on sulphur planes of the doped and undoped cadmium sulphide. The main reason for this was the slightly larger O.C.V. produced by sulphur plane junctions.

7.8 O.C.V. Spectral response as a function of CdS doping and resistivity

Wilson and Woods (1972) showed that for optimum photovoltaic efficiency, the resistivity of the base cadmium sulphide should be $\sim 10^2$ Ωcm. However, in the investigations described here, five types of cadmium sulphide single crystal were investigated. The range of resistivity and dopants used were chosen not to give optimum efficiency but to investigate the dependence of spectral response on resistivity and dopant of the base material. All of the boules had been grown using techniques described by Clark and Woods (1968).

7.8.1 Low resistivity undoped CdS

The uncorrected spectral response of the O.C.V. of a typical cell formed on the sulphur plane of a low resistivity sample of undoped cadmium sulphide is shown in Figure 7.5. There are four curves showing how the spectral distribution varied as a function of bake time in air

at 200°C. The curves are uncorrected since it is easier to distinguish the salient features before correction (but see Appendix 1). There are three main peaks in the curves of Figure 7.5 at wavelengths of 0.92, 0.68 and 0.49 μm. With the as-plated cell, the maximum O.C.V. occurred at 0.92 μm while there was slight evidence of a peak in the vicinity of 0.5 μm. Following the heat treatment at 200°C (a bake in air at 200°C for approximately 2 mins is normally administered to achieve optimum efficiency), the O.C.V. clearly increased in magnitude initially, before decreasing slowly as the baking was prolonged. At the same time, the response became larger in the band at 0.68 μm than in that at 0.92 μm and the peak at 0.49 μm became quite apparent.

It should be recorded that when spectral response measurements were being made, the wavelength was always scanned manually from long to short wavelengths. With the as-plated undoped low resistivity device, the response of the O.C.V. to incident monochromatic radiation was faster than that of the associated instrumentation which was approximately 10 seconds. However after a cell had been baked, the O.C.V. increased rapidly for a few seconds following exposure to monochromatic radiation and then changed slowly over a period of the order of several minutes before reaching a steady state value. Generally, the longer the heat treatment, the slower was the response time. The curves shown in these investigations were obtained by waiting for steady state conditions to be obtained at each wavelength measured.

7.8.2 High resistivity undoped CdS

The spectral distribution of the O.C.V. of a typical cell formed on high resistivity undoped cadmium sulphide is depicted in the curves in Figure 7.6. In contrast with cells discussed in the

FIG. 7.6 O.C.V. SPECTRAL RESPONSE OF A TYPICAL DEVICE FORMED ON HIGH RESISTIVITY ($\rho \approx 10^6 \Omega$ cm) UNDOPED CdS

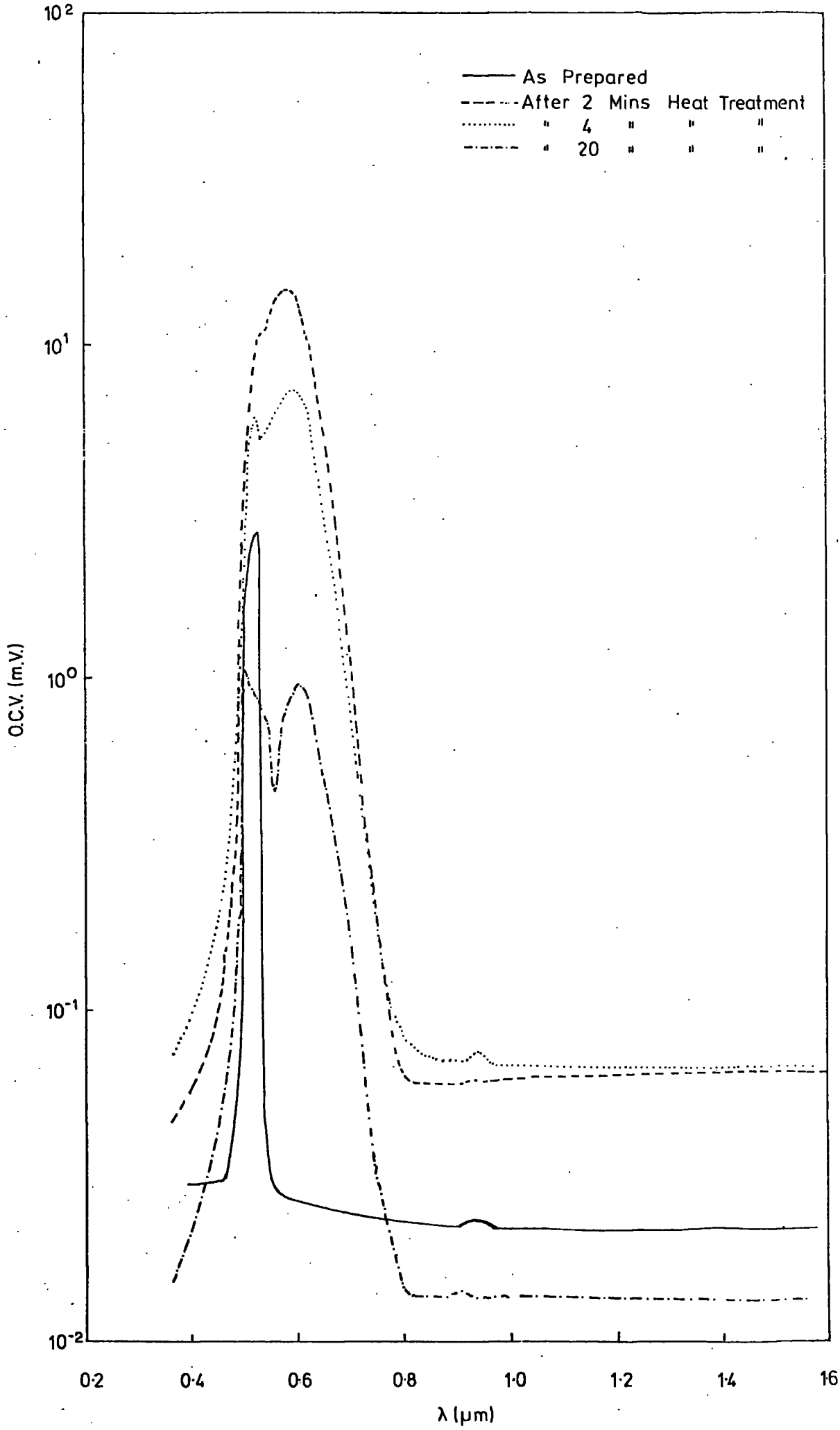

previous section (7.8.1), which had very little response near the band-gap of CdS immediately after plating, these cells had a sharp and narrow response at 0.52 μm. There was no evidence at all of a band in the range 0.6 - 0.7 μm, but there was a small feature at about 0.92 μm which suggested some selective response at this wavelength at least.

After the cell had been baked at 200°C for 2 min. in air, the O.C.V. increased substantially and the spectral response now extended over a wider range of wavelengths leading to a broad band with a maximum near 0.6 μm. Following further heat treatment, the O.C.V. fell in magnitude and the spectral response indicated two bands with maxima at 0.49 μm and 0.6 μm.

The O.C.V. of this type of cell was relatively large, i.e. it exceeded 150 mV when the illumination was provided by ambient daylight. The response time was very long, being of the order of several minutes. Since the internal impedances of these particular cells were very high, care had to be taken to ensure that the instruments used to measure the O.C.V. offered negligible load to the devices.

7.8.3 Copper doped low resistivity crystals

Curves illustrating the spectral distribution of the O.C.V. of cells prepared on low resistivity crystals doped with copper are shown in Figure 7.7. There are clearly certain similarities with the curves of Figures 7.4 and 7.5 which are for the cells formed on low resistivity undoped crystals. However there is one notable difference, namely that the photovoltaic output from an unbaked cell on a copper doped crystal is much higher than that from an unbaked cell on an undoped crystal. Furthermore the relative response in the range 0.7 - 0.8 μm is enhanced. After baking, the spectral peaks at 0.7 and 0.49 μm

FIG. 7.7 O.C.V. SPECTRAL RESPONSE OF A TYPICAL DEVICE FORMED ON CdS:Cu

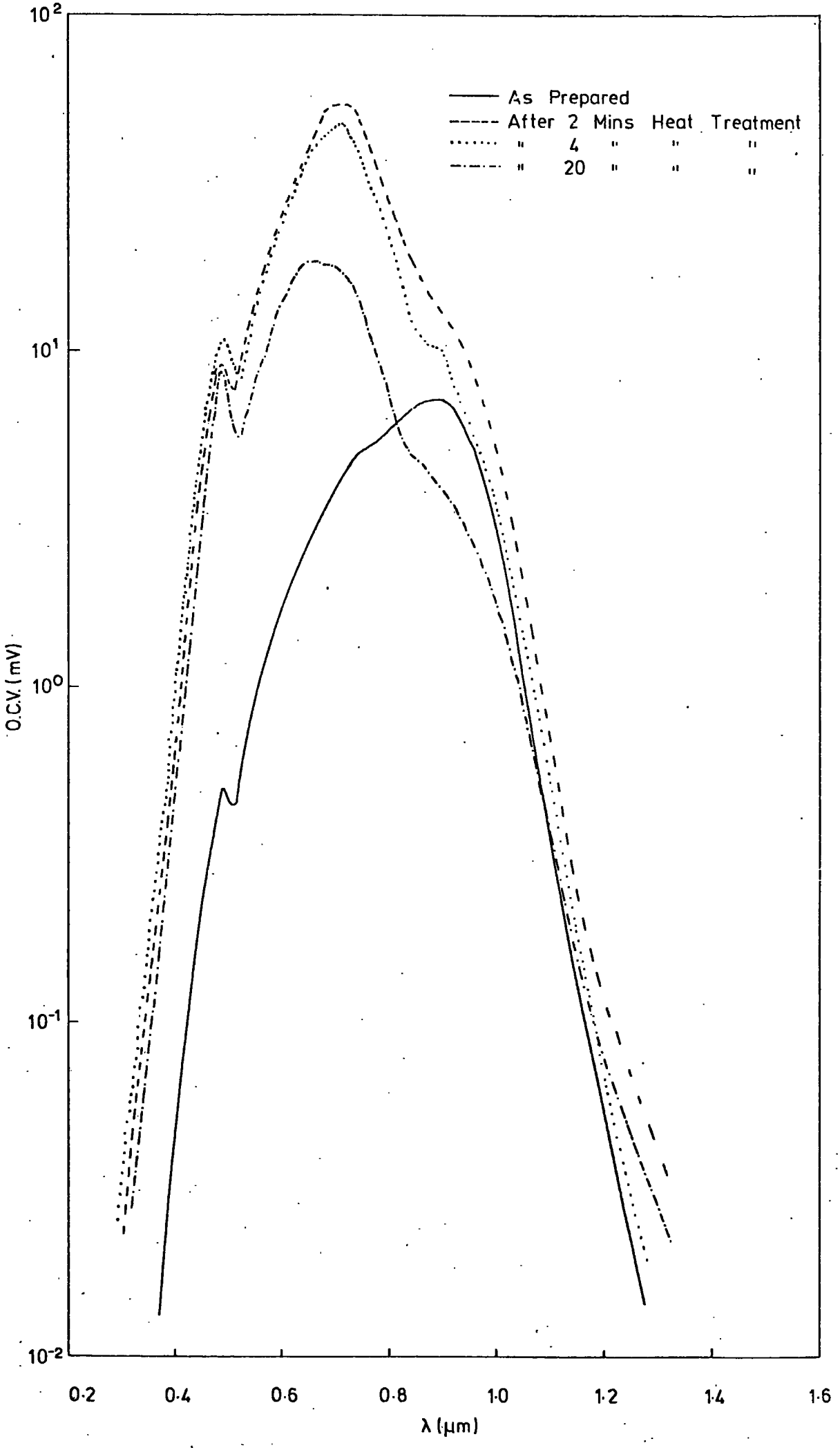

increased in magnitude whereas that at 0.9 μm eventually decreased slightly.

With the as plated device, the response to monochromatic radiation was not immediate. Steady state conditions occurred after about one minute. The response times lengthened as the cell was heat treated.

7.8.4 Indium doped very low resistivity CdS

The set of curves showing the spectral distribution of the O.C.V. of cells heavily doped with indium is shown in Figure 7.8. None of the devices produced on this very low resistivity ($\sim 10^{-2}$ to 10^{-1} Ω cm) cadmium sulphide produced very high O.C.V's. even under the direct illumination from the 1.5 Kw lamp. The voltages obtained using monochromatic illumination were correspondingly lower. Consequently the various peaks are more distinguishable if the O.C.V. is plotted as a relative percentage. The spectral distribution curve of the as-prepared cell shows close similarity in shape, if not in magnitude, to the curve for an as plated device fabricated on low resistivity undoped cadmium sulphide. Clearly the main peak is in the vicinity of .93 μm but there is evidence of an unresolved peak of lower magnitude in the region of 0.7 to 0.8 μm. Following a 2 min bake in air, the O.C.V. increased in magnitude but the shape of the curve did not alter. Further heating caused an overall decrease in sensitivity. After a 10 minute bake in air at 200°C, the peak had shifted to the shorter wavelength of .87 μm and after a total heat treatment of 20 mins, to 0.85 μm. The sensitivity of the device was now less than that of the as-prepared cell.

There was no evidence at any stage of the treatment of any peak in the vicinity of 0.5 μm. Another feature of this cell was that the response time of this device even after prolonged heat treatment

FIG. 7.8 O.C.V. SPECTRAL RESPONSE OF A TYPICAL DEVICE FORMED ON CdS:In

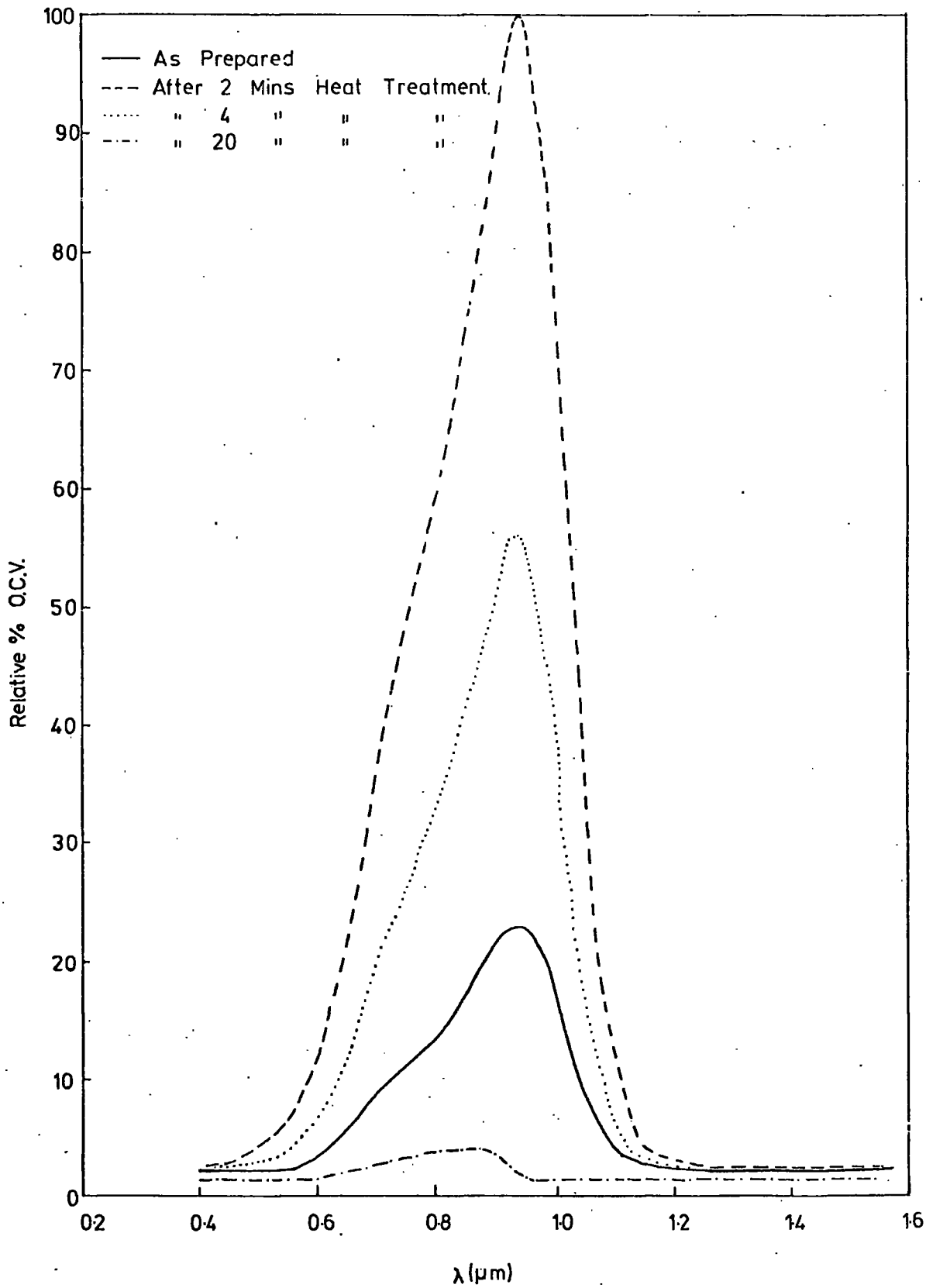

was faster than any of the cells previously investigated.

7.8.5 Chlorine doped CdS

Curves showing the O.C.V. spectral response as a function of heat treatment of devices formed on chlorine doped crystals with very low resistivity (10^{-2} to 10^{-1} ohms cm) are shown in Figure 7.9. These cells have low O.C.V. ($\sim$ mV) under high light intensities ($\sim$ 100 mW cm^{-2}) like those discussed in the previous section (7.8.4). The as prepared device showed a main peak at 0.94 μm with an unresolved 'shoulder' in the vicinity of 0.7 to 0.8 μm. After a 2 min heat treatment in air, the O.C.V. had increased and the main peak was still at 0.94 μm. Further heating caused an overall decrease in sensitivity but a small peak in the vicinity of 0.75 μm appeared. Prolonged heating produced a still lower sensitivity but the 0.75 μm peak broadened significantly.

Devices formed on very low resistivity ($\sim 10^{-2}$ to 10^{-1} Ωcm) CdS, which was heavily doped with indium or chlorine, showed no evidence of a peak in O.C.V. spectral response in the vicinity of 0.5 μm even after continued heat treatment. The response times for both types of device were fast (less than 30 seconds).

7.9 Fabrication of Thin Film Cells

The thin film cells were all prepared from layers of cadmium sulphide evaporated on to different substrates as discussed in Chapter 5. Many such evaporated layers were produced in the 12" vacuum system with a resistively heated source, but this led to a poor quality of film with visible pinholes. It was also very difficult to produce layers more than a few micrometres thick without them beginning to peel

FIG. 7.9 O.C.V. SPECTRAL RESPONSE OF A DEVICE FORMED ON CdS:Cl

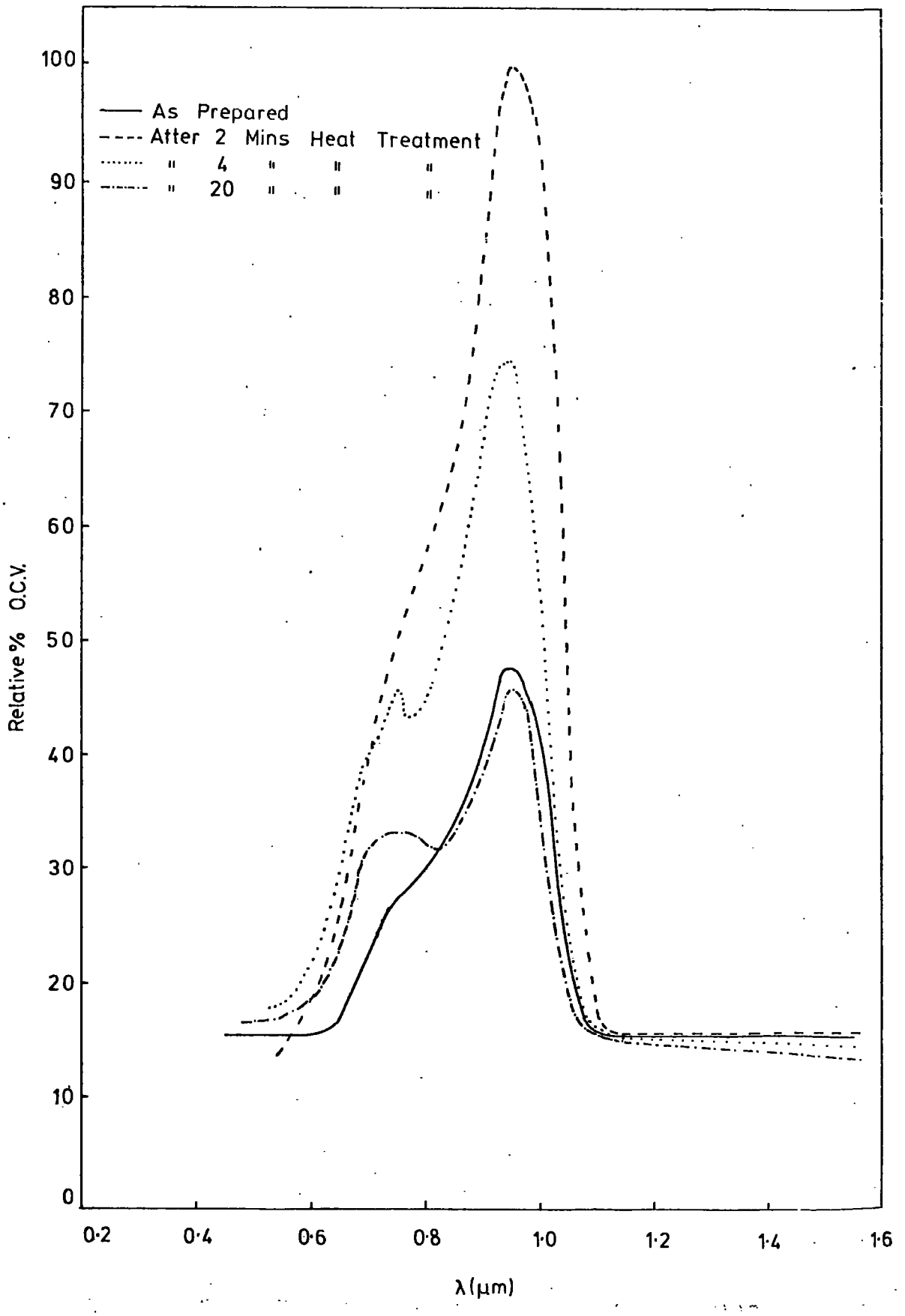

from the substrate. The thicknesses of the evaporated layers were measured using the interferometer and mechanical gauge methods discussed in Chapter 5. It was found that photovoltaic devices could only be fabricated on films produced using the Durham 12 " vacuum system, which were thicker than about 15 μm. The I.R.D. thin films were generally thicker than this.

The edges of the evaporated films were painted with an acid resistant lacquer to prevent the plated copper sulphide from shorting directly to the substrate. The lacquer also served to prevent the film from peeling at its edges when it was immersed in the aqueous plating bath. As with the single crystal cells, it was necessary to etch the film surface lightly before plating, for two reasons, (1) to remove any oxide layers before conversion to copper sulphide, and (2) to etch down the grain boundaries to provide a larger surface area junction. This latter process leads to higher short circuit currents. It was not possible to use hydrochloric acid as an etchant since it was too efficient. Instead a strong solution (1N) of potassium iodide was employed. A dip of several minutes roughened the film surface adequately. After the etching, the cells were washed thoroughly in distilled water.

To form a layer of copper sulphide, the film was immersed in the standard plating solution for 5 secs at 90°C. After a short rinse in distilled water, the cell was dried in a stream of dry nitrogen. Prior to evaluation, or gridding and encapsulation, the thin film cells were stored in the dark in a vacuum dessicator.

Thin film cells for commercial use would normally be gridded to reduce series resistance to the copper sulphide layer. Finally to reduce oxidation, a permanent encapsulation process would be carried out.

It was not possible to do this for cells with which various properties were to be investigated as a function of bake time in various ambients, so methods had to be devised of producing a temporary, removable grid which could be reapplied after each treatment.

A compressed air jig was therefore designed. This is shown in Figure 7.10. With this technique a gold plated grid with 90% transmission was made to contact the copper sulphide layer by applying compressed air to the flexible transparent membrane. This method worked very well and the cell could be removed for subsequent treatments.

In preliminary trials, gold grids were evaporated on to the copper sulphide surface but appeared to have the disadvantage that this caused some degree of heating which changed the cell properties.

Relatively permanent encapsulation and fixing of the grid in contact with the copper sulphide layer was achieved using self adhesive 'Melinex'. This method was convenient and simple but the adhesive weakened with time and contact to the copper sulphide became unreliable.

The standard method of permanent encapsulation and gridding in a clean room was carried out on a number of thin film cells prepared at I.R.D. Ltd. Cells which had been subjected to an optimum heat treatment in air at 200^{o}C were bonded to a molybdenum sheet using silicone adhesive tape. Areas of 1 cm^{2} were cut from 90% transmission gold grid (20 lines/cm) and the grid lines were coated with gold filled epoxy cement. Cover pieces were cut from 25 μm thick Melinex coated with a 10 μm layer of transparent epoxy adhesive. The thin film cell was held to a hot plate/metal base using vacuum suction and the grid and cover plastic were clamped in place using an over pressure of 60 P.S.I. nitrogen acting on a P.T.F.E. disc. The epoxy adhesive was cured by heating to 200^{o}C for

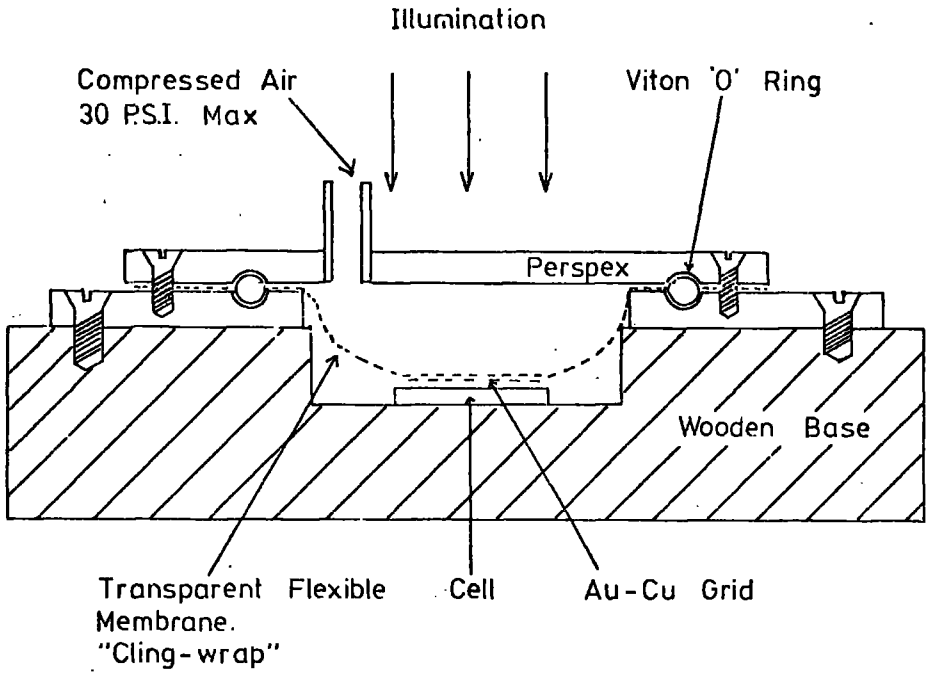

FIG. 7.10 TEMPORARY GRIDDING JIG

several minutes. After cooling to room temperature, the cells were removed and stored in a vacuum dessicator in the dark.

7.10 Spectral Response of Thin Film Cells

The uncorrected spectral distribution of the O.C.V. of a typical thin film cell produced at I.R.D. in the 18" vacuum system is shown in Figure 7.11. Four curves are included to show how the O.C.V. spectral response varied as a function of bake time in air at 200°C. There are two main peaks at 0.92 μm and in the region from 0.6 to 0.7 μm. For the as-plated cell, the main peak is at 0.92 μm and there is evidence of an unresolved peak in the region 0.6 to 0.7 μm. Following heat treatment at 200°C for two minutes in air, the O.C.V. increased greatly in magnitude with the main peak in the vicinity of 0.9 μm and a second unresolved peak in the region of 0.7 μm. Further heating caused an overall decrease in sensitivity and after a total of 16 mins heating in air, the main peak was at 0.63 μm with a second resolved peak at 0.92 μm.

The response time of the unbaked cell was quite fast (~15 secs) but as heat treatment was prolonged, the response time at certain wavelengths (0.6 to 0.7 μm) lengthened to one or two minutes.

Most films evaporated on to tin oxide coated glass in the 12" vacuum system were too thin to enable devices to be prepared, but several did lead to devices with low outputs for which a spectral distribution could be obtained as a function of bake times in air at 200°C. A typical set of curves for such a cell is shown in Figure 7.12. Here the main peak is at 0.9 μm, but an unresolved 'shoulder' in the vicinity of 0.7 to 0.8 μm is clearly visible. Baking for 2 minutes in air led to an overall improvement and it was then possible to resolve both peaks in the region 0.9 μm and 0.72 μm. Heat treatment for 8 minutes

FIG. 7.11 O.C.V SPECTRAL RESPONSE OF AN I.R.D THIN FILM CELL

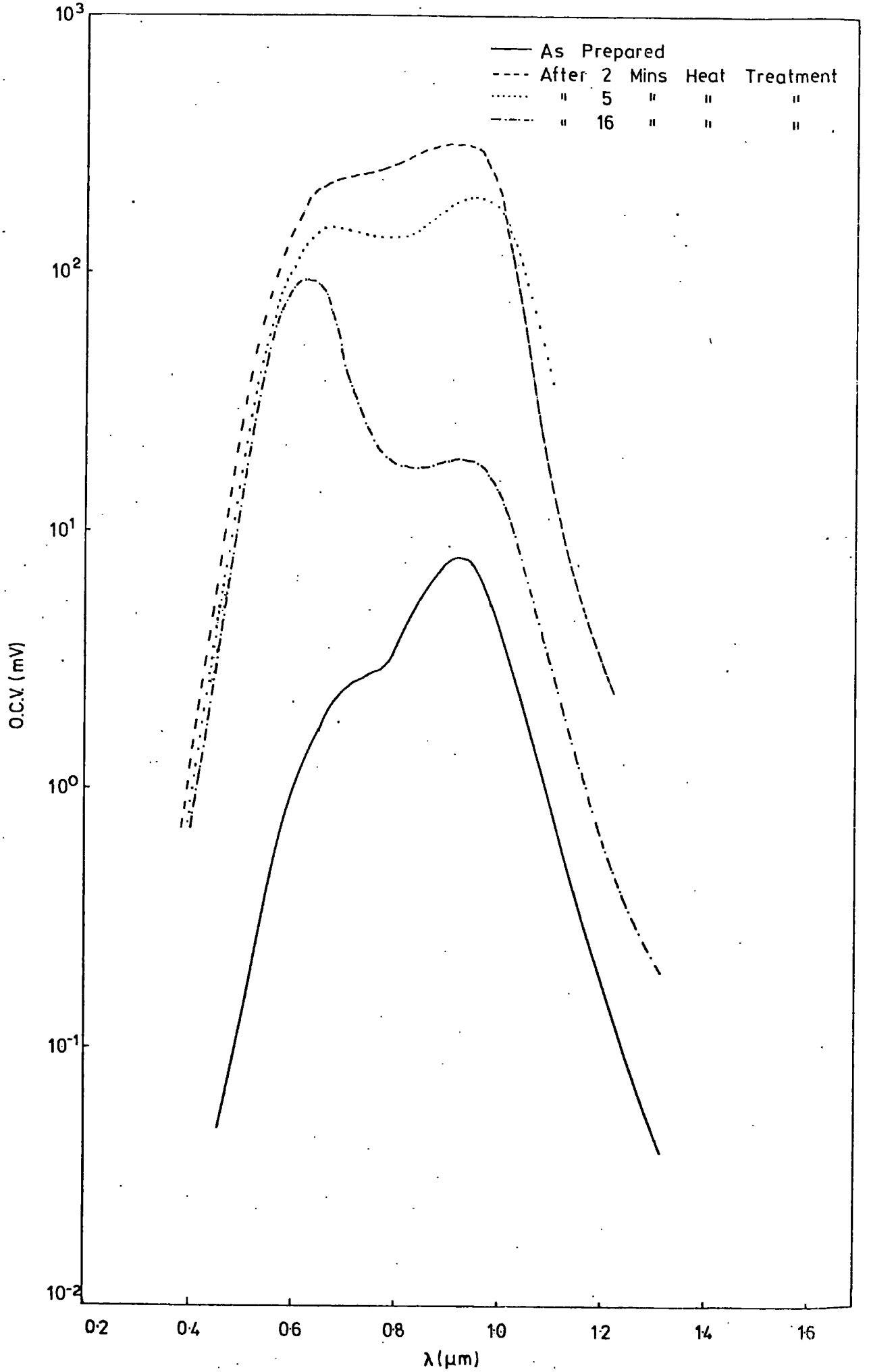

FIG. 7.12 O.C.V. SPECTRAL RESPONSE OF A TYPICAL DURHAM THIN FILM CELL

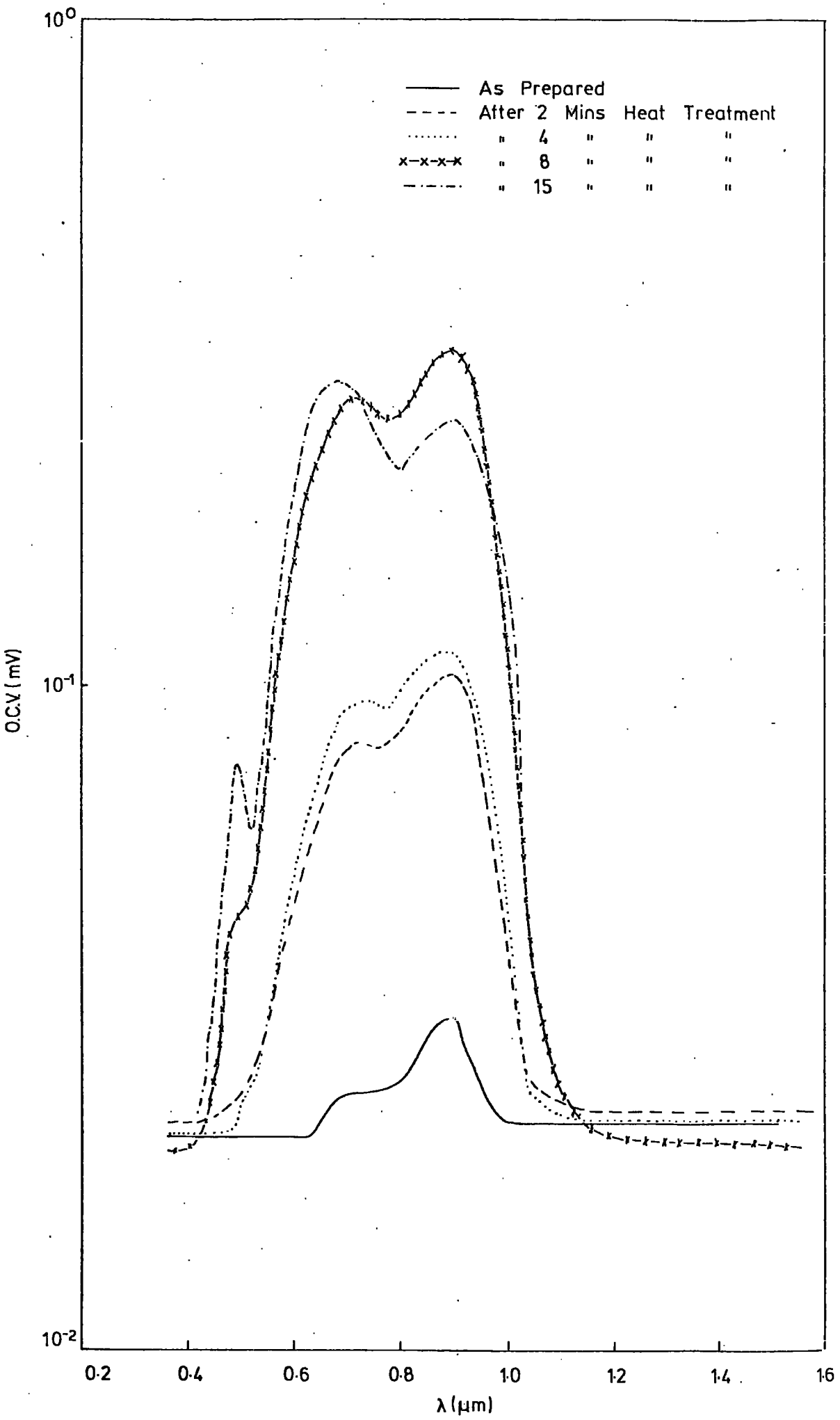

produced the optimum response for this device when the two peaks were at 0.71 and 0.9 μm with that at 0.9 μm being the higher. Prolonged heat treatment for a total of 15 mins caused an overall decrease in sensitivity, but the 0.68 μm peak became dominant.

Although these cells had a low output, the response times even after several minutes heat treatment were relatively fast (less than a minute). Prolonged heat treatment caused the partially converted films to peel off the tin oxide coated substrates. The peak in the vicinity of 0.5 μm became fully resolved only after 15 mins baking, but was in evidence after a 2 min bake.

Several enclosed thin films were produced on tin oxide coated glass substrates using the method discussed in Chapter 5. These films were quite yellow in colour and up to 5 μm thick, but appeared to be of better uniformity than those prepared in the conventional system. Short dip times of 1 to 2 secs were employed with these films since no devices could be formed using longer immersion times. Large open circuit voltages were produced with the as-plated cells, but the short circuit currents were small. It was interesting to observe that the cells were photoluminescent at liquid nitrogen temperatures when irradiated with ultraviolet light. The variation of O.C.V. with wavelength as a function of bake time was not investigated as thoroughly as previous devices since these devices were investigated only when a system failure caused a prolonged disruption in the supply of thin films evaporated in a conventional system. However the spectral response of a device baked for 2 mins is shown in Figure 7.13. There are two peaks, one in the vicinity of .48 μm and another broader peak of higher intensity near 0.67 μm. No peak in the vicinity of 0.9 μm is visible. The response time of the cell was several minutes. In many aspects the properties resembled

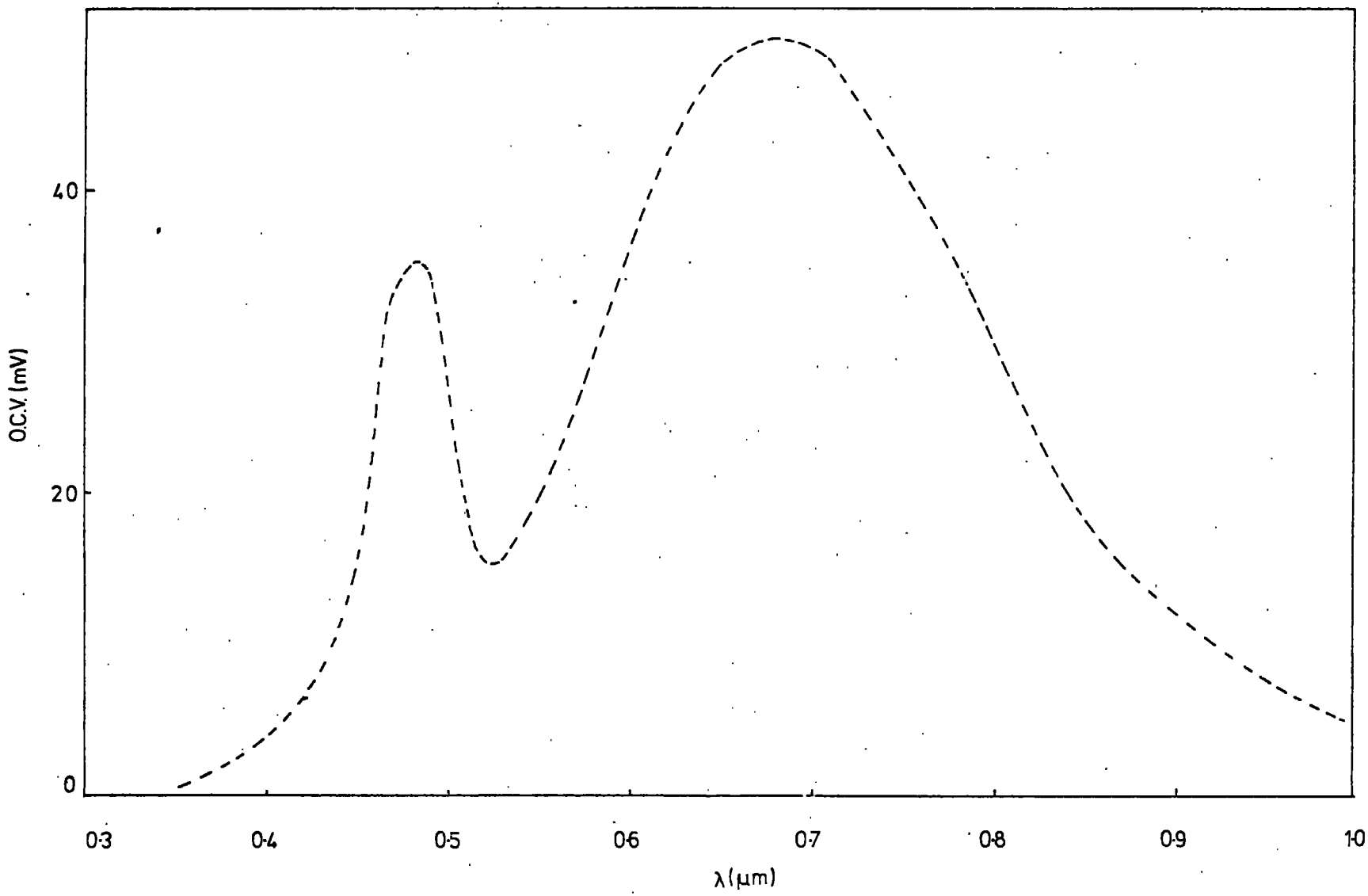

FIG. 7.13 O.C.V. SPECTRAL RESPONSE OF A DEVICE FORMED ON AN ENCLOSED THIN FILM

those of the device formed on single crystal high resistivity cadmium sulphide.

7.11 Measurement of Current-Voltage (I-V) Characteristics

The light source used was a 1.5 kW quartz halogen strip lamp with a parabolic reflector housing. The lamp was mounted in a levelled metal frame which contained a 2 cm deep tray of flowing water. Underneath the tray was a table of adjustable height on which the sample and heat sink/contact unit was mounted. The intensity of illumination at the surface of the sample was adjusted by altering the table height while monitoring the short-circuit current of a calibrated silicon solar cell until A.M.1 conditions (intensity $\sim$ 100 mW cm^{-2}) were obtained. This illumination intensity was used for all of the experiments with this light source.

The open circuit voltage of each cell was measured directly by connecting a Philips GM 2440 ($Z_{in} \sim 10^8$ Ω) valve voltmeter in parallel with the cell. It was generally not possible to measure short circuit currents by the conventional method of determining the voltage developed across a low resistance in parallel with the cell.

Since it was decided to record I-V characteristics directly rather than make point by point plots, a circuit was designed to allow I-V plots to be recorded across high impedance samples up to 10^8 Ω. Reference should be made to Figure 7.14. A cell bias unit was constructed using two separate batteries connected in series with a helical potentiometer. It was possible to produce a voltage between the slider and the battery mid point which was continuously variable between -1.5 and +1.5 volts. The voltage source was connected in series with the cell under test and a standard current sensing resistor. To ensure

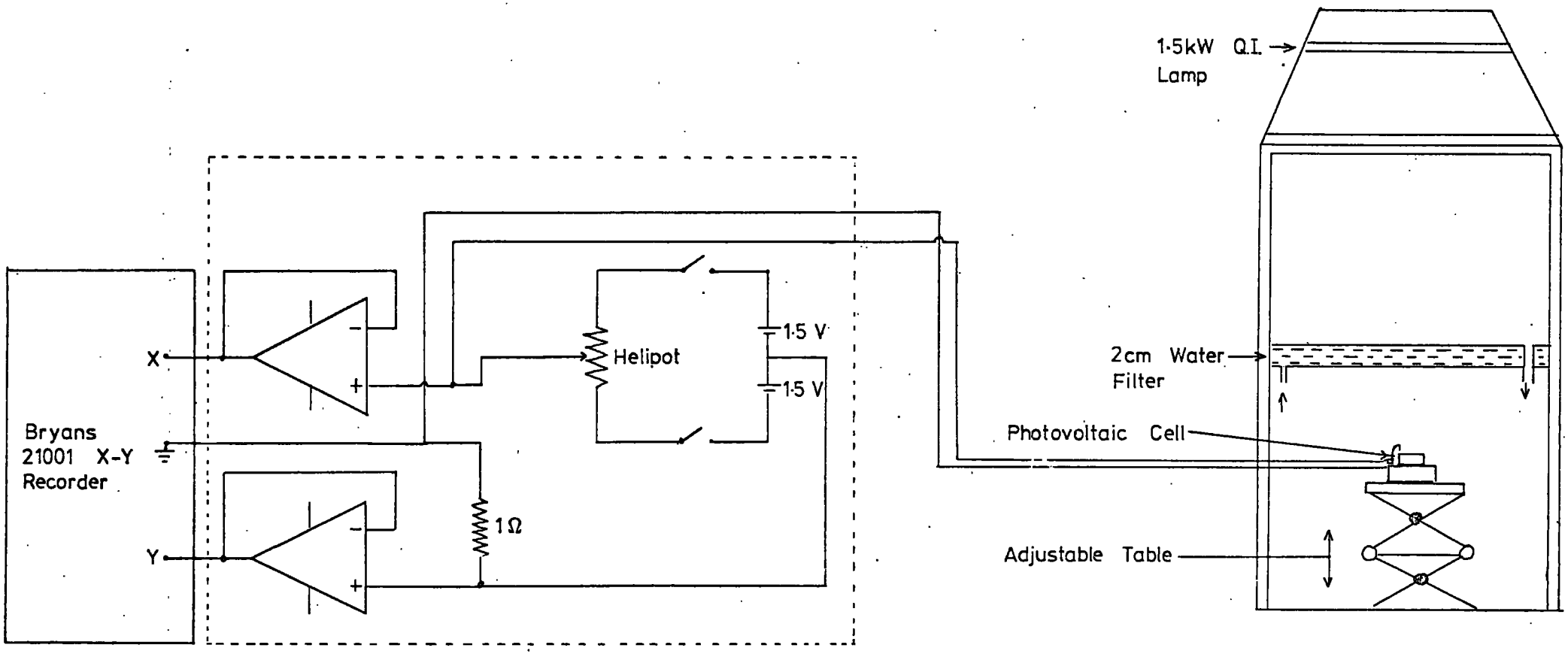

FIG. 7.14 CIRCUIT FOR SEMI-AUTOMATIC PLOTTING OF PHOTOVOLTAIC CELL I-V CHARACTERISTICS

that the X-Y recorder did not introduce any loading effects, buffer amplifiers were connected between the cell and the associated current sensing resistor and the X-Y recorder. These were F.E.T. input operational amplifiers with input impedances in excess of 10^{11} Ω, connected in voltage follower mode. The outputs were connected to the X and Y channels of a Bryans 21001 X-Y plotter. When the potentiometer spindle was rotated the current-voltage characteristics of a device was plotted. With the arrangement used, it was possible to investigate the forward and reverse bias and power production quadrants of the device characteristics.

Measurements of the current-voltage characteristic in forward bias in the dark and under illumination would be expected to demonstrate whether any photoconductive effects occurred. It was with this in mind that the forward bias characteristics of cells formed on low resistivity undoped CdS, low resistivity copper doped CdS and high resistivity undoped CdS were recorded. With the devices on undoped low resistivity bases, the as prepared (prior to baking) cells showed that the I-V characteristics measured in the light (A.M.1) and in the dark, converged but did not cross (Figure 7.15a). After only 2 mins heat treatment in air, the characteristics did intersect but this will be discussed in the next chapter. As-plated cells formed on the copper doped crystals showed the cross-over effect (i.e. intersecting characteristics) before heat treatment. Typical I-V characteristics from this type of device are shown in Figure 7.15b. The crossover effect was very pronounced in cells formed on high resistivity undoped material. With these last devices, the I-V characteristic in the dark was almost coincident with the voltage axis because of the high resistivity of the base material (Figure 7.15c).

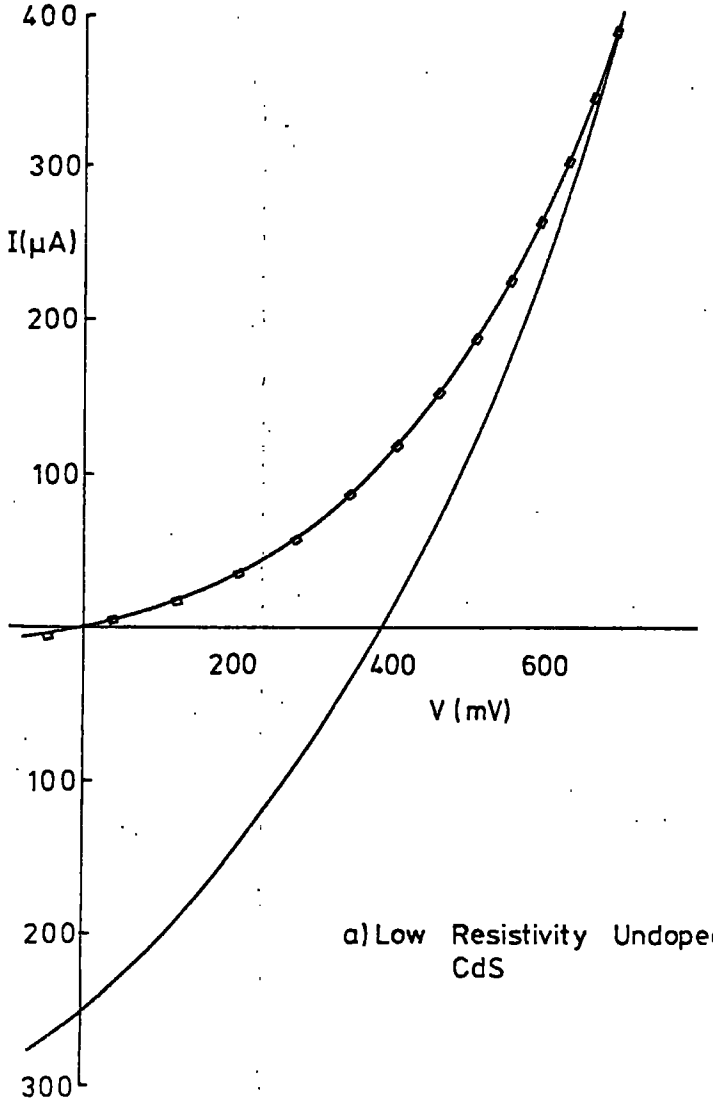

a) Low Resistivity Undoped CdS

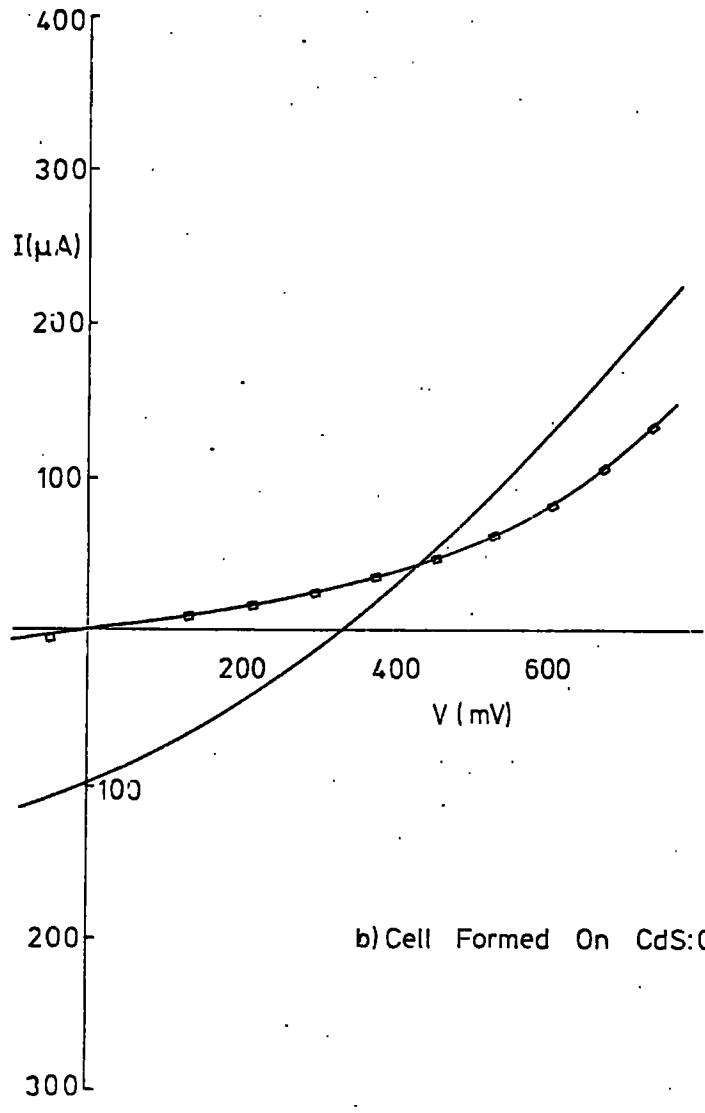

b) Cell Formed On CdS:Cu

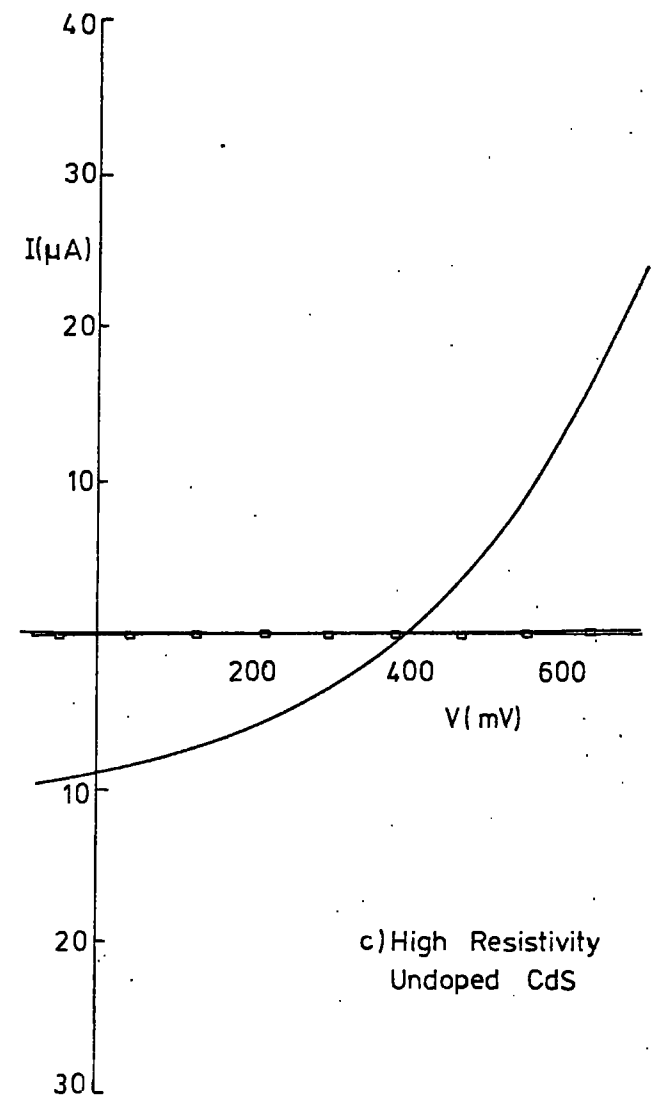

c) High Resistivity Undoped CdS

FIG. 7.15 I-V CHARACTERISTICS OF UNBAKED CELLS UNDER A.M.1 ILLUMINATION (——) AND IN THE DARK (—▫—▫—▫—).

Many I.R.D. thin film devices were investigated in a similar manner and the I-V characteristics were similar to those of the undoped low resistivity cells and did not show the cross-over effect. Some of the devices prepared on enclosed thin films however did show noticeable photoconductive behaviour but to a lesser degree than the devices formed on high resistivity single crystals. The low resistivity cells which had been heavily doped with indium and chlorine did not show a cross-over even after several minutes baking in air at 200°C. Further experiments were carried out in which the I-V characteristics were determined as a function of bake time at 200°C in air. These will be described in the next chapter.

7.12 Measurement of the S.C.C.

7.12.1 Introduction

It is generally accepted that measurements of the short circuit current are more important and sensitive than those of open circuit voltage. For instance, measurements of short circuit current as a function of wavelength gives information about the quantum efficiency at different photon energies which is vital if a more fundamental interpretation of cell operation is to be attempted. However, the small area (4 mm^2) of most of our devices and the fact that the magnitude of the short circuit current was a function of the quality and size of the contact (i.e. a spring loaded phosphor bronze probe) led to very low currents being observed. At the exit slit of the monochromator, the intensity of the radiation was exceedingly low ($\sim$ 100 $\mu W\ cm^{-2}$) and the resultant maximum short circuit current was of the value of 1 μA or less. The method of measuring the short circuit current by measuring the voltage across a low value standard resistor was clearly impracticable because with a 10 Ω load, the load voltage would be 10 μV for a short

circuit current of 1 μA. Towards the finish of the experimental work an electronic circuit was designed to enable small short circuit currents to be measured reliably. This is described in the next section.

7.12.2 Design of Current to Voltage Converter

The circuit to enable low short circuit currents to be measured was essentially a current to voltage converter. Figure 7.16 shows a standard inverting amplifier circuit. In a slightly modified form it may be used to 'convert' current into voltage. The output voltage is proportional to the current flowing into the input. To demonstrate this, it is easiest to assume that the operational amplifier is ideal. No appreciable current flows into the inverting input so the source current i_s which flows out through R_1 must flow in through R_F. Since the voltage at the inverting terminal $v_{(-)} = 0$, Output voltage $v_{out} = i_s R_F$.

The input resistance to the circuit is R_1 and since it does not play any part in the converter, it may be allowed to tend to zero, in which case the input resistance tends to 0 also. However, even if $R_1 = 0$, which is unlikely, because of lead resistance etc., the actual input resistance will not be zero.

To determine its magnitude, a simple operational amplifier model is used (Figure 7.17). Assume that a current I_{Test} flows into the circuit, if V_{Test} can be determined using circuit laws, then it is possible to evaluate the ratio V_{Test}/I_{Test} which is equal to circuit input resistance R_i'. Writing Kirchoffs equation at the inverting node

FIG. 7.16 SIMPLE INVERTING AMPLIFIER CIRCUIT

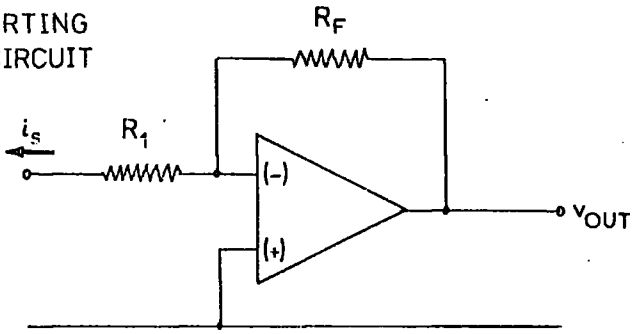

FIG. 7.17 CIRCUIT MODEL FOR FINDING INPUT RESISTANCE OF THE CURRENT TO VOLTAGE CONVERTER

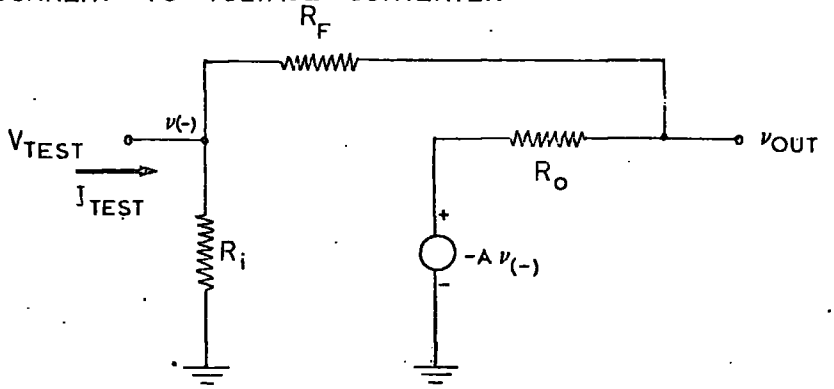

FIG. 7.18 Circuit Diagram Of The Current To Voltage Converter

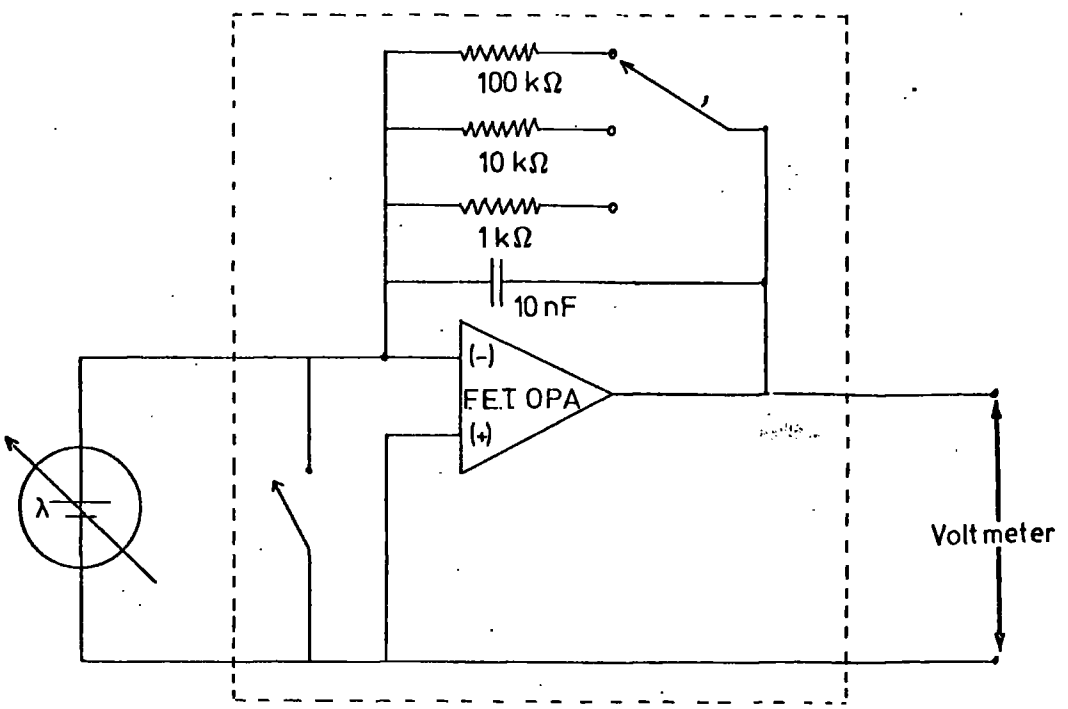

$$I_{Test} - \frac{v_{(-)}}{R_i} + \left(\frac{-A v_{(-)} - v_{(-)}}{R_F + R_o} \right) = 0$$

where R_i = operational amplifier input resistance = $10^{"}$ Ω

A = operational amplifier open loop gain = 100 dB for F.E.T. O.P.A. used

R_o = operational amplifier output resistance = 10^3 Ω

R_F = Feeback resistor

and solving for $v_{(-)}/I_{Test}$,

$$R_i' = \frac{V_{Test}}{I_{Test}} = \frac{v_{(-)}}{I_{Test}} = \frac{1}{\left(\frac{A + 1}{R_F + R_o} + \frac{1}{R_i} \right)}$$

But since $A >> 1$,

$$R_i' \approx (R_F + R_o)/A$$

Assume a value of 1 kΩ for feedback resistor R_F ,

$$R_i' \approx 20 \text{ m}\Omega$$

In theory the circuit should be suitable for measuring short circuit currents down to 10^{-8} A or even less.

The actual circuit used is shown in Figure 7.18. The power supplies and voltage offset adjustment network are omitted for clarity. In order to measure S.C.C., the device would be connected across the input and the voltage across the output was measured. The value of the current was calculated from the relationship

$$i_s = \frac{v_{out}}{R_F}$$

When the spectral response of the S.C.C. was plotted using this circuit, the shape of the curve was similar to that of the corresponding

O.C.V. distribution but with slight differences in magnitudes when plotted as relative percentage responses.

7.13 Discussion of Results

The magnitudes of the O.C.V's. of the as-prepared devices depended significantly on which plane of the orientated single crystals the junction was formed. With the junction on sulphur planes the O.C.V's. were on average some 20% higher than those for junctions on cadmium faces. This would probably explain the discrepancies which were often observed between early devices fabricated from the same crystal boule under apparently the same conditions. The work described in the previous chapter suggests that there are possibly two main reasons for this, namely (1) the greater thickness of copper sulphide formed on the S planes which would mean that more light could be absorbed on the S side, (2) the copper sulphide formed on an etched S plane takes the morphology of the rough S plane and is highly light absorbent. However copper sulphide formed on the smooth Cd plane reflects much of the incident radiation. Another contributory factor could be associated with the existence of microcracks on the Cd plane which could add to the interface states present and thus enhance the free carrier recombination.

Te Velde (1973) independently has reported that O.C.V's. from S plane junctions are greater than those from Cd plane junctions but he did not give any more information than that. On the other hand, Miya (1970) reported that higher O.C.V's. are obtained with Cd plane devices. On closer examination of his work, it appears that he identified his Cd and S planes incorrectly by referring to an early paper of Warekois et al (1962). However Warekois et al subsequently published an erratum in 1966 which explained that their original paper

contained an error. This may well have led to confusion in Miyas results which apart from the possible wrong identification of the polarity, looked similar to those obtained in this present investigation.

Miya further suggested that copper atoms diffuse more readily into junctions formed on cadmium planes and this would obviously affect the spectral response observed after prolonged heat treatment. Apart from the slightly larger overall magnitude of as prepared S plane devices, no overall difference in the spectral distributions of the O.C.V's. of our devices was discernible. After prolonged heating in air for 20 mins at 200^{o}C, it was apparent that copper diffusion had proceeded more rapidly on S plane junctions. This again would agree with Miya's work if his identification of the polarity of the basal plane had been in error. The evidence for the rate of in-diffusion of copper is simply based on the relative magnitudes of the photovoltaic peak at 0.9 μm in the two types of device . It is proposed that this band is associated with indirect optical absorption in the copper sulphide layer. In junctions formed on cadmium planes this particular band decreases slowly in magnitude as the baking at 200^{o}C is continued. With junctions formed on the sulphur planes, prolonged baking at 200^{o}C causes a much more dramatic decrease in the relative magnitude of the 0.9 μm band, while the other features follow the same trends exhibited by cadmium plane devices. It is likely that the thickness of the copper sulphide layer is reduced more rapidly during baking when the junction has been prepared on a sulphur face.

Several authors have demonstrated that the efficiency and stability of a CdS-Cu_2S photovoltaic cell can be improved by baking in air for a short period following the formation of the copper sulphide

layer (see for example Wilson and Woods 1972, Te Velde 1973). The baking treatment usually leads to changes in spectral response such as those illustrated in Figures 7.4 and 7.5. It is suggested here that these changes are strong evidence of the formation of a photoconductive i-layer in the CdS during the heat treatment. Consider first the devices formed on low resistivity undoped material (Figure 7.5). An unbaked cell showed no significant response at the band gap energy of CdS and relatively little at 0.68 μm. The major sensitivity occurred near 0.92 μm when the incident light is absorbed in Cu_2S which has an indirect absorption edge at 1.2 eV (Marshall and Mitra 1965). After baking at 200°C for 2 min in air, the dominant spectral feature was the broad band at 0.68 μm which is attributable to the photoconductive i-layer of CdS i.e. n-type CdS compensated by diffusing copper. This conclusion is supported by the curves of Figure 7.7 which show that an unbaked device fabricated on a copper-doped base, had properties and an output which were almost identical with those of a device formed on an undoped base which had however been baked. The suggestion here is that the copper doped base material already contained a copper compensated layer so no baking was necessary to produce an i-layer. The spectral sensitivity of this i-layer is revealed by the curve in Figure 7.2 showing the spectral distribution of bulk photoconductive sensitivity lying in a broad band centred at 0.7 μm.

The studies of cells formed on undoped high resistivity CdS ($\rho \sim 10^6$ Ω cm) (Figure 7.6) also reinforced the argument. In this case, an unbaked cell already contained a bulk photoconductive layer in close juxtaposition with the topotaxial layer of copper sulphide. However the spectral response of the O.C.V. showed a narrow band at the band gap energy of CdS. It was only after baking for two minutes at

200°C that the broader band at 0.58 μm appeared, i.e. heat treatment was necessary to cause some copper to diffuse into the junction region of the CdS. The conclusion is therefore that the band of sensitivity with its maximum lying variably in the wavelength range from 0.58 μm to 0.7 μm is caused by optical absorption of copper acceptor centres in an i-layer of CdS neighbouring the copper sulphide.

With devices formed on base material heavily doped with indium or chlorine, the cell output remained low, even after heat treatment. The main response was at the indirect absorption edge of chalcocite in the region of 0.92 μm. Even after heat treatment the main peak was at 0.92 μm. Presumably this was so because of relative difficulty of compensating the indium in the heavily doped lattice. It would be much more difficult to produce an i-layer in such a lattice so that the response in the region 0.6 μm to 0.7 μm would be suppressed.

Further support for the existence of photoconductive processes in CdS-Cu_2S photovoltaic cells is provided by the long time constants of all the heat treated devices examined and some of the as-prepared devices. Long time constants are a feature of photoconductivity in CdS. Furthermore the existence of a cross-over between the current voltage curves measured in the dark and under illumination is usually taken as evidence of the existence of a photoconductive i-layer. It is also significant that unbaked cells formed on photoconductive dice showed a cross-over effect (Figures 7.15 a,b,c) whereas the unbaked cells formed on undoped low resistivity CdS did not. After two minutes heat treatment the cross-over effect was observed on this latter type of device. No cross-over was observed in devices fabricated on very low resistivity indium or chlorine doped CdS even after several minutes heat treatment. This would imply that these types of device did not show any photoconductive behaviour.

The proposal that the large spectral peak in the wavelength range 0.58 μm to 0.7 μm is largely due to photoconductive effects, appears to contradict the suggestion (Palz et al 1972, Massicot 1972) that the phase of the copper sulphide may dominate the spectral responses of some devices. This situation does in all probability apply to unbaked cells formed on low resistivity CdS and will be discussed in greater detail in the next chapter. Massicot suggests that the heat treatment oxidises Cu_2S to the lower copper sulphide phase $Cu_{1.96}S$ (djurleite) which is reported to have a bandgap of about 1.8 eV. It is however obvious that the diffusion of copper out of the copper sulphide and into the CdS to form a photoconductive i-layer will automatically require a reduction in the copper content of the Cu_xS layer at the junction. Nevertheless, the close similarity between the measured photovoltaic and photoconductive response shows that photoconductive processes in these types of device had a dominating influence.

With regard to the photoconductive i-layer it is noticeable that the maximum spectral response occurs at slightly different wavelengths in different devices. It is proposed that an increase in copper concentration in the i-layer leads to the formation of acceptors with slightly larger hole ionization energies. This means that the maximum of the spectral band in question shifts from 0.58 μm to longer wavelengths as a cell is baked for increasingly longer times. However this process appears to saturate when the maximum response reaches 0.7 μm.

After prolonged heat treatment in air at 200°C, the overall magnitude of the O.C.V. integrated over all wavelengths decreased significantly for all types of device.. This was probably due to oxidation of the copper sulphide surface and preliminary work involving different

gas ambients such as hydrogen or nitrogen showed a reduction in this effect.

With several thin film devices, the spectral responses of the O.C.V. and S.C.C. were obtained using the current to voltage converter which had been designed and constructed. At the low light levels obtained from the exit slit of the monochromator, the O.C.V. and S.C.C. responses showed the same general features with slight variation in magnitude throughout the wavelength range employed. This behaviour was predicted using the equivalent circuit for the solar cell discussed in Chapter 3. It was decided to measure O.C.V's. of the cells rather than S.C.C's. since great difficulty was experienced in ensuring a good contact to the copper sulphide layer. Furthermore, the form of spectral response of the O.C.V. of an optimised low resistivity undoped CdS cell matched closely that reported by Konstantinova and Kanev (1973) in which they investigated the dependence of short circuit current on wavelength.

CHAPTER 8

OPTIMISATION AND DEGRADATION OF SOLAR CELLS

8.1 Introduction

In general, as prepared CdS/Cu_2S photovoltaic cells do not exhibit high O.C.V's. and S.C.C's. or stable device parameters. However after a short heat treatment in air at 200°C, the properties of the cell are reported to be optimised (Shiozawa et al 1969). During this heat treatment it is likely that copper diffusion takes place. Since the most efficient heterojunction is between CdS and chalcocite, Cu_2S, it may be advantageous to have an excess of copper present to counteract the inevitable deficiency caused by diffusion. To test this idea, attempts have been made to influence the stoichiometry of the copper sulphide layers by electrochemical means and simple life-tests were carried out on some samples. Other possible degradation mechanisms were investigated further by treating the cells with oxidising and reducing agents at room temperature and monitoring the spectral response of the O.C.V. as a function of this treatment. The effects of varying the plating temperature on the properties of the cells have also been investigated.

8.2 Heat Treatment of Devices

8.2.1 Experimental

The effects of heat treatment in air at 200°C on the current-voltage characteristics were studied using the semi-automatic plotter (7.11) and a small heating apparatus (Fig. 8.1). It was possible to bake the devices in different gases, e.g. air, nitrogen and hydrogen. Short circuit currents were derived from the current-voltage plots

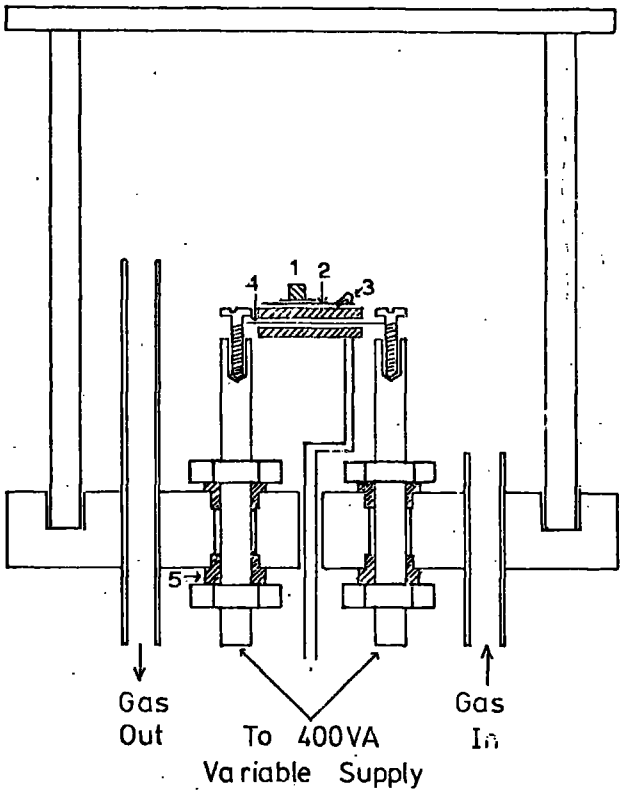

1. Sample
2. Glass Cover Slide
3. Thermocouple
4. Molybdenum Wire
5. P.T.F.E. Spacer

FIG. 8.1 HEAT TREATMENT APPARATUS

since the current to voltage converter had not then been constructed. The characteristics of the as-prepared cells were determined using equivalent AM1 illumination and an independent measurement of O.C.V. was made using a high impedance meter. Each sample was heated in air in the following manner. The glass cover slide (Fig. 8.1) was preheated to 200°C while a gas flow was maintained through the apparatus. Samples were introduced individually into the heating chamber for the time required and the device was then placed in a stream of cool gas. The current-voltage characteristics were again measured under the same conditions as before. Heat treatments were carried out for periods up to 20 minutes and the current-voltage measurements were made periodically. With small area single crystal cells, temporary contact was made to the copper sulphide layer by means of a phosphor bronze spring. The temporary gridding jig was used to make a good contact to thin film cells.

8.2.2 Results

Typical current-voltage characteristics plotted as a function of bake time in air are shown for some of the devices investigated in Figs. 8.2a to e. Only the portion of the characteristic in the power production quadrant is shown, but investigations were also carried out in forward and reverse bias.

Devices formed on low resistivity undoped CdS ($\rho \sim 10^{-1}$ Ωcm) had poor power conversion characteristics in the as-prepared state. However a short (2 min) heat treatment in air at 200°C led to a great improvement in O.C.V. and S.C.C. The area under the curve increased to produce a much larger fill factor. Prolonged heat treatment caused a slight decrease in O.C.V. and a larger decrease in S.C.C.

With devices formed on low resistivity copper doped CdS, $\rho \sim 5 \times 10^{3}\Omega$cm,

FIG. 8.2 I-V CHARACTERISTICS AS A FUNCTION OF HEAT TREATMENT (MEASURED UNDER A.M.1 ILLUMINATION)

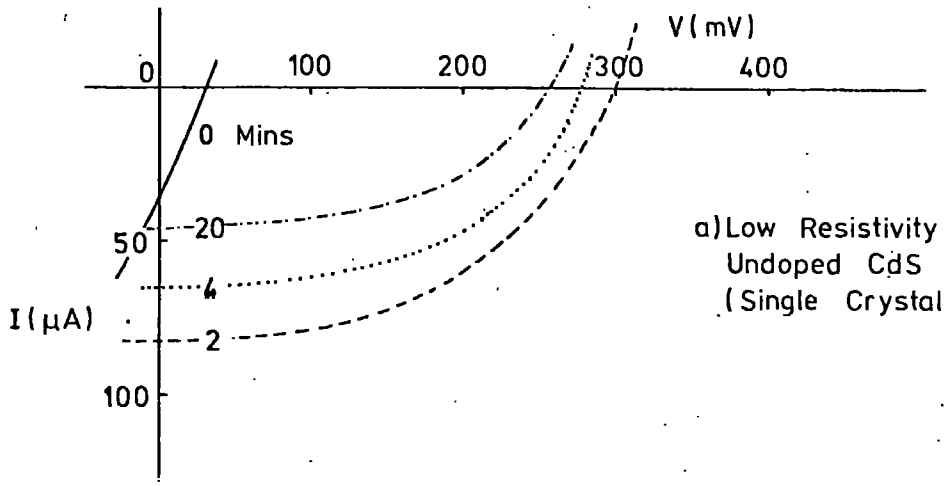

a) Low Resistivity Undoped CdS (Single Crystal)

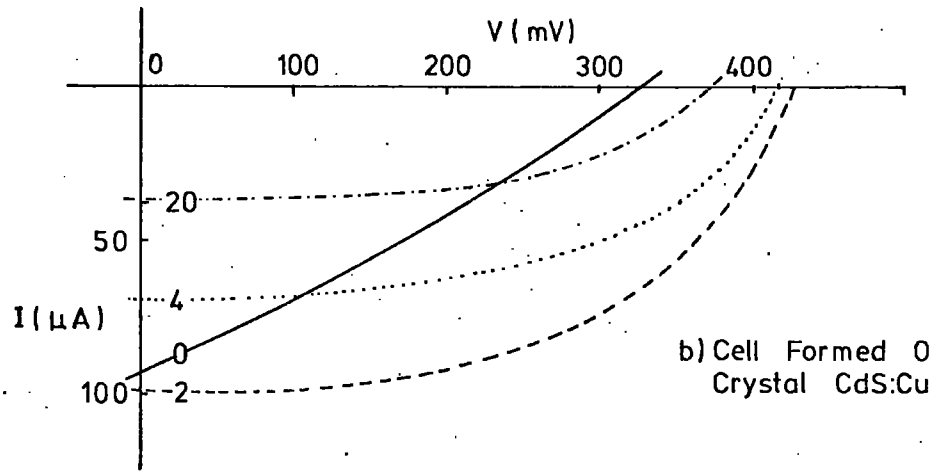

b) Cell Formed On Single Crystal CdS:Cu

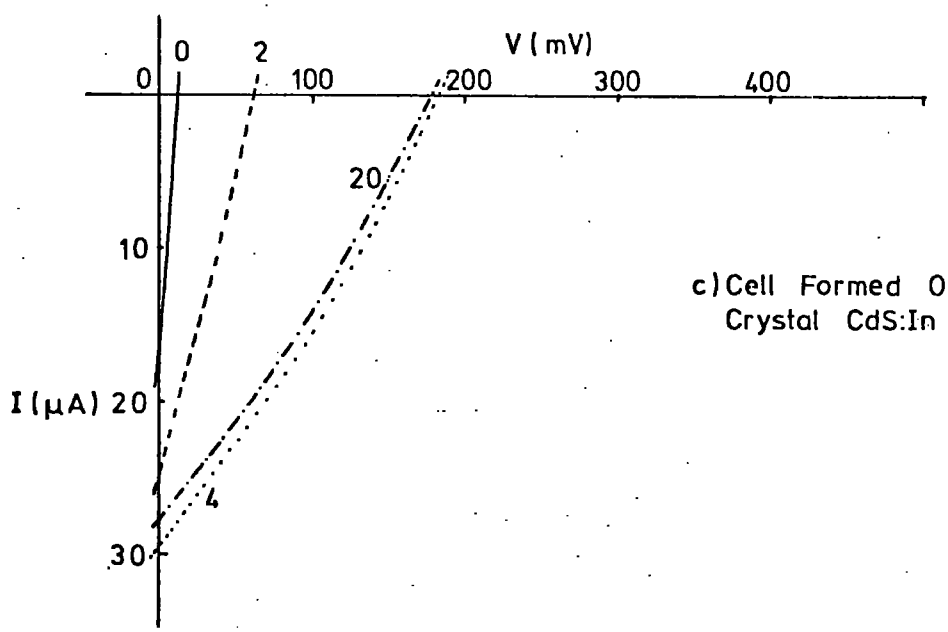

c) Cell Formed On Single Crystal CdS:In

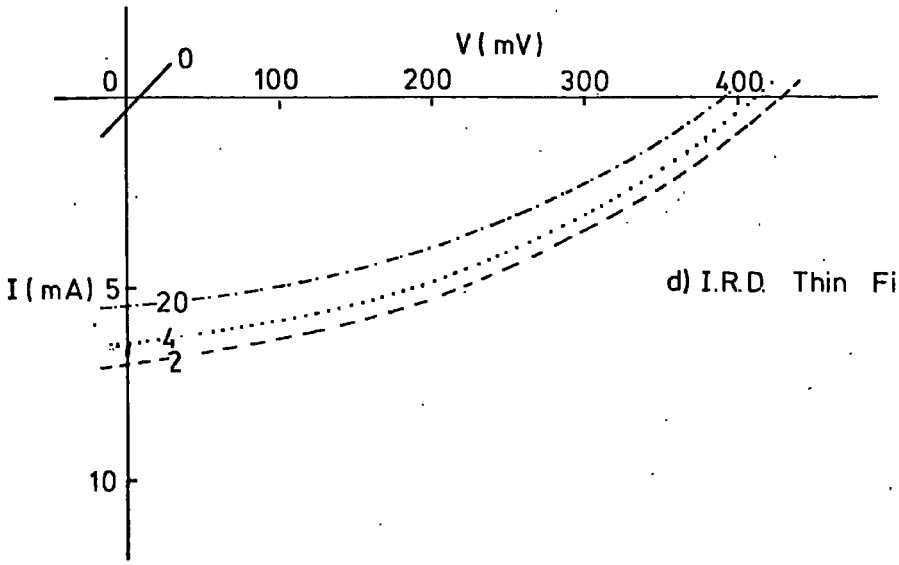

d) I.R.D. Thin Film Cell

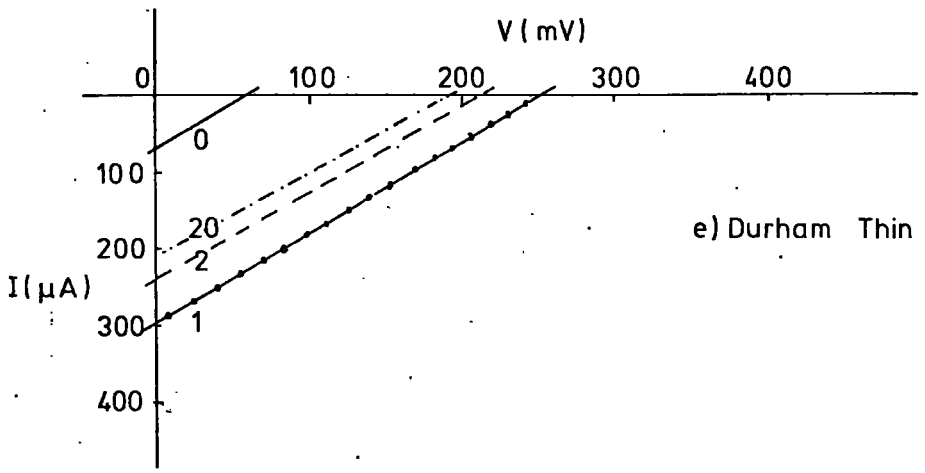

e) Durham Thin Film Cell

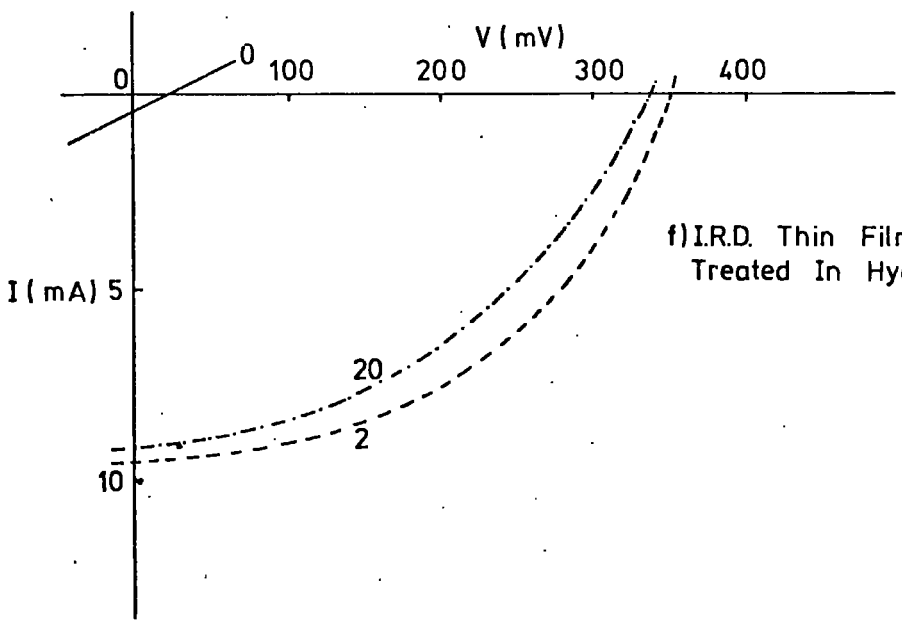

f) I.R.D. Thin Film Cell Heat-Treated In Hydrogen

the O.C.V. of as plated cells was high (greater than 300 mV) and the S.C.C. density was also quite large ($J_{s.c.} \sim 2.2$ ma/cm^2) in view of the relatively poor top contact. A short heat treatment of 2 mins in air led to an improvement in O.C.V. but only a small increase in S.C.C. The curve shape had improved to produce a reasonable fill factor of about 60%. Prolonged baking in air caused a slight decrease in O.C.V. and a greater decrease in S.C.C.

Cells formed on high resistivity undoped CdS ($\rho \sim 10^6$ Ωcm) had current-voltage characteristics with a reasonable shape but the main feature was their high O.C.V. This type of device also had the lowest S.C.C. of all. Heat treatment initially produced a large improvement in O.C.V. and a lesser improvement in S.C.C., but prolonged baking caused degradation of cell parameters.

As-prepared devices formed on indium or chlorine doped crystals with very low resistivity ($\rho \sim 10^{-2}$ to 10^{-1} Ω cm) had similar very poor current-voltage characteristics. Both the O.C.V. and S.C.C. were low and the characteristics were straight lines rather than smooth curves. The devices developed their maximum O.C.V. and S.C.C. values after heat treatment for 2 to 4 minutes, but prolonged baking caused degradation. Even after 20 mins heat treatment, the characteristics remained almost straight lines and the fill factors did not improve significantly. Devices formed on CdS which had been heated in molten cadmium using a process to be described later in this chapter showed many similar features to those of devices formed on indium and chlorine doped CdS.

Of the three types of thin film device investigated, the ones fabricated on I.R.D. films proved to be the most potentially useful. However the as-prepared devices gave almost zero O.C.V's. and S.C.C's. and exhibited straight line characteristics. A short (2 minute) heat

treatment caused a great improvement and prolonged heat treatment caused the usual degradation in cell properties. Devices formed on films evaporated in an enclosed system and the 12" Durham evaporation unit were also investigated. These devices gave poor current-voltage characteristics initially which improved after a short heat treatment. Durham thin film (D.T.F.) devices gave lower O.C.V's. than enclosed thin film (E.T.F.) devices and prolonged baking caused the usual degradation. The current voltage characteristics remained as straight lines throughout the baking treatments.

Values of S.C.C. and O.C.V. as functions of bake time in air at 200^{o}C are shown in Figs. 8.3 and 8.4. The curves are from typical devices of various types. Since the thin film devices were 1 cm^2 in area, while the single crystal cells were 4 mm^2 in area, S.C.C. densities are plotted to allow direct comparison between thin film and single crystal devices.

8.2.3 Heat treatment of thin films in different ambients

It is considered by some workers (e.g. Te Velde, 1973) that heat treatment in an atmosphere containing oxygen is essential for the optimisation of a device. From the results described in the previous section, it is indisputable that a short heat treatment in air improves the O.C.V. and S.C.C. of devices formed on CdS of different resistivities, containing various dopants. It is however likely that surface oxidation of the copper sulphide layer will also take place.

To investigate the effect of heat treatment in ambients containing little oxygen, thin film devices wre baked in nitrogen and hydrogen using the same heat treatment apparatus as before. A typical set of current voltage characteristics for a thin film cell baked in

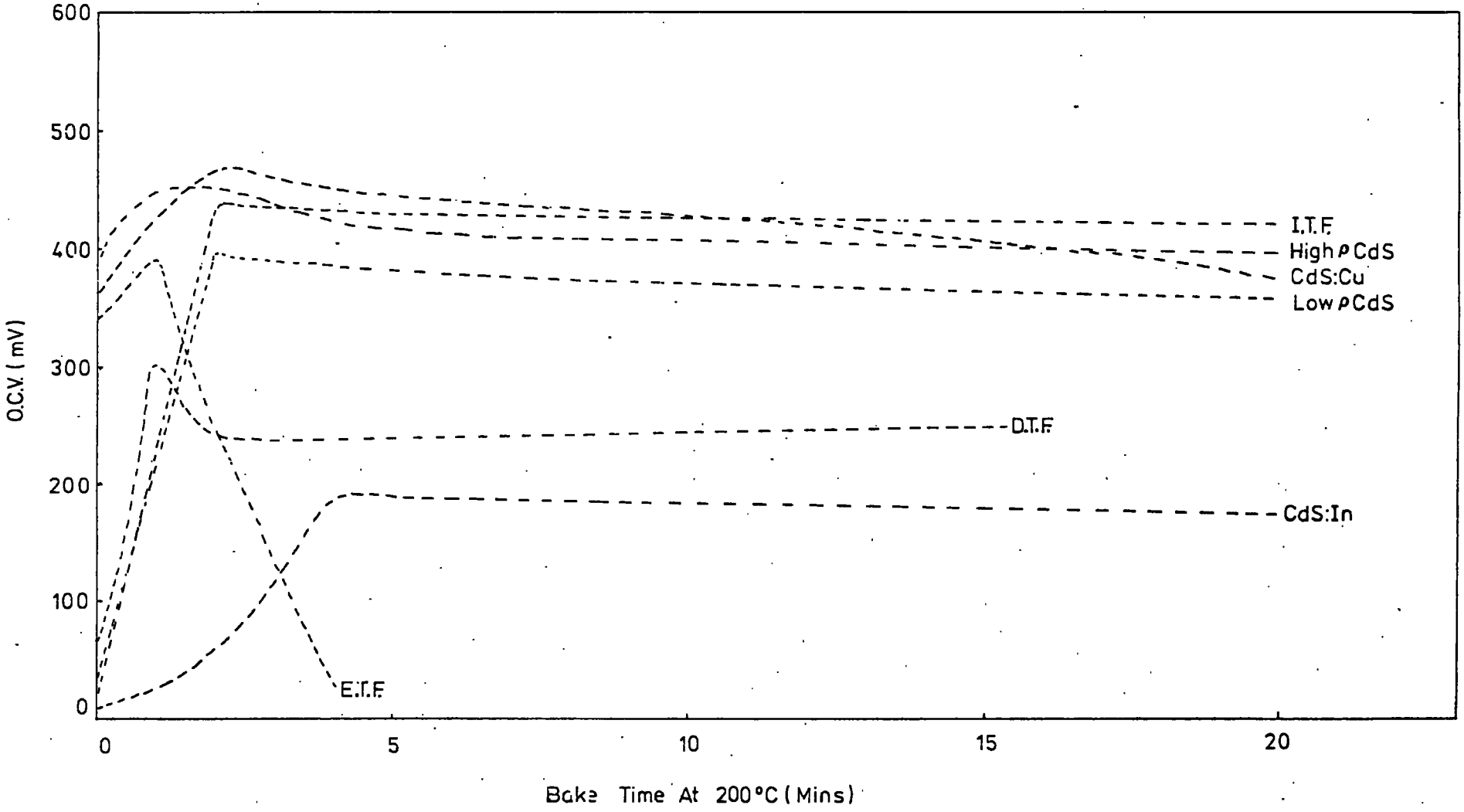

FIG. 8.3 INFLUENCE OF BAKE TIME IN AIR ON THE O.C.V. OF SINGLE CRYSTAL AND THIN FILM CELLS

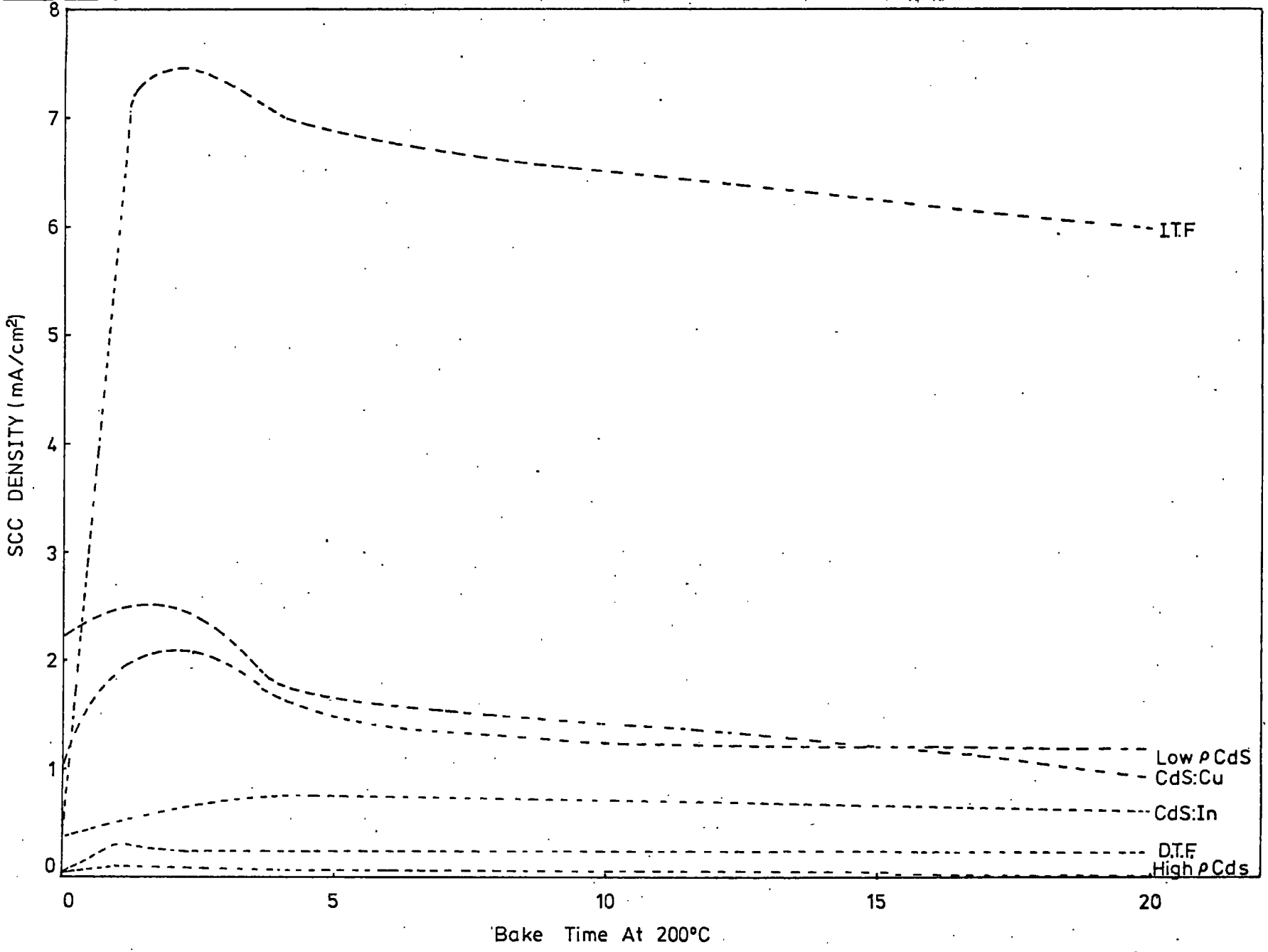

FIG. 8.4 INFLUENCE OF BAKE TIME ON S.C.C. DENSITY OF SINGLE CRYSTAL AND THIN FILM CELLS

hydrogen is shown in Fig. 8.2(f). Low O.C.V. and S.C.C's. were observed for the as-plated devices but a short heat treatment of 2 to 4 minutes caused the usual improvements. However as baking was continued, the rate of degradation of O.C.V. and S.C.C. was lower than that for cells baked in air. Devices were also heated in dry oxygen-free nitrogen and features similar to those of hydrogen treated cells were observed. Preliminary investigations showed a degradation behaviour intermediate between that of devices treated in air and hydrogen. The O.C.V. spectral response of thin film cells measured as functions of bake time in hydrogen and nitrogen were not fully investigated but the position of the maximum shifted to lower wavelengths after a short bake in either gas. Observation of the current-voltage characteristics in forward bias in the dark and under A.M.1 illumination for these types of thin film device showed that there was a crossover after a short heat treatment, in the same way as for devices baked in air.

8.3 Oxidation and Reduction of Cells

One process which may be at least partly responsible for cell degradation is simple oxidation of the copper sulphide layer, which is accentuated by prolonged heating in an atmosphere containing oxygen. Devices may be degraded as a result of atmospheric oxidation under illumination or simply in storage. To investigate the effect of surface oxidation on degradation and on the spectral responses, the following experiments were carried out.

Freshly prepared cells which had been fabricated using the wet barrier method were wrapped loosely in aluminium foil to keep light out, but to allow air to reach the surface of a cell. The cells were kept in the laboratory for six weeks and the O.C.V. spectral responses were

measured at the end of this time. Their O.C.V's. had degraded to 10% of the original value and the maximum in the spectral response had shifted to lower wavelengths, see Figure 8.5. A small peak was visible at 0.49 μm, but the main sensitivity was at 0.67 μm and there was evidence of an unresolved peak in the vicinity of 0.9 μm.

Hydrazine hydrate, which is a very strong reducing agent in liquid form, is used in the preparation of the standard plating solution. Its purpose is to ensure that the copper ions present in the bath remain in their un-oxidised cuprous ions form. It was thought that a strong reducing agent might have some effect on any oxidised surface layer of copper sulphide present in the devices. The degraded devices were therefore dipped for 5 mins at room temperature in undiluted liquid hydrazine hydrate solution. After this treatment the cells were removed, rinsed in distilled water and dried in a stream of oxy-free nitrogen. The spectral response of the O.C.V. was re-measured (Fig. 8.5). The peak which had previously been centred at 0.48 μm had decreased in magnitude while the major response at 0.67 μm had shifted to larger wavelengths at 0.72 μm and the existence of an unresolved peak at 0.9 μm was confirmed. There had also been an overall increase in magnitude (by a factor of two).

The cells were then dipped in the hydrazine hydrate for a further 50 hours to see if any additional improvement could be obtained. Following this it was necessary to remount the cells on to new baseplates since hydrazine hydrate dissolved the silver cement between ohmic contact and baseplate. After the long treatment in hydrazine hydrate, the spectral distribution of the O.C.V. was measured again. Now the peak at 0.49 μm had disappeared completely and the dominant response was at 0.94 μm. Further, the original peak in the vicinity of 0.7 μm could

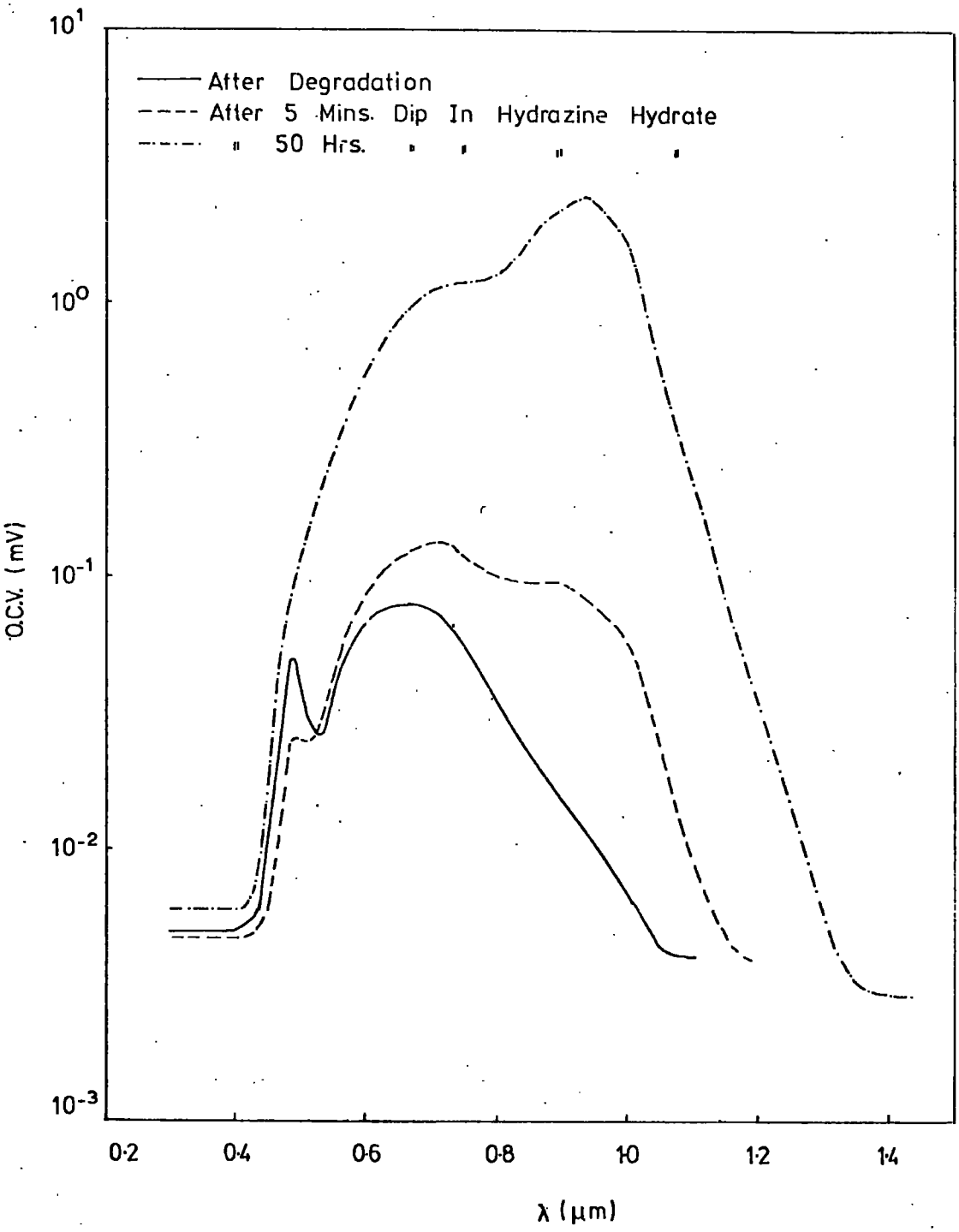

FIG. 8.5 RECOVERY OF DEGRADED SINGLE CRYSTAL CELL

not be fully resolved. The magnitude of the maximum O.C.V. had increased some 20 times compared with that of the degraded cell.

Experience shows that cells represented by curves in Fig. 8.5 oxidise slowly if left in the open laboratory. Rather than having to wait several weeks to allow the atmosphere to oxidise the solar cells, it was decided to perform this artificially by using a strong oxidising agent in liquid form. Most of the agents considered attacked the copper sulphide layer or substrates, but 100 vol. hydrogen peroxide showed promising results. Single crystal cells were prepared in the usual way together with thin film cells which had been fabricated on Au-Cr-glass substrates. The spectral distributions of the O.C.V's. were measured and showed the usual features, i.e. a main peak at 0.92 μm with an unresolved peak in the region of 0.7 μm. The cells were then immersed in 100 vol. hydrogen peroxide for periods of up to 45 minutes at room temperature to ensure that oxidation would be significant. Attempts were then made to determine the spectral response of the O.C.V., but no response could be detected above the noise level of the measuring apparatus (Fig. 8.6). However, after a short (5 min.) dip in hydrazine hydrate at room temperature, it was possible to detect a response. Peaks at 0.7 and 0.85 μm were visible and a further 15 hours dip in the strong reducing agent gave rise to an O.C.V. response curve which was similar in shape to the one measured for the freshly prepared cells. The curves shown (Fig. 8.6) are for a thin film cell but similar results were obtained for devices formed on low resistivity undoped CdS.

Thin films of chalcocite have also been converted to digenite ($Cu_{1.8}S$) by exposure to ammonium sulphide fumes (Ellis 1967). Ellis reported that chalcocite films 0.25 μm thick evaporated on to glass were converted in 45 seconds and the effects of ammonium sulphide on

FIG. 8.6 DEGRADATION AND RECOVERY OF A THIN FILM CELL (UNBAKED)

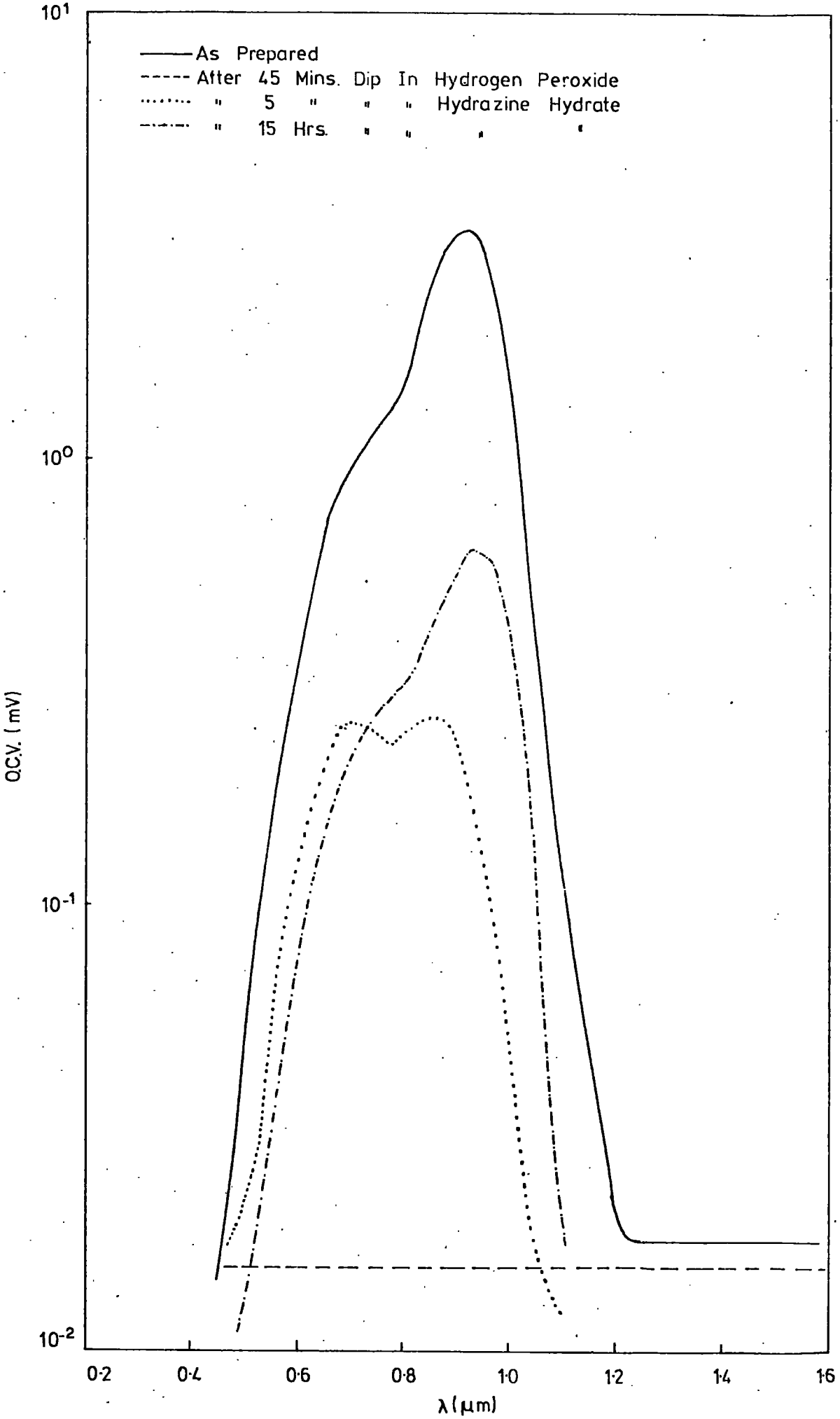

our solar cells have been investigated. The spectral responses of the O.C.V. of single cystal and thin film cells were measured in the usual way (Fig. 8.7). Devices were then held over some ammonium sulphide in a fume cupboard for about 15 seconds. The spectral responses of the O.C.V's. were then re-measured. Cell outputs had degraded to a very large extent to about the noise level of the measuring equipment. There was, however, evidence of a peak in the vicinity of 0.75 μm. A five minute dip in hydrazine hydrate at room temperature produced a dramatic recovery. The overall shape of the response curve was again similar to that of an as prepared device but the magnitude of the response was only half that of the original.

These oxidation and recovery processes were carried out on single crystal and thin film devices and so long as the resistivities of the base CdS were of the same order, analogous effects were observed. With thin film devices, it was necessary to investigate those formed on Au-Cr-glass substrates since the flexible substrates of Zn-Ag alloy on yellow Kapton dissolved in hydrazine hydrate. The devices prepared on tin oxide coated glass were of generally poor quality, but similar oxidation and recovery cycles could be performed.

8.4 Control of stoichiometry by Electrochemical methods

8.4.1 Introduction

Several workers have suggested that the stoichiometry of the copper sulphide layer can be stabilised as chalcocite by controlling the electro chemical potential of the cell during the plating process, see for instance Aerschodt and Reinhartz (1970) and Rickert and Mathieu (1969). Aershodt and Reinhartz reported however that with CdS films evaporated under different conditions, the optimum value of the potential

FIG. 8.7 DEGRADATION AND RECOVERY OF AN UNBAKED SINGLE CRYSTAL CELL

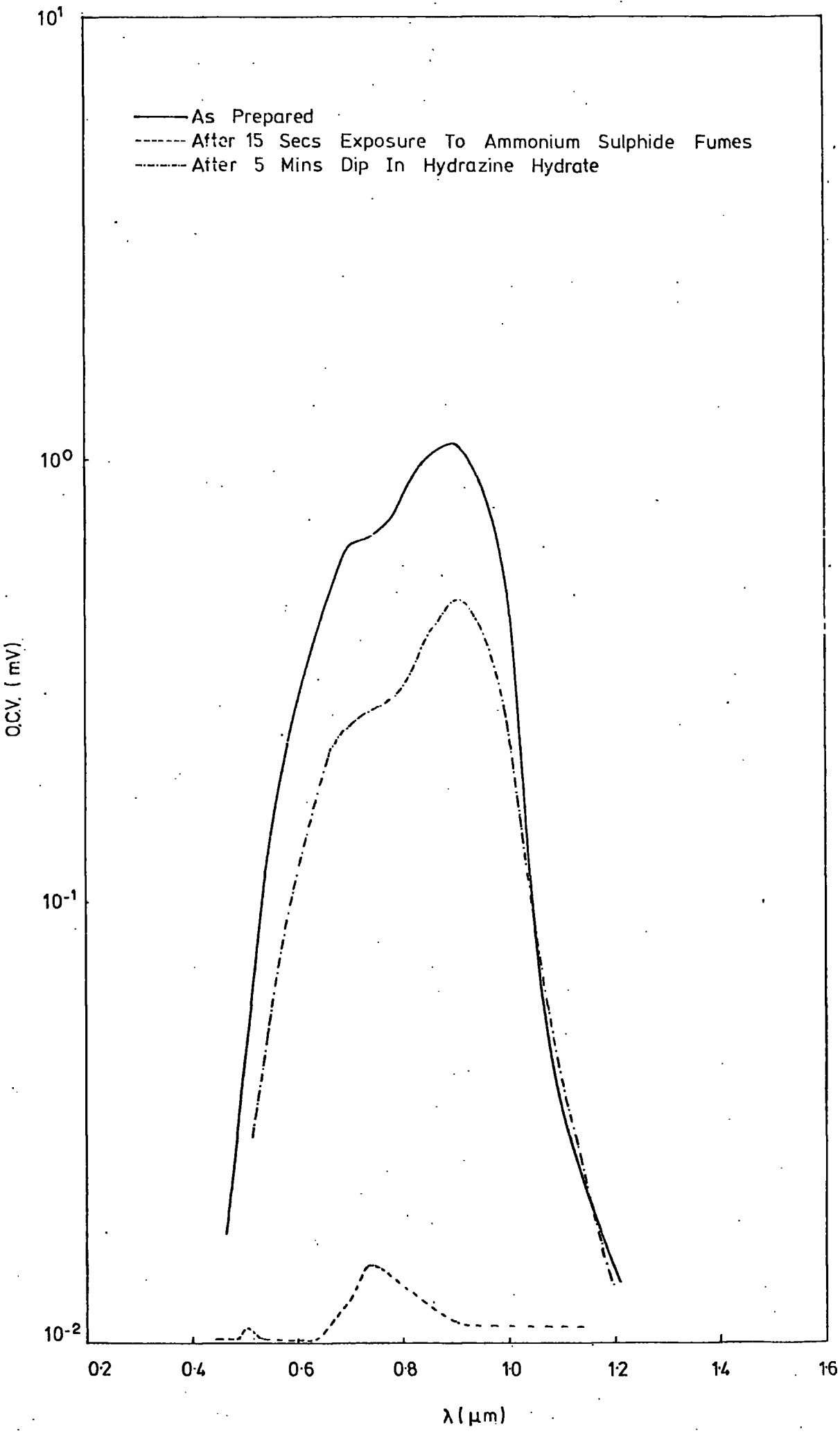

to be applied to the cell surface during fabrication varied between + 100 mV and - 100 mV. The investigation carried out here was designed to identify the optimum sign of electropotential to be applied to a cell.

8.4.2 Device preparation

Investigations of the influence of plating potential on device parameters were carried out on large area (~ 1 cm^2) devices with a base CdS resistivity of approximately 10^2 Ω cm. The CdS slices were prepared in the same way as described in Chapter 6 and they were clamped to a strip of perspex using a molybdenum clip. Contact to the free surface was made with a piece of 0.5 mm diameter platinum wire clamped under this clip. The other face and sides of the CdS had been coated with the acid resisting lacquer. Platinum, molybdenum and perspex were used because these materials did not precipitate copper from the solution. A reference electrode of oxy-free copper was placed in the plating solution which was held at 90°C. It was possible to control the potential between the reference electrode and the CdS surface before introducing the sample to the bath by means of a potentiometer across a low voltage d.c. supply.

It was decided to employ three voltages, namely + 100 mV, 0 and - 100 mV with respect to the copper reference electrode. The potential between cell surface and copper electrode was set to the required value and the samples were introduced into the plating bath for 10 secs at 90°C. Plated cells were rinsed in distilled water, acetone (to remove the lacquer) and distilled water again. Finally they were dried in a stream of nitrogen. The cells were then heated for 2 minutes in air at 200°C, after which gold grids were flash evaporated on to the copper sulphide layers in two stages.

8.4.3 Measurement of Cell Degradation

Rather than simply determining the cell parameters such as S.C.C., O.C.V. and O.C.V. spectral distribution for the cells freshly plated with different voltages applied, it was decided to monitor life-tests on these parameters as a function of time while under constant illumination. To simplify the design of the apparatus and to accelerate the degradation process, the life-test experiment was carried out in air rather than in an inert atmosphere. If the cells had been left in an unloaded condition and the light were of sufficient intensity to produce O.C.V's. in excess of 383 mV, then load effect degradation would have occurred. This type of behaviour has been investigated by Spakowski and Forestieri (1968) and Stanley (1968) and is now well understood. The problem was avoided in the present set of investigations by using a low power (100 W) tungsten lamp as a light source, but leaving the cells on open circuit since the O.C.V's. developed were lower than the load effect threshold. Unfortunately the tungsten radiation contained more infra-red than the solar spectrum. The power density at the cell positions was approximately 12.5 mW/cm^2 so that with lamp and cells enclosed in the light proof testing box the cell temperatures were raised to about $60^{\circ}C$. To exercise more control over this temperature, the cells were mounted on a water cooled aluminium plate (Fig. 8.8). This arrangement kept the device surface temperature to less than $30^{\circ}C$. Contact to the cells was made by wires soldered to the copper base plates and phosphor bronze spring contact to the gold grid evaporated on to the copper sulphide.

Spectral response curves for the three types of device (with 0 or ± 100 mV applied during plating) were obtained after the evaporation of the gold grid. Samples were mounted in the life-test box. Current-

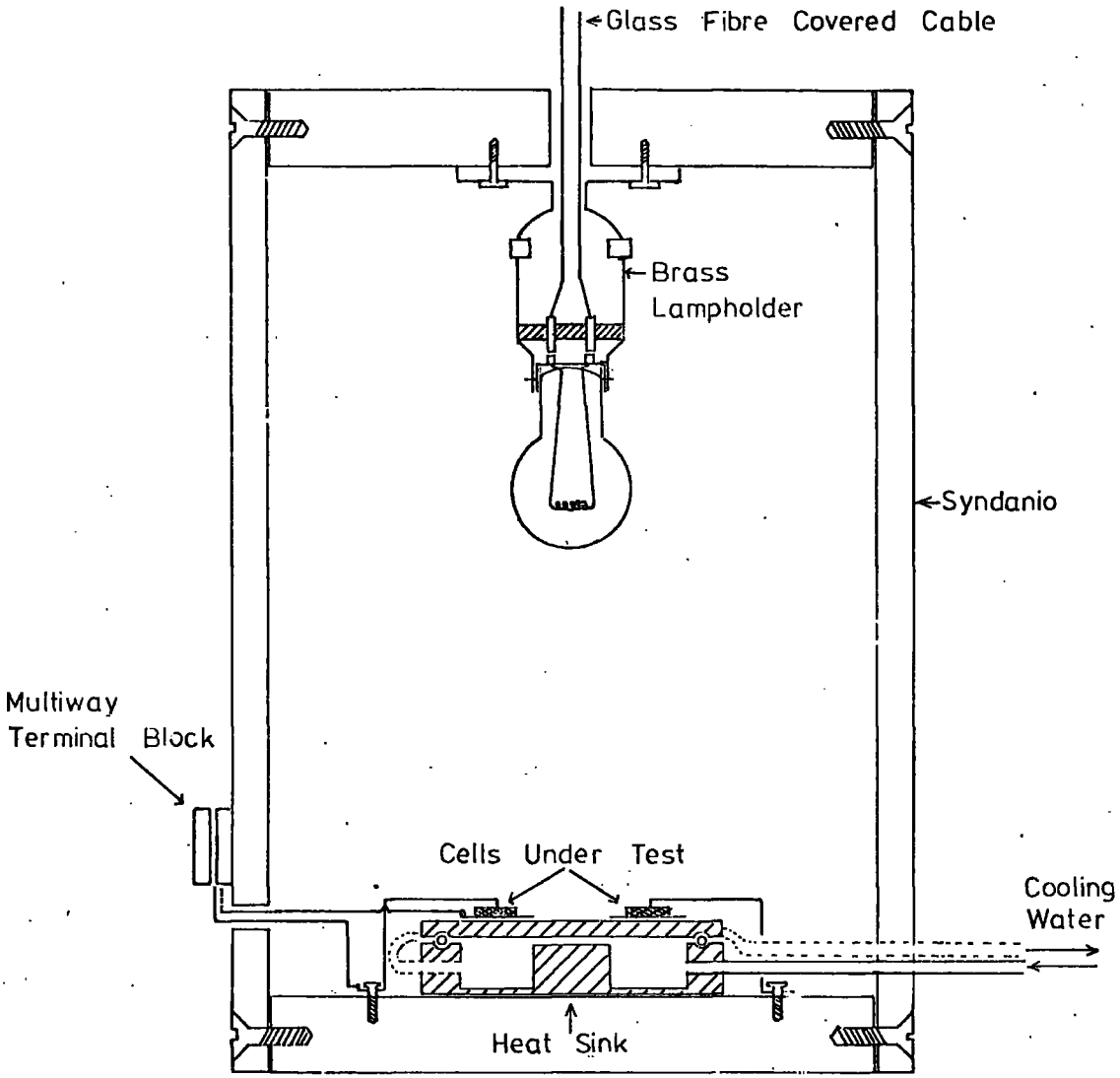

FIG. 8.8 PHOTOVOLTAIC CELL LIFETEST APPARATUS

voltage characteristics were obtained in the usual way. After 24 hours illumination, the current-voltage characteristics of these devices were again plotted and the devices were removed from the box and spectral responses of the O.C.V. were determined. The devices were replaced in the box in their original positions and their current-voltage characteristics were measured every 24 hours whenever possible up to a time of about 1500 hours. At this point they were removed and the spectral distributions of the O.C.V. were measured yet again.

8.4.4 Results

Over the 1500 hours period of the investigation under open-circuit conditions, the S.C.C's. of each type of device degraded significantly (Fig. 8.9) regardless of the electrode potential applied during plating. The S.C.C. of the cell to which + 100 mV had been applied with respect to the copper reference electrode had degraded the most to about 30% of the original value. A degradation to about 42% of the initial value had occurred for the cell to which no potential had been applied. The least degradation (about 57%) was suffered by the cell to which - 100 mV had been applied.

Similarly the O.C.V's. had all degraded to some extent (Fig. 8.10). Again the cell with + 100 mV applied had degraded by the largest amount (to about 35% of its original value) whereas the cell with zero potential applied had degraded to 80% of its starting value. In contrast the cell to which - 100 mV had been applied had only degraded slightly to about 95% of its initial value.

It was not possible to monitor the spectral response of the O.C.V's. continuously since the devices had to be removed from the life-test box for these measurements and could not be replaced in exactly the

FIG. 8.9 DEPENDENCE OF S.C.C ON ILLUMINATION TIME FOR SINGLE CRYSTAL CELLS

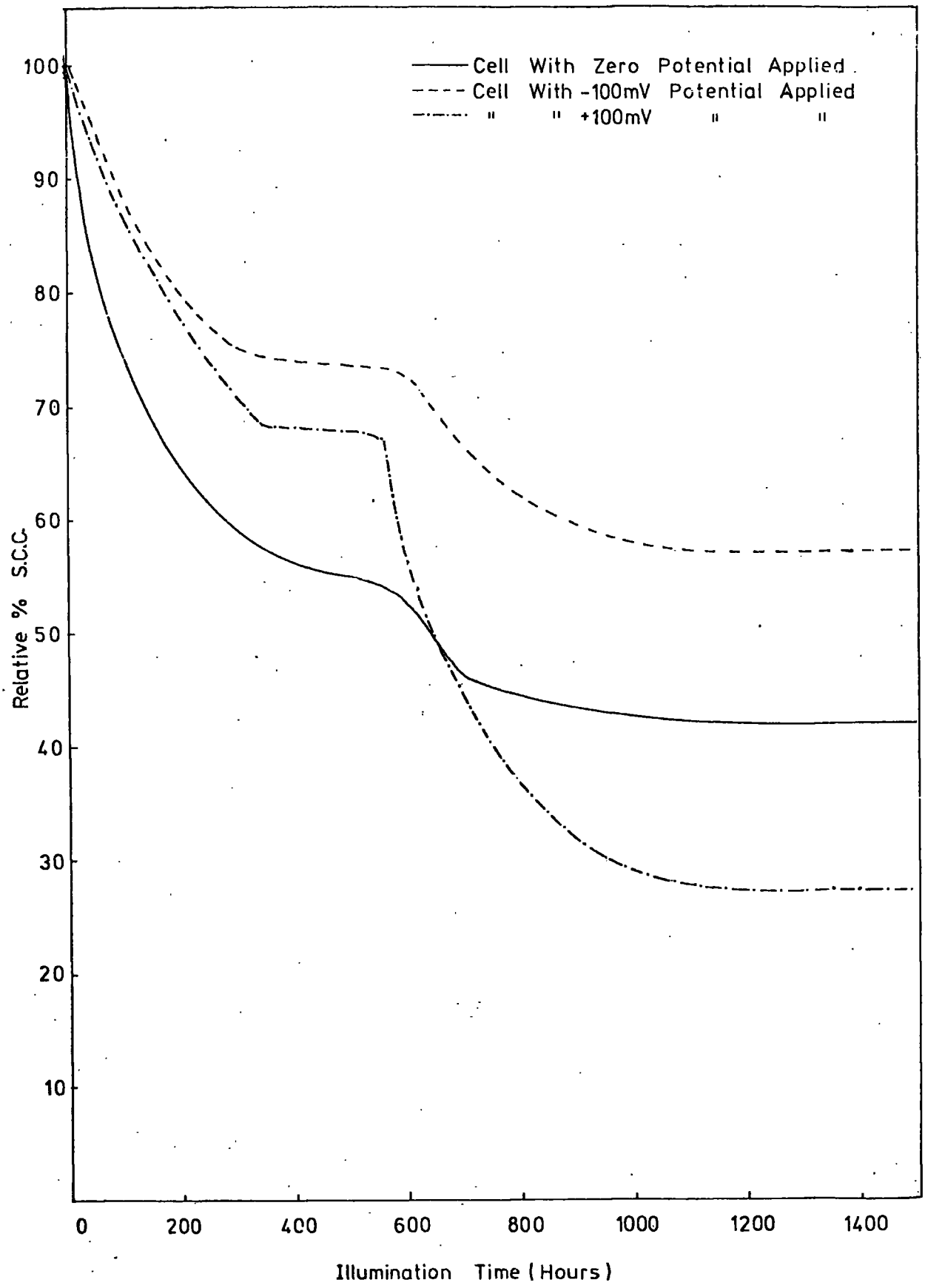

FIG. 8.10 DEPENDENCE OF O.C.V ON ILLUMINATION TIME FOR SINGLE CRYSTAL CELLS

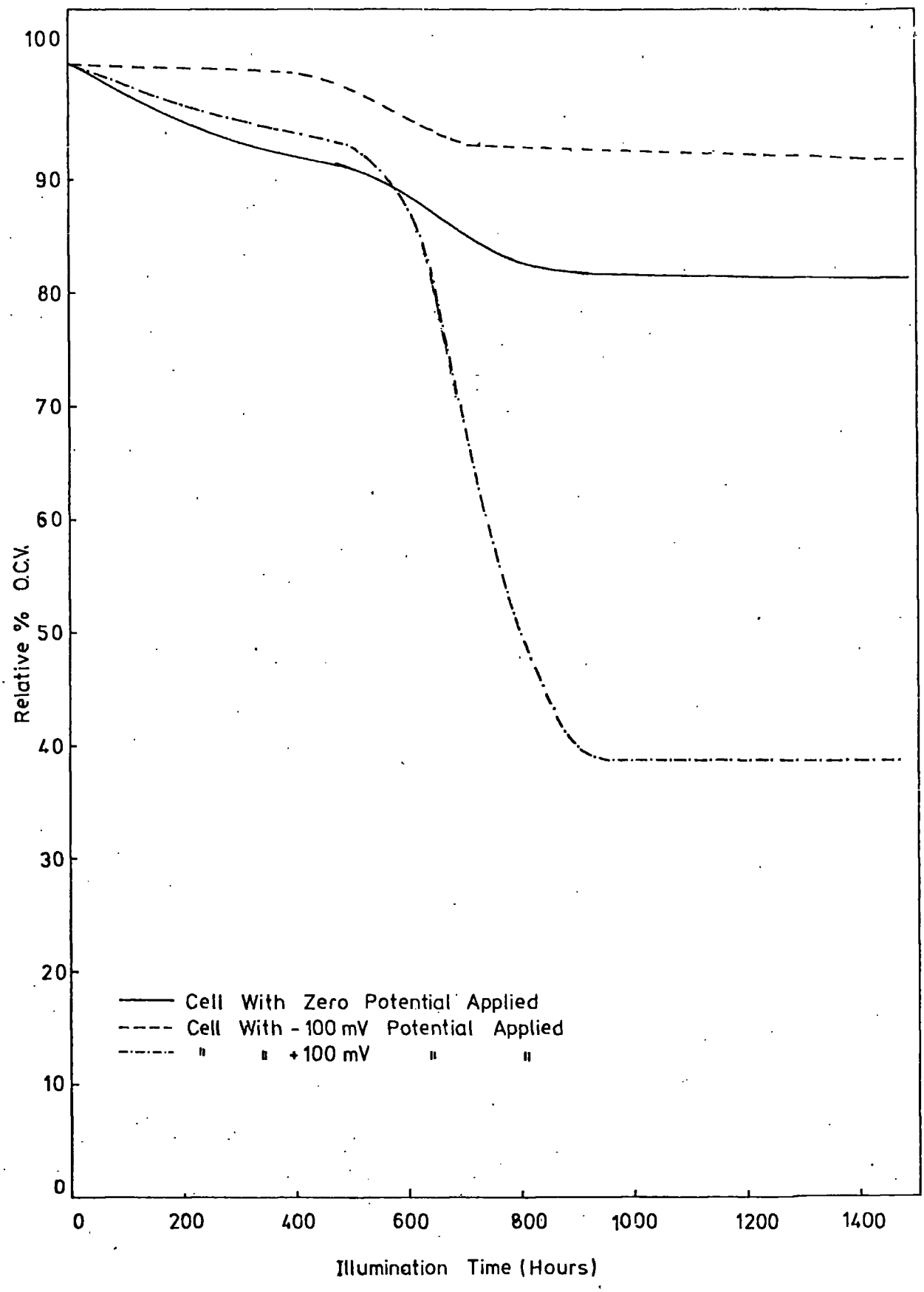

same position. After the 2 min heat treatment in air at 200°C, and the flash evaporation of the gold electrodes, all three types of device had main resolved peaks at 0.75 μm and 0.48 μm with evidence of an unresolved peak of low magnitude in the vicinity of 0.9 μm. This type of response was that expected for heat treated devices. After 24 hours illumination, the peaks had shifted slightly to shorter wavelengths but no significant difference in the spectral distribution of the O.C.V. of any of the three types of device was discernible. However after 1500 hours illumination, the main peak of the device with zero applied potential had shifted to 0.69 μm whereas that of the device to which + 100 mV had been applied during plating had shifted to about 0.67 μm. In contrast the main peak of the device with - 100 mV applied had shifted to 0.7 μm.

8.5 O.C.V. as a Function of the Intensity of Illuminstration

All current-voltage characteristics described in this thesis have been measured using a high illumination level of approximately 100 mW cm^{-2} except for the lifetest investigations described in the previous section. However for terrestrial use as photovoltaic energy converters, it is unlikely that cells would be used at noon only. Obviously the intensity of illumination would vary considerably and would be lower than A.M.1 for most devices being used as solar cells. Furthermore, low light intensities only (approximately 100 μW cm^{-2}) were available at the exit slit of the monochromator and this fact is reflected in the low O.C.V's. produced for most cells investigated. One problem in measuring spectral response was that the intensity of illumination was not uniform throughout the wavelength range investigated (0.3 μm to 1.5 μm) because of the energy distribution of the

tungsten lamp. It was possible to correct spectral responses for this if required (Appendix 1) provided the response as a function of wavelength was known. For all of these reasons it is clearly necessary to investigate how the cell O.C.V. depends on the intensity of illumination.

The steady state O.C.V. as a function of the intensity of illumination from a tungsten source was investigated over four orders of magnitude from about 100 mW cm^{-2} down to 10 μw cm^{-2}. A 1.5 kW tungsten halogen lamp was used for this purpose with a 2 cm water tray underneath it to remove some of the infra-red radiation. Each cell to be investigated was placed in a light tight container. Contact was made to the layer of copper sulphide with a phosphor bronze spring for the single crystal devices and the temporary gridding jig for the thin film devices. Various combinations of neutral density filters were placed between the device and source and the O.C.V. was monitored using the Philips GM 6020 valve voltmeter with 10^8 Ω input impedance.

The curves of O.C.V. as a function of intensity for thin film cells produced in the I.R.D. and Durham 12" vacuum systems both have similar forms but the overall magnitude of the O.C.V. of the I.R.D. films was significantly higher. With these latter devices, low O.C.V's. were observed for as-plated cells (approximately 2.5 mV under A.M.1 illumination). The O.C.V. was a linear function of intensity above 1 mW cm^{-2} (Fig. 8.11). At lower intensities the response was relatively insensitive to light intensity. Response times were a few seconds for this type of device. After a 1 min bake in air at 200°C, the O.C.V. had improved by two orders of magnitude and exhibited saturation effects at high light levels. A further heat treatment of 1 min caused a slight increase in O.C.V. generally but the shape of the curve did not alter.

FIG. 8.11 DEPENDENCE OF O.C.V. ON ILLUMINATION INTENSITY FOR AN IRD. THIN FILM CELL

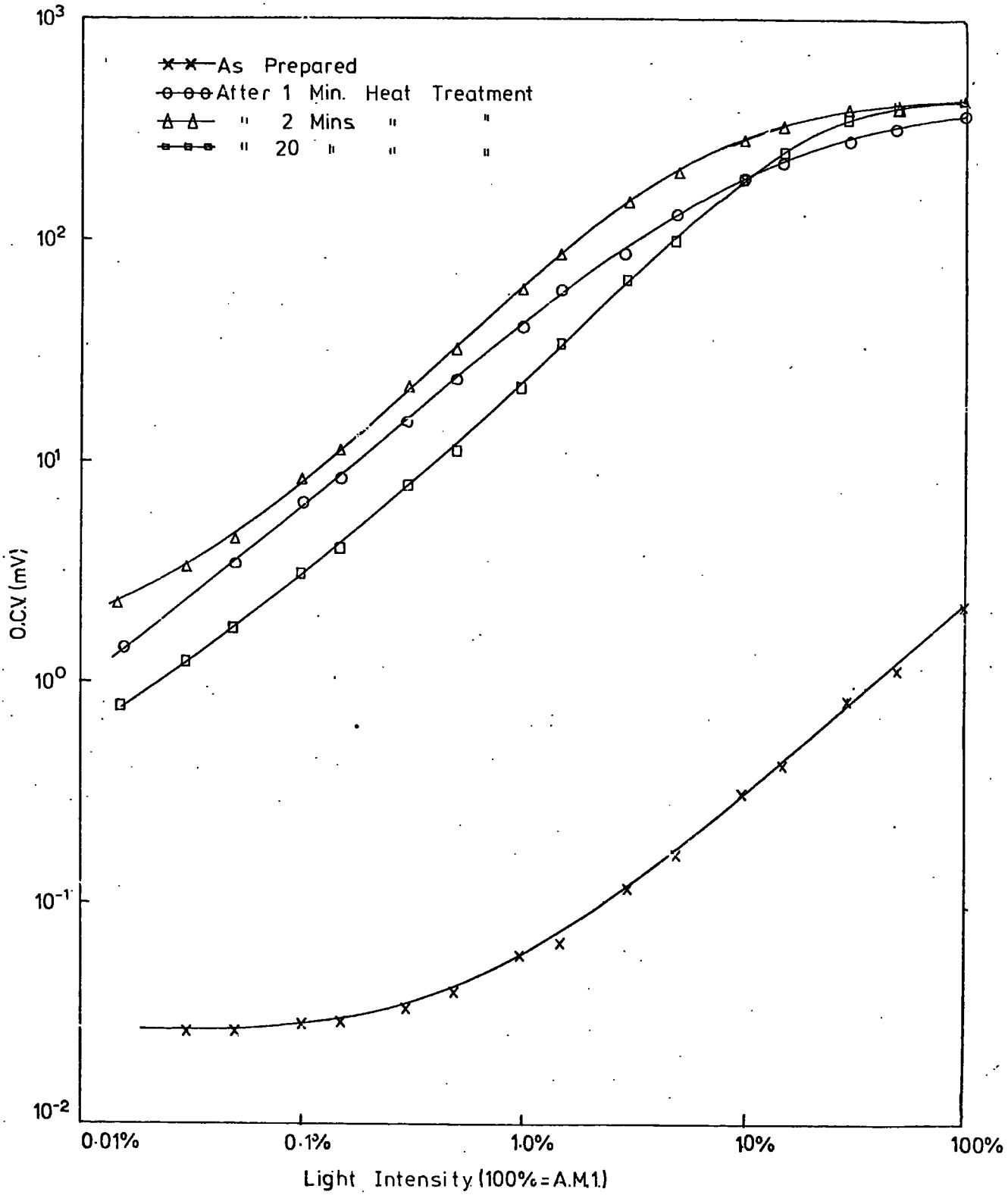

Prolonged heat treatment caused an overall decrease in O.C.V. but that at low light levels was greater than that at levels near A.M.1 illumination intensity. Saturation of the O.C.V. still occurred at the high light levels.

Single crystal devices fabricated on low resistivity undoped cadmium sulphide ($\rho \sim 10^{-2}$ Ω cm) were also investigated and the spectral response of the O.C.V. as a function of intensity resembled closely that of the I.R.D. thin film cells. The O.C.V's. of as-prepared cells were some 15 times larger (approximately 30 mV under A.M.1 conditions) than the I.R.D. film devices.

As-prepared devices formed on copper-doped single crystals gave high O.C.V's. (~60 mV) under A.M.1 illumination and the response was approximately linear (Fig. 8.12). After a very short heat treatment for 1 min, high O.C.V's. were produced at all levels of illumination. Saturation of the O.C.V. was very marked and several tens of mV were generated at light levels of 0.1 mW cm^{-2}. Response times of two or three minutes were observed even in as-plated devices. The slow response was particularly noticeable at low light levels. Prolonged heat treatment led to an overall degradation and longer response times.

Cells prepared on indium and chlorine doped CdS had low O.C.V's. even with incident light intensities of 100 mW cm^{-2}. A set of curves for a typical indium doped cell is shown in Fig.8.13. The dependence of O.C.V. on intensity for the as-plated cell was linear at higher light levels. Heat treatment produced a gradual improvement in O.C.V. at all levels and the response became substantially linear after 2 minutes heat treatment. The optimum O.C.V's. were reached after baking for 4 minutes, but evidence of saturation of the O.C.V. at the highest light levels was slight. Response times remained faster than

FIG. 8.12 DEPENDENCE OF O.C.V. ON ILLUMINATION INTENSITY FOR A SINGLE CRYSTAL DEVICE FORMED ON CdS:Cu

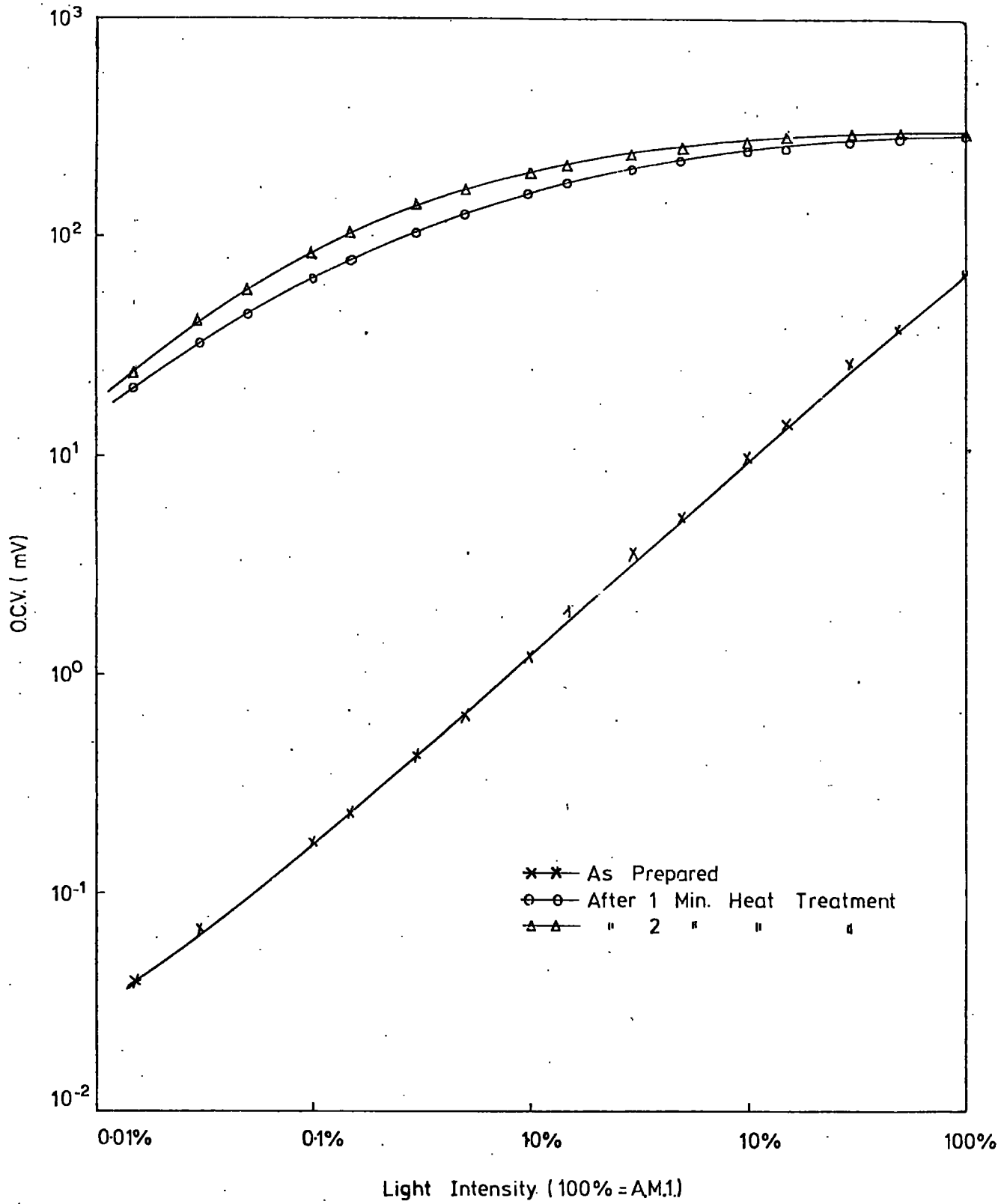

FIG. 8.13 DEPENDENCE OF O.C.V. ON ILLUMINATION INTENSITY FOR A SINGLE CRYSTAL DEVICE FORMED ON CdS:In

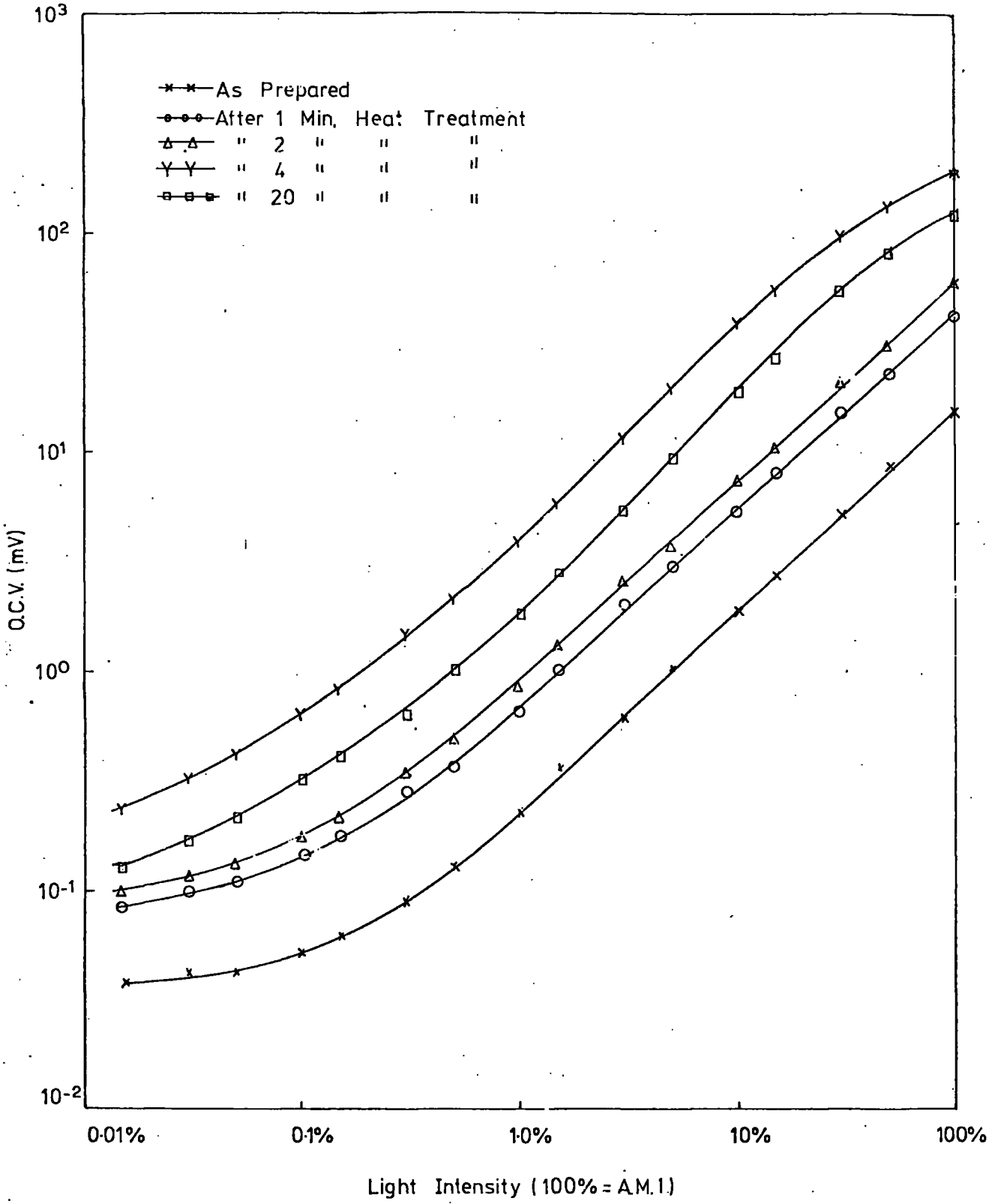

one minute at all stages of treatment but were significantly longer at low levels than at high.

Devices prepared on high resistivity undoped CdS gave very high O.C.V's. (~ 150 mV) even under the ambient lighting conditions in the laboratory. The curves of O.C.V. vs intensity closely resembled those of heat treated devices formed on photoconductive, copper-doped CdS. The saturation of the O.C.V. was very marked in the as-prepared cell and was present down to 1 mW cm^{-2} level). Heat treatment caused a slight overall improvement.

8.6 Removal of Impurities by Solvent Extraction

Several devices were fabricated on dice cut from a single crystal boule of CdS which had been grown in a capsule with a cadmium reservoir and which was therefore expected to be of low resistivity. The boule was dark in colour and showed a slight red photoluminescence at liquid nitrogen temperatures under excitation with ultra violet light. The bulk resistivity was significantly higher (~ 25 Ωcm) than for similar boules prepared under supposedly identical conditions. Dice were prepared in the usual way and the sulphur planes were plated for 10 secs at 90°C. The spectral response of the O.C.V. showed two peaks; the main one at 0.7 μm and a smaller one at 0.5 μm. There was some evidence of an unresolved peak between 0.8 and 1.0 μm (Fig. 8.14). These results were clearly surprising in view of the fact that the boule was supposed to be undoped. A similar problem occurred with several other boules grown using the standard procedures. These boules displayed an anomalously high resistivity (up to 10^6 Ω cm) and exhibited photoconductive behaviour in the region of 0.65 to 0.75 μm. One possible impurity may have been copper.

FIG. 8.14 SPECTRAL DISTRIBUTION OF THE O.C.V OF DEVICES FORMED ON AS GROWN AND SOLVENT EXTRACTED CdS

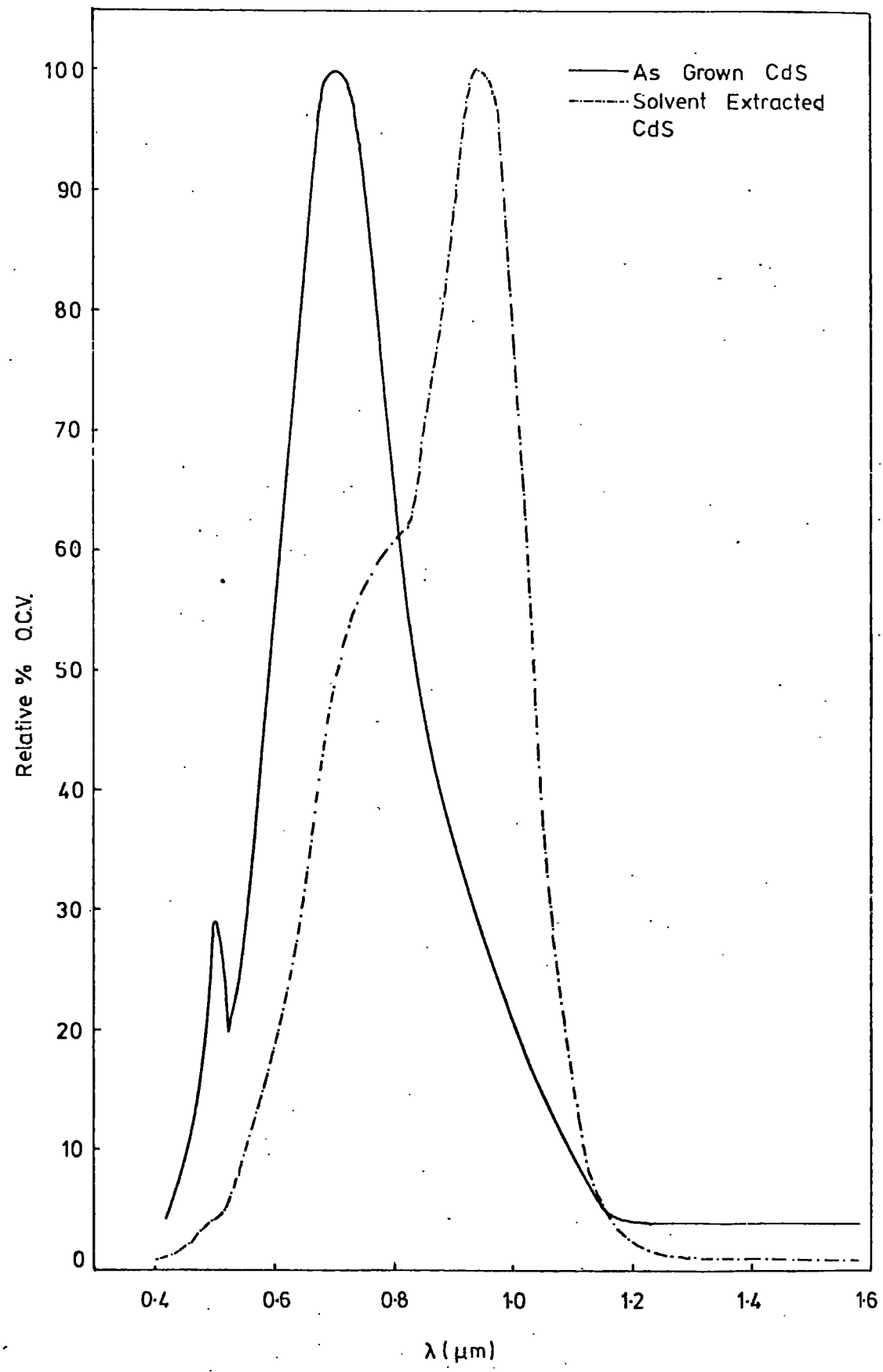

It has been shown (Aven and Woodbury 1962) that impurities such as silver and copper can be removed from ZnSe by heating the crystal in molten zinc. These impurities are more soluble in pure zinc than the impure ZnSe crystal and hence segregate out into the zinc. It was decided that a similar procedure might be suitable for removing impurities which could be present in the CdS boules. A method was therefore devised to enable the crystals to be heated in molten cadmium metal to reduce the impurity content and alter the resistivity.

The treatment was carried out in a silica tube as shown in Fig. 8.15. To remove grease etc. the silica glass was washed in acetone and then immersed in freshly prepared aqua regia for a short time. Finally the glassware was rinsed in distilled water. The tube was then baked in an oven at 100^{o}C for several hours to dry it. A short section cut from a capillary tube was used to facilitate the separation of the crystals from the molten metal after treatment. Several dice were sealed in the rounded end of the tube and about 5 gm of 6 N cadmium shot was sealed in at the opposite side of the capillary. The impurity extraction tube was evacuated and flushed with argon several times before being sealed off at a pressure of about 2 x 10^{-5} torr. After attaching a clamping rod, the tube was suspended in a vertical furnace and maintained at 650^{o}C for several days. At the end of this time, the tube was removed momentarily from the furnace and inverted to separate the molten cadmium from the crystals. The tube was then re-inserted, crystal end uppermost, into the furnace and allowed to cool down slowly to room temperature.

The dice which had been dark in colour and hardly photo-luminescent before heat treatment were not much lighter in body colour. After a short 2 second etch in cold concentrated hydrochloric acid, a

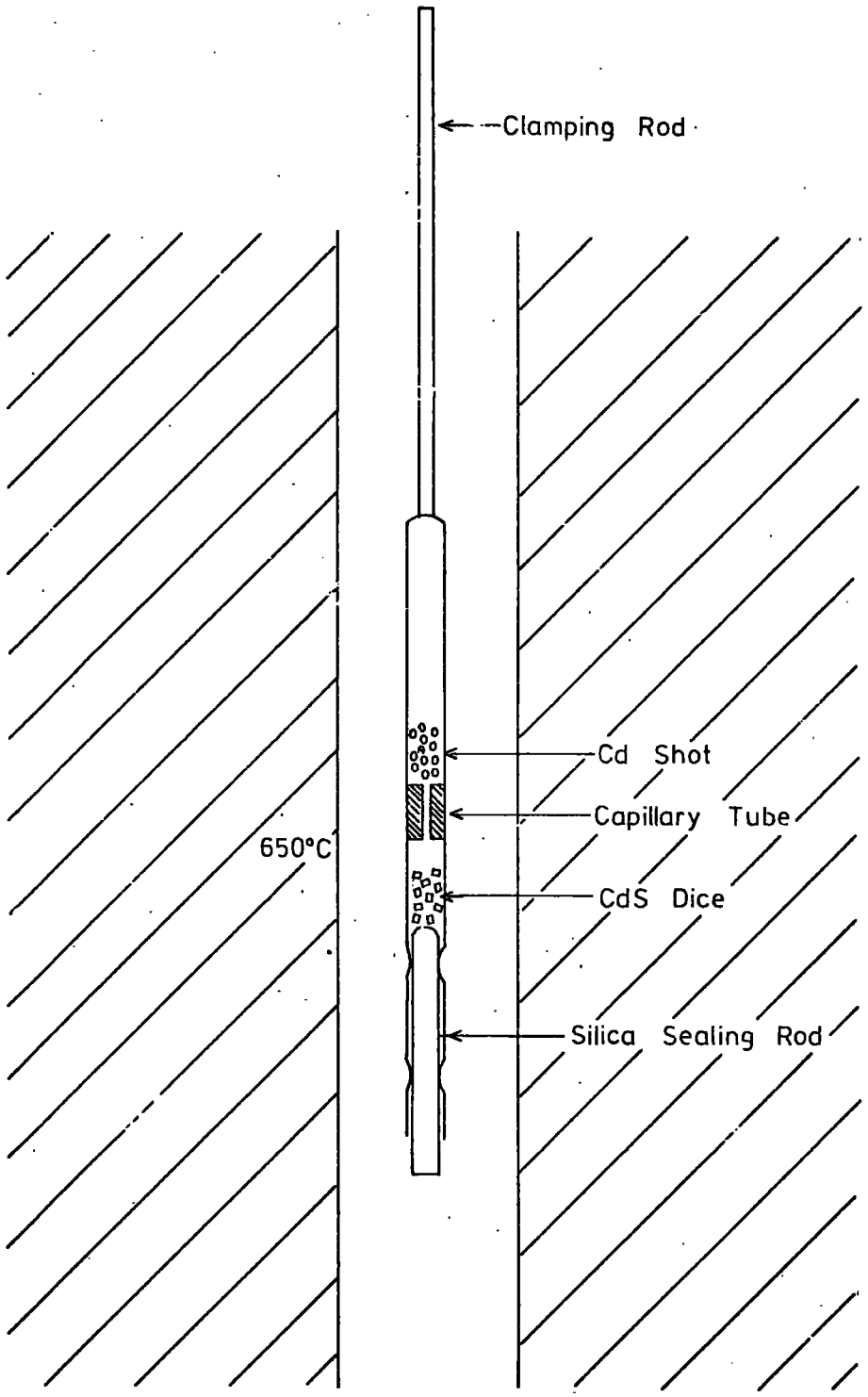

FIG. 8.15 TUBE USED FOR SOLVENT EXTRACTION OF IMPURITIES IN CdS

strong green photoluminescence was observed at 77 K. The resistivity of the material had decreased to about 10^{-1} to 10^{-2} Ω cm.

Devices were fabricated from the treated samples by plating at 90°C for ten seconds and the spectral response of the O.C.V. was measured. These devices produced low O.C.V's. (~ few mV) in common with all other low resistivity devices, but the main response was in a band at 0.94 μm with an unresolved peak in the region of 0.7 to 0.8 μm (Fig. 8.14). The spectral distributions of the O.C.V. for typical devices formed on as-grown and solvent extracted CdS have been plotted on the same axes using relative percentage O.C.V. and wavelength axes since the positions of the band maxima formed the main interest of the investigations. The magnitudes of the O.C.V. of solvent extracted devices were much lower than for those devices prepared on the as-grown CdS. However, subsequent baking of such devices caused the usual improvement in the magnitudes of the O.C.V's.

8.7 Influence of Plating Temperature on the Properties of Cells

8.7.1 Introduction

Most workers who have investigated CdS/Cu_2S solar cells have produced the topotaxial layer of copper sulphide by means of the 'wet' chemical method. A temperature of 90°C is usually employed (Shiozawa et al 1969) but very little work had been reported to justify that this is the optimum temperature to use. Bogus et al (1970) found that properties of a cell were very dependent on the plating temperature in the range 70 to 95°C. They showed that devices formed at 95°C gave higher S.C.C's. than those fabricated at 65°C, but they did not attempt to explain these results in terms of the phase of copper sulphide present. Other workers have shown that the most efficient phase of

copper sulphide with which to form the heterojunction is chalcocite (Cu_2S) (Nakayama et al 1971). Since the Cu-S system is of rather a complex nature (Shiozawa et al, 1969), special precautions may be necessary to ensure the reproducible production of chalcocite. It is possible that strict temperature control of the cuprous ion solution is necessary to produce the desired phase of copper sulphide. The spectral responses of the O.C.V. of devices formed at two different temperature ($90^{o}C$ and $45^{o}C$) were obtained and attempts were made to relate the responses to the phases of copper sulphide present as identified by the R.E.D. technique as discussed in Chapter 6.

8.7.2 Experimental Details

The preliminary investigations were carried out on 25 μm thick evaporated layers of low resistivity CdS ($\rho \sim 10^2 - 10^3$ Ω cm) which had been prepared on flexible substrates (Clark et al, 1971). These evaporated layers were cut into 1 cm^2 areas and the edges were treated with an acid resisting lacquer (Lacomit) to prevent the formation of shorting paths when the topotaxial layer of copper sulphide was formed. Each sample was dipped in a 1 N potassium iodide solution to roughen the surface and remove oxide layers.

The plating solution was made up as described in Chapter 6 and was cooled slowly to room temperature whilst maintaining a flow of oxy-free nitrogen through the liquid. Several thin film samples were dipped for periods of five seconds at various temperatures between 20 and $95^{o}C$ as the plating solution was gradually heated. Care was taken to ensure that the pH was 2.5 at each dip temperature. After dipping, all the devices were washed in distilled water and dried in a stream of nitrogen.

Initial measurements using a high impedance voltmeter showed that all of the cells gave low open circuit voltages ($\approx$ several mV) even under intense illumination. Thin film cells usually require an optimisation heat treatment (Section 8.1) and so all of the devices were heated under as near the same conditions as possible for 2 minutes at 200°C in air.

Contact was made to the copper sulphide layers using a 90% transmission, gold plated copper grid and the temporary gridding jig described in Chapter 7. The advantages of this type of contact were, firstly that it did not scratch through the layer, and secondly that it did not subject the devices to any further heat treatment as might well be incurred by using an evaporated gold grid. After the temporary contact had been made to the copper sulphide layer, the cells were illuminated in turn with a 1.5 Kw tungsten halogen lamp under approximate A.M.1 conditions and the O.C.V's. were recorded.

Since the idea was to try and relate the spectral responses of the O.C.V. with the phase of copper sulphide present as identified using reflection electron diffraction techniques, it was necessary to fabricate devices on single crystal CdS with the same resistivity as the thin films investigated above. Single crystal dice were plated for 10 seconds at 45°C and 90°C i.e. the same temperatures used in the R.E.D. studies. The spectral responses of the O.C.V's. of the devices prepared at the two different temperatures were then determined.

8.7.3 Results

All of the thin film devices which had been prepared at temperatures between 20°C and 95°C improved after the short heat treatment in air. The O.C.V. after heat treatment is plotted as a function

of plating temperature in Figure 8.16. Cells on which the copper sulphide had been formed at low temperatures (between 20°C and 70°C) gave low O.C.V's. (~ 1 mV). For samples dipped in the range from 75°C to 85°C, the O.C.V's. increased sharply and then levelled off again at about 90 to 95°C. This behaviour was reproducible for several sets of samples.

The spectral distributions of the O.C.V's. of the devices prepared at 90°C and 45°C are shown in Fig. 8.17. The devices prepared at 45°C produced lower O.C.V's. than those fabricated at 90°C but the O.C.V's. are shown as normalised relative percentages since the investigation was more concerned with the positions of the maxima than absolute magnitudes. In the devices plated at 90°C, there was an unresolved peak in the vicinity of 0.7 μm, but the usual main peak was in the vicinity of 0.9 μm. However for the devices plated at 45°C, the dominant peaks were at 0.7 μ, and 0.52 μm with an unresolved peak in the vicinity of 0.9 μm. Both types of device responded within seconds to changing illumination.

Current-voltage characteristics were obtained from devices produced at 45°C and 90°C under approximate A.M.1 illumination and in the dark. These curves measured in forward bias for illumination and no illumination converged for each type of device, but did not cross.

8.8 Assessment of Stoichiometry by Observation of Phase Transformation

Palz et al (1972) reported that the stoichiometry of copper sulphide could be determined by studying the variation of the S.C.C. with temperature. It is possible to assess the stoichiometry in this way since the cell series resistance (Chapter 3) is due mainly to the

FIG. 8.16 DEPENDENCE OF O.C.V. ON PLATING TEMPERATURE FOR HEAT TREATED THIN FILM CELLS

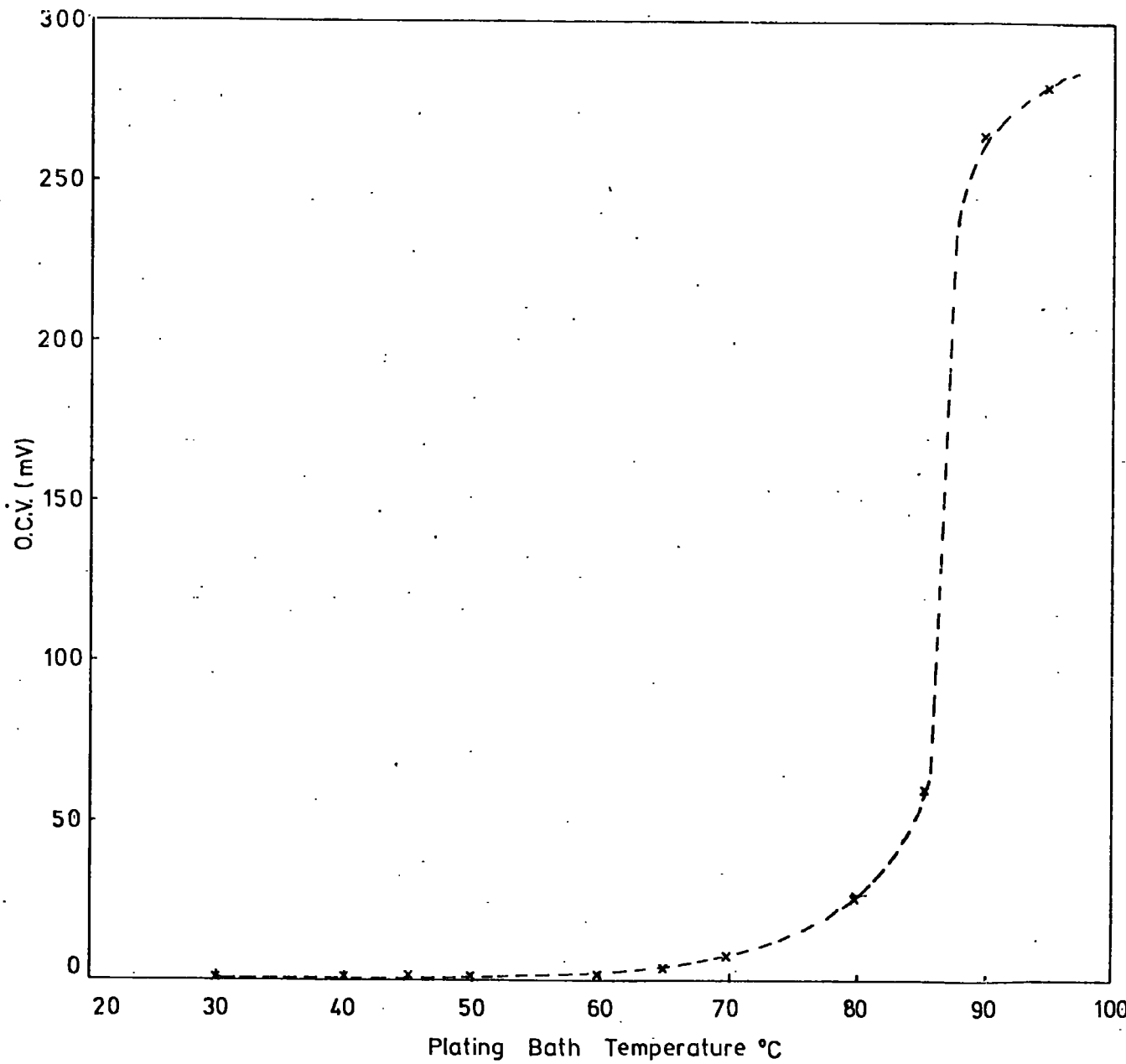

FIG 8.17 SPECTRAL RESPONSE OF THE O.C.V OF UNBAKED DEVICES FORMED AT 90°C AND 45°C

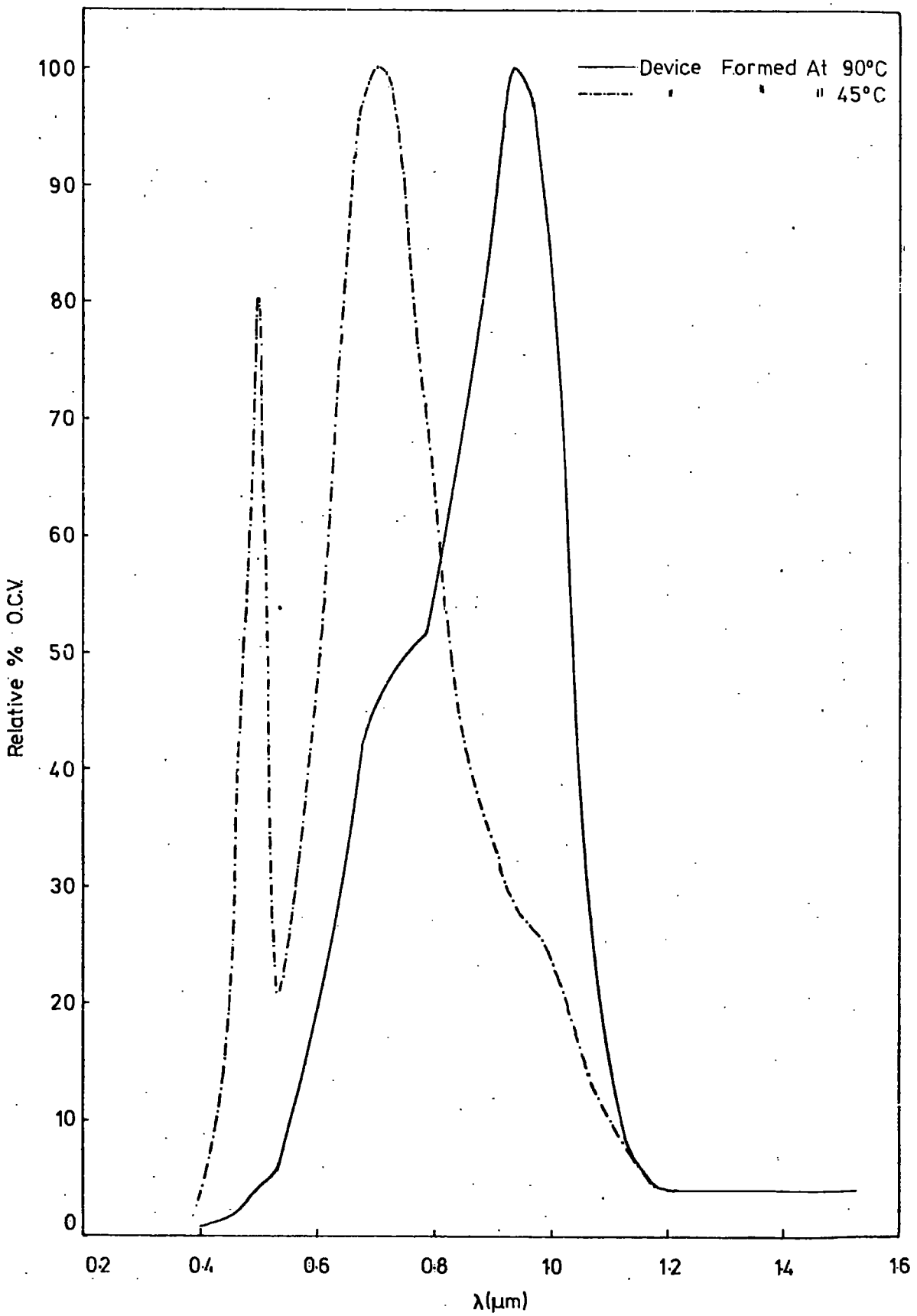

sheet resistance of the copper sulphide layer. It is well established that $Cu_{1.8}S$ and $Cu_{1.96}S$ undergo phase transformations at 90°C and 93°C respectively whereas the transition temperature of Cu_2S rises from 98°C to 108°C as the composition approaches the stoichiometric value (Okamoto and Kawai, 1972).

Single crystal devices were positioned on a metal heating block which was capable of fast heating to 150°C and fast cooling by means of compressed air. The small area devices were illuminated using the standard 1.5 kW light source. The S.C.C. was measured using the current to voltage converter, the output of which fed the Y amplifier of a Bryans 21001 X-Y recorder. The temperature was measured using a copper constantan thermocouple clamped to the cell surface. The signal was amplified and fed into the other channel of the recorder. Thermocouple voltage and S.C.C. were monitored as the cell was heated to 150°C and then cooled quickly to room temperature.

Results of these experiments on the small area (4 mm^2) single crystal devices were not conclusive since the small area of the device and the spring contact did not lead to high S.C.C's. The phase transition could be observed but it was not a well defined parameter. The heat losses from the sample did not help in this respect. It was possible to observe the transition for large area thin film cells which had been gridded and encapsulated several months before, but these devices were at least partially degraded and did not give much information. This technique may therefore give useful information concerning the copper sulphide stoichiometry for large area (>1 cm^2) evaporated film or silk screen printed cells but not for single crystal cells employing the particular geometry used in these investigations.

8.9 Discussion of Results

As-prepared single crystal or thin film solar cells did not exhibit good device parameters. Their O.C.V's. and S.C.C's. were generally low and the current-voltage characteristics of illuminated cells were not 'square'. This low curve factor was probably caused by the existence of an abrupt CdS/Cu_2S junction in these as-plated cells which may well have permitted tunnelling behaviour and shunting paths across the junction. Devices formed on low resistivity ($\rho \sim 10^{-2}$ to 10^{-1} Ω cm) CdS gave low O.C.V's. This was almost certainly due to the low shunt resistance which the cells would possess. It has been reported that shunt resistances less than 10 Ω result in significant loss of curve factor and efficiency (Clark et al, 1971). Devices fabricated on high resistivity, undoped CdS ($\rho \sim 10^{6}$ Ω cm) gave high O.C.V's. (tens of mV) but such devices possessed very high series resistance. This accounts for the low S.C.C's. which were obtained from these devices. Cells produced on copper doped CdS exhibited properties intermediate between those of the high and low resistivity devices. I.R.D. thin film devices gave lower O.C.V's. and curve factors than single crystal devices with similar resistivities. This was probably due to numerous shorting paths between the Cu_2S and the bottom contact in the thin film devices. Grain boundaries and pinholes would increase the number of paths.

A short (2 min) heat treatment seems to have one main effect. This is the growth of an i-type copper compensated layer between the p-type Cu_2S and n-type CdS. Evidence of the formation of a photo-conductive i layer is supplied by the lengthening of device response times as the heat treatment was extended. Differences in the current-voltage characteristics gave additional support to this proposal. As-prepared devices formed on low resistivity undoped CdS ($\rho \sim 10^{-1}$ Ω cm)

showed that the curves measured in the dark and under illumination converged. After a short heat treatment, the curves intersected showing that photoconductive behaviour had been induced by the heat treatment process. Other workers (Shiozawa et al, 1969) have reported that when thin film cells are heated in vacuum or inert gas, there is a slow irreversible increase in series resistance. They also proposed that this increase was due to the growth of an i-layer by copper diffusion.

Te Velde (1973) alternatively suggested that the heat treatment must be carried out in an atmosphere containing some oxygen to produce higher efficiency cells. He proposed that after a short heat treatment in air, oxygen is absorbed at the interface of CdS and Cu_2S and causes an increase in barrier height between these two regions. The amount of oxygen required for this process is too small to determine. This model for the modification of cell properties as a function of heat treatment does not include the effects of copper diffusion at all.

The greatest improvement in cell parameters after a 2 minute heat treatment in air was found with the I.R.D. thin film devices. Apart from the improvement in curve factor which results from the formation of the i-layer, the effects of the shorting paths present would also have been decreased by the dissociation of Cu_2S and diffusion of copper from the grain boundaries and pinholes. Cells produced on single crystal CdS of similar resistivity showed smaller improvement since the number of shorting paths would be fewer than in thin film devices.

Cells formed on low resistivity single crystal CdS ($\rho \sim 10^{-2}$ Ω cm) did not improve on baking as much as the other types of device. This was probably because the formation of a photoconductive 'i' layer was more difficult to achieve in heavily indium or chlorine-doped CdS. These types of device all exhibited a low reverse breakdown voltage rather like that of a Zener diode.

Devices fabricated on the high resistivity undoped CdS ($\rho \sim 10^6$ Ω cm) did not improve much on heat treatment either, but this was because these devices had high built-in shunt and series resistances. Cells formed on copper doped CdS behaved in a similar manner in the sense that the as-prepared devices produced high O.C.V's. because the heterojunction was between Cu_2S and CdS:Cu. The base starting material of the cell was similar to the 'i' type layer normally produced after heat treatment.

Te Velde (1973) also proposed that heat treatment in hydrogen had the effect of reducing the barrier between the CdS and Cu_2S and presumably therefore did not lead to an improvement in the performance of a device. However preliminary measurements on our thin film devices did not support this suggestion. Te Velde has already suggested that the amount of oxygen involved in the optimisation process is very small (Te Velde, 1973) and it is likely that the evaporated CdS layers contained some oxygen. Consequently, optimisation would still occur if the devices were heated in hydrogen and surface oxidation decreased.

It appears that surface oxidation of the Cu_2S occurs during prolonged baking in air and leads to a loss in O.C.V. and S.C.C. In the investigations reported in this chapter it has been demonstrated that this oxidation process is reversible to a great extent. Devices were successfully rejuvenated by exposure to a strong reducing agent after oxidation in the laboratory atmosphere over a period of several weeks. It also proved possible to degrade cells at room temperature with hydrogen peroxide liquid and ammonium sulphide vapour. In the latter case it is probable that the following reaction occurred

$$Cu_2S + 0.111\,S \longrightarrow 1.111\,Cu_{1.8}S$$

Again it was possible to rejuvenate devices by dipping them in the strong reducing agent.

Aerschodt and Reinhartz (1970) showed theoretically, using thermodynamic considerations, that the most efficient CdS/Cu_2S solar cell could be obtained by applying a voltage of between + 0.2 and 0.25 V to the copper sulphide surface during plating. Their experimental observations did not agree with this however. The results presented in this thesis suggest that the use of a potential of - 100 mV produces more stable devices than potentials of zero and + 100 mV. It is possible to explain the results observed here in terms of a simple electrolytic model. If a negative potential is applied to the copper sulphide layer with respect to a copper electrode similarly immersed in a bath of copper ions, it should be possible to produce a thin film of metallic copper on the surface. After heat treatment, the copper would diffuse through the copper sulphide and into the CdS and an 'i' layer would be formed in the usual way without leaving a deficiency of copper in the copper sulphide. Bogus and Mattes (1972) reported that more stable devices could be produced by depositing an additional thin layer of copper on to the chalcocite before heat treatment.

The S.C.C's. of all devices fabricated to investigate the effects of applied potentials degraded during the 1500 hours illumination. This degradation was most marked for devices prepared using a positive applied potential during plating and it is proposed that these devices had Cu_2S layers initially deficient in copper. It is likely that surface oxidation aided the degradation but that diffusion of copper into the 'i' layer occurred to some extent during the investigations. O.C.V's. were similarly degraded but to a lesser extent. Devices formed with a negative applied potential may have had a thin layer of copper electroplated on to the copper sulphide and so the effects of

oxidation would have been less than with the other two sets of cells. The shifts in the spectral distribution of the O.C.V. during the 1500 hours illumination time would support the suggestion that a gradual oxidation causes a shift of maxima to lower wavelengths and that the effect is slightly less if excess copper is present.

The examination of the influence of the intensity of illumination on the O.C.V. gave some useful information concerning the operation of the devices. I.R.D. thin film devices, when optimised, showed a saturation level at high intensities but at lower light levels there was a change of gradient below which a nearly linear dependence was observed. This behaviour agrees with that predicted by the equivalent circuit (Chapter 3) since at low levels, the diode is forward biased by a small voltage and the effective resistance R_d is large, such that $R_d >> R_i + R_{sh}$. As the intensity of illumination is increased, the value of R_d decreases relative to R_{sh} but eventually R_d tends to a limiting value. This leads to a limiting value of O.C.V. The as-plated devices exhibited a linear dependence of O.C.V. on illumination intensity since R_{sh} is low because of the shorting paths.

Devices produced on high resistivity ($\rho \sim 10^6$ Ω cm) CdS exhibited an anomalous variation of O.C.V. with intensity of illumination. No linear dependence could be discerned even at low light levels. This behaviour could be explained if the lumped shunting resistance R_{sh} is large compared with that in the I.R.D. thin film devices. Shiozawa et al (1969) observed a similar effect in ceramic CdS solar cells. Devices fabricated here on copper doped CdS single crystals displayed similar effects but to a lesser extent.

The cells fabricated on low resistivity ($\rho \sim 10^{-2}$ to 10^{-1} Ω cm) CdS had a linear dependence of O.C.V. on intensity of illumination over the full range investigated. It is suggested that this is caused by the very

low value of R_{sh} in such devices. Prolonged heat treatment of such cells did not produce saturation presumably because of the difficulty of producing an 'i' type layer. R_{sh} probably remained essentially unchanged.

The main effect of heating pieces of CdS in molten cadmium was to reduce the resistivity of about 10^{-1} Ω cm. If the anomalous behaviour of the as-grown material is due to inadvertent contamination with copper impurity, it is likely that some of the impurity was removed during the heating, but there is no proof of this. Copper is certainly removed by this process in other II-VI compounds such as ZnSe. The resistivity of the treated CdS was too low to be useful for the fabrication of devices which would produce reasonable O.C.V's.

It seems that the temperature of the plating solution used must be controlled to produce reproducible layers of copper sulphide of the correct stoichiometry. Devices produced by dipping for 5 secs at temperatures below 70°C to 80°C gave consistently low O.C.V's. even after heat treatment. Conversely devices plated at temperatures above 85°C produced high O.C.V's. In the region between these two temperatures, the plating temperature had a strong influence on the O.C.V. Devices formed at 90°C had a maximum response at 0.9 μm which, it is suggested, is due to the indirect optical absorption process in chalcocite. A temperature of 45°C was chosen at which to study the low temperature formation of copper sulphide since this temperature was in the plateau region of the variation of O.C.V. with plating temperature, and was therefore far removed from the very temperature sensitive region. For devices plated at 45°C, the dominant response was in the vicinity of 0.7 μm. It is suggested that this peak is associated with indirect optical absorption in djurleite ($Cu_{1.96}S$). Support for this proposal

can be obtained from investigating the dependence of the spectral response of the S.C.C. on the stoichiometry of the copper sulphide (Palz et al, 1972). In Palz's work it was reported that the peak S.C.C. response for a CdS/$Cu_{1.955}S$ heterojunction was at 0.69 μm. Direct evidence of the phase of copper sulphide formed at 45°C has been described in Chapter 6. The layers formed after a long (45 min) dip time were indeed identified as djurleite $Cu_{1.96}S$.

Finally it should be noted that the response with a maximum at 0.7 μm for heat treated devices (Chapter 7) was attributed to photoconductive effects in an 'i' type layer which had been formed by diffusion of copper into CdS at the interface. It is obvious that the diffusion process will cause a copper deficient phase but it is proposed that as-prepared devices formed at 90°C are CdS/Cu_2S heterojunctions whereas those formed at 45°C are CdS/$Cu_{1.96}S$ diodes.

CHAPTER 9

SUMMARY OF CONCLUSIONS

9.1 CdS Thin Films

During the three year period of investigation, many thin films of CdS have been prepared. Three evaporation systems were used. These were: (1) The I.R.D. resistively heated system, (2) the Durham resistively heated system and (3) the system utilising enclosed tubes. The first method produced 25 μm thick evaporated layers with a resistivity in the range 10^2 to 10^3 Ω cm and few visible defects. These layers were successfully converted into solar cells. Evaporated layers produced in the Durham resistively heated system in general were of lower resistivity, 10^{-1} to 10 Ω cm, probably due to excess cadmium. The films were up to about 15 μm thick and contained some visible defects such as pinholes. It would have been possible to produce layers of the desired thickness with a more powerful heating source, but none was available. The relatively low power source meant that the system became too hot during the resultant very long evporation process and re-evaporation occurred, thus reducing the film thickness. The enclosed tube method produced thin films of high resistivity ($>10^5$ Ω cm) showing photoconductive behaviour. It was only possible to produce thin layers (~ 5 μm) but the film quality seemed quite good. Although thin film cells were eventually made from films evaporated using systems (2) and (3), these did not exhibit desirable properties.

R.E.D. studies on 10 μm thick films of CdS demonstrated that there was a considerable degree of orientation of the crystallites as reported by other workers. Transmission electron microscope studies showed that relatively expitaxial films of CdS could be grown on {100}

faces of NaCl using the Durham resistively heated source. These epitaxial layers relaxed from the cubic phase to the wurtzite phase after storage in the laboratory for several months.

9.2 CdS/Cu_2S Photovoltaic Cells

It was found that copper sulphide could be grown topotaxially on cadmium sulphide but that the conversion proceeded 1.5 times faster on sulphur faces than on cadmium planes. The crystal orientation and face on which the copper sulphide was formed also proved to be important. The photovoltages of unbaked cells with the cuprous sulphide formed on sulphur planes were some 20% larger than those observed in devices formed on cadmium planes.

The resistivity and dopants in the base CdS also had a great influence on the properties of devices. High resistivity CdS ($\rho \sim 10^6$ Ω cm) gave rise to devices with high O.C.V's. and low S.C.C's. with the main response for unbaked devices in the region of .53 μm. These devices had slow response times ($\sim$ minutes). In contrast, devices doped with indium and chlorine and with very low resistivity in the range 10^{-2} to 10^{-1} Ω cm produced low O.C.V's., S.C.C's. and curve factors. The main response for such unbaked devices was in the vicinity of 0.9 μm. Cells fabricated on undoped low resistivity CdS ($\rho \sim 10^{-1}$ Ω cm and above) produced similar characteristics to those of the indium and chlorine doped devices, but higher outputs were observed. The best overall unbaked devices were produced using copper doped CdS and these devices resembled the undoped CdS devices which had been subjected to a short heat treatment.

The best thin film devices were produced on evaporated layers from the I.R.D. system, but gave low outputs until a short heat treatment

had been performed. Thin films produced in the Durham resistively heated system did not lead to very good devices.

Heat treatment of thin film and single crystal devices for 2 to 4 minutes in air at 200°C led to great improvement in all devices investigated. This short heat treatment caused a shift downwards in the spectral responses of the O.C.V. and caused a lengthening of the response time. In addition, the short heat treatment caused the current-voltage characteristics of thin film and undoped single crystal devices formed on low resistivity CdS ($\rho \sim 10^{-1}$ Ω cm and upwards) measured under illumination and in the dark to cross, whereas previously they had converged. Crossover was observed on the as-plated devices formed on photoconductive copper doped or undoped CdS, but was not observed on the indium or chlorine doped cells even after prolonged heat treatment.

It is proposed that the short heat treatment had one overriding effect. This was the dissociation of some of the chalcocite into copper which diffused into the underlying cadmium sulphide. The copper compensated CdS was photoconductive and modified the O.C.V. spectral response in most cases. It is suggested that the peak in the vicinity of 0.7 μm is due mainly to the 'i' layer. However it is obvious that copper diffusion will cause a copper deficient phase of copper sulphide to be formed at the interface. Prolonged heat treatment caused overall degradation of cell parameters. It is suggested that the deterioration is due mainly to surface oxidation. This process was shown to be reversible to a large extent by oxidising the cells at room temperature to enhance degradation and by dipping in a strong reducing agent to restore the original sensitivity.

Experiments involving electrode potentials applied to the copper sulphide surface during plating showed that the resultant stability

of devices could be controlled to some extent. Devices to which - 100 mV were applied during plating were found to be more stable over a 1500 hour illumination period than cells prepared without applied potentials. In contrast, devices prepared with a + ve potential were less stable than conventional cells. It is suggested that the improved stability is due to the deposition of a thin layer of copper during the plating process for - ve applied potentials.

The temperature at which the plating is carried out is another important parameter. Temperatures of 90°C and above promoted the growth of chalcocite (Cu_2S) as identified directly using R.E.D., and indirectly by measurement of spectral responses. The peak in the O.C.V. response in the vicinity of 0.9 μm is associated with absorption processes in chalcocite. Devices produced at temperatures below 65°C gave low O.C.V's. and cells plated at 45°C were subjected to more detailed examinations. R.E.D. investigations showed that the formation of a copper deficient phase, Djurleite, was promoted at this temperature. This correlated with changes in the O.C.V. spectral response which showed that the main peak for unbaked devices is at 0.7 μm which may be associated with absorption processes in Djurleite ($Cu_{1.96}S$).

Heat treated devices prepared at 90°C show a main peak at 0.7 μm due to the formation of a photoconductive 'i' layer, whereas the unbaked devices prepared at 45°C show a similar response, but this is mainly due to the formation of a copper deficient phase of copper sulphide.

9.3 Suggestions for future work

The results described in this thesis indicate several interesting areas for future work. These are:

(1) The thin film and single crystal work should be extended to a study of sprayed and sintered powder layers. Powdered CdS cells would consume still less energy in production than evaporated layers Much larger area devices could also be fabricated. The author has only carried out preliminary work on sintered CdS discs and the main problem would appear to be that the resistivity of the sintered layers is much too high or low.

(2) The work concerning heat treatment of solar cells should be investigated much more fully in ambients other than air. Baking in hydrogen may produce more efficient solar cells. Specially prepared thick layers of Cu_2S (200 μm or above) on CdS should be observed at each stage of heat treatment using R.E.D.

(3) Investigations on the control of the stoichiometry of the copper sulphide by applying electrode potentials during plating should be continued in view of the discrepancy between theory and the observations reported here, and by other workers. R.E.D. investigations may prove to be of use in monitoring the chemical phase of the copper sulphide as a function of illumination time.

(4) Zinc should be introduced into the lattice of CdS using the solvent extraction process described in Chapter 8. This will produce a mixed crystal which would give rise to topotaxial copper sulphide layers under less strained conditions. There would be fewer interface or recombination states and higher O.C.V's. should be obtained. Eventually this work could be extended to powdered solar cells.

APPENDIX 1

CORRECTIONS TO SPECTRAL RESPONSE CURVES

None of the spectral response curves presented so far in this thesis have been corrected for the variation of energy with wavelength of the light source or for the varying dispersion of the prism monochromator. To make these corrections it was necessary to measure the spectral distribution of the output of the tungsten lamp. This was done using a Hilger and Watts Schwartz Compensated Linear Vacuum Thermopile Type F.T. 16.301/60287 at the exit slit of the monochromator. The input from the tungsten lamp at the entrance slit to the monochromator was mechanically chopped at 10 Hz and the resulting output of the thermopile was fed to a Barr and Stroud Type E.L. 7921 tuned amplifier. A moving coil meter in this amplifier gave a reading directly proportional to the energy falling on the thermopile. The meter output is plotted as a function of wavelength for the light source in Fig. A.1. This calibration enabled the spectral response of the O.C.V. to be corrected for equal incident energy when required. However, although simple, the correction process is laborious and so a computer program was written to perform this more easily and plot the response automatically. The flow chart and program listing are shown in Figs. A.2 and A.3. A corrected curve is shown in Fig. A.4. This should be compared with the uncorrected response shown in Fig. 8.17.

The corrections of many O.C.V. responses at various stages of heat treatment were carried out, but the conclusion is that no additional information is revealed after the correction process, but there is a slight downward shift in wavelength of corrected peaks relative to uncorrected responses. The main features can certainly always be distinguished on the uncorrected responses. Furthermore, in the previous

FIG. A.1 ENERGY DISTRIBUTION OF TUNGSTEN LAMP RUN AT 200 V.D.C.

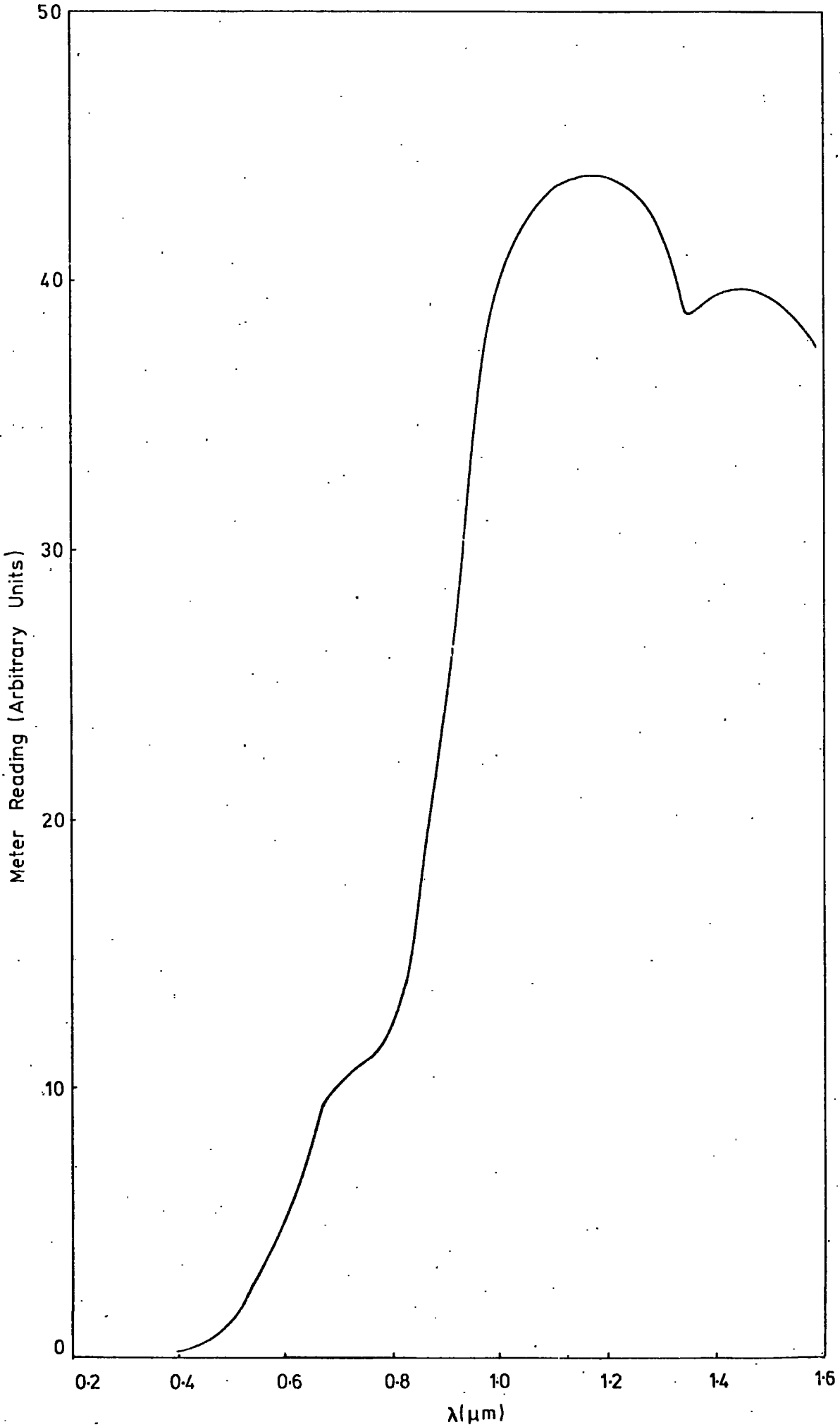

FIG. A.2 FLOW CHART OF SPECTRAL RESPONSE CORRECTION PROGRAM

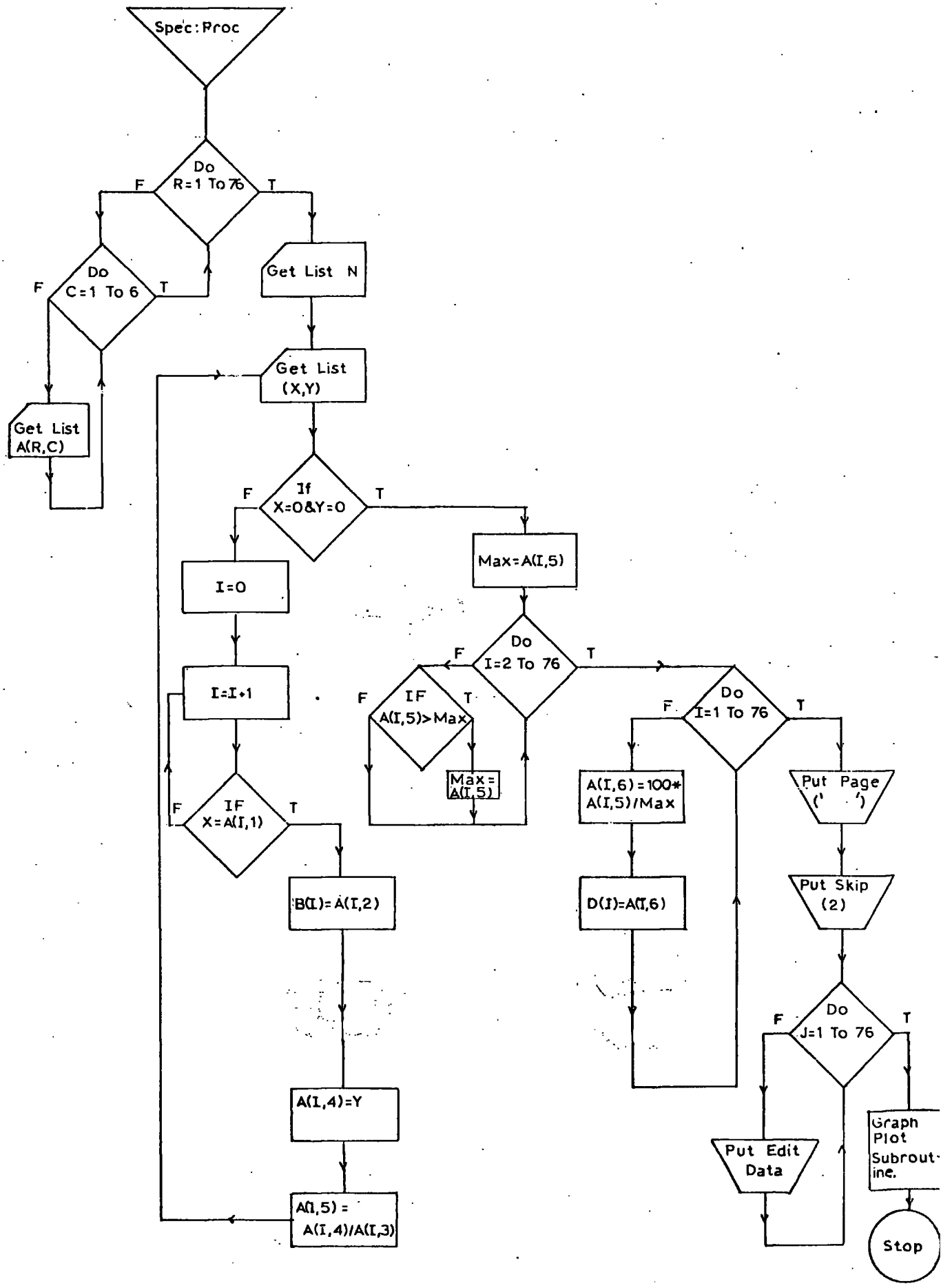

FIG. A.3 LISTING OF SPECTRAL RESPONSE CORRECTION PROGRAM

```
    SPEC:PROC OPTIONS(MAIN);
         DCL(R,C,N,I,J,K)FIXED BIN(31),(X,Y,MAX)FLOAT(16),A(76,6)FLOAT(
16),(B(76),D(76))FLOAT(6);
         DO R=1 TO 76;
         DO C=1 TO 6;
         GET LIST(A(R,C));
         END;
         END;
         GET LIST(N);
   START:GET LIST(X,Y);
         IF X=0 & Y=0 THEN GO TO STOP;
         I=0;
    CONT:I=I+1;
         IF X=A(I,1) THEN DO;
         B(I)=A(I,2);
         A(I,4)=Y;
         A(I,5)=A(I,4)/A(I,3);
         GO TO START;
         END;
         ELSE GO TO CONT;
    STOP:MAX=A(1,5);
         DO I=2 BY 1 TO 76;
         IF A(I,5)>MAX THEN MAX=A(I,5);
         END;
         DO I=1 TO 76;
         A(I,6)=100*A(I,5)/MAX;
         D(I)=A(I,6);
         END;
         PUT PAGE EDIT('       DRUM READING          WAVELENGTH          CO
RRECTION FACTOR          O.C.V.          CORRECTED O.C.V.          % O.C.V.
 ')(A);
         PUT SKIP(2);
         DO J=1 TO 76;
         PUT SKIP EDIT(A(J,1),A(J,2),A(J,3),A(J,4),A(J,5),A(J,6))(X(9),
F(7,3),X(12),F(7,3),X(13),F(7,3),X(14),F(7,3),X(12),F(7,3),X(13),F(7,3)
);
         END;
         BEGIN;
         CALL PLTSIZ(7.874E-1);
         DCL 1 DUM,2(I FIXED BIN(31),CHPAR CHAR(80) VAR ),FPAR DEFINED
CHPAR;
         CALL PLTOFS(0.3E0,0.2E0,0.0E0,1.0E1,1.5E0,0.5E0);
         CHPAR='WAVELENGTH IN MICRONS.';
         I=-22;
         CALL PAXIS(1.5E0,C.5E0,FPAR,I,6.5E0,0.0E0,0.3E0,0.2E0,0.5E0);
         CHPAR='PERCENTAGE O.C.V.';
         I=17;
         CALL PAXIS(1.5E0,C.5E0,FPAR,I,1.0E1,9.0E1,0.0E0,1.0E1,1.0E0);
         K=1;
         N=76;
         J=-1;
         R=4;
         CALL PLINE(B(1),D(1),N,K,J,R,99.9E0);
         CALL PLTEND;
         END;
         END SPEC;
```

FIG. A.4 CORRECTED SPECTRAL RESPONSE CURVE

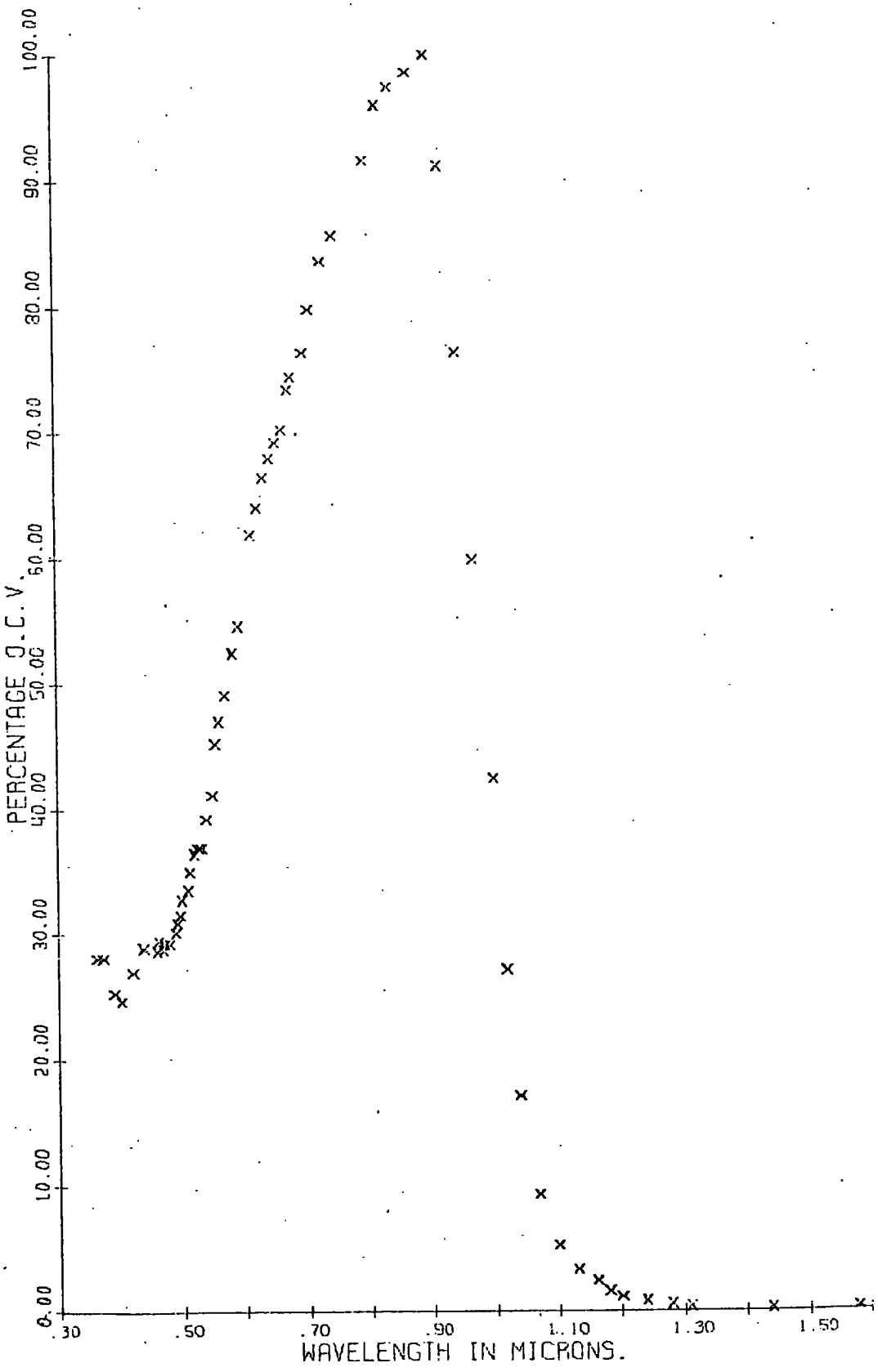

work reported from this laboratory, response curves have not been corrected and hence it is easier to make comparisons between cells produced in previous investigations and in the present series if no corrections are made.

REFERENCES

Abdullaev G B et al (1968) Phys. Stat. Sol. 26 65

Addiss R R (1963) Trans. 10th Nat. Vac. Symp. (Macmillan) 354

Aerschodt A E van and Reinhartz K K (1970) Proc. ECOSEC Int. Coll. on Solar Cells (Gordon and Breach) p.95

Aitchson R F (1951) Nature 167 812

Anderson J G (1966) 'The Use of thin films in Physical Investigations' (Academic Press)

Anderson W and Mitchell J T (1968) Appl. Phys. Lett. 12 334

Andrews A M and Haden C R (1969) Proc. IEEE 57 99

Aven M and Cook D M (1961) J. Appl. Phys. 32 960

Aven M and Prener J A (1967) 'Physics and Chemistry of II-VI Compounds' (North Holland)

Aven M and Woodbury H H (1962) Appl. Phys. Lett. 1 53

Balkanski M and Chone B (1966) Rev. de Phys. Appl. 1 179

Barrett S and Massalski T B (1966) 'Structure of Metals' (McGraw-Hill)

Becquerel E (1839) Compt. Rend. 9 145

Berger H (1961) Phys. Stat. Sol. 1 739

Berger H et al (1964) Phys. Stat. Sol. 7 679

Berger H et al (1968) Phys. Stat. Sol. 28 K97

Bleha W P et al (1970) J. Vac. Sci. Tech. 7 135

Bleha W P and Peacock R N (1970) J. Appl. Phys. 41 4992

Bockenmuehl R J et al (1961) J. Appl. Phys. 32 1324

Bogus K and Mattes S (1972) Proc. 9th P.V. Spec. Conf. 121

Bogus K et al (1970) Proc. ECOSEC Int. Coll. on Solar Cells (Gordon and Breach) p.241

Bonnet D and Rabenhorst H (1972) Proc. 9th P.V. Spec. Conf. 129

Bowman R L and Mirtich M J (1967) A.I.A.A. Journal 6 378

Bramley A (1955) Phys. Rev. 98 246

Brandhorst H W et al (1968) J. Appl. Phys. 39 6071

Brucker G J et al (1966) Proc. I.E.E.E. 54 895

Bube R H (1955) Proc. I.R.E. Dec. 1836

Bube R H (1960) 'Photoconductivity of Solids' (Wiley)

Buckley R W and Woods J (1973) J. Phys. D:Appl. Phys. 7 197

Buckley R W and Woods J (1974) J. Phys. D:Appl. Phys. 7 663

Bujatti M (1967) Phys. Lett. (Netherlands) 24 36

Bujatti M (1968) B.J.A.P. 1 983

Bujatti M and Muller R S (1965) J. Electrochem. Soc. 112 702

Caswell B G et al (1975) J. Phys. D:Appl. Phys. 8 1889

Chamberlin R R and Skarman J S (1966) (a) Sol. St. Electron 9 819

Chamberlin R R and Skarman J S (1966) (b) J. Electrochem. Soc. 113 86

Chapin D M et al (1954) J. Appl. Phys. 25 676

Chernow F et al (1968) Appl. Phys. Lett. 12 339

Chockalingham M J et al (1970) Ind. J. Pure and Applied Physics 8 744

Chopra K L (1969) 'Thin Film Phenomena' (McGraw-Hill)

Chopra K L and Khan I H (1967) Surf. Sci. 6 33

Clarke R L (1959) J. Appl. Phys. 30 957

Clark L and Woods J (1968) J. Cryst. Growth 3 126

Clark L et al (1971) Proc. Brighton Power Conf. 643

Comas J and Cooper C B (1966) J. Appl. Phys. 37 2820

Cook W R et al (1970) J. Appl. Phys. 41 3058

Cummerow R L (1954) Phys. Rev. 95 16

Curtis B J (1969) J. Appl. Phys. 40 433

Cusano D A (1963) Sol. St. Electron. 6 217

Cutter J R and Woods J (1975) J. Phys. D:Appl. Phys. 8 314

Davydov B I (1938) Zh. Tekh. Fiz. 5 79

de Klerk J and Kelly E F (1965) Rev. Sci. Instrum. 36 506

Dresner J and Shallcross F V (1962) Sol. St. Electron. 5 205

Duc Cuong N and Blair J (1966) J. Appl. Phys. 37 1660

Durand S et al (1972) Thin Solid Films 11 237

Ellis S G (1958) Phys. Rev. 109 1860

Ellis S G (1967) J. Appl. Phys. 38 2906

Elster J and Geitel H (1895) Wied. Ann. 55 685

Esibtt A S (1965) Phys. Stat. Sol. 12 K35

Fabricus E D (1962) J. Appl. Phys. 33 1597

Fischer A G (1963) U.S.A.F. Final Report No. AF 19(604)8018

Fischer A G (1966) 'Electroluminescence in II-VI Compounds'
pp.541-602, Published in 'Luminescence of Inorganic Solids'
Ed. by Goldberg P (Academic Press)

Foster N F (1967) J. Appl. Phys. 38 149

Frenkel J (1933) Nature 132 312

Frenkel J (1935) Physik. Z. Sovieturnion 8 185

Frerichs R (1947) Phys. Rev. 72 594

Fukunishi S and Niizeki N (1969) Jap. J. Appl. Phys. 8 1274

Galkin B D et al (1968) Sov. Phys. Crystallog. 12 766

Gill W D et al (1968) Proc. 7th P.V. Spec. Conf. p.47

Goldstein B and Pensak L (1959) J. Appl. Phys. 30 155

Goryunova N A et al (1970) Phys. Stat. Sol. (a) 2 K117

Greene L C et al (1958) J. Chem. Phys. 29 1395

Grimmeis H G and Memming R (1962) J. Appl. Phys. 33 2217, 3596

Haering R R (1964) Sol. St. Electron 7 31

Hallwachs W (1888) Ann. Physik. 33 301

Hertz H (1887) Ann. Physik. 31 421 983

Heyraud J C and Capella L (1968) J. Cryst. Growth 2 405

Hietanen J R and Shirland F A (1967) Proc. 6th P.V. Spec. Conf.

Hill E R and Keramidas B G (1966) Rev. de Phys. Appl. 1 189

Hirahara E (1951) J. Phys. Soc. Japan 6 422

Hirashima M (1955) J. Phys. Soc. Japan 10 1055

Hirsch P B et al (1965) 'Electron Microscopy of Thin Crystals' (Butterworths)

Holland L (1958) B.J.A.P. 9 410

Holland L (1963) 'Vacuum Deposition of Thin Films' (Chapman and Hall)

Holloway H and Wilkes E (1968) J. Appl. Phys. 39 5807

Holt D B (1969) J. Mat. Sci. 4 935

Holt D B and Wilcox D M (1971) J. Cryst. Growth 9 193

Honda M et al (1972) Fujitsu Scientific and Technical Journal 161

Imaoka E et al (1971) Oyo Buturi (Japan) 40 729

Kahle W and Berger H (1970) Phys. Stat. Sol. (a) 2 717

Keating P N (1963) J. Phys. Chem. Sol. 24 1101

King P J (1969) B.J.A.P. 2 1349

Kitada M and Kamoshita S (1972) J. Vac. Soc. Japan 15 205

Kitamura S (1960) J. Phys. Soc. Japan 15 2343

Konstantinova E M and Kanev S K (1973) Compt. Rend. Acad. Bulg. Sci. 26 867

Kunioka A and Sakai V (1965) Sol. St. Electron 8 961

Kuwabara G (1954) J. Phys. Soc. Japan 9 97

Lakshmanen T K and Mitchell J M (1963) Trans. 10th Nat. Vac. Symp. 335

Landau L D and Litshitz E M (1936) Physik. Z. Sovietunion 9 477

Lawrance R (1959) B.J.A.P. 10 298

Loferski J J (1956) J. Appl. Phys. 27 777

Loferski J J (1963) Proc. I.E.E.E. 51 667

Lorenz R (1891) Chem. Ber. 29 1501

Lorenz M R (1962) J. Appl. Phys. 33 3304

Mankarious R G (1964) Sol. St. Electron. 7 702

Manufacturing Optician (1958) 11 288

Marchenko A I et al (1970) Ukr. Fiz. Zh. (USSR) 15 1530

Marshall R and Mitra S S (1965) J. Appl. Phys. 36 3882

Martinuzzi S et al (1970) Phys. Stat. Sol. (a) 2 K9

Massicot P (1972) Phys. Stat. Sol. (a) 11 531

McMahan L L (1967) Proc. 6th P.V. Spec. Conf. Florida U.S.A. 210

Mecalf W E and Fahrig R H (1958) J. Electrochem. Soc. 105 719

Micheletti F B and Mark P (1967) Appl. Phys. Lett. 10 136

Micheletti F B and Mark P (1968) J. Appl. Phys. 39 5274

Miya N (1970) Jap. J. Appl. Phys. 9 768

Moss H I (1961) R.C.A. Rev. 22 29

Mott W F (1939) Proc. Roy. Soc. A171 281

Mulder B J (1972) Mat. Res. Bull. 7 1532

Mytton R J (1973) Phys. Technol. 4 92

Mytton R J et al (1972) Proc. 9th P.V. Spec. Conf. 91

Nadzhakov G et al (1954) Izv. Bulg. Acad. Nank. 4 4

Nakayama N (1969) Jap. J. Appl. Phys. 8 450

Nakayama N et al (1971) Jap. J. Appl. Phys. 10 1415

Nelson R C (1955) J. Opt. Soc. Amer. 45 774

Neugebauer C A (1968) J. Appl. Phys. 39 3177

Nicoll F H and Kazan B (1955) J. Opt. Soc. Amer. 45 647

Okamoto K and Kawai S (1973) Jap. J. Appl. Phys. 12 1130

Otake T et al (1972) Oyo Buturi (Japan) 40 1224

Palż W et al (1968) Proc. 7th P.V. Spec. Conf.

Palz W et al (1972) Proc. 9th P.V. Spec. Conf. p.91

Palz W et al (1974) Proc. 10th P.V. Spec. Conf. p.69

Pavelots S Yu and Fedorus G A (1966) Ukr. Fiz. Zh. 11 686

Petritz R L (1956) Phys. Rev. 104 1508

Pfann W G and Roosbroeck W van (1954) J. Appl. Phys. 25 1422

Pilling N B and Bedworth R E (1923) J. Inst. Met. 29 529

Pinder R S and Clark L (1974) Proc. Brighton Power Conf.

Piper W W and Polich S J (1961) J. Appl. Phys. 32 1278

Potter A E and Schalla R L (1967) N.A.S.A. Report TND 3849

Prince M B (1955) J. Appl. Phys. 26 534

Purohit R K et al (1969) J. Appl. Phys. 40 4677

Putner T (1959) B.J.A.P. 10 332

Pizzorello F A (1964) J. Appl. Phys. 35 2730

Rappaport P (1959) R.C.A. Rev. 20 373

Ratcheva S T et al (1972) Phys. Stat. Sol. (a) 10 209

Ray B (1969) 'II-VI Compounds' (Pergamon)

Reynolds D C and Czyzak S J (1950) Phys. Rev. 79 543

Reynolds D C and Czyzak S J (1954) Phys. Rev. 96 1705

Reynolds D C et al (1954) Phys. Rev. 96 533

Rickert H and Mathieu H J (1969) E.S.R.D. Contract Report 14

Rittner E S (1954) Phys. Rev. 96 1708

Riviere J C (1957) Proc. Phys. Soc. B70 676

Rose A (1963) 'Concepts in Photoconductivity and Allied Problems' (Interscience/Wiley)

Rozgonyi G A and Foster N F (1967) J. Appl. Phys. 38 5172

Sakai Y and Okimura H (1964) Jap. J. Appl. Phys. 3 144

Shalimova K V et al (1961) Sov. Phys. Dok. 6 404

Shalimova K V et al (1964) Sov. Phys. Crystallog. 8 618

Shallcross F V (1966) Trans. Met. Soc. of A.I.M.E. 236 309

Shallcross F V (1967) R.C.A. Rev. 28 569

Shiozawa L R et al (1966) Contract A.F. 33(615)-5224 (2nd Q.P.R.)

Shiozawa L R et al (1969) Clevite Corp. 10th Quarterly Report AF33(615) - 5224 p.27

Shiozawa L R et al (1969) Aerospace Research Labs. Report ARL 69-0155

Shirland F A et al (1962) A.S.D. Tech. Doc. Report 62

Shirland F A (1966) Adv. Energy Conv. 6 201

Shitaya T and Sato H (1968) Jap. J. Appl. Phys. 7 1348

Singer J and Faeth P A (1967) Appl. Phys. Lett. 11 130

Smith W (1873) Am. J. Sci. 5 301

Smith R W (1955) Phys. Rev. 97 1525

Spakowski A E (1967) Proc. 6th P.V. Spec. Conf.

Spakowski A E and Forestieri (1968) N.A.S.A. TMX-52485

Sreedhar A K et al (1970) 'Radiation Effects' (Gordon and Breach) p.103

Stanley J M (1956) J. Chem. Phys. 24 1279

Stanley A G (1968) Proc. I.E.E.E. 57 292

Stoyanov V E et al (1971) Compt. Rend. Acad. Bulg. Sci. 24 1469

Strong J (1944) 'Modern Physical Laboratory Practice' (Blackie)

Suzanne J and Male D (1971) Thin Solid Films 5 379

Szeto W and Somorjai G A (1966) J. Chem. Phys. 44 3430

Tauc J (1962) "Photo and Thermoelectric Effects in Semiconductors' (Pergamon)

Tell B and Gibson W M (1969) J. Appl. Phys. 40 5320

Te Velde T S (1973) Sol. St. Electron. 16 1305

Te Velde T S and Dieleman J (1973) Phillips Res. Repts. 28 573

Thomas P A et al (1970) Rev. de Phys. Appl. 5 683

Thomsen S M and Bube R H (1955) Rev. Sci. Instrum. 26 664

Thomson G P and Cochrane W (1939) 'Theory and Practice of Electron Diffraction' (Macmillan) p.146

Tyagi M S (1971) Proc. Symp. on Electronics (Madras)

Van Aerschodt A E et al (1968) Proc. 7th F.V. Spec. Conf.

Vecht A (1966) 'Physics of thin films' 3 (Academic Press)

Veith W (1950) Compt. Rend. Acad. Sci. 230 947

Vlasenko N A and Kononets Ya F (1971) Ukr. Fiz. Zh. 16 238

Vodakov Ya A et al (1960) Sov. Phys. Sol. St. 2 1

Vojdani S et al (1973) Electron. Lett. 9 128

Vojdani S and Douroudian M (1973) Proc. Sun in Service of Mankind, Paris p.159

Wagner S and Shay J L (1975) Appl. Phys. Lett. 26 229

Wallmark J T (1957) Proc. I.R.E. 45 474

Warekois E P et al (1962) J. Appl. Phys. 33 690

Warekois E P et al (1966) J. Appl. Phys. 37 2203

Watanabe S and Mita Y (1972) Sol. St. Electron. 15 5

Waxman A et al (1965) J. Appl. Phys. 36 168

Wendland P H (1962) J. Opt. Soc. Amer. 52 581

Werring N J (1972) Ph.D. Thesis Thames Polytechnic

Wilcox D M and Holt D B (1969) J. Mat. Sci. 4 672

Williams R (1960) J. Chem. Phys. 32 1505

Williams R and Bube R H (1960) J. Appl. Phys. 31 968

Wilson J I B (1971) Ph.D. Thesis University of Durham

Wilson J I B and Woods J (1972) J. Phys. D: Appl. Phys 5 1700

Wilson J I B and Woods J (1973) J. Phys. Chem. Sol. 34 171

Witt W et al (1966) Proc. I.E.E.E. 54 897

Wolf M (1960) Proc. I.R.E. 48 1246

Woodbury H H (1965) J. Appl. Phys. 36 2287

Woodcock J M and Holt D B (1969) B.J.A.P. 2 775

Woods J and Champion J A (1959) J. Electron. and Control. 7 243

Wright H L et al (1968) B.J.A.P. 1 1593